CONTROL OF WATER SUPPLY AND SPECIFIC NUTRIENT APPLICATION IN CLOSED GROWING SYSTEMS

Th.H. Gieling

Promotor:	prof. dr. ir. G. van Straten hoogleraar in de Meet-, Regel- en Systeemtechniek
Co-promotor:	dr. J. Bontsema plv. hoofd Afdeling Geavanceerde Systemen, Plant en Energie (IMAG)
Samenstelling promotie commissie:	prof. dr. O. van Kooten (Wageningen Universiteit) prof. dr. E.J.R. Sudhölter (Wageningen Universiteit) Prof. Dr. rer. hort. habil. H.-J. Tantau (Universität Hannover) dr. ir. J.J.W. Westra (Priva Hortimation B.V., De Lier)

CONTROL OF WATER SUPPLY AND SPECIFIC NUTRIENT APPLICATION IN CLOSED GROWING SYSTEMS

Th.H. Gieling

Proefschrift

ter verkrijging van de graad van doctor
op gezag van de rector magnificus
van Wageningen Universiteit,
prof. dr. ir. L. Speelman
in het openbaar te verdedigen
op maandag 5 november 2001
des namiddags te 16.00 uur in de Aula.

CIP-gegevens Koninklijke Bibliotheek, Den Haag

Gieling, Th. H.
Control of water supply and specific nutrient application in closed growing systems.
Dissertation Wageningen University - With ref. - With summaries in English and Dutch.

ISBN 90-5808-525-2

IMAG

This dissertation is also available as publication No. 2001-15 (ISBN 90-5406-201-0) of the Institute of Agricultural and Environmental Engineering (IMAG), P.O.Box 43, 6700 AA, Wageningen, The Netherlands.

Stellingen

1. Het vrijwel enige - maar in ieder geval belangrijkste - proces, dat bij de water- en nutrienten toediening moet worden geregeld, vindt plaats in het substraat (dit proefschrift).

2. Indien "ion sensitive electrodes" of "ion selective field effect transistors" worden gebruikt om de individuele ionconcentratie in de retourvloeistof van planten constant te houden geldt - in tegenstelling tot de stelling van Heinen (1997) - dat vooral levensduur en stabiliteit ervan doorslaggevend zijn voor toepassing in de glastuinbouw, terwijl de absolute meetfout nauwelijks van belang is (dit proefschrift).

3. De impact van de besturing van water- en nutriënttoediening via terugkoppeling met signalen van ion specifieke sensoren zal in de glastuinbouw op de bedrijfsvoering, de productie, de productkwaliteit en het milieu tenminste dezelfde zijn als die van de invoering van de computerregeling voor kasklimaat (dit proefschrift).

4. Beleidsmakers en bestuurders zouden verplicht een studie systeem- en regeltheorie moeten volgen. Ze zouden dan eindelijk inzicht krijgen in de effecten van systeemkenmerken zoals reactietraagheid, doorlooptijd en instabiel regelgedrag, die het beoogde resultaat van hun beslissingen ten aanzien van mensen nu zo vaak doen tenietgaan.

5. Planten zijn soms net mensen. Als het slecht met ze gaat, gaan ze over nageslacht nadenken.

6. Sinds de privatisering van het onderzoek wordt de kwaliteit van het eindresultaat beoordeeld door de boekhouder.

7. Totdat in een gesprek met de androïde bediende kan worden gekletst over Ajax, en de gezamenlijke afschuw over Feyenoord kan worden gedeeld, zijn robotachtige apparaten te betitelen als "automaten".

8. Het huidige gebruik in de wedstrijdmensport, om jonge paarden direct zonder beperkingen in te zetten in de hoogste klasse, zou moeten worden veranderd overeenkomstig het gebruik in de dressuur- en springsport voor rijpaarden, waarbij de inzet van paarden in een hogere klasse gebeurt via promotie na succes in de onderklasse.

Stellingen behorende bij het proefschrift:
"Control of water supply and specific nutrient application in closed growing systems"
van Th.H. Gieling. 5 november 2001,Wageningen Universiteit.

voor mijn vader R.H. Gieling die ik te kort kende
voor mijn moeder Th.J.Gieling-Peters die zorgde dat ik studeerde
en vooral voor Ada, waar ik van hou

He that will not apply new remedies must expect new evils,
for time is the greatest innovator.
(Francis Beacon)

CONTENT

ABSTRACT

Gieling Th.H. (2001). Control of water supply and specific nutrient application in closed growing systems. Dissertation, Agricultural University, Wageningen, The Netherlands. 172pp, 73 figures, 24 graphs, 16 photos, and 9 tables. Summaries in Dutch and English.

Plants in modern greenhouses receive water and nutrients from a diluter of chemical solutes. Supply lines of a trickle irrigation system dispense the nutrient solution by means of thin capillary hoses, to each individual plant. Dependent on the type of growing system - either a NFT or a substrate system - the drain will run-off immediately or it will linger for some time in the substrate mat. In a closed system for water and nutrient supply, the drain water returns to the nutrient dispenser, where it is prepared for reuse by mixing it with clean water. The thesis starts with an overview of the state of the art of water supply and nutrient application systems.

The purpose of the design study in this thesis is to enable completely closed growing systems for water and nutrients, to be applied in horticulture practise, and to improve the technological level of their control to such an extend that it is comparable to the level of computerised climate controllers in greenhouses. It is argued that as a basic requirement the system should have the ability to control the drain flow and the concentration of individual ions in the drain to any predefined set value. An analysis is given of the dynamics of movement of water and nutrients in substrates in relation to nutrient uptake, supply-flow and mass-flow. From a mass balance of nutrients, a control strategy for nutrient application in closed growing systems is suggested that is useful in the design of control algorithms. This strategy keeps the concentration of the individual ions in the drain constant by feedback of ion concentration and drain flow. In doing so, it compensates intrinsically for the plant's uptake of ions.

The creation of a system with feedback control requires appropriate sensors and the ability to blend nutrient solution for values demanded by the controller. The ion specific feedback control of fertiliser application implies that ions need to be measured individually. The thesis describes a novel type of ion specific analyser, based on a set of Chemfet sensors. This instrument, as a result of this research, is the prototype of the first series of commercially available equipment for horticulture. Continuous measurement implies sensors with an electrical output, connected to an automatic data acquisition system with in-line calibration. In horticulture applications the lifetime expectancy of a sensor should at least be 6 to 9 months.

In contrast to open loop control based on a prediction of uptake, feedback control automatically compensates for fluctuations in evapo-transpiration and nutrient uptake. Uptake by the plant is treated as a disturbance. Comparison of simulation results, with data from an implemented controller in a greenhouse, shows the success of the design.
The so-called "Tichelmann" layout of supply lines is proposed to improve the dynamic properties of the supply system. The design study demonstrates and recommends robust controller design as a tool to achieve robust performance and robust stability as qualities of the controlled process to compensate for seasonal changes in the root mat or imperfect models. The modifications to the ideal design arising from the desire in practice for pulse wise water and nutrient injection, as well as aspects related to the blending are considered as well.

Keywords: Tichelmann layout, constant drain flow, constant drain concentration, mass-flow, diffusion flow, sensor, Isfet, Chemfet, closed growing system, robust control, loop-shaping, Simulink®, MIMO controller, SISO controller, simplex routine, simplex matrix.

VOORWOORD

Tijdens het eerste symposium 'Sensors in Horticulture' in 1991 kwam het tot een discussie over de hoeveelheid werk die moet worden verzet voor een promotie. Daarbij werd opgemerkt dat er - naast een goed onderwerp - vooral financiering nodig zou zijn en de rest was eigenlijk niet meer dan een nietje door de publicaties, een voor- en achterkant eromheen en klaar is het. Sjaak Bakker was hierbij de uitdager en Theo Gieling het aangesproken slachtoffer. Sjaak, het is er dus toch van gekomen. Alleen, het is wel iets meer werk geweest! Toch bedankt voor het implanteren van die eerste gedachte.
Een gesprek met mijn directeur, ir. A.A. Jongebreur, bevestigde de uitgangspunten. Hij ondersteunde vanaf het eerste moment in de volle breedte mijn verzoek. Ook om hieraan IMAG tijd te mogen besteden, mits ingekaderd in projecten met betaalde opdrachten als basis, zoals hij dat formuleerde. Een dergelijke ondersteuning, ge'push't door de wetenschappelijk directeur dr. ir. J. Metz, is onontbeerlijk voor het doen slagen van zo'n onderneming. Hoewel de organisatie van IMAG tijdens de uitvoering verschillende keren is gewijzigd, kreeg ik op elke nieuwe plek weer de gelegenheid dit onderzoek te continueren. Die ondersteuning kreeg ik vooral tijdens de laatste perioden van dit onderzoek, op de afdeling Geavanceerde Systemen onder leiding van Dr. J. Bontsema.
Een verzoek aan Prof. dr. ir. G. van Straten, gaf de uiteindelijke doorslag, en ik kon proberen het waar te maken. Prof. van Straten gaf mij de steun die een HBO-er nodig heeft om de stap naar PhD in één keer te kunnen maken. Begeleid door een ondersteunende commissie kon vruchtbaar worden gediscussieerd.

De leden van deze commissie wil ik bedanken voor hun kostbare tijd en geduldige oor:
Promotor en commissievoorzitter Prof. G. van Straten, copromotor Dr. J. Bontsema en de commissieleden Drs. S. Boonstra, Dr. J. W. Engbersen, Dr. E.J. van Henten, Dr. C. Stanghellini, Dr. B.W. Veen, Dr. W. Verboom en - last but not least - Dr. J.J.W. Westra.
Jan Westra vormde tijdens mijn promotieonderzoek de schakel naar het bedrijf PRIVA Hortimation, dat bij de ontwikkelingen rond ionspecifiek regelen en besturen zeer nauw betrokken was en ook in de toekomst zal zijn. Hij zorgde ervoor dat alles goed kwam, ook als het met de sensoren weer eens tegen zat.
Belangrijke projectmedewerkers van de Priva Groep: In het prille begin: A van de Meer, H. H. van den Vlekkert en H. Kouwenhoven. Aan het eind van het project: J.J.W. Westra, S. Boonstra, G. Hermans, A. Arkesteijn, M. Grote Gansey en P. Emmerink.
De eigen investeringen van PRIVA, de financiering van het Ministerie van Economische Zaken via het Bureau Senter, de programmafinanciering van het Ministerie van LNV en de eigen SEO investeringen van IMAG en DLO maakten dit project mogelijk.

In 1981 bezocht de afdeling Fysische Proces Techniek op initiatief van W.P Mulder de Universiteit Twente. Dit bracht het geheel rond Isfets en glastuinbouw aan het rollen, met een presentatie over Isfet sensoren van Prof. P. Bergveld. Op ons initiatief kwam het tot een gesprek met directeur J. Prins van PRIVA, die daarna onderhandelde met CME en UT Twente. Met als gevolg de start van een onderzoekstraject dat nu, 20 jaar later, uiteindelijk zal gaan leiden naar een automatisch doseersysteem voor water en nutriënten in gesloten teeltsystemen in de glastuinbouw. Een doseersysteem dat functioneert op basis van feedback van specifieke ionconcentratie.
Waterhuishouding en nutriëntentoediening heeft nu eindelijk van de automatiseerders de aandacht gekregen die het verdient. Binnen enkele jaren zal het op tenminste hetzelfde niveau worden gebracht, waar nu de regeling van het kasklimaat al is en het zal daarmee een inte-

graal besturingssysteem vormen. Het is mijn inschatting dat de impact op bedrijfsvoering, productie, productkwaliteit en milieu dezelfde zal zijn als bij de invoering van de computerregeling voor het klimaat in de tuinbouw kas.
Als eerste werd het EU projectvoorstel MACQU gehonoreerd, onder coördinatie van Prof. N. Sigrimis, Universiteit van Athene. Dit verschafte de benodigde basis-financiering en een eerste kader waarin zou kunnen worden gewerkt en gepubliceerd. Ervaringen met ionsensoren, opgedaan in voorgaande projecten met PRIVA-Hortimation, kwamen hierbij goed van pas. De hernieuwde belangstelling van PRIVA voor de inzet van ionsensoren, na enkele jaren van een pas op de plaats, was aanleiding voor een nieuw project met parallel hieraan het promotieproject.
De samenwerking in deze beide projecten met de collega's van de betrokken PRIVA bedrijven en DLO instellingen, maar vooral de collega's van het IMAG en van de leerstoelgroep Meet- Regel- en Systeemtechniek van de Wageningse Universiteit, gaf de onontbeerlijk uitdaging.
Wim van Meurs wil ik bedanken voor zijn inbreng en niet aflatende support. Dertig jaar in tuinbouwonderzoek, vaak samen met jou Wim, is niet niks. Voor mij heeft het o.a. geleid tot hetgeen hier voor je ligt. Maar daarnaast vooral tot veel plezier om ons minimalistisch-woordenloze onderlinge verstaan van - en welgemeende kritische kijk op - de wereld om ons heen. Onszelf vooral niet uitgesloten!
Naast Wim zijn vooral Hans Janssen en Erik van Os te noemen als degenen die het dichtst bij de kwaliteit van het eindresultaat zijn betrokken.
Vooral tijdens het EU MACQU project was een groot aantal studenten actief bezig. Jan Bontsema, toen docent van de Wageningse Universiteit, was vaak 'leverancier' van deze studenten. Hij vormde samen met zijn studenten een tomeloze aandrijving voor mijn bescheiden ambities. Het zou te ver voeren om ze allemaal te noemen, maar vooral Leo Lukasse, Arjan van Antwerpen, Ronald Steeghs, Toine Bouwmans, Henk Vree, Peter Loef, Michiel Suurmond en Adrien van den Berge wil ik speciaal bedanken voor hun heel zichtbare aandeel in de publikaties en het geheel van dit proefschrift.
Sinds enige tijd is Jan Bontsema inmiddels IMAG collega en plv. hoofd van de afdeling Geavanceerde Systemen Plant en Energie, mijn baas dus. Jan, in beide functies heb je me fantastisch geholpen en welhaast voortgeduwd naar het eindresultaat.
Een iets wijdere kring van IMAG collega's was betrokken bij de organisatie rond het project, de financiële afhandeling ervan, of het daadwerkelijke onderzoek: Steef van Aggelen, Ferry Corver, Johan van Gaalen, Eldert van Henten, Simon van Heulen, Sjaak Jongejan, Ton Janssen, Loretta van Kollenburg, Geert Kupers, Arjan Lamaker, Marcel Maertens, Jan Meuleman, Wim Rossing, Cecilia Stanghellini, Bart van Tuijl, de Afdeling Beschermde Teelten, de Proeftuin Mansholtlaan, de Werkplaats en I&S.
De medewerkers van de Afdeling Geavanceerde Systemen, Plant en Energie, speciaal de cluster Mechatronica en Procesbesturing, gunden me de gelegenheid dit af te maken, zelfs in voor de afdeling moeilijke tijden in verband met reorganisatie en financiën.

Ada, niets bij zo'n avontuur zou zijn geslaagd zonder jou. De ruimte die ik kreeg, van jou Ada, in tijd, geduld en in achterstand op klussen die eigenlijk mijn pak-aan zijn, maakte dat het uiteindelijk toch kon slagen. Ook als het me even iets moeilijker af ging. Zelf heb je inmiddels een vergelijkbare klus achter de rug, hetgeen jou beduidend beter af ging dan mij.
Dit klusje is nu af en ik beloof je, dat de klussen die thuis nog steeds moeten, nu uiteindelijk ook af zullen komen.

Theo Gieling
Juni 2001.

ACCOUNT

The below numbered chapters of this thesis are covered by the mentioned papers:

§1.1 Gieling, Th.H., E.A. van Os, P.C.J. Hamer and A.W.J. van Antwerpen, 1996. EU project MACQU: Greenhouse water supply, application of nutrients and their environment. In: *Greenhouse reference model*, Chapter 2 (part one).

Kupers, G, J. van Gaalen, Th.H. Gieling and E.A. van Os, 1992. Diurnal changes in ion concentration of the supply and return water of a tomato crop. In: *Acta Hort. 304.*

Jongebreur, A.A., Th.H. Gieling, J.J.W. Westra, 1999. Closed growing systems for supply of water and nutrients. In: *Proceedings of BRAIN International Symposium 2000*. IAM-BRAIN, Japan, November 1999, pp 44-51.

§2.1 Gieling, Th.H., J. Bontsema and L.J.S. Lukasse, 1994. The dynamic behaviour of salinity changes in a closed NFT growing system. In: *Acta Hort. 361*, pp 218-225

§2.2 Gieling, Th.H., J. Bontsema, A.W.J. van Antwerpen and L.J.S. Lukasse, 1995. Model of a water supply system in a greenhouse. In: *Acta Hort. 401*, pp 365-372.

Gieling Th.H., E.A. van Os, P.C.J. Hamer and A.W.J. van Antwerpen, 1996. EU project MACQU: Greenhouse water supply, application of nutrients and their environment. In: *Greenhouse reference model*, Chapter 2 (second part).

§2.3 Gieling, Th.H., G. van Straten, B.W. Veen, 2000. Analysis of solute movement in inert substrates. In: *Proceedings of IFAC Conference on modelling and control in agriculture, horticulture and post-harvest processing.*

§3.1 Gieling, Th.H. and K. Schurer, 1995. Sensors and measurement. In: *Acta Hort. 421.*

§3.2 Gieling, Th.H., J.F.J. Engbersen, J.J.W. Westra, 1998. Chemically modified field effect transistors to monitor ion concentration in nutrient solution. In: *Proceedings of the 3^d symposium on sensors in horticulture.* Tiberias Israel.

Gieling, Th.H. and H.H. van den Vlekkert, 1996. Application of ISFETs in closed-loop systems for greenhouses. In: *Adv. Space Res.* Vol 18, No. 4/5, pp 135-138, Pergamon.

§4.1 Gieling, Th.H., H.J.J. Janssen, G. van Straten and M. Suurmond, 1998. A greenhouse water supply controller: a design based on system identification. Computers and Electronics in Agriculture, Vol 26, (2000) pp 361-374.

Gieling, Th.H., H.J.J. Janssen, H. de Vree and P. Loef, 1998. Feedback control of water supply in an NFT growing system. In: *Proceedings 3^d workshop on "Sensors in Horticulture"*, Tiberias Israel.

§4.2 Gieling, Th.H., J. Bontsema, T.W.B.M. Bouwmans and R.H. Steeghs, 1997. Modelling and simulation for control of nutrient application in closed growing systems. Netherlands Journal of Agricultural Science 45, pp127-142.

Gieling, Th.H., J. Bontsema and E.A. van Os, 1997. Monitoring and control of water and nutrient supply in closed growing systems, 1997. In: E. Goto *et al.* (Eds). *Plant production in closed ecosystems*, pp103-121. Kluwer Netherlands.

§4.3 Gieling, Th.H., J.J.W. Westra, 2000. Supply of fertiliser stock fluids. Internal report IMAG.

SYMBOLS AND DIMENSIONS

Basic SI dimensions: [1] dimensionless, [L] length, [M] mass, [T] time, [K] temperature (Kelvin), [I] ampère

symbol	eqn	description	dimensions	units
Ψ		Evaporation (Figure 2.3.01)	$[L \cdot T^{-1}]$	$m^3 \cdot m^{-2} \cdot s^{-1}$
Ψs		substrate/soil evaporation (Figure 2.3.01)	$[L \cdot T^{-1}]$	$m^3 \cdot s^{-1}$
D_{tube}	2.1.01	diameter supply line in between plant rows	[L]	m
F_n	2.1.01	solution flow through a nozzle	$[L^3 \cdot T^{-1}]$	$m^3 \cdot s^{-1}$
L	2.1.01	length	[L]	m
$U_j(t)$	2.1.02	nutrient uptake rate at plant j	$[M \cdot T^{-1}]$	$mol \cdot \cdot s^{-1}$
V	2.2.02	volume	$[L^3]$	m^3
$\underline{v}$	2.2.06	kinematic viscosity	$[L^2 \cdot T^{-1}]$	$m^2 \cdot s^{-1}$
η	2.2.06	dynamic viscosity	$[M \cdot L^{-1} \cdot T^{-1}]$	$Pa \cdot s$
ρ	2.2.06	density	$[M \cdot L^{-3}]$	$kg \cdot m^{-3}$
λ	2.2.06	coefficient of friction	[1]	-
ΔP_w	2.2.06	pressure loss over a tube	$[M \cdot L^{-1} \cdot T^{-2}]$	Pa
d	2.2.06	diameter	[L]	m
P	2.2.06	pressure	$[M \cdot L^{-1} \cdot T^{-2}]$	Pa
Re	2.2.06	Reynolds number	[1]	-
ϖ	2.2.06	velocity	$[L \cdot T^{-1}]$	$m \cdot s^{-1}$
t_d	2.2.07	residence time in a tube	[T]	s
$t_{j,w}$	2.2.07	residence time in part of a supply line with n capillaries, between capillary j and w, n = w-j	[T]	s
a_i	2.2.09	partial flow fraction through capillary i	[1]	-
κ	2.2.10	extinction coefficient	[1]	-
Δ	2.2.10	temperature dependancy of saturation vapour pressure	$[M \cdot L^{-1} \cdot T^{-2} \cdot K^{-1}]$	$Pa \cdot K^{-1}$
λ_v	2.2.10	latent heat of vaporisation	$[L^2 \cdot T^{-2}]$	$J \cdot kg^{-1}$
e_a	2.2.10	air vapour pressure	$[M \cdot L^{-1} \cdot T^{-2}]$	Pa
e_a*	2.2.10	air saturated vapour pressure	$[M \cdot L^{-1} \cdot T^{-2}]$	Pa
E_t	2.2.10	evaporation flux density	$[M \cdot L^{-3} \cdot T^{-1}]$	$kg \cdot m^{-2} \cdot s^{-1}$
r_a	2.2.10	internal resistance of canopy to water vapour transfer	$[L \cdot T^{-1}]$	$s \cdot m^{-1}$
$\Phi_\perp$	2.2.11	solar radiation on a horizontal surface	$[M \cdot T^{-3}]$	$W \cdot m^{-2}$
LAI	2.2.12	leaf area index	[1]	-
r_c	2.2.12	aerodynamic resistance		$s \cdot m^{-1}$
r_s	2.2.12	leaf stomatal resistance	$[L^{-2} \cdot T]$	$s \cdot m^{-2}$
VPD	2.2.13	saturation deficit	$[M \cdot L^{-1} \cdot T^{-2}]$	Pa
Φ	2.2.14	radiation	$[M \cdot T^{-3}]$	$W \cdot m^{-2}$
CO_2	2.2.14	volume parts CO_2 per million volume parts	[1]	vpm
Φ_g	2.2.15	global radiation	$[M \cdot T^{-3}]$	$W \cdot m^{-2}$
θ	2.3.01	volumetric water content per unit volume	[1]	$m^3 \cdot m^{-3}$
f_{in}	2.3.01	volumetric flow rate of water entering the control volume per unit volume	$[T^{-1}]$	$m^3 \cdot m^{-3} \cdot s^{-1}$
f_{out}	2.3.01	volumetric flow rate of water leaving the control volume per unit volume	$[T^{-1}]$	$m^3 \cdot m^{-3} \cdot s^{-1}$
S_r	2.3.01	root surface area per unit volume	$[L^{-1}]$	$m^2 \cdot m^{-3}$
W	2.3.01	water uptake rate per unit root surface area	$[L \cdot L^{-2} \cdot T^{-1}]$	$m^3 \cdot m^{-2} \cdot s^{-1}$
C_b	2.3.02	molar concentration in the bulk of a control volume	$[M \cdot L^{-3}]$	$mol \cdot m^{-3}$
C_{in}	2.3.02	molar concentration of nutrient in incoming water	$[M \cdot L^{-3}]$	$mol \cdot m^{-3}$
C_{out}	2.3.02	molar concentration of nutrient in outgoing water	$[M \cdot L^{-3}]$	$mol \cdot m^{-3}$
U^*	2.3.02	nutrient uptake from bulk solution per unit root surface	$[M \cdot L^{-2} \cdot T^{-1}]$	$mol \cdot m^{-2} \cdot s^{-1}$
F_{dr}	2.3.05	volumetric outflow (drain)	$[L^3 \cdot T^{-1}]$	$m^3 \cdot s^{-1}$
F_{in}	2.3.05	volumetric inflow (supply)	$[L^3 \cdot T^{-1}]$	$m^3 \cdot s^{-1}$
$f_W(\theta)$	2.3.08	empirical function expressing the ratio of the actual water uptake and unrestricted uptake	[1]	-
W_{sup}	2.3.08	unrestricted water uptake at sufficient water content	$[L \cdot T^{-1}]$	$m^3 \cdot m^{-2} \cdot s^{-1}$
$f_U(Cb, \theta)$	2.3.09	empirical function expressing the ratio of the actual nutrient uptake and unrestricted uptake	[1]	-

symbol	eqn	description	dimensions	units
M	2.3.10	molar mass {= $V \cdot Cb \cdot \theta$}	[M]	mol
Q	2.3.10	molar mass flow {= $F \cdot C$}	$[M \cdot T^{-1}]$	$mol \cdot s^{-1}$
U^*_{sup}	2.3.10	unrestricted nutrient uptake from the bulk at sufficient water and nutrient content everywhere in the substrate	$[M \cdot L^{-3} \cdot T^{-1}]$	$mol \cdot m^{-3} \cdot s^{-1}$
r	2.3.11	radial distance	[L]	m
$v(r)$	2.3.11	water flow velocity perpendicular to rootsurface at distance r from root	$[L \cdot T^{-1}]$	$m \cdot s^{-1}$
$r0$	2.3.12	radius of root	[L]	m
δ	2.3.16	boundary layer thickness	[L]	m
C_{r0}	2.3.16	concentration at root surface	$[M \cdot L^{-3}]$	$mol \cdot m^{-3}$
D	2.3.16	effective diffusion coefficient	$[L^2 \cdot T^{-1}]$	$m^2 \cdot s^{-1}$
U	2.3.16	nutrient uptake rate at root surface per unit root surface	$[M \cdot L^{-2} \cdot T^{-1}]$	$mol \cdot m^{-2} \cdot s^{-1}$
k_m	2.3.18a	Michaelis-Menten coefficient	$[M \cdot L^{-3}]$	$mol \cdot m^{-3}$
C_x	2.3.20	(virtual) influx concentration {= U/W}	$[M \cdot L^{-3}]$	$mol \cdot m^{-3}$
$K^{pot}_{i,j}$	3.1.01	potentiometric selectivity = sensitivity coefficient of ion J in a membrane of type I	[1]	-
a_I	3.1.01	activity of ion type I in an aquaous solution	$[M \cdot L^{-3}]$	$mol \cdot m^{-3}$
E	3.1.01	electrical potential, developed across a membrane due to the capture of charged particles by ligands in the membrane	$[M \cdot L^2 \cdot T^{-3} \cdot I^{-1}]$	mV
E_0	3.1.01	potential across a reference sensor	$[M \cdot L^2 \cdot T^{-3} \cdot I^{-1}]$	mV
z_i	3.1.01	electrical charge of ion of type i	$[T \cdot I]$	$A \cdot s$
E_{mem}	3.2.01	membrane electrical potential	$[M \cdot L^2 \cdot T^{-3} \cdot I^{-1}]$	mV
μ	3.2.02	electron mobility	$[L \cdot T^{-2}]$	$J \cdot mol^{-1}$
C_{ox}	3.2.02	gate insulator electrical capacitance of a FET device	$[L^{-2} \cdot M^{-1} \cdot T^4 \cdot I^2]$	pF
I_D	3.2.02	electrical drain current of a FET device	[I]	mA
V_{DS}	3.2.02	drain to source potential	$[M \cdot L^2 \cdot T^{-3} \cdot I^{-1}]$	mV
V_{GS}	3.2.02	gate to source potential	$[M \cdot L^2 \cdot T^{-3} \cdot I^{-1}]$	mV
AD	3.2.04	ageing drift of output signal of a sensor in calibration fluid	$[M \cdot L^2 \cdot T^{-3} \cdot I^{-1}]$	$mV \cdot s^{-1}$
pI	3.2.04	logarithm of activity a of ion type I in an aquaous solution (i.e. pH = $-\lg [10^{-3} \cdot \{a(H^+)\}]$ or pNa = $-\lg [10^{-3} \cdot \{a(Na^+)\}]$)	[1]	-
S_{T0}	3.2.04	sensitivity of a Chemfet sensor	$[M \cdot L^2 \cdot T^{-3} \cdot I^{-1}]$	$mV \cdot pI^{-1}$
STC	3.2.04	temperature dependency of sensitivity	$[M \cdot L^2 \cdot T^{-3} \cdot I^{-1} \cdot K^{-1}]$	$mV \cdot pI^{-1} \cdot K^{-1}$
TD	3.2.04	sensor output signal temperature drift in calibration fluid	$[M \cdot L^2 \cdot T^{-3} \cdot I^{-1} \cdot K^{-1}]$	$mV \cdot K^{-1}$
H, G	4.1.01	transfer function	[1]	-

underscore	total or spatially average
<i>	index for nutrient elements (i.e.: N, P, K, S, Ca, Mg)
affix ^	cycle averaged value
f(...)	function of the arguments
subscript ss	steady state

CHAPTER 1

STATE OF THE ART

§1.1 WATER AND NUTRIENT SUPPLY IN PROTECTED CULTIVATION

§1.1 Water and nutrients in protected cultivation

Based on:
Diurnal changes in the ion concentration of the supply and return water of a tomato crop on rockwool. In: Acta Hort. 304. Kupers, G., J. van Gaalen, Th.H. Gieling and E.A. van Os, 1992.
Greenhouse water supply, application of nutrients and their environmental impact. In: EU project MACQU: Greenhouse Reference Model Chapter 2. Gieling, Th.H., E.A. van Os, P.C.J. Hamer and A.W.J. van Antwerpen, 1996.
Closed growing systems for supply of water and nutrients. In: Proceedings of BRAIN International Symposium 2000. IAM-BRAIN, Japan, November 1999, p. 44-51. Jongebreur, A.A., Th.H. Gieling and J.J.W. Westra, 1999.

1. Protected cultivation

Greenhouse production - by its nature - is a labour, capital and knowledge intensive branch of the agricultural industry. In order to be able to earn a living in economically harsh circumstances, the grower is forced to be an innovative entrepreneur. The modern grower carefully observes and adopts new developments, even if there are only slight indications of return on investment.

In the minutiae of his history of greenhouses, Van den Muijzenberg (1980) shows examples of the same kind of attitude of 'growers' from ancient times in China, Egypt and India, mediaeval Belgium and Holland and 19th century England and France (Figure 1). Although Jacobs (1995) states that England should be regarded as the cradle of the modern greenhouse industry, he stresses that in 1950 the Dutch horticultural industry responded to the rapidly growing European market by taking advantage of its favourable geographic position in the centre of that market. He mentions as reasons for the position of Dutch horticulture over a period of 30 years to become the world leader and main centre of glasshouse production:

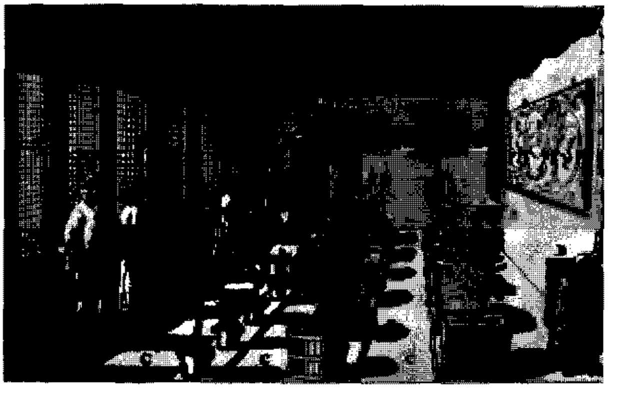

Figure 1 - Technical documentation of a 17th and 18th century predecessor greenhouse. They were found as 'oranjerie' to protect orange trees during winter near Manors and Mansions. The letters in the drawing (A, B, C) explain the function of the equipment (Van den Muijzenberg, 1980).

- the creation of a co-operative auction system,
- the introduction of a co-operative banking system,
- the government policy to support the industry's professional training,
- research and advisory services free of charge available for the grower (until 1990).

Climate control computers

A commercial firm used the Dutch Horticultural Fair of 1974 to show the first system that claimed to be the 'computer hart' of an automatic climate controller. It is of value to mention this event, since it was the ultimate cause to release funds for institutions in The Netherlands to aim their research efforts on the application of the computer as controlling element in greenhouse processes. These research efforts did benefit research in computerised controllers for climate as well as the development of automatic water supply systems (Figure 2).

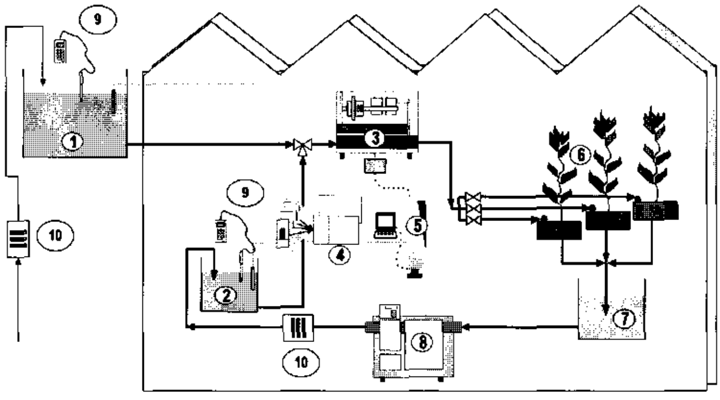

Figure 2 - Water supply system: ① basin for rain water collection ② tank for clean drain water ③ equipment to dilute and distribute fertilisers (either direct injection or mixing tank) ④ on-line ion concentration analyser (ISE or Chemfet sensors) ⑤ fertiliser dilution control ⑥ closed growing system ⑦ tank for untreated drain water ⑧ disinfecting unit for drain water (Heat treatment, UV radiation, Ozon, Biological-active filtering ⑨ hand-held ion concentration sensors (ISE or Chemfet sensors) ⑩ membrane system to remove sodium selectively (picture used by courtesy of Priva Hortimation).

The energy crisis of 1972 and beyond boosted horticultural research into a direction of saving energy. Next to measures like screens for energy saving and improvements in greenhouse construction, automatic control appeared to be a major contributor to energy efficient operation of greenhouse processes. Redundant and robust automatic control systems for climate and nutrient solution supply became a value in its own. Suddenly there was a need for control systems, that:

- are cost effective
- are less susceptible to interference and show less down time
- guarantee stable and precise control
- are programmable to the grower's wishes
- are able to fulfil the plant's demands.

From that time on, growing systems were adjusted to accommodate the new demands raised by automation and control instead of the other way around.

Legislation for sustainable crop growth

Starting in 1985, the last 15 years can be characterised by an awakening of environmental consciousness. The industrial world has been confronted with environmental legislation during this period of time. At first, governments of the industrialised countries mainly tackled the major industrial contaminators. Only during the last years, these governments are turning to the large group of minor contaminators, in which farmers and growers form a specific group.
Dutch government issued various memoranda aiming at a given level of reduction in pollution by the year 2000. The National Environmental Policy Plan (1989) aimed to achieve a safe, sustainable and competitive horticultural sector. Following the Agricultural Structure Memorandum (1989) glasshouse growers should grow their products in closed systems, separated from the subsoil. The target for 1994 was, that 80% of the glasshouse vegetables and pot

plants and 30% of the flowers should not be grown in open soil cultivation, whilst 30% of the area should reuse the drain water.
It appeared that there were so many differences in growing systems in use in the sector that general legislation was not useful. In the Wastewater Disposal Decree, very detailed targets are set for nurseries to be fulfilled at a certain point of time between 1995 and 2000. Such targets are the result of negotiations between government and horticultural representatives and are based on research done in the five years before. The results of this research showed the advantages and shortcomings of soilless systems for all glasshouse crops.
Among several others, the most important targets are:

- recirculation of the nutrient solution when soilless growing systems are used,
- the use of a rain water basin,
- maximum limits on water supply for soil grown crops,
- the first shower of a rainy period after a period of dryness should be kept separate,
- registration of consumption of water, fertilisers and pesticides.

The Multi-Year Crop Protection Plan (1991) gives guidelines to minimise the dependency on chemical pesticides (e.g. more biological control). If applied, to reduce its use (e.g. more precise depositing to reduce spraying frequency) and to reduce its emission to the environment (e.g. air, ground and surface water). Compared to 1991, the target to a total reduction in use of pesticides in 1995 was set to be 35% and more than 50% in 2000 for the whole agricultural sector. For glasshouse horticulture, the figures are more stringent: 50% reduction in 1995 and 65% in 2000. At the same time considerable reductions in emission of pesticides should be obtained in 2000: 50% reduction in emission to the air, 75% to soil and ground water and 90% to surface water.
Now, with the introduction of the 1997 covenant between horticultural employers and the government, the grower is allowed to follow his own way to achieve the legal targets set for 2000 till 2010. In co-operation with the advisory service each grower puts together his own "Environmental Business Plan", in which he sets out how to achieve the goals. For each measure in the field of energy, minerals and crop protection, he gets points. Each year he needs a certain amount of points, which he can obtain by the introduction of protective measures. E.g. recirculation of drain water, registration of usage of fertilisers, use of biodegradable utensils (supporting strings, packaging), recycling of substrates, double energy screens, biological control of pests, etc. (Hietbrink *et. al.*, 1999; Van Os, 1999)

2. Growing systems

2.1 Soil-bound crops

Generally speaking, under present legislation, vegetable crops with many plants per m^2 (lettuce, radishes) still may be grown in soil. Research confirmed that a complete change to soilless growing is economically not feasible for all growers (Ruijs, 1994). In reaction, conceptual methods for water management have been developed to preserve the water resources and prevent ground water from becoming brackish, even in soil bound cultivation.
Figure 3 depicts a system where two tensiometers measure soil humidity at different depths. Tensiometer sensors and hydraulic models dictate when and how much water should be given to the crop and secure that no water leaches out of the cultivation layer into the groundwater
This water management concept for open growing systems is based on the idea of keeping the water available in the top layer (root zone) of the soil. Below this layer, there will be an inactive dry soil layer, which acts as a buffer between the root zone and the ground water. In this

way water in the top layer of the soil and in the groundwater do not connect. It results in a lower demand for irrigation water and in fewer problems with leaching. The crop production system will behave as a "virtually" closed system for water and fertilisers. By irrigating more often with lower amounts, the water is enabled to spread in a horizontal rather than a vertical way in the wet root zone of the higher soil layers. This type of irrigation in open-, soil-bound growing systems has been subject of several adjacent studies, not part of this thesis (Balendonck *et al.*, 1998; De Veld, 1997; Sonneveld, 1996).

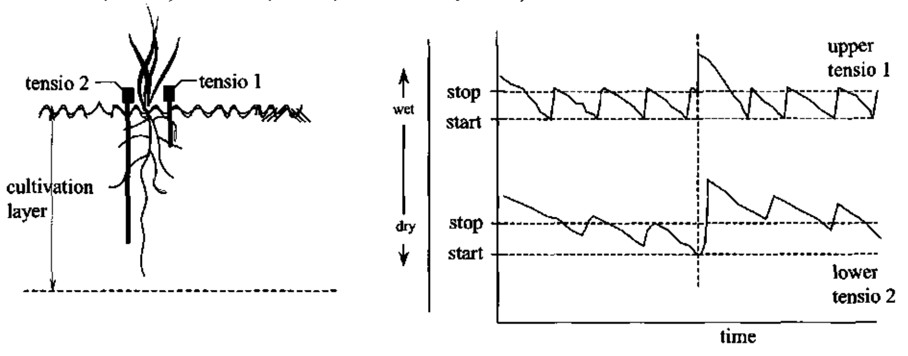

Figure 3 - Two tensiometers placed at different depths in the root zone (left). Changes of upper and lower tensiometers output signals as function of time (right).

2.2 Soilless growing systems

The reasons to put vegetables, flowers and fruits in sheltered or covered conditions - and control the application of artificial heating, lighting, CO_2, water and fertilisers - are found in boosting production, minimising labour cost and producing year round. Nowadays products are sold on a more and more exacting market, with the implication that pursue of high product quality - in all its aspects - is the major goal. Improvement of quality starts with the control of the production process, which includes climate, water and nutrients.

Especially in the field of water and nutrient supply, a lot of changes came about. One would expect that only in ancient times buckets and water hoses were used to water plants. Nevertheless, it is only since 1960 that automatic control of water supply and of supply of nutrients came about. Ranging from a simple electro-mechanical water supply clock with a relay operated valve multiplexer, to a more sophisticated analogue or digital integrator for solar radiation with programmable valve selection.

In the period from 1950 to 1958 research was carried out on soilless water cultures in Belgium and on gravel systems in The Netherlands, whilst in 1969 the first systems with rockwool as an artificial growing medium were introduced in the Scandinavian countries (Verwer, 1976). In combination with good functioning water and nutrient supply systems, rockwool - modified to accommodate plant production - proved to be a perfect medium for fruit-vegetable crops such as tomato, sweet pepper and cucumber. In The Netherlands the area with commercially grown soilless cultures in rockwool rapidly increased from 1975 and onwards (Verwer, 1976; Sonneveld, 1988). In 1993 the use of rockwool was estimated to be 70% for fruit vegetables and 24% for flowers.

From then on, adapting growing systems from soil-grown crops to soilless cultures could be observed in all major horticultural areas, since the major benefit of growing in artificial media - avoid the use of highly toxic chemicals to disinfect the soil - had become more than evident.

Additional reasons for the change were higher production, energy saving, stopping the spread of soil-born pathogens and a better control over growth and quality.
In 1999 approximately 4000 ha of vegetables and flowers are grown in soilless growing systems (KWIN, 1999). Almost all fruit vegetables (3000 ha) and a few flower crops (rose, gerbera, orchids and anthurium; totally 1000 ha) are grown on a rockwool (3200 ha) based system. In Belgium approximately 800 ha is grown on substrate (Van Os, 1999; van Os and Benoit, 1999). In Southern Europe, Spain is the leader in soilless systems with around 3000 ha (Heuvelink and Miguel Costa, 2000), France 1200 ha, Germany 600 ha and the UK 500 ha (Van Os, 2000). Outside Europe, Canada has an important area with more than 500 ha, Japan 750 ha and Korea 600 ha (Steiner, 1997).
Experiments at research institutes, experimental stations and at nurseries were supported by supplier firms to develop properly functioning growing systems and to learn to handle them and get familiar with growing crops in them. Problems that had to be tackled were:

- the lay out of the growing system,
- the kind and size of the substrate,
- the water supply system, e.g. capillaries, supply lines, tanks and pumps
- the control of the system, e.g. root temperature, the amount of supply water, the EC, the pH and the fertiliser recipe in the nutrient solution.

Soon, practical experience with artificial media in open systems showed drawbacks. An excess of water of 30% of the amount for crop transpiration is needed to rinse out the accumulated nutrients from the rockwool slabs and to even out transpiration induced variation in water uptake per plant. In open systems, the surplus of water and fertilisers runs off freely from the growing media and simply flushes into the subsoil. It has never been seen as a problem, until environmentalists awakened the general public, who forced the politicians to become aware of the negative aspects of pollution. Polluting effects of fertilisers on ground- and surface water and on the sub-soil aquifers became an issue. Since then, next to the more common quality aspects - like flavour, smell, colour, texture, tenability, firmness, etc. - the feature that the process of growing in itself should do no harm to the environment or in any other way endanger public health, is seen as a modern additional quality aspect. To fulfil this latter aspect, the traditionally open growing systems were forced to change into closed growing systems (Figure 2-⑤), often with an artificial growing medium.

2.3 Closed growing systems

When the introduction of closed growing systems started, nutrient film technique (NFT) was the only type of closed growing system available at a high technical standard. However, NFT never became very popular as a commercial system in practice, mainly because of the risks involved (spreading of diseases, no buffer).
In the years that followed, closed systems for many different types of crops were developed as a result of the increasing awareness of the environmental aspects of open systems. Simulation studies were performed for different groups of crops, investigating the economical, technical and environmental aspects of closed soilless growing systems (Ruijs and Van Os, 1991; Van Os *et al.*, 1991; Ruijs, 1994). These studies showed that each group of crops needs a growing system with crop-specific properties. To fulfil the demand for sustainability, materials and growing media had to be useable over a long period of time. The studies also showed that for a number of crops the economic prospects of growing in (closed) soilless systems were insufficient (e.g. chrysanthemum).

In the last years one can see a stabilisation in the development of new growing systems (Van Os, 1998). For the grower economic reasons gain again in importance, forcing a lower ranking in importance for environmental issues. Furthermore, the adaptation of legislation from sector to nursery is now apparent: each grower may have his own plan to fulfil the regulations, how the targets are reached is of less importance.
Registrations at nurseries affirmed that water and fertiliser consumption could be decreased dramatically (Vernooij, 1992). Nowadays guidelines are available for closed, sustainable growing systems that decrease pollution of ground water and surface water and avoid the creation of new waste flows (Van Os, 1994):

- materials should be low cost, have a life span of at least 4 years, have constant physical properties during use (resistant to steam-cleaning), be safe and be recycled by the supplier,
- substrates should be low cost, have a life span of at least 3 years, show no decrease in physical properties during use (resistant to steam-cleaning) and be recycled by the supplier,
- per plant or per substrate slab the growing system should have a separate drain water outlet to the mainstream drain flow (decrease the risk of spreading diseases).

Layout of closed systems
The technical layout of the growing system and the way the crop is placed in the greenhouse offers opportunities to classify a crop (Van Os, 1994).

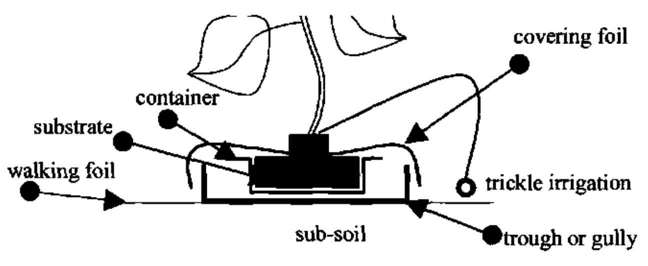

Figure 4 - Growing system with rockwool in container and trough

- Fruit vegetable crops with 2-6 plants per m^2 like tomatoes, cucumbers and sweet peppers. They are grown in multi-year usable substrates, e.g. rockwool, polyurethane foam. The slabs of growing material are enveloped in plastic foil or placed in long-shaped polypropene containers (Figure 4). The enveloped slabs lay in a flat or profiled polypropylene or coated-steel trough.

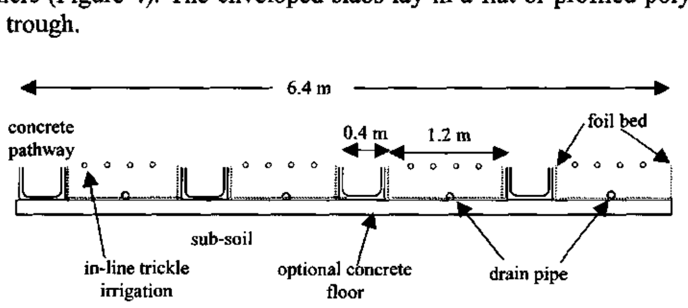

Figure 5 - Growing system with plants in beds and pathways in-between.

- Crops that are grown in 3-4 beds with pathways per 6.40m span, like carnations, freesias and alstroemerias. Upon a perfectly slopeless soil 1.00m - 1.50m wide beds are created,

made of 1.5mm - 2.0mm thick polyethylene foil, aluminium or concrete (Figure 5). The beds are filled with a loose substrate such as peat, sand, perlite or volcanic sands.
- Crops with many plants per m^2, such as chrysanthemums, lettuce and radishes. They are grown span-wide and need a system of dug-in polyethelene foil, with a loose substrate like sand, volcanic sand or perlite (Figure 6).

Latest developments show that only the first group of systems (Figure 4) is really in commercial use (Van Os, 1998, 1999), the others are too expensive (Figure 5 and 6). For the same reason there is no increase of the area of soilless growing systems anymore in the Netherlands. Government even adapted its legislation: when growing on substrates then in a closed system, whilst for some crops growing in soil is still permitted. However, leaching of nutrients should be minimised and the use of water should be more efficient.

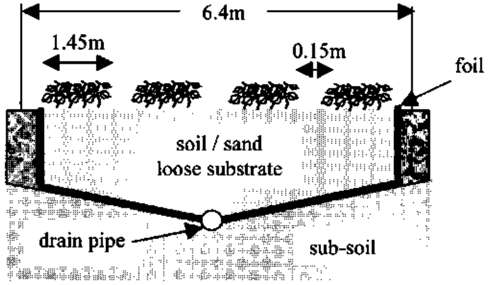

Figure 6 - Growing system with loose substrate

3. Supply systems

3.1 Clean water sources and water quality

An important part in a recirculating closed water supply system is the fresh water source. Dependent on water uptake, fresh water needs to be added to the already circulating nutrient solution. The quality of the fresh water depends on the concentrations of the dissolved ions, algae and residues. Sodium- and chloride content are the two most important quality factors of fresh water. These ions are hardly absorbed by the plants.
Chloride is taken up in larger quantities than sodium. Sodium will cause the first problems. In order to keep the cells free of damaging concentrations of sodium, the roots have a very efficient mechanism that 'pumps' the sodium out. However, this mechanism is not very efficient at high sodium concentrations and - finally - Na will accumulate to toxic concentrations for the crop. As a result, the roots will not be able to keep sodium out at high levels of sodium concentration. The concentration level at which this occurs, the 'Na damage threshold', is specific for each type of crop.

Table 1 - For various crops Na^+ uptake (in mmol Na^+ per liter water uptake) and Na^+ damage threshold concentration ($mmol \cdot l^{-1}$). Na^+ discharge (% of water use).

	Chrysanthemums	Cucumber	Tomato	Sweet pepper
Na^+ uptake [$mmol \cdot l^{-1}$]	0.2	0.8	1.0	0.1
Na^+ damage threshold [$mmol \cdot l^{-1}$]	8.0	6.0	8.0	6.0
Na^+ discharge (in % of water use)				
If rain water is used at 0.5 $mmol \cdot l^{-1}$ Na^+ content	4 %	0 %	0 %	7%
If tap water is used at 2.0 $mmol \cdot l^{-1}$ Na^+ content	23 %	23 %	14 %	32 %

Table 1 shows figures from the situation in practice for several crops. It shows that 100% circulation is not possible for all crops, even when good quality rain water is used. Rain water is captured and stored in a basin. When there is a shortage of rain water, even from the basin, the use of a mixture of rain water and tap water is common practice.
The iron content of the clean water source may differ between various types of sources (e.g. tap water in comparison to well water). It is an important factor, especially in trickle irrigation systems, where - due to the pH difference between the fresh water and the irrigation water - iron may cause coagulation and blockage of the capillaries.

3.2 Water supply

Plants grown in protected cultivation, in a closed growing system, are deprived of natural water supply (e.g. rain or natural water table) and hence require artificial supply of water and nutrients. Different systems of growing a crop require different methods of watering, only some of which are suitable for adding nutrients (e.g. nutrient film technique, trickle irrigation). In greenhouses conventional irrigation, sprinkling and spraying techniques are in use, (like: overhead sprinklers, mist and fog supply systems, low level sprinklers and trickle irrigation systems, capillary action), of which only the last three are suited for nutrient supply.

In closed growing systems water is the transport medium for nutrients. Either, the growing system contains a substrate to support the roots of the plants (like: rockwool, perlite, glasswool, peat, sawdust, etc.), or the plants stand bare rooted in gullies, troughs or containers (like: NFT, Aeroponics, Plant Plane growing system, Deep Flow growing system, Ein-Gedi growing system) (Gieling *et al.*, 1996). When present, the growing medium serves as buffer for water and nutrients.

Time delays in the supply system

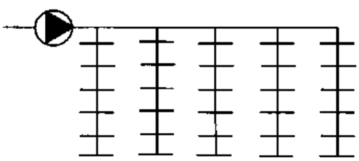

Figure 7 - Water supply lines with pump and capillaries to feed individual plants.

The time delays in the water supply lines in a greenhouse are mainly caused by the time it takes the water to move through the pipes from capillary to capillary. It may take more than 30 minutes for any molecule (water molecule or ion) injected at the water injection point to reach the last capillary (Figure 7). This delay is important for a specific particle (i.e. ions) or property of the water (temperature, colour). In relation to just water molecules, it holds that an amount injected at the inlet will instantaneously cause the same amount to leave at the capillaries because of the incompressibility of water. So, delay time for water supply is mainly found in the substrate, gully and the mixing tank. Changes in ion concentration at the injection point will be subjected to both the delay times in travelling from injection point to delivery point at the substrate (capillary) and the delay time in the substrate. Chapter 2 deals with the problems related to this subject and suggests a special layout of the supply lines.

Scheduling of supply

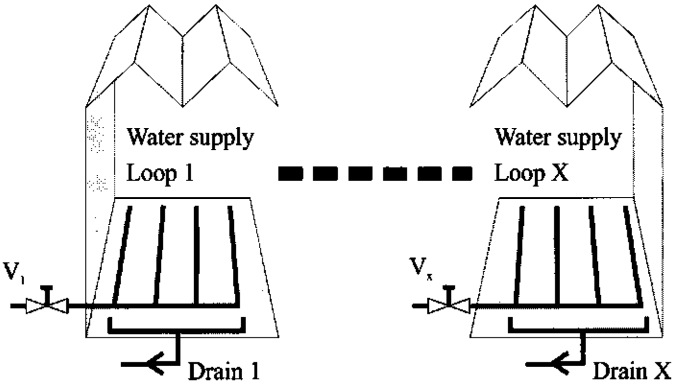

Figure 8 - Layout of {1...x} number of supply loops. V_1..V_x are on/off valves

It is common practice that in large area greenhouses (> $3000m^2$) the supply system for water or nutrient solutions is split up in several supply loops, each controlled by a valve (Figure 8). The nutrient diluter and dosing system is time-multiplexed over these valve-operated loops. As a consequence opening that specific valve will only activate each of the loops whilst all the other valves are kept closed. Time multiplexing of the supply loops consequently implies that the delivery of nutrient solution to the plants is done as a supply pulse. The supply pulses are either modulated in their repetition frequency with a fixed pulse width or at a fixed repetition frequency with a modulation of the pulse width. During the off time, the other valves are sequentially activated.
Supply of nutrient solution is controlled based on a set of parameters. It is good practice that the grower has some optional settings available to influence the behaviour of his equipment. For reasons of easiness of handling, the grower only needs a limited set of choices to make and parameters to enter. An example of a set of options is given below:

1. The next start of the supply cycle is controlled based on a fixed (but user defined) time of day, with a fixed (but user defined) duration of supply time for each supply loop controlled by a separate valve.
2. The next start of the supply cycle is determined based on a fixed (but user defined) time of day. The duration of water supply for each loop is dependent on a model $\Psi(RH, \Phi_g)$ or on a constant amount of drain. (RH = relative humidity, Φ_g = global solar radiation)
3. The next start of the supply cycle is delayed based on a model $\Psi(RH, \Phi_g)$ or based on the amount of drain. The time duration of water supply pulse for each supply loop is dependent on a fixed (but user defined) time period.

A design intended for application in practice should take into account these constraints and incorporate optional settings for at least one of the two opportunities from Figure 9. Preferably option c, since with option c fixed time scheduled operation of the valves is possible. If water is supplied in pulses to a growing system, the control action cannot resolve more time-related details than is determined by the time difference between two pulses.

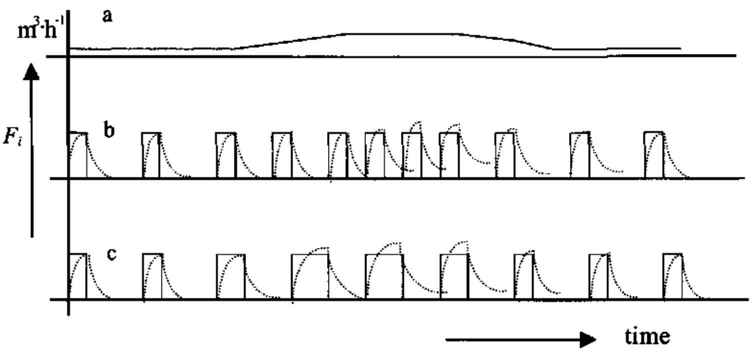

Figure 9 – Supply flow F_{in} [m^3·h^{-1}] as time-multiplexed supply pulses.
Continuous line in b and c is excitation, broken line is response:
a time average, both for b) and c) the same,
b fixed pulse width, modulated repetition rate,
c fixed repetition rate and modulated pulse width.

According to the reasoning in Chapter 4, it is favourable to control the flowrate of the drain-water. However, pulses of solute applied to a growing system will result in an almost first order reaction (Figure 10). In a concept aimed at a controlled flowrate, an exact description should be given to define which flowrate it is that should be controlled. During the design procedures and tests that were carried out for the research as basis for this thesis, the mean value during the time of one supply cycle was taken as the value to control. In other words, the flowrate averaged over the time between the start of one supply pulse and the start of the next supply pulse. It implies that the drain flow signal has to be averaged between the start of two subsequent pulses. The specific accumulated flow value and the time to average over is only known at the moment the next pulse starts.

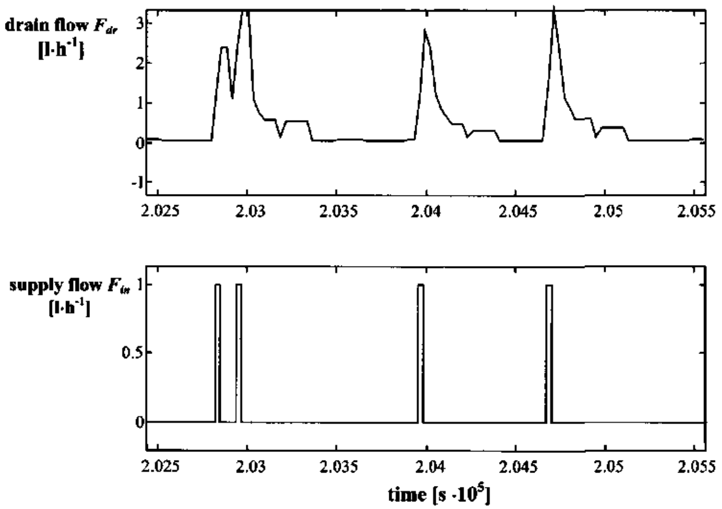

Figure 10 – Actual measured response of the drain flow F_{dr} of 4 plants in a short measuring gully on excitation with a supply flow F_{in} that is modulated both in pulse width and pulse repetition rate. Pulse one and three are of the same duration, but shorter than pulse two and four, which again are equal in time duration.

3.3 Nutrient application, state of the art

In practice there are two different approaches in processing water and nutrients, before supplying it to the plants: a system with a mixing tank unit and a system with direct fertiliser injection unit.
Both systems are commercially available as so-called A/B-dilutors or as a dilutor of simple fertilisers. Nutrient concentrates are added automatically, either from liquid stock fertilisers or from A/B tanks containing dissolved powders in 100-fold concentration. The EC value, measured in the nutrient solution supplied to the plants, is used as the controlled variable and is kept at a value of approximately 1.5 and 3 [$dS \cdot m^{-1}$]. Metering pulsating pumps (or pumps in combination with accurate flow sensors) add nutrient ions until the desired EC level is reached. An additional acid or lye is supplied to keep the pH value of the supplied nutrient solution within the range of approximately 5.5-6.5.
However, using EC as feedback signals has as disadvantage that it is a measure for the total salt content and does not provide information on the concentrations of individual ions. To overcome this drawback, it is common practice to have the recirculating water analysed by a lab each fortnight. The lab suggests the optimal mix of the different fertilisers for the next 14 days and the grower adjusts accordingly the composition of the A/B storage solutions or the recipes supplied by the simple liquid dilutor.
Occasionally, the solute recirculating in the closed growing system is flushed to remove unwanted (or unused) ions that would otherwise build up and have a toxic effect on the crop. Toxic effects are postponed by a good water quality, a good quality of the stock fertilisers, by mixing the nutrient solutions in the correct proportions and by timely dispose of unwanted ions that did accumulate in the recirculating solute. The balance between the nutrients in the recipe is of importance. Nutrients with a single valency like ammonium, potassium and nitrate are more easily taken up than nutrients with a double valency like calcium, sulphate and magnesium.
The concentration of some nutrient ions should be limited at a maximum level, which is specific for each crop and each ion. The production of the crop may decrease when the limit of the concentration of the individual ions is exceeded. An EC measurement does not provide information on concentration of individual ions, which may be seen as a big drawback of the present situation in practice.
In some situations, the recirculating solution is heated to maintain a constant temperature to ensure that root temperature is near to optimal for the plant.

A/B systems
The A/B-dilutor is the most common practice at this moment. It consists of two tanks (an A-tank and a B-tank), in which standard solutions are made at a concentration hundred times the normal concentration needed for the plant (Figure 11). An optional third (and fourth) tank is filled with an acid or a base to control the pH. Sulphate and phosphate should not be dissolved in the A-tank. Calcium and iron-chelate should not be dissolved in the B-tank. This partitioning is strict, otherwise calcium-sulphate, calcium-phosphate and magnesium-phosphate will precipitate due to a too high concentration in both solutions. The solutions in the tanks may consist of liquefied solid fertilisers (powder salts) or single or simple element liquid fertilisers.
Solid fertilisers are sold in large bales and therefore quite a physical effort is needed to make the required solutions. The dust produced during handling is very bad for the grower's health. Solid fertilisers are polluted with ballast or carrier material, which is not taken up by the crop and may cause problems in recirculating systems. Accumulated ballast material in the irrigation water may coagulate and block the trickle irrigation nozzles.

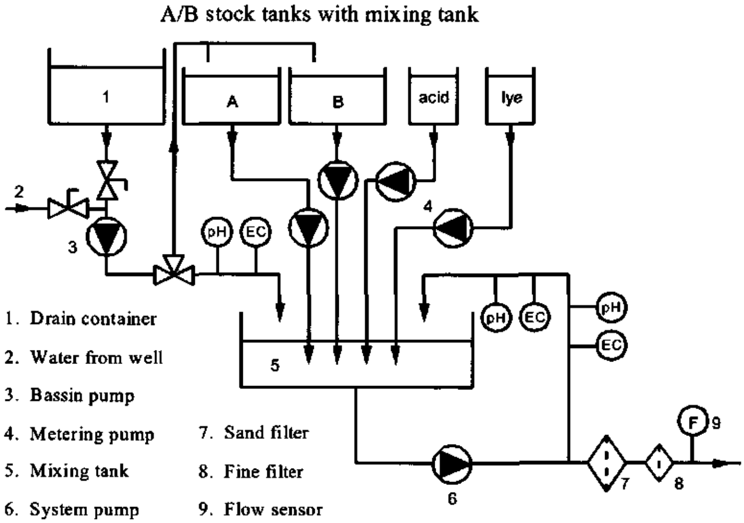

Figure 11 - Layout of a supply system with A/B stock solutions and a mixing tank.

A/B supply with a mixing tank: when a mixing tank unit is used, all the fertiliser sources (A/B or single element) and the water streams (clean water and return water) flow into the mixing tank. The composition needed for the crop is fixed in the A/B recipe, in the relative amount of each single nutrient ion.

The irrigation solute is then taken out of the mixing tank and brought into the system by means of a system pump. The mixing tank serves as a buffer between the fertiliser and the irrigation water, which makes it less sensitive for disturbances (Figure 11).

This is an advantage over direct injection. However, buffering has the disadvantage that a quick response on a change in setpoint is no longer possible. First the buffer has to be emptied before a solution with a different composition can be prepared. On the other hand, the mixing process in a mixing tank is less susceptible to an unsteady flow.

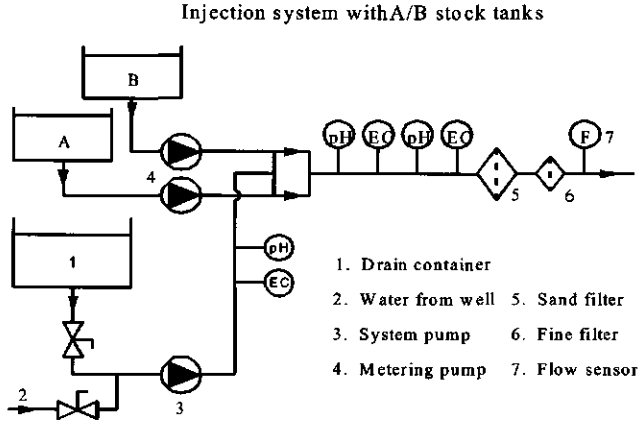

Figure 12 - Layout of a supply system with A/B stock solutions and direct injection of A/B fluids.

A/B supply with direct injection: when direct injection is used (Figure 12), the A-B fertilisers are separately injected directly into the water supply pipe. Direct injection does not use a mixing tank. The mixing has to take place in-line with the supply pipe itself, by means of a static mixer.
Direct injection is very sensitive to disturbances. A change in flow rate has a direct effect on the addition of fertilisers. Also, bicarbonate in the recirculating water will react with injected fertilisers. This process takes some time, which causes the actual pH level in the capillaries to differ from the pH level directly after injection.

Simple element injection

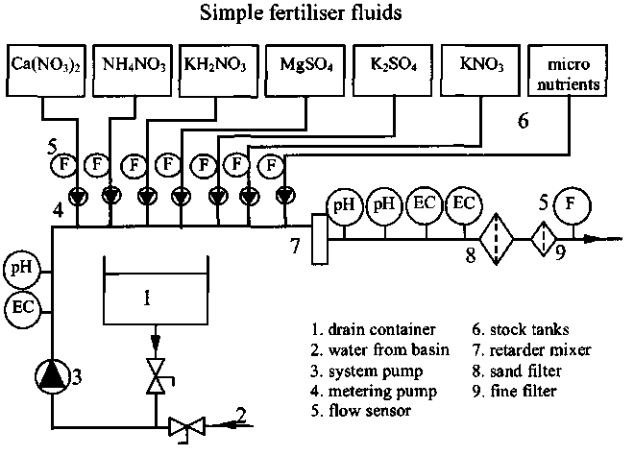

Figure 13 - Layout of a supply system with injection of single element stock solutions.

Simple element fluid fertilisers are highly concentrated and pure (Figure 13). Extra precautionary safety measures have to be taken because of the high concentration of the fertilisers.
The advantages of liquid fertilisers are to be found in the little workload and the capability for easy and precise automatic dosing. Since the equipment is in contact with highly concentrated acid and lye fluids, the high susceptibility to failure of the equipment and the high service costs is a disadvantage. Injection of the fertiliser fluids is done in different ways:

- a venturi system, where the main pump builds up a pressure drop over a restriction (venturi) in the main supply pipe. This pressure drop is used to suck the different fertiliser fluids through a flow meter into the water stream. The value of the pressure difference is a problem for some fertilisers, since it may degasify the fluid. The nutrient-enriched water is either pumped into a mixing tank or is used as the main water stream to supply the plants directly.
- peristaltic pumps, gear pumps, piston pumps or rotating piston pumps without valves are used to pressurise the fertiliser fluids and inject it into the main water supply stream. Here a flow meter is not needed since the amount of injected fertiliser is linear with the rotation/pulse frequency of the pumps. Most of these pumps need inlet and outlet valves - often consisting of a spring-loaded ball - to handle the different pressurise and suction phases. The spring and the ball easily wear out, especially in the highly concentrated acid and lye fluids. All direct injection systems need a static retarder to mix the fluids. The order in which the fluids enter the main stream is of importance, since it might come to a reaction between the highly concentrated fluids. They may then crystallise, precipitate and block the supply pipe and/or capillaries.

Control of nutrient application

In most commercial available control systems that apply water and nutrients in closed growing systems, nutrient application is controlled by means of a feedback of the total salt content in the supplied solution by means of measuring EC (Electrical Conductance). The pH value of the supplied water is checked with an on-line pH sensor and compensated, either by means of adding an extra amount of lye or acid from the concentrated simple stock solutions (Figure 13) or in A/B systems by adding an extra acid or lye from a special tank (Figure 11).

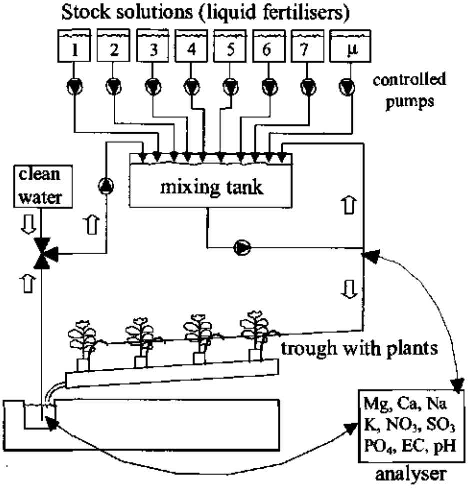

Figure 14 - A dispenser system for liquid fertilisers, with mixing tank and ion specific sensors.

When using closed loop systems, a few essential points are evident:

- The plant is selective in absorbing nutrients and/or water from the solution (Chapter 2). The nutrient supply system uses a mix of return water, supplementary pure water with varying quality over time and stock fertilisers. It implies that the concentration of each ion in the mixture of return water and clean water has to be determined to know how much of each specific nutrient ion needs to be added for a new recipe (Figure 14).
- Some ions are not absorbed or only slowly absorbed by the plant, e.g. sodium and chlorine. The "clean" water that is added again and again often contains considerable amounts of these unwanted ions. Hence, the concentration of these ions in the irrigation water tends to rise gradually as a result of ongoing accumulation. Consequently, sodium and chlorine concentrations have to be monitored, to check if (and when) they become toxic.

3.4 Design of an ion specific nutrient dispenser

Changes in ion concentration

In order to demonstrate the need for measurement and control of individual ions rather than EC feedback of total salt content, below some results of monitoring concentration of individual ions are presented in Table 2 and in Figures 15 and 16.

During three weeks samples were taken from the supply and drain of a tomato crop grown on rockwool with a closed loop nutrient supply system. Feedback control was established by measuring the EC and pH of a mixture of drain water and clean water. During one day, every hour samples were taken from the supply water and the return water. Sampling started at

07.00 h and ended at 19.00 h. During twelve days, three samples were taken every day, at approx. 09.00h, at 12.00h and at 17.00h from the supply water. In these samples PO_4^{3-}, NO_3^-, SO_4^{2-}, NH_4^+, K^+, Ca^{2+} and Mg^{2+} were measured afterwards, using different laboratory type of measuring techniques, like flame photometer, HPLC and spectro-photometer. Values for supply flow and drain flow were not established.

Since the flow values of supply and drain have not been established, the data can neither be interpreted quantitatively nor can it be used to determine the transfer of the controlled system for water supply or for nutrient application. It only allows for a qualitative approach. Remarkable changes during one day are shown by the graphs of Figure 15 and 16. It was not established, whether instabilities in the control system, changes in nutrient uptake of the plants or irregularities in preparing a new mixture for the stock solutions caused this phenomenon. In either case it is an indication that the controllers, as they are found in this kind of commercial nutrient supply systems, are not able to cope with these disturbances in the ion concentration. In the first place not the daily fluctuations (Figure 16) and in the second place not the long-term drift (Figure 15). The above remarks indicate that improvements in the controller part of the nutrient supply system are necessary. A direct feedback loop on the concentration of the different ions may solve some problems. However, this needs direct on-line measurement of the concentration of each ion involved. Although promising developments in ISFET technology (Ion Selective Field Effect Transistor sensors, to be called 'Isfet') are immanent (Chapter 3), it is expected that it will take some years before all macro ions can be measured individually. It indicates the need for models or algorithms, which correlate the uptake of non-measurable ions to measurable ions or other measurable variables.
The data of the return water (Figure 16) indicate that some of the ions have reached almost complete depletion. From a point of view of 'uptake compensation' this is not an ideal situation. Furthermore, the growing system in use here consists of NFT with plants in 10 x 10 cm rockwool seedling blocks in gullies. It does not have rockwool slabs as buffer in the gullies and - for this reason - will react much faster to disturbances. According to Bailey (1988) NFT systems may react in less than 25 minutes, which is fast compared to systems with substrate slabs.
At the time the measurements were carried out, the root system of the plants was fully developed. Together with the seedling blocks it influences the hydrodynamic behaviour of the growing system considerably and is the main cause of the time lag. In both cases - NFT or full rockwool system - the hydrodynamic characteristics of growing systems with trenches or gullies changes as the root system develops. In designing feedback control loops for the different ion concentrations, one should take into account these changing hydrodynamic time lags. One way of dealing with the changing parameters or perturbations of the controlled process, is in designing the controller according to a set of robust criteria.

In Chapter 4 an attempt is made to cope with this kind of perturbations, and design the controller by using the 'robust design' method (Doyle *et al.*, 1992). With the robust design method, a whole class of system models can be controlled based on a controller that has been designed for the nominal model. Robustness in control distinguishes between robust stability and robust performance. In this particular case, the robust design method deals with uncertainties in the model description of the real process, i.e. variability of the flow and seasonal changes of the models. Loopshaping is used as a design tool for the controller. This way of designing the controller takes into account the uncertainties mentioned above and a desired performance.

Table 2 - A Concentration of 6 ions from samples of the supply water during 15 days in August 1990. B Concentration of 6 ions measured on the 24th of August 1990. The first 13 lines show data from the supply water samples. The second 13 lines show data from the return water samples.

A	8 - 23 August 1990							B	1990 Aug 24						
Date dd	time hh.mm	K	NO3	PO4	NH4	Mg	Ca	time hh	K	NO3	PO4	NH4	Mg	Ca	
		mg·L⁻¹							mg·L⁻¹						
8	9.20	218	1180	160.00	32.90	38.23	221	7	164	576	32.70	2.70	13.29	103	
8	16.35	220	1180	165.00	29.20	38.40	202	8	156	558	25.40	3.79	12.25	95	S
9	9.10	220	1090	165.00	26.00	38.57	185	9	148	531	22.60	3.43	11.81	97	
9	16.10	240	1180	179.00	28.20	41.83	202	10	118	545	12.20	1.23	10.68	92	U
10	11.55	88	788	1.01	0.10	23.54	166	11	124	571	13.80	2.97	10.63	91	
13	10.45	100	749	1.25	0.00	20.11	158	12	154	580	25.50	3.77	11.56	91	P
13	17.00	102	740	1.29	0.03	20.32	160	13	176	620	33.20	4.22	12.26	91	
14	9.15	110	793	1.38	0.00	21.64	165	14	184	606	37.10	4.44	12.61	90	P
15	9.45	108	761	0.73	0.07	21.03	166	15	184	664	35.40	4.35	12.65	93	
15	17.00	104	704	0.55	0.08	19.04	154	16	180	638	32.50	4.02	12.65	94	L
16	9.45	104	735	0.73	0.00	20.04	158	17	182	638	32.40	3.51	12.66	94	
17	9.00	108	700	0.86	0.07	19.01	153	18	180	633	32.80	3.72	12.62	94	Y
17	16.50	104	696	1.38	0.03	18.98	151	19	170	633	29.80	4.04	12.39	93	
18	9.00	106	638	2.33	0.19	15.66	130	7	134	616	1.74	0.08	13.21	112	
20	11.00	108	647	0.77	0.04	15.91	133	8	136	607	1.62	0.30	12.92	112	R
20	16.30	112	665	0.86	0.05	15.61	131	9	138	687	1.59	0.28	12.83	114	
21	8.30	116	669	0.55	0.04	16.06	134	10	138	647	1.50	0.32	12.83	111	E
21	12.00	118	651	0.86	0.01	15.41	129	11	140	660	1.38	0.33	12.88	110	
21	16.45	120	647	0.95	0.10	15.51	128	12	142	664	1.32	0.09	12.52	110	T
22	8.15	122	656	1.96	0.01	15.26	126	13	140	673	1.59	0.37	12.58	110	
22	12.00	122	638	0.77	0.08	15.48	127	14	140	660	1.47	0.76	12.64	109	U
22	16.00	122	638	1.22	0.08	14.96	124	15	142	638	1.99	0.57	12.59	109	
23	8.30	120	616	0.92	0.01	9.02	116	16	146	656	2.94	0.66	12.48	108	R
23	12.00	118	607	0.64	0.06	7.25	113	17	146	682	2.54	0.59	12.62	109	
23	16.00	118	602	0.95	0.12	12.72	109	18	150	669	3.18	0.58	12.99	110	N
								19	152	700	3.55	0.17	12.92	112	

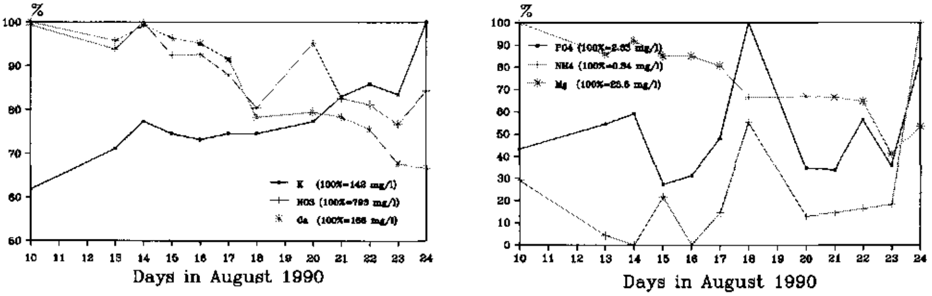

A B

Figure 15 - Long term variations of concentration of ions measured in supply water in % of maximum value according to Table 2-column A.

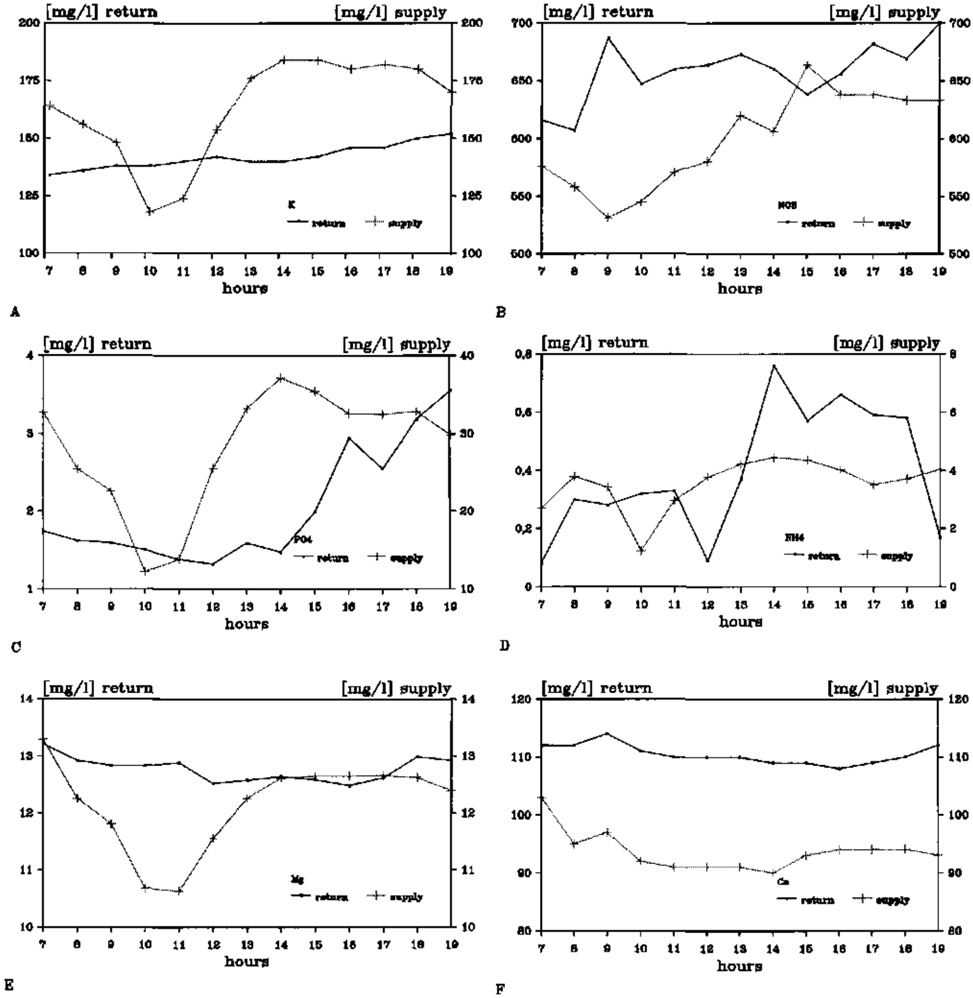

Figure 16 - Concentration of macro ions measured in the supply and drain of a closed growing system, according to Table 2-column B.

3.5 Aim of the thesis

The main controlled variables in the process at hand are in the drain (Figure 17). As long as the value of the drain flow is measurable, from a point of view of control technique alone, there is no real reason to take a specific value. So its value can be chosen freely to fit to the demand of the plant and the needs of the physical processes in the substrate.
There is no reason to assume that the absolute value of the drain flow has an influence on the physiological processes or even the water uptake process. It implies that the absolute value of the drain flow can be chosen to comply with constraints in the system, i.e.: the amount of drain needed to flush out accumulated ions from the substrate or minimum flow requirements set by the inaccuracy of a low-cost drain flow sensor.

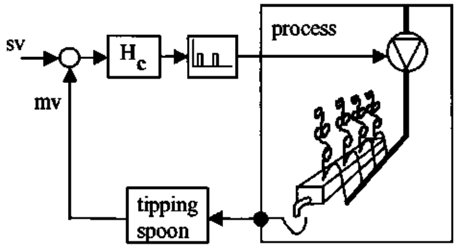

Figure 17 - The controlled process of drain flow, kept constant at the set value (sv).

In contrast, the set value for the EC of the bulk solution does have an influence on the physiological processes in and around the roots. Since EC is the result of total salt content and consequently from all ion concentrations together, the absolute value of EC and concentration of individual ions does have a distinguished physiological meaning. The set values for the drain concentration of each individual ion is not free to choose, because of the relation between the bulk concentration in the substrate slab, the concentration at the root surface and the drain concentration (Chapter 2). Root surface concentration of some ions on itself - and drain concentration in relation to it - seems to be of importance to the physiological processes in the plant, in particular the growthrate. The set value of the drain concentration should be related to it. These considerations lead to an overall block diagram of the controlled process (Figure 19).

Demand compensation

During crop production, the major aim of the nutrient solution supply process is to supply the amount of water and nutrient ions to the plant's needs, i.e. to fulfil its demand for evaporation and growth. Another aim can be the sub-optimal supply of nutrients to introduce opportunities for quality steering, i.e. only fulfil say: α x demand, where $\alpha<1$. If water is supplied to such an extend that an amount of drain water (being the water that is not used by the plant) exists, this amount and its specific nutrient content can be measured and used in a feedback control system. At least a measurable amount of drain water should be available under all circumstances in order to be able to establish the uptake at each moment. The control system can be designed to control the water supply to exactly compensate the plant's uptake, by keeping the drain flow - or drain concentration - constant (Chapter 2).

Viewed in this way, the water uptake and nutrient uptake of the plant is a disturbance of the 'constant drain flow process'. In order to keep the drain flow precisely constant, a tight feedback control is needed. A large time constant or dead time can harm proper functioning of this controlled process. These time constants are found in the measuring loop (flow back of drain to the water treatment area) and in the solution supply loop (mixing tank, supply lines and drippers and substrate).

Speaking plants on a measuring gully

In order to overcome the problems related to the big time delays in the measuring loop (Kupers *et al.*, 1992) the idea was introduced of using a 2.5m long measuring gully that contains approx. 8 plants.

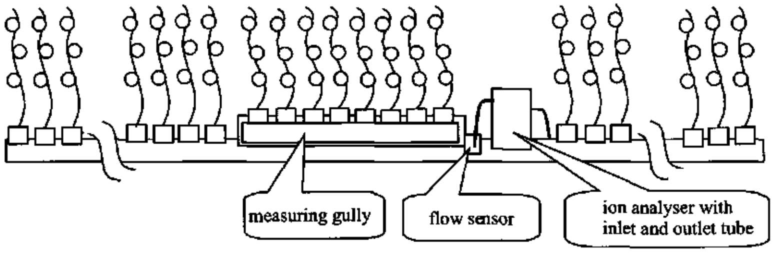

Figure 18 - One row of a canopy of plants on a trench with measuring gully, ion analyser and flow sensor

The measuring trench or gully is used to measure drain flow and drain concentration of one valve controlled greenhouse section (Figure 18). A measuring gully - installed in the middle of one of the crop's rows - can be used as a monitoring device for the water relations of the whole crop in that valve controlled section, just like a 'measuring box' with temperature and humidity sensors represents the climate of a complete greenhouse compartment. The supply of the plants in the measuring gully is from the same supply line as all the other plants in that row. During the research for this thesis, the measuring gully was considered to be a good enough representation of the overall uptake process of the valve-controlled greenhouse section. Here, it was assumed that the rest of the valve-controlled section would be adequately served, if the plants on the gully were adequately served. Commercial controller equipment is already available that uses this kind of set-up. However, before introduction in practice on a large scale, it should still be proven that the suggested relation is valid. Then also the question should be answered how many plants are needed on the measuring gully to be a good enough representation of the whole valve-controlled section. The plants in the gully can be monitored even more thoroughly. Extra sensors (like sap flow, water uptake, evaporation, water potential and turgor of the leaves, change of fresh weight of the whole plant and photosynthesis) give opportunities for more direct data input in models that predict the plant's short term behaviour. The gully itself may even be constructed as a weighing device (Bruggink *et al.*, 1988; Stanghellini, 1987; Van Meurs and Stanghellini, 1991; Gieling and Schurer, 1995a&b, Van Ieperen, 1996).
The advantage of using a short measuring gully is found in the relative short delay times between the outflow of drain from the substrate slab and the place where the drain flow is measured. In this way the dead time of the trenches, which lead the drain back to the water treatment area, is cancelled out (Chapter 2).
Some models that are used in predicting uptake of nutrients by the plant may need data on solution flow to the plant and on drain flow from the plant over the same corse of time, with a short as possible time delay between them. The effects of this type of delay time on the interpretation by models of the measured data of the inlet concentration in comparison with data of the drain concentration, may be overcome by measuring the inlet concentration just at the capillary in the measuring gully. So the ion analyser equipment needs at least two fluid input channels, one for the drain concentration and one for the input concentration of the measuring gully (Chapter 3).

The controlled process
The process to be controlled is taking place in the substrate. Here, in the substrate, the problems are situated. In words it is best described as: how to manipulate the supply of water and nutrients in such a way that the plant's demand can be delivered to the root system by the substrate and *avoid limiting situations* in regard to water uptake and nutrient ion uptake.

The ultimate goal of the control actions, as depicted in Figure 19, is to keep drain flow from the substrate and the concentration in the drain at a constant set value. In doing so, the demand of the plant is satisfied by compensation of the plant's uptake from the substrate, where the plant's uptake is merely treated as a disturbance of the controlled process in the substrate. The very purpose of this thesis is to elucidate the steps needed in the development of such a system.

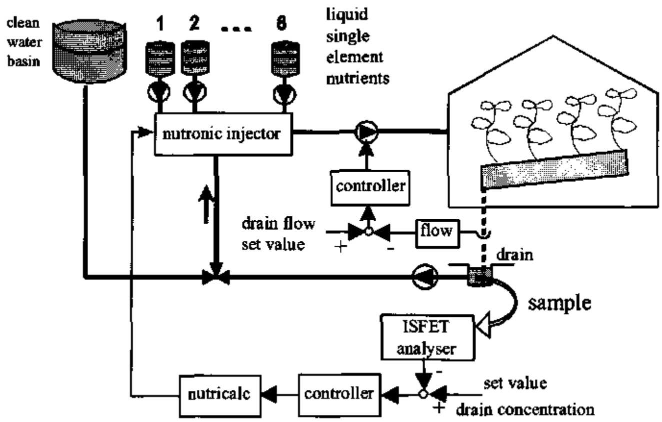

Figure 19 - Block diagram of the controlled system. Drain flow is controlled to be equal to a set value, by measuring the drain flow from a model gully. Drain concentration is measured in a sample from the model gully drain and controlled to be equal to a set value.

The concentration controller generates a new recipe vector that consists of new concentrations for all ions. A program (NUTRICALC® in Figure 19), which uses algorithms from mixture theory, generates the time duration values needed to activate the valves for the addition of liquid fertiliser fluids by the injection unit in the main solution stream (Schrevens and Cornell, 1990). The program takes into account constrains to avoid precipitation due to crystallisation reactions and rules to select supply for some ions from multiple sources. Radiation can be used as a feed forward control action to cancel out delays in the chain from transpiration to uptake (Chapter 4).

Feed forward control

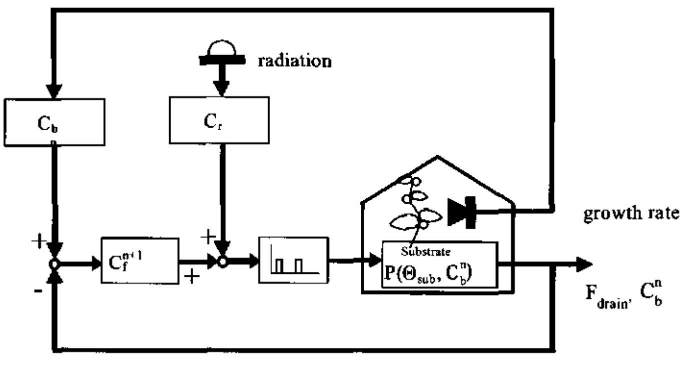

Figure 20 - Diagram of feed forward control. Θ_{sub} is the substrate humidity and C_b^n is the vector of the concentrations of *n* nutrient ions in the substrate. F_{drain} and C_b^n are the output variables. C_f^{n+1} is a vector of *n+1* SISO controllers, one for water supply and *n* for nutrient application. C_r is feeding forward radiation on water supply and C_p^n determines the set values of *n* ion concentrations in the substrate.

Information from the plant (i.e. growth rate) is used to adjust the *n* set values of the *n* ion concentrations (Figure 20). However, model based control, that uses plant physiological models supported by sensor signals from the real world (Speaking Plant Concept) and describes the relationship between controller actions and climate- and root environment related variables, is on itself not a subject of the research efforts described in this thesis.

3.6 Epitome

New developments in practice-oriented closed growing systems need an automatic nutrient dilutor/dispenser that can prepare the irrigation solution in accordance with the pre-calculated composition per ion for each new cycle of supply water. It is a prerequisite that affordable and reliable techniques become available for measuring the concentration of each nutrient (Chapter 3). An automatic nutrient dispenser should consist of five essential elements (Figure 14):

- Technology to keep in stock and dispense eight highly concentrated liquid fertilisers. Often two ions (e.g. $Ca\text{-}(NO_3)_2$) are coupled in one nutrient stock fertiliser. Controllers should include algorithms for the calculation of the amounts of concentrated stock fertilisers to add, for the next recipe. Extra attention should be paid to the aspect, whether MIMO (Multiple Input Multiple Output) or SISO (Single Input Single Output) controllers need to be applied (Chapter 4).
- Both a mixing tank and metering pumps to dilute the stock fertilisers with pure water and return water; in case the stock fertilisers are directly injected in the main stream of the solution, suitable injection equipment and retarders are essential.
- Sensors to measure the concentration of individual ions, EC and pH in the supplied solution and in the drain solution. The use of ion selective electrodes in practice is primarily hampered by the problems encountered with these electrodes, however, developments in Isfet sensors are promising (Chapter 3).
- Software for measurement, communication and control. The control software should contain adequate control algorithms to cope with the time delays in the real-world systems and with the perturbations of the models (Chapter 4).
- Dispensing technology to multiplex the expensive dilutor equipment over a number of compartments and transport the solution with short as possible delays to the individual plants. Since the main process of interest for control takes place in the substrate, attention should be paid to the question: is the substrate able to deliver, in time, the water and nutrients to the root system according to the plant's needs and the grower's intention (Chapter 2).

CHAPTER 2

TRANSPORT OF WATER AND NUTRIENTS

§2.1 THE STANDARD WATER SUPPLY SYSTEM

§2.2 FLUID FLOW IN A SET OF SUPPLY PIPES

§2.3 ANALYSIS OF SOLUTE MOVEMENT IN INERT SUBSTRATES

§2.1 The standard water supply system

Based on:
The dynamic behaviour of salinity changes in a closed NFT growing system. In: *Acta Hort. 361*, pp 218-225.
Th.H.Gieling, J. Bontsema and L.J.S. Lukasse, 1994.

1. Introduction

Plants in modern greenhouses receive water and nutrients from a diluter of chemical solutes. To recapitulate: supply lines of a trickle irrigation system dispense the nutrient solution by means of thin capillary hoses, connected to the supply lines at equal distances, to each individual plant. The drain from the plants returns into a small pit. Whenever the level in the small pit reaches a pre-set value, a pump transports the solution to a drain reservoir. Dependent on the type of growing system - either a NFT or a substrate system - the drain will run-off immediately or it will linger for some time in the substrate mat. In a closed system for water and nutrient supply, the drain water is mixed with clean water for reuse.

Almost all of the water taken up by the roots passes through the plant and evaporates from the leaves in the process of transpiration. The remaining water is retained by the constituent parts of the plant and removed when the crop is harvested, leaves are removed or the plants are destroyed and moved out of the greenhouse at the end of their productive live.

Transpiration plays on important role. By evaporative cooling, it prevents the leaf temperature from going too high. Furthermore, as sap flow it serves as a means to transport nutrients to the different plant organs. Yield reductions are linked with low transpiration, e.g. because the latter creates nutrient deficiencies. An increase of water supply causes extra drain flow, which reduces the build up of salts in the rockwool. However, supply of too much water creates an abundance of drain water that has to be cleaned before it can be reused. A costly process that should be minimised, if minimisation does not introduce limitations in uptake of water or nutrients.

To define an effective control strategy for water supply, it is necessary to be able to predict how transpiration depends on the climatic conditions. Direct measurements of transpiration are difficult to achieve, particularly in commercial situations. Paragraph 2.2 section 2 gives an overview on some of the transpiration models that are in use in climate control practise in greenhouses.

Although the forcing factors for water and nutrient uptake are in transpiration and growth, the process to control in relation to water supply and nutrient application takes place in the growing medium in the root zone. Water, as a means of transport, substrate or soil as a growing medium and - in case of NFT - water as a growing medium, will have to be able to fulfil the demand of the plant. Therefore, both in NFT growing systems as in substrate growing systems, this area needs to be well described.

When a NFT system is in use, a certain amount of the water supplied to the plants will seep through the bare roots into the gully underneath. When flowing back to the return pit, the drain water will contact the root system of subsequent plants in the gully. On top of the supply

from the capillaries, the drain water from preceding plants will make additional water and nutrients available to the plants downstream in the gully.
In order to gain some insight, Paragraph 2.1 section 2 provides an illustration of the problems related to the dynamics of a closed system (responses, residence time and time delays). In relation to the capillary index number, it describes the residence time at a capillary hose position along the length of the supply line in a preliminary model. Measuring EC [$dS \cdot m^{-1}$] at some distinct positions in the gullies validates this model.

A growing medium like soil or artificial substrates (e.g. rockwool slabs wrapped in plastic foil) does react quite differently than an NFT growing system. Heinen (1997) developed a model for simulations in relation to water and nutrient status in soils and in artificial substrates. His model provides outputs for a standard Dutch rockwool substrate growing system during the growing season of a crop. For control purposes, however, one needs to know the true dynamic behaviour of water- and nutrient related state variables in all parts of the growing system, whether it is in the installation tubing and supply lines, the gully, the storage tank, the trickle irrigation system or the substrate itself.
Paragraph 2.3 starts a discussion on the dynamics in the flow of water and nutrients through the substrate, in relation to the most important disturbance of the controlled process in the substrate: the uptake of the plant.

2. Illustration of supply tube and return channel behaviour

This section illustrates problems - related to supply and drain - encountered in practise oriented closed growing systems, by some popular hydraulic relations as a preliminary model on the delay times and residence times in the supply tubes and return channels.

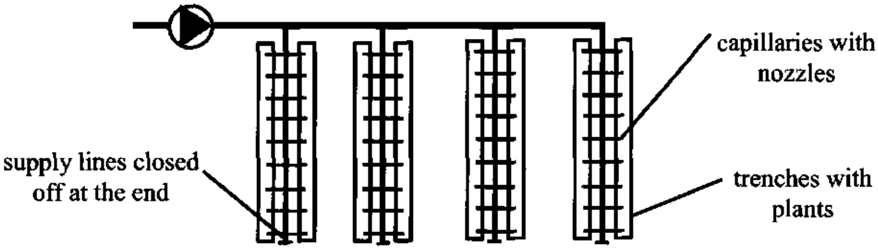

Figure 1 - Growing system with trickle irrigation nozzles, supply lines, a transport tube and a feeding pump. In the standard growing system above, the supply lines are closed off with an end cap.

In Figure 1, the tubes with a pump and the growing channels of a standard water and nutrient supply installation are shown. The channels capture the drain water and return it into a drain reservoir for reuse. Each individual plant is fed with water by a nozzle connected to a capillary hose. The capillaries receive the water from a supply line that is installed in-between the channels.
First, it is of interest to take a closer look at the delay time in the supply lines, the mixing and storage reservoirs. The mixing reservoir is a stirred tank and as such its behaviour may be considered as a first order response. The time delay can easily be determined from the dimensions of the tank itself.
Figure 2 shows a supply line with n capillary hoses. The time t [s] it takes a specific water molecule, or nutrient ion or small (almost dimensionless) particle, to travel from the begin-

ning of the supply line to a specific capillary, is determined by the time it takes all downstream capillaries to empty the volume between the beginning and that specific point.

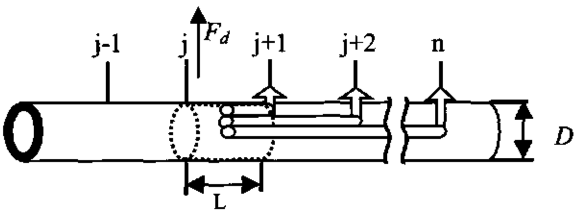

Figure 3 - Supply line with *n* capillaries connected to it. F_d is the solution flow through each nozzle. The volume between nozzle *j* and *j+1* is flown through by (*n-j*) partial flows of value F_d each. *L* [m] is the length of the supply line, *D* [m] is the inner diameter of the supply line.

Equation 1 presents the relationship between the delay time t_j for the nozzle in position j, the nozzle flow F_d and the index number j of the nozzle.

$$t_j = \frac{L \cdot D^2 \cdot \pi}{4 \cdot Fd} \cdot \sum_{j=1}^{n-1} \frac{1}{n-j} \tag{1}$$

If values for the standard research greenhouse (used throughout the research) are used (D = 0.018m, L = 0.3m, F_d = 37 mL·min^{-1}, n = 74), then for each nozzle position j the delay time t_j can be calculated from (1).
In this same greenhouse, measurements have been taken to determine t_j at seven distinct nozzle positions along a supply line. Figure 3 shows the results of the prediction for t_j from equation 1, the measured data points and the 95% reliability interval.

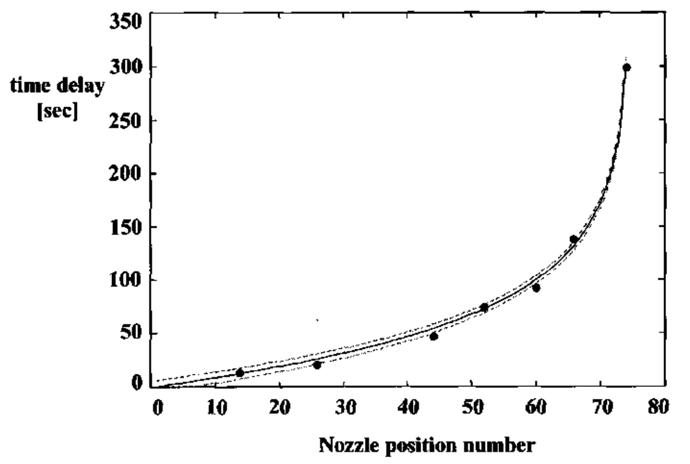

Figure 3 - Measured (dots) and modelled (solid) time delays [s] of a supply pulse to arrive at the nozzles with 95% reliability interval (dashed), as a function of index number of nozzle along the supply line.

As can be seen from Figure 3, equation 1 sufficiently describes the time delays as a function of the index number of the capillary. During the test, it appeared that the capillaries were gradually blocked, a disturbance not accounted for in equation 1. Therefore, the reliability interval changes and the time delays increase.

The conclusion of the above is that a standard layout of the supply lines intrinsically introduces time delays. These time delays show the tendency to be of longer duration with increasing index number along the length of the supply lines. This phenomenon causes an unequal distribution of the supplied nutrients over the length of the supply lines and thus over the overall greenhouse.

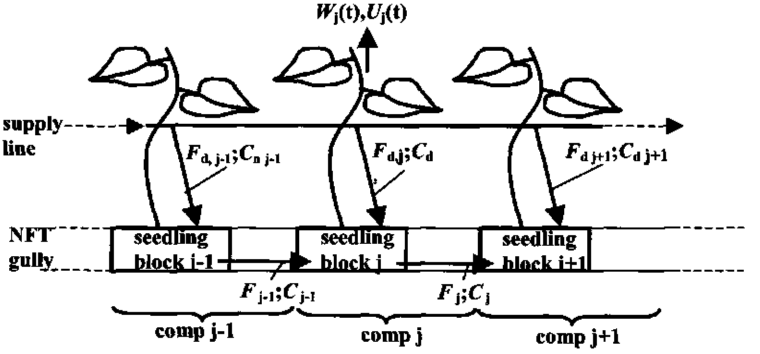

Figure 4 - Nutrient supply pipe with capillary hoses (nozzles), plants and growing channel, subdivided in compartments. F = flow [$m^3 \cdot s^{-1}$], C =concentration of a specific nutrient ion [$mol \cdot m^{-3}$], n = at the nozzle, j = at compartment j, F_j = flow at the exit of compartment j, $F_{d,j}$ = flow from nozzle j, $W_j(t)$ = water uptake flow into plant j, $U_j(t)$ = nutrient uptake rate of plant j.

Figure 4 shows a cut-through in the length of one of the growing trenches of Figure 1. The channel is subdivided into a chain of compartments, where each compartment is considered to behave like a stirred tank (Lukasse, 1994). Properties - like residence time and dead zone times - can be calculated for each compartment separately. Then, for the whole channel, it can be collected together in an overall residence time.

In a NFT growing system, an obstacle in the channel like a rockwool seedling block, if present in each compartment, may be thought of as a part of the properties of that compartment.

C [$mol \cdot m^{-3}$] is a property that will stick to water in the due process of transport. The same holds for e.g. EC or pH. Each compartment has two inputs, the nozzle flow and the output flow of the former compartment F_{j-1}. A compartment has two outputs, the drain flow to the next compartment F_j with its ion concentration C_j [$mol \cdot m^{-3}$] and the plant water uptake $W_j(t)$ [$m^3 \cdot s^{-1}$] with plant nutrient uptake $U_j(t)$ [$mol \cdot s^{-1}$].

In equation 2, the mass balance of a compartment in a NFT channel is described for e.g. ionic content of the nutrient solution. Equation 3 depicts the incompressibility of water (sum of all flows is equal to zero).

Change = - outflow via gully + inflow via gully + nozzle inflow - uptake

$$V_j \cdot \frac{dC_j(t)}{dt} = -F_j(t) \cdot C_j(t) + F_{j-1}(t) \cdot C_{j-1}(t) + Fn_j \cdot Cn_j(t) - U(t) \qquad (2)$$

$$F_j(t) = F_{j-1}(t) + Fn_j(t) - W_j(t) \qquad (3)$$

The discrete time model of equation 4 can replace the equations 2 and 3:

$$C_j(k+1) = a \cdot C_j(k) + b_1 \cdot C_{j-1}(k-n_1) + b_2 \cdot Cn_j(k-n_2) - \frac{U_k}{F_j} + e_j(k) \qquad \textbf{(4)}$$

In equation 4, parameter n_1 and n_2 are the time delays - expressed as an integer number of sample intervals - of compartment *j-1* and *j* respectively. $e_j(k)$ is the modelling error in compartment *j* at sample interval *k*.
With the aid of the program Matlab®, the model of equation 4 is validated with real measured data. The real measured data was collected from tests in a greenhouse with tomato plants grown on rockwool in channels. EC sensors were placed at some capillary outputs in a growing channel to measure the time between the start of a supply pulse and the moment the EC pulse passes the EC sensor. Data of this experiment fitted on difference equation 4 determines the parameters as:

$$C_j(k+1) = 0.986 \cdot C_j(k-1) + 0.0033 \cdot C_j(k-38) + 0.017 \cdot Cd_{j-1}(k-1) \qquad \textbf{(5)}$$

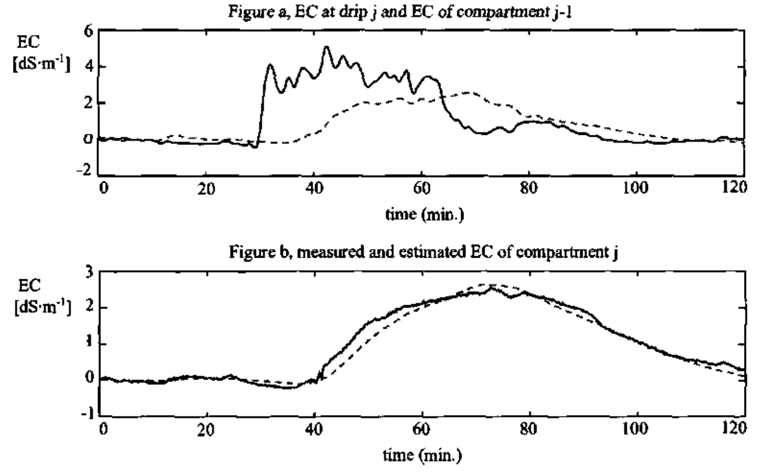

Figure 5 - a) Input EC [mS·m^{-1}] of compartment *j* (full line) as measured at output of compartment j-1 and at nozzle *j* (dotted line).
b) Measured (full line) and estimated (dotted line) output of compartment *j*.

3. Conclusion

Figure 5 shows results of a simulation run with the validated model of equation 5 in comparison with real measured data. Figure 5a shows the inputs of compartment *j*, i.e. the output of the former compartment and the signal at the nozzle, respectively. Figure 5b shows the good fit between the measured concentration and the modelled concentration of compartment *j*. It demonstrates that it is feasible to build discrete time domain models of the growing channels and the trickle irrigation pipes to define the dynamic behaviour of an NFT growing system.

§2.2 Fluid flow in a set of supply pipes

Based on:
Monitoring and control of water and fertilizer distribution in greenhouses. In: *Acta Hort. 401*: pp365-372. Th.H.Gieling, J. Bontsema, A.W.J. van Antwerpen and L.J.S. Lukasse, 1994.
Greenhouse water supply, application of nutrients and their environment. In: *Macqu Final Report EU AIR3-CT93-1603.* Chapter 2. Th.H.Gieling, E.A. van Os, P.C.J. Hamer, 1996.

1. Introduction

In a standard layout (Figure 1 a) water and nutrients are transported to the individual plants by supply lines. The supply lines, which are installed along the plant rows and have a capillary hose per plant, are cut-off and sealed up at the end of the row. These dead-ends in the trickle irrigation supply lines have a special effect on the residence time of water and nutrients in the supply lines. They cause an increase of the residence time along the length of the supply tube, as is shown in the former section.
Towards the end of a supply line, water of fewer capillaries flows through the cross-section of it in comparison to its beginning. This causes the peculiar effect of exponential increase of delay time with increasing index number (Figure 3 of former section) and a dramatic inequality of the distribution over the greenhouse. In heating systems, as they are often applied in greenhouse engineering, this problem also occurs. It is solved by a decrease of the diameter of the heat supply pipe towards the end of the supply pipe, in order to keep the distribution equal over the whole supply pipe.
However, in case of nutrient solution supply, this would increase the pressure drop over the supply lines, with an unequal capillary water flow by the first and last capillary.

A better approach for nutrient supply systems is found in a different layout of the supply lines.

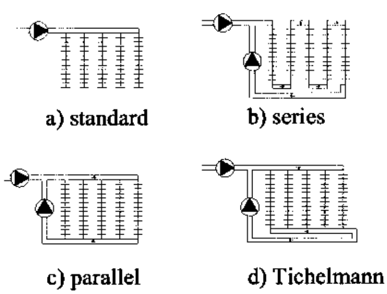

Figure 1 - Four optional piping diagrams for water supply in a greenhouse.

Adding an extra pump and interconnecting the supply lines at their ends, creates a supply system with a circulating water stream over the system of supply lines and their interconnecting tubes (Figure 1b, c, d).

- The first alternative on the standard way of connecting the supply lines is a series connection of the supply lines (Figure 1b). It means that the supply lines are connected outlets to inlets. This layout causes the pressure difference over the entire system to be very large and an unequal distribution of water through the capillary hoses is the result of it.
- The second option connects the outlets of the tubes in the same way as the inlets (Figure 1c). The main supply then situates at the same side as the main outlet. It means that the route of the water through the first supply tube is much shorter than the route through the last supply tube. Thus, the residence time of water in the entire system is not uniform.
- A third option is a special version of a layout known from heating systems technique as the Tichelmann system (Buitelaar *et al.*, 1975; Von Zabeltitz, 1978, Knoll and Wagenaar, 1994). The outlet of the system situates on the opposite side of the inlet (Figure 1d). The length of the routes in the system and the route of the water through the system is equal for all supply lines. The distribution of water is nearly uniform, since the resistances in the different routes are the same. The resistance of inlet and outlet tubes should be small in comparison to the resistance of the supply tube (Von Zabeltitz, 1978).

The experimental greenhouses used throughout the research of this thesis consist of eight plant rows. A single row at each greenhouse wall and three double rows in the middle. Single plant rows contain 36 plant positions, each position provided with a trickle irrigation capillary. Five supply lines feed nutrient solution to the plants. One supply line for each single row and one supply line in between each double row. This leads to 36 trickle irrigation capillaries for a single row supply line, 72 trickle irrigation capillaries for a supply line of a double plant row, resulting in 288 capillaries for this greenhouse.
In Figure 5, the cultivation area is 150 m^2, F_d = nozzle flow [30ml·min^{-1}], maximum water supply = $n_d \cdot F_d$ =288·0.030 = 8.64 [l·min^{-1}] = 1.44·10^{-4} [m^3·s^{-1}], F_b = base flow; F_a = inlet flow = $(F_b + n_d \cdot F_d)$, L_d = nozzle distance on supply tube [0.3m], L_v = length of inlet tube [41.2m], L_z = length of outlet tube [25m], d_d = diameter of supply tube [0.018m], d_v = diameter of inlet tube [0.0284m]. a_i = fraction flow of tube *i*, w_i = number of nozzles on tube *I*, n_d = total number of nozzles = 288. *i, a, w, n* are dimensionless numbers.

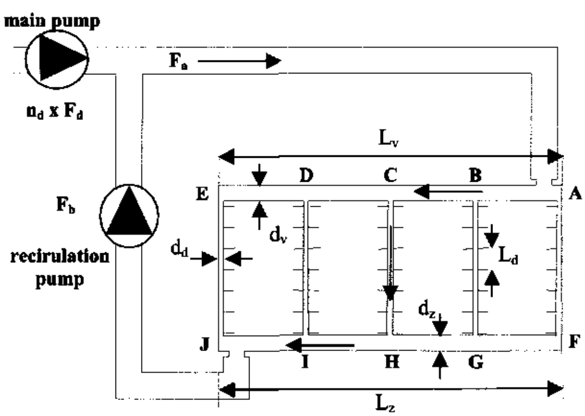

Figure 5 - Actual layout of a Tichelmann connection of five supply tubes.

This supply pipe layout has been used in the following fluid flow analysis.
At one point in time, at one point in the system there can only exist one pressure. At the main inlet of the system (point A in Figure 5), a pressure exists that is created by the pump. At the

main outlet of the system (point J in Figure 5), a pressure exists that is lower than at point A and is caused by the pressure drop over the pipes in the system.
These two pressure points are common for all parallel flow paths. The pressure drop ΔP [Pa] across the supply lines and their connecting tube sections must be the same. A model of the hydraulic properties relating pressure and flow of water in tubes (equation 6) and residence time of changes in concentration in tubes is given in equation 7 (Van Antwerpen, 1995; Gieling *et al.*, 1994).

$$\Delta P_W = \lambda \cdot \frac{L}{d} \cdot \frac{1}{2} \cdot \rho \cdot v^2 = \frac{128 \cdot \eta \cdot L \cdot F}{\pi \cdot d^4}; \; v = \frac{4 \cdot F}{\pi \cdot d^2}; \; \lambda = \frac{64}{Re}; \; Re = v \cdot \frac{d}{\nu}; \; \nu = \frac{\eta}{\rho} \tag{6}$$

$$t_d = \frac{L \cdot \pi \cdot d^2}{4 \cdot F}; \text{ residence time in a tube}$$
$$t_{j,w} = \frac{L \cdot \pi \cdot d^2}{4 \cdot F} \cdot \sum_{x=j}^{w-1} \frac{1}{n-x}; \text{ residence time in a } n\text{-capillary line between capillaries } j \text{ and } w \tag{7}$$

ΔP_w = pressure loss over tube [Pa], λ = coefficient of friction [1], L = length tube [m], d = tube diameter [m], v = velocity [$m \cdot s^{-1}$], ρ = density [$kg \cdot m^{-3}$], F = flow through the tube [$m^3 \cdot s^{-1}$], ν = kinematic viscosity [$m^2 \cdot s^{-1}$], Re = Reynold number [1], η = dynamic viscosity (Pa·s).

The viscosity is equal for all points. The hydraulic resistance of the tubes depends on the dimensions of the tubes and the distribution of the flow through the supply lines. Each of the equations in the following system of equations (8) is a result of the pressure differences over a supply tube.

$$\begin{aligned}
\Delta P_{AF} + \Delta P_{FG} &= \Delta P_{AB} + \Delta P_{BG} \\
\Delta P_{BG} + \Delta P_{GH} &= \Delta P_{BC} + \Delta P_{CH} \\
\Delta P_{CH} + \Delta P_{HI} &= \Delta P_{CD} + \Delta P_{DI} \\
\Delta P_{DI} + \Delta P_{IJ} &= \Delta P_{DE} + \Delta P_{EJ} \\
a_1 \cdot F_a + a_2 \cdot F_a + a_3 \cdot F_a + a_4 \cdot F_a + a_5 \cdot F_a &= F_a
\end{aligned} \tag{8}$$

$a_1 ..... a_5$ [1] are the partial flows through each supply tube. Equations 6 and 7 can be substituted in equation 8 and generalised for k supply lines. The system then consists of (k-1) equations and one equation stating that the sum of all partial flows equals one (equation 9).

$\{1 \le i \le k-1 | k \in 1, 2, ... n\}$; k is the number of supply lines, variables as in Figure 5.

$$a_1 + a_2 + ... a_i + ... a_k = 1$$

$$\frac{L_{d_i}}{d_d^4} \sum_{x=1}^{w_i} (a_i \cdot F_a - x \cdot F_d) + \frac{L_z}{d_z^4} \sum_{x=1}^{i} (a_x \cdot F_a - w_x \cdot F_d) = \frac{L_v}{d_v^4} \left(1 - \sum_{x=1}^{i} a_x \cdot F_a \right) + \frac{L_{d_{i+1}}}{d_d^4} \sum_{x=1}^{w_{i+1}} (a_{i+1} \cdot F_a - x \cdot F_d) \tag{9}$$

In case of the greenhouse mentioned before, the system consists of five supply lines (k = 5). An analytic solution exists for the system of equations. However, numerical solutions are calculated with mathematical software (Matlab® and Mathcad®). F_b varies from 0 to $8.64{\cdot}10^{-4}$ [$m^3{\cdot}s^{-1}$]. Each F_b results in a specific solution of the system of equations. The diagram in Figure 6 shows that the distribution over the supply lines is poor for low values of the circulation flow rate. At a circulation flow rate of approximately $5.5{\cdot}10^{-4}$ [$m^3{\cdot}s^{-1}$] and onwards, the actual distribution stays within a boundary of +2.5% to –2.5% of the ideal distribution, which is in case of 5 supply lines: 100% divided over 5 lines = 20% of the total flow per supply line.

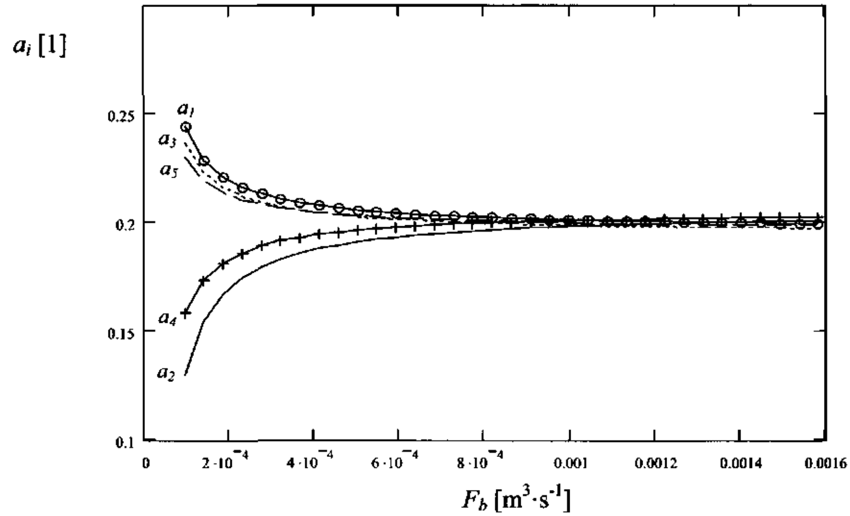

Figure 6 - The diagrams $a_1..a_5$ [1] represent the partial flows through five supply tubes as a function of the circulation flow F_b, at a capillary flow rate F_d of $5{\cdot}10^{-7}$ $m^3{\cdot}s^{-1}$.

Table 1 - The delay time (min.) of the standard water supply system

			supply line #				
			1	2	3	4	5
main inlet line			6,00	6,00	6,00	6,00	6,00
distribution	1	A-B		0,11	0,11	0,11	0,11
"	2	B-C			0,18	0,18	0,18
"	3	C-D				0,30	0,30
"	4	E-F					0,84
supply line			21,25	12,40	12,40	12,40	21,25
total delay time			27,25	18,51	18,69	18,99	28,68

Table 2 - The delay time (min.) of the Tichelmann water supply system

			supply line #				
			1	2	3	4	5
main inlet line			4,04	4,04	4,04	4,04	4,04
distribution	1	A-B		0,12	0,12	0,12	0,12
"	2	B-C			0,19	0,19	0,19
"	3	C-D				0,28	0,28
"	4	D-E					0,53
supply line			0,83	0,89	0,91	0,90	0,84
total delay time			4,86	5,05	5,25	5,25	6,00

The data in Table 1 and Table 2 show the improvement in total delay time due to forced circulation over the supply lines and connecting tubes. The delay time decreases from approximately 20 minutes in the standard layout to approx. 5 minutes in the Tichelmann layout. Comparison of the values of time delay in the supply lines of both tables shows, that the distribution of the inlet flow over the five supply lines is more uniform in the Tichelmann layout, than in the standard layout. In Table 1, the supply lines 1 and 5 show a much larger time delay than 2, 3 and 4. The reason is that these two supply lines only have 37 capillaries to empty them and the other three have 72 capillaries. Table 2 does not show these differences, since here time delay is more the result of the circulation speed and less of the loss through the capillaries.

2. Models for water uptake

Introduction
The aim of irrigation of glasshouse crops is to provide enough water to meet the needs of the plants and to avoid water stress. About 95% of the water that is taken in by the roots passes through the plant and evaporates from the leaves in the process of transpiration. The organs and other constituent parts of the plants retain the remaining water. It is removed when the crop is harvested, leaves are removed or the plants are destroyed and moved out of the greenhouse at the end of the productive live.
In broad outlines, transpiration plays an important role:

- by evaporative cooling: prevent the leaf temperature from going too high,
- as a means of transporting nutrients to the different plant organs.

Yield reductions are linked with low transpiration, because the latter creates nutrient deficiencies. The control of water supply can be used as a tool to control crop growth and to improve the quality of the product.
Furthermore, water supply is increased to reduce the build up of salts in rockwool. Supply of too much water creates a lot of drain water that has to be cleaned before ruse.
To define an effective control strategy for water supply, it is necessary to be able to predict how transpiration depends on the climatic conditions. Direct measurements of transpiration are difficult to achieve, particularly in commercial situations.

Transpiration
Most of the existing models for predicting transpiration, E_t [kg·m^{-2}·s^{-1}], are based on the thermal balance equation of the canopy and are similar to the Penman-Monteith equation (Monteith and Unsworth, 1990):

$$\lambda_v \cdot E_t = \frac{\Delta \cdot \Phi_n + (\rho \cdot c_p / r_a)(e_a^* - e_a)}{\Delta + \gamma(1 + r_c / r_a)} \qquad \textbf{(10)}$$

Here, λ_v [J·kg^{-1}] is the latent heat of vaporisation, Δ [Pa·K^{-1}]is the rate of change of saturation vapour pressure with temperature and γ [Pa·K^{-1}] is the psychrometer constant. Φ_n [W·m^{-2}] is the net radiation, ρ [kg·m^{-3}] and c_p [J·kg^{-1}·K^{-1}] are respectively the density and air specific heat at constant density. e_a* [Pa] is the air saturated vapour pressure, e_a [Pa] is the air vapour pressure. r_c [s·m^{-1}] is the internal resistance of the leaf canopy to transfer of water vapour and r_a [s·m^{-1}] is the aerodynamic resistance.

Equation 10 assumes that the net radiation is completely absorbed by the crop canopy - which it does not in practice - and therefore the radiation term should be multiplied by $\{1-\exp(-\kappa \cdot LAI)\}$, where κ [1] is the radiation extinction coefficient and LAI [$m^2 \cdot m^{-2}$] the leaf area index. The net radiation absorbed by a crop can be described in terms of the short-wave radiation (received from the sun and sky and reflected from the ground) and long-wave flux (received from the atmosphere and emitted by the ground).
A suitable general form of the equation describing the radiation budget is found in equation 11.

$$\Phi_n = a \cdot \Phi_\downarrow + b \tag{11}$$

In equation 11, $\Phi_\downarrow$ [$W \cdot m^{-2}$] is solar radiation on a horizontal surface and a, b are coefficients. For high values of solar radiation, for example in mid-summer and at mid-day, $a \cdot \Phi_\downarrow >> b$ and net radiation is directly related to solar radiation. About two thirds of the solar radiation measured outside a greenhouse is transmitted into the greenhouse.
Other environmental variables - which influence the transpiration rate - are the air temperature and the saturation deficit ($VPD = e_s{*} - e_a$) [Pa]. For a hypostomatous crop the internal resistance of the canopy can be related to the leaf stomatal resistance (r_s) [$s \cdot m^{-1}$] by assuming:

$$r_c = \frac{r_s}{LAI} \tag{12}$$

Stomatal resistance depends on solar radiation, vapour pressure deficit, temperature and CO_2 concentration (Stanghellini, 1987).
The above inventory shows that solar radiation, vapour pressure deficit and leaf area index are the main variables affecting transpiration of greenhouse crops. Furthermore, solar radiation and VPD usually correlate strongly within a greenhouse. An aim of crop management is to produce a full crop canopy as soon as possible and to maintain a balance between the amount of leaf and the rest of the plant parts. Most models relate transpiration to either solar radiation or VPD or to both and differ in the method of calculation of the solar radiation and the stomatal resistance.

Some well known transpiration models
Jolliet and Bailey (1992) checked a range of models against measurements on a tomato crop. The simplest models were of the form:

$$E_t = a \cdot \Phi_i + b \cdot VPD + c \tag{13}$$

In equation 13 Φ_i is the solar radiation inside the greenhouse and a, b and c were constants mainly derived from regression analyses. Most of the simple models do not take account of VPD (i.e. $b = 0$) and c has a positive value to take account of the transpiration that occurs at night (when $\Phi_i = 0$) and when the light levels are low. In effect these models use constant values for the stomatal resistance and result in poor accuracy when compared with measurement.

The best accuracy is obtained when the transpiration is calculated from measurements of leaf area index, calculations of aerodynamic resistance (from measurements of the width and length of leaves and windspeed) and a model of stomatal resistance. For example, Stanghellini (1987) used functions to relate stomatal resistance r_s to a minimum stomatal resistance (r_{min})

and resistance functions related to temperature *r(T)*, the concentration of CO_2, *r(CO_2)* and the vapour pressure deficit, *r (VPD)*:

$$r_s = r_{min} \cdot r(\Phi) \cdot r(T) \cdot r(VPD) \cdot r(CO_2) \qquad (14)$$

where:

$$r_{min} = 82.0 \; ; \; r(I) = \frac{(I + 4.30)}{I + 0.54)} \; ; \; r(T) = 1 + 2.3 \cdot 10^{-2}(T_0 - 24.5)^2$$

$$r(VPD) = 1 + 4.3(e_0 - e_a) \qquad e_0 - e_a < 0.8 \text{ [kPa]}$$

$$r(VPD) = 3.8 \qquad e_0 - e_a \geq 0.8 \text{ [kPa]}$$

$$r(CO_2) = 1 \qquad I = 0 \text{ [W}\cdot\text{m}^{-2}\text{]}$$

$$r(CO_2) = 1 + 6.1 \cdot 10^{-7}(CO_2 - 200)^2 \qquad CO_2 < 1100 \text{ [vpm]}$$

$$r(CO_2) = 1.5 \qquad CO_2 \geq 1100 \text{ [vpm]}$$

The model requires model information or direct measurement of: solar radiation, leaf area index, leaf temperature, air temperature, vapour pressure (usually determined from measurements of air temperature and relative humidity) and CO_2 concentration.

Most of these measurements are recorded in greenhouses in which the environment is controlled by computer. Separate sub-models are required to estimate *LAI* and leaf temperature.

Jolliet and Bailey (1992) used a simplified version of the Stanghellini model by leaving out of consideration the influence of CO_2 concentration and air temperature on stomatal resistance. There was a loss of accuracy when the models were tested against an independent set of data. The Stanghellini model predicted transpiration to within 2% whereas the Jolliet & Bailey model prediction was within 8%. Both models are a considerable improvement on the simple models relating transpiration to solar radiation; such models gave poor accuracy (typically 50%).

However, this approach is not easy to implement for irrigation control since estimates of stomatal resistance require models to describe energy fluxes at the leaf surface.

The approach taken by Hamer (1997) was to generate data on crop water uptake, using a modified version of the Stanghellini model and to relate the modelled values to the easily measured environmental variables solar radiation and saturation deficit (*VPD)* inside the greenhouse. A greenhouse simulation model (Chalabi and Bailey, 1989) was used to generate data. The model simulates the transient environment inside a greenhouse from hourly observed weather variables. The data were restricted to a crop with a complete canopy and divided into day and night periods. Regression analysis related transpiration to solar radiation and *VPD* (as in equation 13). However, there is considerable seasonal variation in the coefficients a, b, and c of equation 13. At night the seasonal variation in the coefficients b and c (a = 0 at night) are less pronounced, particularly when the relation is constrained to pass through the origin (c = 0). Hamer (1997) produced a single relation for day and night use:

$$\lambda \cdot E_t = 0.174 \cdot \Phi g + 693.6 \cdot (1 - 0.89 \cdot e^{-0.00225 \cdot \Phi g}) \cdot VPD \cdot f(VPD) \qquad (15)$$

where: Φ_g (W·m^{-2}) is the global solar radiation measured outside the greenhouse, and

$$f(VPD) = \frac{4}{(1 + 255 \cdot \exp(-5.55 \cdot VPD))^{0.25}} \qquad (16)$$

Hamer (1997) based the general form of the relationship on an expression used by Jolliet (1994). He validated the model by measuring water use (assumed to be $\lambda \cdot E_t$) of crops grown using the nutrient film technique (NFT) and the rockwool run-to-waste system (Hamer 1998). Hamer (1998) lists possible explanations why the NFT grown crop in his experiments uses more water than the rockwool grown crop and why the model underestimates crop water use when the saturation deficit is large. These estimations include:

- restrictions of water movement in the rockwool due to low water potential
- the root system is not in full contact with its growth environment.

3. Conclusions

The Tichelmann layout, as presented at the start of this chapter, ensures that the flow in a set of supply lines is equal for all lines. However, the circulation flow needs a value of 3 to 6 times the total capillary flow, to ensure this equal distribution of the inlet flow over the supply lines. The pressure drop across the supply tubes, caused by the circulation flow, might induce a difference in water supply between the first and the last capillary in a plant row. It is advisable to use capillaries - or nozzles - with a capillary flow that is relatively independent of the pressure in the supply lines. It is also advisable to use nozzles, which only open after the pressure exceeds a threshold value. The pressure threshold of the nozzles should be chosen to exceed the pressure generated by the circulation pump. In this way the supply lines stay filled with water after switching off the water supply pump - and do not need refilling - whilst the circulation pump stays on to keep the water circulating over the now closed loop of the Tichelmann system.

Nowadays, transpiration models are available in a broad range of versatility. Quality of the prediction is a trade off against complexity of the algorithms and the number of inputs needed. In the models, measured values are used as inputs (i.e. global radiation, CO_2 level in the greenhouse, inside air temperature, air humidity, etc.) that are often already available from the normal climate control system. The most elaborate models only need e.g. ski temperature or greenhouse roof temperature as extra measured variable.
Lysimeters are used to validate the models in a greenhouse in near-practise situations. As a research instrument it is well accepted and reliable. Correction of artefacts in the dataset, caused by disturbances at the lysimeter's balance, often need human intervention, which causes it to be an unreliable on-line instrument for usage in horticultural practice.
This incorrectness of the on-line measurement in real world situations causes it to be of much lower fidelity than the output of an on-line model.

§2.3 Analysis of solute movement in inert substrates

Based on:
Analysis of solute movement in inert substrates. In: Pre-prints of the Proceedings of IFAC Conference on modelling and control in agriculture, horticulture and post-harvest processing: 357-363. Th.H.Gieling, G. van Straten, B.W. Veen, 2000.

1. Introduction

The paragraph is not intended to describe all problems related to water and nutrient movement in substrates. It merely gives a description that can be of help to identify the dynamic properties of a closed growing system in a greenhouse with rockwool as growing medium, based on a mass balance of nutrients and water. A control strategy and a controller - both in classical as in model-based (predictive) controller design - require:

- insight in the important elements in the set-up of the control configuration: which variables to measure, which to use for the control algorithm, where to measure, which actuators to use,
- insight in the steady state behaviour of the system, or in the time-averaged behaviour,
- insight in the dynamics of the system, in order to design the controller,
- analysis of the options for feed-forward compensation, to improve reaction time and precision.

The process to be controlled is the uptake of water and nutrients by the roots, and in doing so, completely or partially fulfils the demand of the plant. It is important to know if the substrate is able to timely deliver the nutrients and water in an amount needed by the plant. Furthermore, it is of interest to be able to control the uptake in such a way that the results of plant processes - like product quality (taste, smell) and the avoidance of deficiency related diseases - can be influenced.
Section 1.2 on this introductory paragraph, relates to an outline of the problem definition. Sections 1.3 and 1.4. provide a review on some mechanisms in nutrient transport. To gain some insight in a viable strategy for nutrient control, some of the phenomena of ion transport across the bio-membrane into the roots are briefly elucidated.
The value of this introduction is to be found in the need for a plant related control strategy during the development phase of a controller. This strategy helps to show that the equipment, the algorithms and overall systems design, function within the expected parameters in a greenhouse. In a later phase, no doubt, plant physiologists will provide better strategies, which are better suited to achieve the goal of steering the needs of the plant in relation to growth and quality.

Transport of ions across the bio-membrane of the cell wall
Singer and Nicholson (1972) describe the structure of the cell's plasma membrane in their fluid mosaic model, which continues to be the basis for modern thinking about the dynamic structure of bio-membranes. To quote Jacobson *et al.*, (1995) "... *the fluid mosaic model has been revisited and enhanced with respect to protein locomotion and/or confinement to certain restricted areas on the cell's surface. In the fluid mosaic model, the membrane consists of a*

lipid bilayer with proteins floating in them. Many of the membrane proteins are anchored to each other or to the intracellular structures by filaments in the cytoskeleton, which may be involved in the modulation of membrane protein function. The cell's plasma membrane defines the cell's boundaries and selectively interacts with the environment".

In relation to uptake of nutrients by plants, it is important to mention three main types of ion transport across the membrane that are defined within the context of the fluid mosaic model (Chang, 1990; Mulder, 1991; Zimmerman, 1997): simple diffusion, facilitated diffusion, active transport.

1. Simple diffusion, where ions pass through the membrane from regions with high to regions with low concentration, either across the lipid bilayer or through protein pores or 'ion channels' (ion channels with gating mechanisms: ligand gating, membrane voltage gating, stretch gating).
2. Facilitated diffusion involves carrier-assisted transport from regions with high to regions with low concentration. The nutrient ion to be transported complexes with a carrier molecule. The complex formed is soluble in the lipid bilayer. Consequently, the rate of facilitated diffusion is much higher than that of simple diffusion.
3. Active transport moves substances across the membrane against a concentration gradient. This non-spontaneous thermodynamic process needs an external energy source. As in facilitated diffusion, a carrier molecule, e.g. ATPase, is needed for complexing the nutrient ions. In case of the so-called sodium-potassium pump, the active transport of Na^+ and K^+ ions is linked together. The energy supplier is the ATP molecule, which yields ADP and inorganic phosphate. This spontaneous process then couples to sodium-potassium ATPase to drive the moving of ions against a concentration gradient.

The above literature references support the statement that uptake of nutrients by the root across the root membrane is an autonomous process not directly related to water uptake.

Older literature and recent publications (discussed below) take into account the viewpoints laid down in modern thinking about the mechanisms and processes involved in nutrient uptake.

In a chapter on kinetic studies in his monograph on '*Uptake of ions by plant roots*', Bowling (1976) gives a mechanistic approach in view of the selectivity of (root) cells. He elaborates on the general idea (Epstein and Hagen, 1952), that ions bind with specific carrier molecules or molecule complexes in the membrane - analogous to the binding of a substrate to an enzyme - which transport the ions across the membrane. Jungk *et al.* (1990) demonstrate this so-called Michaelis-Menten type of behaviour on phosphate uptake kinetics of maize and soybean roots. However, they conclude that plants markedly adapt P uptake kinetics to their P status. Their main conclusion is that none of the three Michaelis-Menten parameters (C_{min}, V_{max} and K_m), that are used to describe P uptake kinetics of soybean and maize roots, can be regarded as constant. All three variables depend on the P concentration the plants were formerly exposed to, and to which they were adapted in their internal P concentration. Other workers also described this phenomenon in relation to potassium and nitrate uptake. Wild *et al.* (1979) report on the phenomenon that *Lolium* grown at low $[K^+]$ has a more efficient mechanism for K^+ uptake, which continues to operate for some time after the plants have been transferred to a higher concentration, resulting in a higher influx of ions.

Deane-Drummond (1982) shows results of experimental data on instantaneous and long-term uptake of nitrate by barley seedlings from nutrient solutions at various concentrations that confirms the above findings. The plant can achieve uptake to its needs at surprisingly low concentrations (in free nutrient solutions). When such an adapted plant is exposed to higher concentrations, there is temporarily a higher uptake, depending upon concentration, probably until the internal mechanism has been adjusted. In the long run the uptake is adjusted to ac-

commodate the needs of the plant, dictated by some kind of stoichiometric ratio, which implies that the long-term uptake demand is coupled to growth. In order to achieve this under various environmental conditions in the root zone, the plant adjusts its internal mechanisms. In her Figure 1 and Table 1, Deane-Drummond (1982) shows that the net uptake rate of nitrate into the seedlings strongly depends on the concentration they were previously grown in: a high uptake rate of the seedlings previously grown on a low concentration and vice versa.
The above findings on the influence of the nutrient status of the plant suggest that:

a) the concept of a fixed kinetic model for nutrient uptake, which solely depends upon the instantaneous concentration in the substrate/soil solution, is not a sufficiently accurate description of reality.
b) control of the nutrient flux to the plants, by manipulating the external concentration alone, is not straightforward.

Nutrient uptake is better described by a nutrient demand model that is related to growth or growth rate (B. Veen, personal communication; De Willigen and Van Noordwijk, 1987). The question to be answered by a model should be: can the demand be satisfied given the transport phenomena towards the roots and the prevailing concentration in the substrate. Nutrient ions in the substrate are distributed by the water and nutrient dosage control (Figure 2). If not, the actual uptake is limited; if this is a problem, the controller should increase the dosage.
The objective is to propose control strategies that can prevent nutrient limitation or supply a specific amount of nutrients to the plants. The design is based upon an analysis of simple, lumped microscopic and macroscopic mass balances in the substrate mat. The balances hold for the areas around the roots, below the point were the nutrient solution enters the substrate slab by means of nozzles at end of capillary hoses.

Water and nutrient uptake, description of the current status

In his paper on objectives and constraints in irrigation management of greenhouse crops, Baille (1993) presents a global scheme of water fluxes in a greenhouse (Figure 1) and an analysis on the interactions between crop and greenhouse climate. It is an excellent starting point to describe the system of movement of nutrient solution through the growing medium towards the root surface, with state variables and parameters in connection to 'first principles' from physics.
As was already mentioned in the previous section, uptake of water and uptake of most macronutrients by the roots are physiologically two distinct mechanisms, which are independent of each other. Water uptake is a process with as driving force the difference in water-potential [Pa], which, to a large extend, is maintained by transpiration. The transpiration uptake causes a hydrostatic pressure drop in the xylem. In general, to a much less extend it is driven by the osmotic potential, which is generated by ion uptake in the xylem. Again, as said before, most macro-nutrients (e.g. nitrogen, phosphorous, potassium) are absorbed actively. The rate of uptake is determined by the demand of the plant, which is dependent on the growth rate and on the plant's nutrient content. The root is able to adapt its ion uptake to the needs of the plant, even with very low concentrations at the root surface. Active ion uptake of an adapted root is independent of the concentration at the root surface until very low concentrations (Wild *et al.*, 1979). In order to prevent direct evaporation from the substrate surface to the greenhouse air (Ψ_s), the substrate is enveloped in a plastic cover. Slits at either ends or the sides of the plastic envelope enable excess water to leave the growing medium as drain. The plastic cover prevents the drain to get in touch with the substrate after it leaves the enveloped substrate slab.

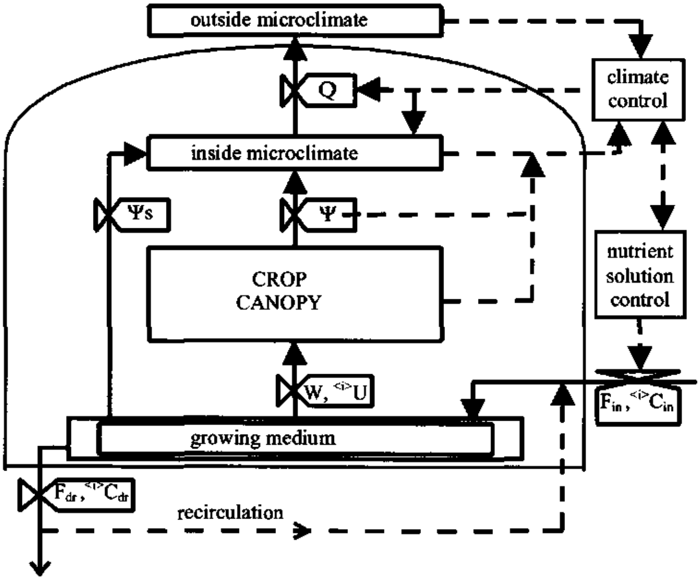

Figure 1 - Model for water and nutrient flows in a greenhouse (courtesy of A. Baille). Ψ and Ψ_s are crop transpiration and substrate/soil evaporation respectively. W is water uptake, $^{<i>}U$ is the uptake of nutrient i, F_{dr} is drainage flow, F_{in} is supply flow, $^{<i>}C_{in}$ and $^{<i>}C_{dr}$ are concentration of nutrient ion i in the supply and the drain respectively, Q is the exchange with outdoor climate.

Water uptake and nutrient uptake together are referred to as the influx. It is a hypothetical solute flow from the root surface into the root, consisting of the water taken up due to evapotranspiration, with as its ion concentration the nutrients taken up. When growing conditions change, transpiration and growth rate may change independently and the influx concentration will vary due to variations in either the transpiration (water uptake) or the growth rate (ion uptake) (Figure 2).

Uptake from the direct vicinity of the roots of water (transpiration driven) and nutrient ions (growth rate dependent) is replenished by flow and diffusion from the capillaries in the bulk of the growing medium. The flow rate of the solution towards the roots is equal to the flow due to water uptake. The concentration of nutrients of this evaporative flow is equal to nutrient ion concentration of the bulk solution in the substrate. This flux of nutrients and water to the roots is called the mass-flow.

In the vicinity of the root surface nutrient ions will accumulate (the boundary layer) if mass flow carries a higher concentration to the roots than the actual influx concentration takes away. If mass flow carries a lower concentration to the roots than the influx concentration, then all the nutrients are absorbed and the direct vicinity of the roots (the boundary layer) may reach depletion. A process of diffusion transports accumulated nutrients to the bulk of the liquid phase in the substrate. An excess supply of solution may contribute as "over-drain" to the transport of accumulated nutrients to the drain. By transporting nutrients into the root area, the same process of diffusion and excess supply may compensate a 'shortage'. The rate of compensation is dependent on the diffusion coefficient of the substrate, or in analogy with Ohm's law, dependent on the apparent hydraulic resistance of the substrate and on the excess supply of water or extra "over-drain".

2. Mass balance over a control volume

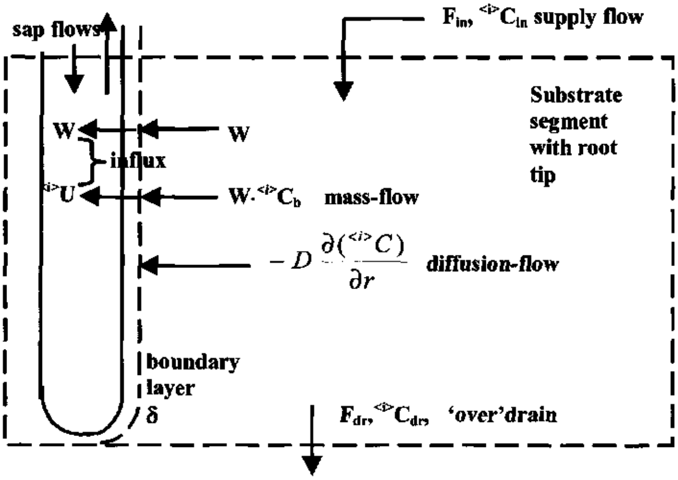

Figure 2 - Root tip in substrate cube with boundary layer, fluid flows and transport of nutrients

Consider a small *uniform* control volume containing a root (Figure 2). The volumetric water balance (equivalent to mass balance at constant density) is as in equation 1.

$$\frac{d\theta}{dt} = f_{in} - f_{out} - S_r \cdot W \tag{1}$$

In equation 1: θ is volumetric water content per unit volume [$m^3 \cdot m^{-3}$], f_{in} is volumetric water flow rate per unit volume entering the control volume [$m^3 \cdot m^{-3} \cdot s^{-1}$], f_{out} is the volumetric water flowrate per unit volume leaving the volume [$m^3 \cdot m^{-3} \cdot s^{-1}$], S_r is the root surface area per unit volume [$m^2 \cdot m^{-3}$] and W is the water uptake rate per unit root surface area [$m^3 \cdot m^{-2} \cdot s^{-1}$].

Nutrient molar balance over the control volume:

$$\frac{d(C_b \cdot \theta)}{dt} = f_{in} \cdot C_{in} - f_{out} \cdot C_{out} - S_r \cdot U^* \tag{2}$$

In equation 2: C_{in}, C_b and C_{out} are the molar concentrations of nutrients [$mol \cdot m^{-3}$], respectively in the incoming solution, in the bulk of a control volume and in the outgoing water. U^* is the nutrient uptake rate by the root per unit root surface area [$mol \cdot m^{-2} \cdot s^{-1}$]. Expanding equation 2 leads to:

$$C_b \cdot \frac{d\theta}{dt} + \theta \cdot \frac{dC_b}{dt} = f_{in} \cdot C_{in} - f_{out} \cdot C_{out} - S_r \cdot U^*$$

Combining the above result with equation 1:

$$\theta \cdot \frac{dC_b}{dt} = f_{in} \cdot (C_{in} - C_{out}) - f_{out} \cdot (C_{out} - C_b) - S_r \cdot (U^* - W \cdot C_b)$$

By definition a control volume is uniform, i.e. $C_{out} = C_b$, so:

$$\theta \cdot \frac{dC_b}{dt} = f_{in} \cdot (C_{in} - C_b) - S_r \cdot (U^* - W \cdot C_b) \tag{3}$$

It is not defined yet how the rate of inflow and the concentration of incoming solute into a control volume - at a deliberate location within the growing medium - relate to the supply flow rate and solute concentration from the dosage system. In order to find this relation, the total volume should be subdivided in a set of N sequential control volumes, which is worked out in section 2.2. of this paragraph. An important exception to the above observations is found in a pure hydroponics system (NFT), because there the control volume is the total volume. In addition, it is needed to specify how W depends upon θ, and how U^* depends upon C_b and θ, i.e. the functions $W(\theta)$ and $U^*(C_b, \theta)$ would be needed. The equations 1, 2 and 3 give rise to the following interpretation:

The bulk concentration in a control volume is the result of plant processes (the second right hand side term) and of controllable processes (the first right hand side term). In a later section the role of C_b in determining the nutrient uptake will be discussed in more detail. For now, it is assumed that there exists a bulk concentration at which the nutrient uptake of the plant is not impaired. Therefore, it could be legitimate purpose of a controller to keep the bulk concentration constant. In this case, equation (3) provides a means to pre-calculate how the control input C_{in} should be adjusted in order to keep the bulk concentration C_b at the same value, despite variations in water and nutrient uptake. Simply setting the derivative equal to zero leads to:

$$C_{in,c} = C_b + \frac{S_r \cdot (U^* - WC_b)}{f_{in}}.$$

Here, in $C_{in,c}$ the additional subscript c is used to denote that this is a kind of control law. Next, it is assumed that the water content in the gully is kept constant, which is equivalent to keeping the drain flow constant, by manipulating the inflow. Thus, the steady state version of equation 1 can be substituted into the equation above, to yield:

$$C_{in,c} = \frac{f_{out,sp} \cdot C_{b,sp} + S_r \cdot U^*}{f_{out,sp} + S_r \cdot W}.$$

Here, the subscript sp denotes set value. The set value is assumed to be constant in this derivation. The interesting aspect of this pseudo-control law is that under more or less stationary conditions the plant uptake can be estimated from the control signal, as can be seen as follows. From the controller of the drain flow $f_{out,sp}$ is measured, while f_{in} as output of the controller is known. Therefore, $S_r \cdot W$ can be computed from equation 1. On the other hand, a controller that succeeds in keeping the bulk concentration constant will eventually have a known $C_{in,c}$ given by the equation above. So, all terms except $S_r \cdot U^*$ are known, and the uptake can be reconstructed. It should be noted that this derivation does not take into account the transient effects, which, especially in the case of the nutrients, will be substantial. Therefore, the reconstruction of the uptake should probably be done with an observer. The development of such an observer is the subject of a successor project (Van Kooten, 2000) and is outside the scope of this thesis.

In the following sections, a more detailed analysis will be given of the microscopic and macroscopic mass balances, leading to more elaborate considerations about the control concept. There, it will be argued that no diffusion limitation towards the plant's roots can occur if the bulk concentration is equal to the so called influx concentration, which is defined as the ratio

$U^* W^1$. If the average value of this concentration is chosen as the C_b set value, it can be seen by time-averaging of equation 3, that a steady state is possible only if C_{in} is made equal to C_b. Consequently, a controller that steers C_{in} towards this C_b will ensure that no limitations can occur. Note that the value of the C_b set value will be determined by the plant. As before, this derivation does not take the dynamic effects into account, but it may serve as an excellent starting point for the design of alternative nutrient controllers.

Mass balance over an ensemble of sequential control volumes

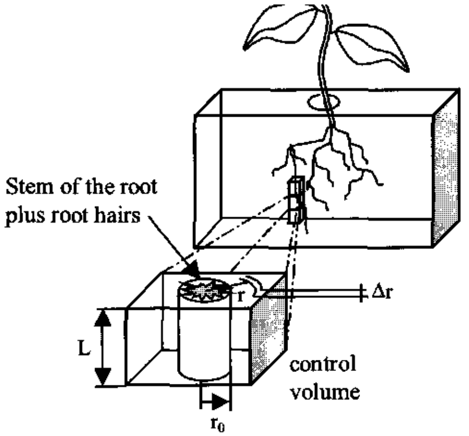

Figure 3 - Root tip in rockwool block with control volumes in sequential chains. The cylinder determined by r_0 and L stands for the total of root hairs around the stem of the root and the root stem itself. The root hairs are efficient enough to consider the concentration in the space between the root hairs to belong to the surface of the root cylinder.

Suppose that a number of control volumes is connected as a sequential chain, such that the outflow from the upstream volumes act as inflow for the downstream ones, as in Figure 3.

The mass balance for water reads:

$$\begin{aligned}
V_1 \cdot d\theta_1/dt &= V_1 \cdot f_{in,1} - V_1 \cdot f_{out,1} - V_1 \cdot S_{r,1} \cdot W(\theta_1) \\
V_2 \cdot d\theta_2/dt &= V_1 \cdot f_{out,1} - V_2 \cdot f_{out,2} - V_2 \cdot S_{r,2} \cdot W(\theta_2) \\
V_3 \cdot d\theta_3/dt &= V_2 \cdot f_{out,2} - V_3 \cdot f_{out,3} - V_3 \cdot S_{r,3} \cdot W(\theta_3) \\
&\dots \\
V_N \cdot d\theta_N/dt &= V_{N-1} \cdot f_{out,N-1} - V_N \cdot f_{out,N} - V_N \cdot S_{r,N} \cdot W(\theta_N)
\end{aligned} \tag{4}$$

$\underline{\theta}$ is the total volumetric moisture content, defined by: $\underline{\theta} = \sum_i \frac{V_i \cdot \theta_i}{V}$

i.e.: the total volumetric moisture content is equivalent to the spatially averaged volumetric moisture content. Similarly, the total active root surface per unit total volume is defined by:

$$\underline{S}_r = \sum_i \frac{V_i \cdot S_{r,i}}{V}$$

F_{in} is the volumetric inflow rate defined by:

$$F_{in} = V_1 \cdot f_{in,1}$$

Furthermore, F_{dr} is the total drain flow leaving the substrate, define:

$$F_{dr} = V_N \cdot f_{out,N} \cdot$$

It needs an additional assumption to derive the water balance for the substrate slab as a whole: the system is operated such that the water flux towards the roots, needed for water uptake, nowhere depends upon the water content. In equation form:

$$W(\theta_i) = W,\ i \in \{1, 2, \ldots n\}$$

It is now easy to see - by adding up the equations of (4) - that the total volumetric moisture content, $\underline{\theta}$, is given by the overall water balance:

$$V \cdot \frac{d\theta}{dt} = F_{in} - F_{dr} - V \cdot S_r \cdot W \qquad \textbf{(5)}$$

provided, that $W(\theta_i) = W,\ \forall\ \theta_i$.

Remark: The plant determines W (not controllable from the root zone without violating the former assumption, however, potentially controllable by the greenhouse climate), while F_{dr} normally depends upon the moisture content. Use of the equation for simulations requires the specification of $F_{dr}(\underline{\theta})$. In principle, this relation is given by the pF curve. It usually shows hysteresis, which means that the relationship is not purely algebraic.

The mass balance for dissolved nutrients reads:

$$\begin{aligned}
&V_1 \cdot d(\theta_1 \cdot C_{b,1})/dt = V_1 \cdot f_{in,1} \cdot C_{in,1} - V_1 \cdot f_{out,1} \cdot C_{out,1} - V_1 \cdot S_{r,1} \cdot U^*(C_{b,1}, \theta_1) \\
&V_2 \cdot d(\theta_2 \cdot C_{b,2})/dt = V_1 \cdot f_{out,1} \cdot C_{out,1} - V_2 \cdot f_{out,2} \cdot C_{out,2} - V_2 \cdot S_{r,2} \cdot U^*(C_{b,2}, \theta_2) \\
&V_3 \cdot d(\theta_3 \cdot C_{b,3})/dt = V_2 \cdot f_{out,2} \cdot C_{out,2} - V_3 \cdot f_{out,3} \cdot C_{out,3} - V_3 \cdot S_{r,3} \cdot U^*(C_{b,3}, \theta_3) \\
&\ldots \\
&V_N \cdot d(\theta_N \cdot C_{b,N})/dt = V_{N-1} \cdot f_{out,N-1} \cdot C_{out,N-1} - V_N \cdot f_{out,N} \cdot C_{out,N} - V_N \cdot S_{r,N} \cdot U^*(C_{b,N}, \theta_N)
\end{aligned} \qquad \textbf{(6)}$$

Define:

$$\underline{\theta} \cdot \underline{C}_b = \sum_i \frac{V_i \cdot \theta_i \cdot C_{b,i}}{V}, \text{ then: } \frac{d(\underline{\theta} \cdot \underline{C}_b)}{dt} = \frac{1}{V} \sum_i V_i \cdot \frac{d(\theta_i \cdot C_{b,i})}{dt}$$

and substituting the terms of the system of differential equations (6), leads to:

$$\frac{d(\underline{\theta} \cdot \underline{C}_b)}{dt} = \frac{1}{V} \left\{ \underbrace{V_1 \cdot f_{in,1}}_{F_{in}} \cdot C_{in,1} - \underbrace{V_N \cdot f_{out,N}}_{F_{dr}} \cdot C_{out,N} - \underbrace{U^* \cdot \sum_i V_i \cdot S_{r,i}}_{U^* \cdot S_r} \right\}$$

i.e.: $\underline{C}_b$ is the spatially averaged molar concentration, defined as the total nutrient molar mass divided by the total water volume. Derivation of the overall nutrient balance from the individual control volumes requires one additional assumption: the system is operated such that the nutrient uptake flux by the roots nowhere depends upon the bulk concentration and the water content. In equation form: $U^*(C_{b,i},\theta_i)=U^*, i\in\{1,2,\dots N\}$

Defining C_{dr} as the concentration in the drain outflow, C_{in} as the concentration of the incoming flow, and taking into account the former assumption, the overall balance is derived by adding up the separate balances, to yield:

$$V\frac{d(\underline{\theta}\cdot\underline{C}_b)}{dt}=F_{in}\cdot C_{in}-F_{dr}\cdot C_{dr}-V\cdot\underline{S}_r\cdot U^* \qquad (7)$$

Remark: U^* is determined by the plant and is not controllable from the root zone without violating the last assumption (potentially it is controllable by the greenhouse climate factors which determine growth).
Furthermore, C_{dr} will depend upon the average bulk concentration and the moisture content. Use of the equation for simulations requires specification of $C_{dr}(\underline{C}_b, \underline{\theta})$.

The overall mass balances under partial depletion conditions
The conditions in the previous section may not be easy to obey in practical situations. When the capillary is just a tube, a cone-like moisture and nutrient profile can be expected, leaving some parts relatively dry (Figure 4).

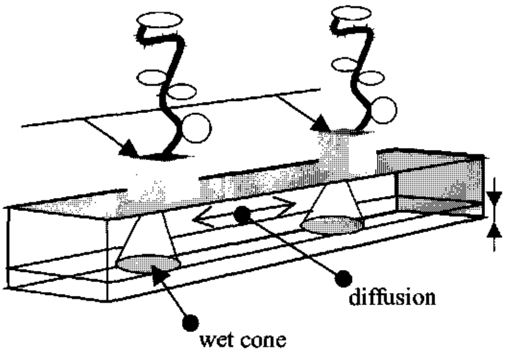

Figure 4 - Cone shaped parts of the substrate that are wetted each water supply pulse. Drain leaves the substrate trough slits in the plastic cover.

Nutrient levels in those dry areas are not necessarily low, especially if the drying out is due to a continuous flow of water towards the surface of the substrate, where it evaporates (neglected in the previous derivation), which leads to crystallisation and accumulation of nutrient salts. Wrapping of the slabs with a plastic cover minimises this process. However, low nutrient levels may occur at specific locations when supply is not sufficient to meet the demands of all roots.
Heinen (1997) shows results of simulations of solute flows and concentration distributions in a rockwool slab, with plants situated in rockwool seedling pots on top of the slab.
As is depicted in Figure 4, Heinen (1997, in his Figure 8-11 A, C) also suggests that a capillary placed in the seedling pot, by the process of dispersion and diffusion, creates a small cone

of high solute flux density [kg $_{H2O}$·m^{-2}] just below the capillary. His model predicts a higher solute flux density and nutrient concentration in the cone than in the remaining rockwool slab. The regions with high root density are situated in this cone. A relative high flux density indicates that the apparent hydraulic resistance is low and-or the diffusion coefficient is relatively large.

To accommodate this situation in a rather empirical way, the derivation needs to be modified. Averaging over all control volumes yields an average uptake that is at most equal to - but generally lower than - the maximum possible uptake belonging to the actual active root surface. The equations then become (including the relationships for F_{dr} and C_{dr}) :

$$V\frac{d\underline{\theta}}{dt}=F_{in}-F_{dr}(\underline{\theta})-V\cdot\underline{S}_r\cdot W_{\sup}\cdot f_W(\underline{\theta}) \tag{8}$$

and:

$$V\frac{d(\underline{C}_b\cdot\underline{\theta})}{dt}=F_{in}\cdot C_{in}-F_{dr}(\underline{\theta})\cdot C_{dr}(\underline{C}_b,\underline{\theta})-V\cdot\underline{S}\cdot U^*_{\sup}\cdot f_U(\underline{C}_b,\underline{\theta}) \tag{9}$$

In equation 8, W_{sup} is the unrestricted water uptake at sufficient water content throughout and in equation 9, U^*_{sup} is the unrestricted nutrient uptake from the bulk at sufficient water and nutrient content throughout; $f_W(\underline{\theta})$ and $f_U(\underline{C}_b,\underline{\theta})$ are (empirical) functions smaller than or equal to 1. Note that W_{sup} and U^*_{sup} usually will be functions of time. Equations 8 and 9 are more general than equations 6 and 7. Equations 6 and 7 are encompassed via the following relationships:

$$f_W(\underline{\theta})=1,\forall\underline{\theta}\quad\text{and}\quad f_U(\underline{C}_b,\underline{\theta})=1,\underset{i}{\forall}C_{b,i},\underline{\theta}$$

Steady state conditions for the macroscopic balances

Equations 8 and 9 lead to the following macroscopic conditions to obey, in order to achieve steady state:

$$0=F_{in,ss}-F_{dr,ss}(\underline{\theta}_{ss})-V\cdot S_r\cdot W_{\sup,ss}\cdot f_W(\theta_{ss})$$

$$0=F_{in,ss}\cdot C_{in,ss}-F_{dr,ss}(\underline{\theta}_{ss})\cdot C_{dr,ss}(\underline{C}_{b,ss},\theta_{ss})-V\cdot S_r\cdot U^*_{\sup,ss}\cdot f_U(\underline{C}_{b,ss},\underline{\theta}_{ss})$$

Multiplying the first equation by $C_{dr,ss}$ and subtracting the second leads to the alternative steady state condition:

$$0=F_{in,ss}\cdot(C_{dr,ss}-C_{in,ss})-V\cdot S_r\cdot(W_{\sup,ss}\cdot f_{W,ss}\cdot C_{dr,ss}-U^*_{\sup,ss}\cdot f_{U,ss})$$

This leads to the interpretation: If the purpose of the control is to assure growth that is unrestricted by nutrient (un)availability, then it needs to ensure that:

$$f_{W,ss}=1\wedge f_{U,ss}=1\wedge[F_{in,ss}\cdot(C_{dr,ss}-C_{in,ss})=V\cdot S_r\cdot(W_{\sup,ss}\cdot C_{dr,ss}-U^*_{\sup,ss})] \tag{10}$$

Time averaged behaviour of the macroscopic balances
For practical reasons, water supply is performed in cycles (Chapter 4). If these cycles are numbered by 1, ... *k*-1, *k*, *k*+1, ... *n*, then each time cycle *k* a pulse of nutrient solution is supplied to the plants. Equation 8 can be written formally as a discrete time equation:

$$V \cdot (\theta_{k+1} - \theta_k) = F^{\wedge}_{in,k} - F^{\wedge}_{dr,k}(\theta) - V \cdot S_r \cdot W^{\wedge}(\theta)$$

Here, $\underline{\theta}_{k+1}$ and $\underline{\theta}_k$ are taken at the same "cycle relative" instant during the cycle (e.g. always at the end of a cycle, so its value is only known after the active status ended), and the ^ indicates cycle-averaged values.
Since $F^{\wedge}_{dr,k}$ depends upon $\underline{\theta}$, keeping $F^{\wedge}_{dr,k}$ constant - as is done with " the constant drain flow controller" (Chapter 4) - ensures maintenance of a certain moisture content (hopefully non-limiting), thus creating a 'cycle-averaged steady state' ($\underline{\theta}_{k+1} - \underline{\theta}_k = 0$) and a control input $F^{\wedge}_{in,k}$ that closely follows the water uptake $V \cdot \underline{S}_r \cdot W^{\wedge}$.
Tuning of this controller requires insight in the transfer dynamics from $F^{\wedge}_{in,k}$ to $F^{\wedge}_{dr,k}$, which can either be obtained from system identification by means of experiments, or from a detailed hydraulic model. The question may be raised, if a similar strategy for the nutrients can be considered. When equation 9 is averaged over one nutrient cycle, it yields:

$$V \cdot [(\underline{C}_b \cdot \underline{\theta})_{k+1} - (\underline{C}_b \cdot \underline{\theta})_k] = [F_{in} \cdot C_{in}]^{\wedge}_k - [F_{dr}(\underline{\theta}) \cdot C_{dr}(\underline{C}_b, \underline{\theta})]^{\wedge}_k - V \cdot S_r \cdot U^{*\wedge}_k$$

Redefining the terms as:
$M = V \cdot \underline{C}_b \cdot \underline{\theta}$, the molar mass in the substrate slab [mol] and $Q = F \cdot C$, the molar mass flow [mol·s^{-1}], then it holds:

$$M_{k+1} - M_k = Q^{\wedge}_{in,k} - Q^{\wedge}_{dr,k} - V \cdot S_r \cdot U^{*\wedge}_k$$

Following the same reasoning as with the water controller:
Keep the cycle-averaged molar flow out of the drain constant at a sufficiently high level, while at the same time maintaining sufficient water content using the "constant drain flow" controller, will ensure a certain bulk concentration in the system. Thus, the left-hand side tends to zero, and the control - i.e. the molar mass flow coming in - closely follows the demand. Tuning of this controller requires insight in the transfer dynamics from $Q^{\wedge}_{in,k}$ to $Q^{\wedge}_{dr,k}$, which can either be obtained from system identification by means of experiments, or from a detailed nutrient distribution model.
Remark: Both the water controller and the nutrient controller require that the drain water flow and drain molar flow be kept at a sufficiently high level, in order to prevent limitations during the cycle of solute supply pulses. In fact, this requirement may be more difficult to meet in strongly dynamic conditions, e.g. during strong evaporation or high nutrient demand periods. Apart from experiments, microscopic modelling may shed some light on this issue.

Microscopic balances
The process to be controlled is the uptake of water and nutrients by the root, by a complete or partial supply of the demand of the plant.
The roots find their source of water and nutrients in the direct vicinity, the boundary layer around them. Apart from the overall or macroscopic ion balances, it is important to know the relations that govern the microscopic balances in the direct neighbourhood of the root. Barber (1962) presents a succinct and mechanistic approach to the contribution of mass-flow and the different diffusion and dispersion processes to the movement of ions towards the roots. As a conclusion, he distinguishes different processes influencing ion movement (Figure 5):

1. ion exchange due to diffusion between soil/substrate solution and root surface
2. exchange of ions due to direct diffusion between substrate particles and root surface
3. mass-flow from nutrient solution to root surface
4. replenishment/accumulation by ion diffusion between substrate particles and nutrient solution
5. replenishment from outside the growing system

In Figure 5, C_1 is ion concentration in the solution, C_2 and C_4 at the soil/substrate surface and C_3 in the mass-flow [all C's: mol·m^{-3}]. D_1, D_2 and D_4 are the diffusion coefficients of the diffusion processes from solution to root surface and from particle into solution respectively [m^2·s^{-1}]. R [m^3·s^{-1}] is the replenishment of water and nutrients from outside and W is mass-flow through the growing medium (Barber, 1962). The over-drain F_{dr} (added by the author) flushes water and nutrients out of the soil/substrate to the drain.

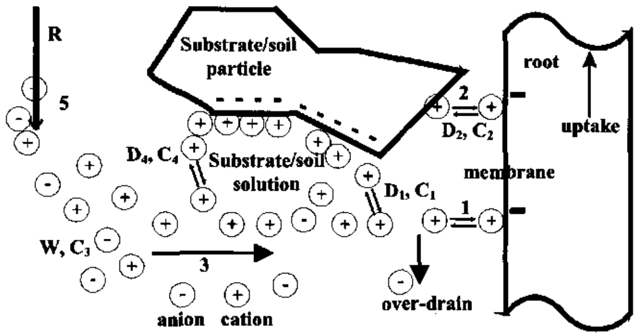

Figure 5 - Processes 1 through 5 are involved in the movement of ions from the growing medium to the root surface (after Barber, 1962). In this figure over-drain is added by the author.

The influence of each of these processes may overshadow the other ones, depending on the plant species and the growth stage of the plant. In an open growing system, or a closed growing system with over-drain, extra nutrient solution is supplied that carries-in extra nutrients or washes out accumulated ions.
In order to build models that describe the dynamics in the movement of ions to the root surface, the diffusion processes and the process of mass-flow and over-drain are of importance. This is the more so, if the drain flow and drain concentration is taken as an indicator for the uptake process of water and nutrients.

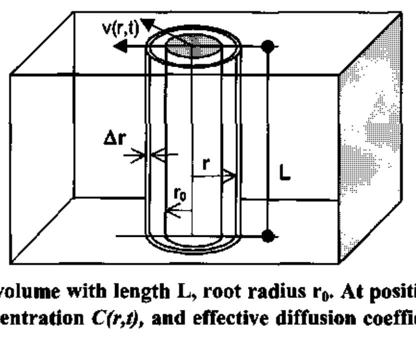

Figure 6 - Root hair in control volume with length L, root radius r_0. At position r: water flow $v(r,t)$, moisture content $\theta(r,t)$ nutrient concentration $C(r,t)$, and effective diffusion coefficient $D(\theta_v)$ and radial expansion of r with Δr.

Consider the transport in the neighbourhood of a cylindrical root, which can be a virtual root that lumps the root hair effects (Figure 3 and 6). Define all transport positives $v(r,t)$ in the positive r direction, outward from the root centre (Figure 6).

The water balance derivation:
The change over time at each position $r > r_0$ of the volumetric water content of the control volume (Figure 6):

$$2\pi r \cdot \Delta r \cdot L \frac{\partial \theta(r,t)}{\partial t} = -v(r+\Delta r) \cdot 2\pi \cdot (r+\Delta r) \cdot L + v(r) \cdot 2\pi r \cdot L$$

Where: L is the length of the root, and $v(r)$ the water flow velocity at distance r. When $2\pi r \cdot L$ and Δr are divided out it holds:

$$\frac{\partial \theta(r,t)}{\partial t} = \lim_{\Delta r \to 0} \left\{ -\frac{v(r+\Delta r,t) - v(r,t)}{\Delta r} - \frac{1}{r} \cdot \frac{v(r+\Delta r,t) \cdot \Delta r}{\Delta r} \right\} = -\frac{1}{r} v(r,t) - \frac{\partial}{\partial r} v(r,t)$$

At the root surface (where $r = r_0$), the flow is equal to the water uptake, i.e. the boundary condition at $r = r_o$ is:

$$-2\pi r_0 \cdot L \cdot v(r_0,t) = 2\pi r_0 \cdot L \cdot W(t) \quad \Leftrightarrow \quad v(r_0,t) = W(t).$$

Therefore, the water balance including the boundary condition is:

$$\frac{\partial \theta(r,t)}{\partial t} = -\frac{v(r,t)}{r} - \frac{\partial v(r,t)}{\partial r} \qquad \textbf{(11)}$$

Boundary condition: $r = r_o$ $\quad v(r_o,t) = W(t)$ **(12)**

The nutrient balance derivation:
The change over time at each position $r > r_0$ of the volumetric molar (nutrient) content of the control volume (Figure 6) is:

$$2\pi r \cdot \Delta r \cdot L \cdot \frac{\partial \{\theta(r,t) \cdot C(r,t)\}}{\partial t} = -2\pi \cdot (r+\Delta r) \cdot L \cdot v(r+\Delta r) \cdot C(r+\Delta r) + 2\pi \cdot r \cdot L \cdot v(r) \cdot C(r) +$$
$$+ D(\theta_{r+\Delta r}) \cdot 2\pi \cdot (r+\Delta r) \cdot L \cdot \left.\frac{dC}{dr}\right|_{r+\Delta r} - D(\theta_r) \cdot 2\pi \cdot r \cdot L \cdot \left.\frac{dC}{dr}\right|_{r}$$

Dividing out $2\pi\, r \cdot L$ and Δr leads to:

$$\frac{\partial \{C(r,t) \cdot \theta(r,t)\}}{\partial t} = \lim_{\Delta r \to 0} \frac{-(r+\Delta r) \cdot v(r+\Delta r) \cdot C(r+\Delta r) + r \cdot v(r) \cdot C(r) + D(\theta_{r+\Delta r}) \cdot (r+\Delta r) \cdot \left.\frac{\partial C}{\partial r}\right|_{r+\Delta r} - D(\theta_r) \cdot r \cdot \left.\frac{\partial C}{\partial r}\right|_{r}}{r \cdot \Delta r}$$

After algebraic manipulation it holds:

$$\frac{\partial\{C(r,t)\cdot\theta(r,t)\}}{\partial t}=\lim_{\Delta r\to 0}\left[-\frac{v(r+\Delta r,t)\cdot C(r+\Delta r,t)-v(r,t)\cdot C(r,t)}{\Delta r}+\right.$$

$$\left.+\frac{D\{\theta(r+\Delta r,t)\}\cdot\left.\frac{\partial C}{\partial r}\right|_{r+\Delta r}-D\{\theta(r,t)\}\cdot\left.\frac{\partial C}{\partial r}\right|_{r}}{\Delta r}-\frac{v(r+\Delta r)\cdot C(r+\Delta r)}{r}+\frac{D(\theta_{r+\Delta r})\cdot\left.\frac{\partial C}{\partial r}\right|_{r+\Delta r}}{r}\right]$$

and:

$$\frac{\partial\{C(r,t)\cdot\theta(r,t)\}}{\partial t}=-\frac{1}{r}\left\{v(r,t)\cdot C(r,t)+D\{\theta(r,t)\}\cdot\frac{\partial C(r,t)}{\partial r}\right\}-\frac{\partial}{\partial r}\left\{v(r,t)\cdot C(r,t)-D\{\theta(r,t)\}\cdot\frac{\partial C(r,t)}{\partial r}\right\} \qquad \textbf{(13)}$$

In equation 13 the change in time of the nutrient content of a control volume due to water and nutrient uptake is written as function of the radial distance from the root surface. At the root surface *($r = r_o$)* the nutrients transported by flow and diffusion towards the root surface must equal the uptake, assuming no capacity for storage at the surface, which results in:

$$-2\pi r_0\cdot L\cdot v(r_0,t)\cdot C(r_0,t)-D\{\theta(r_0,t)\}\cdot 2\pi r_0\cdot L\cdot\left.\frac{\partial C(r,t)}{\partial r}\right|_{r_0}=2\pi r_0\cdot L\cdot U(t),\quad \text{or:}$$

$$U(t)=W(t)\cdot C(r_0,t)-D\{\theta(r_0,t)\}\cdot\left.\frac{\partial C(r,t)}{\partial r}\right|_{r_0}$$

$\frac{\partial\{C(r,t)\cdot\theta(r,t)\}}{\partial t}$ expands to: $\theta(r,t)\cdot\frac{\partial C(r,t)}{\partial t}+C(r,t)\cdot\frac{\partial\theta(r,t)}{\partial t}$

So, equation 13 can be rewritten (for reason of simple notation, the function arguments *r* and *t* are left out):

$$\theta\frac{\partial C}{\partial t}+C\frac{\partial\theta}{\partial t}=-\frac{v.C}{r}+\frac{D}{r}\cdot\frac{\partial C}{\partial r}-C\frac{\partial v}{\partial r}-v\frac{\partial C}{\partial r}-\frac{\partial(D\cdot\frac{\partial C}{\partial r})}{\partial r}$$

Substitution of the water balance relation of equation 11: $\frac{\partial\theta}{\partial t}=-\frac{v}{r}-\frac{\partial v}{\partial r}$ and replacing of

$\frac{\partial(D\cdot\frac{\partial C}{\partial r})}{\partial r}$ by $\frac{1}{r}\cdot\frac{\partial(D\cdot r\cdot\frac{\partial C}{\partial r})}{\partial r}+\frac{D}{r}\cdot\frac{\partial C}{\partial r}$ and some additional algebraic manipulation leads to:

$$\theta(r,t)\cdot\frac{\partial C(r,t)}{\partial t}=-v(r,t)\cdot\frac{\partial C(r,t)}{\partial r}+\frac{1}{r}\cdot\frac{\partial}{\partial r}\left(D_r\cdot r\cdot\frac{\partial C(r,t)}{\partial r}\right) \qquad \textbf{(14)}$$

$$\textit{boundary condition } r=r_0: U(t)=W(t)\cdot C(r_0,t)+D(\theta(r_0,t))\left.\frac{\partial C(r,t)}{\partial r}\right|_{r_0} \qquad \textbf{(15)}$$

U and *W* positive if transport towards the roots, ∂ measured outwards.

It should be noted that D_r depends on r, because it depends upon $\theta(r)$. The effects of time variations in D are ignored in the derivation. Furthermore, the equations do not consider non-radial flow or non-radial diffusion in de boundary area.
Equations 11 and 14 could be solved analytically for idealised boundary and initial conditions. An example can be found in Passioura (1963), who solves the equation (without considering the variation in water content) from an initial uniform system without through flow (no drain).
The equations could also be solved numerically in conjunction with the macroscopic balances, but then additional assumptions are needed. The steady state profiles would be of interest, as well as the impulse response.
The boundary condition of equation 15 is important. It shows that if: $W(t) \cdot C(r_o, t) = U(t)$ (so if Uptake = Mass-flow), there is no gradient towards the root and also no diffusion term. Its importance is found in the control strategy that can be derived from it, as is shown below in the last section of this paragraph.

Approximation of the diffusion term in the microscopic balance
The diffusive flux in one dimension at the root boundary can be expressed in terms of the concentration difference between the bulk and the root surface.
Formally expressed as Fick's first law (Fick, 1855):

$$Q_{diffusive} = -D \cdot \frac{\partial C}{\partial x}$$

Here, the minus sign means that diffusion takes place in the direction of decreasing concentration. In the case of Figure 6, r is taken outwards positive and $C_b > C_{ro}$, which means that the flux towards the roots is:

$$Q_{diffusive} = D_{r_0} \left. \frac{\partial C}{\partial r} \right|_{r_0} = \frac{D_{r_0}}{\delta} \cdot (C_b - C_{r_0})$$

In fact, this substitution merely defines the boundary layer thickness, which is a complicated function of the past.

Passioura's derivation (1963) for instationary diffusion as a function of time shows a similar appearance:

$$D_{r0} \left. \frac{\partial C}{\partial r} \right|_{r0} = \frac{D_{r0} \cdot f}{r_0} \cdot (C_b - C_{r0})$$

Here f is a monotonically decreasing function of $D_{ro}T/r_o^2$, where T is the time elapsed since the constant initial bulk concentration was applied. Typical values for f are 2.7 for very short times to 0.6 for long times. This suggests that $\delta = r_o/f$ is time variant but in the same order of magnitude as the root radius. The use of this expression via equation 15 allows linking of C_b and C_{ro}:

$$W \cdot C_{r0} + (C_b - C_{r0}) \frac{D_{r0} \cdot f}{r_0} = U \qquad \textbf{(16)}$$

Equation 16 can be rewritten as:

$$U = \left[W - \frac{D_{r0} \cdot f}{r_0} \right] \cdot C_{r0} + \frac{D_{r0} \cdot f}{r_0} \cdot C_b \qquad \textbf{(17)}$$

Equation 17 expresses what C_{ro} will prevail at a given uptake and a given bulk concentration after a while. Figure 7 and 8 represent a plot of uptake U versus C_{ro} as straight lines as function of changes in W and of C_b.
If water uptake W increases, and nutrient uptake U remains unchanged, then the slope of the line in Figure 7 increases. The slope is negative, as depicted in Figure 7, if $D_{r0} \cdot f \cdot r_0^{-1} > W$, which is normally the case. $D_{r0} \cdot f \cdot r_0^{-1}$ is in the order of 10^{-2} [$m \cdot s^{-1}$], while W is in the order of 10^{-7}-10^{-10} [$m^3 \cdot m^{-2}_{root\ surface} \cdot s^{-1}$]). The concentration at the root surface (C_{ro}) will increase due to increased mass-flow.

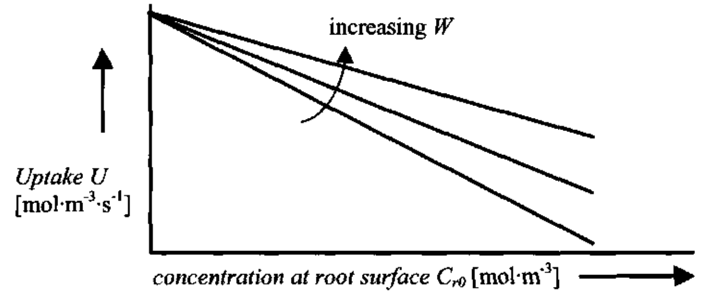

Figure 7 - A straight line represents the relationship between uptake and concentration at the root surface according to equation 17. Increase of mass-flow, by the increase of *W* will increase the slope of the line.

For various values of C_b equation 17 represents a set of parallel straight lines (Figure 8). The triplet W, D_{ro}, C_b will cause a line with a certain slope and intercept. Increase of C_b will create a set of parallel straight lines, each with their own characteristic intercept.

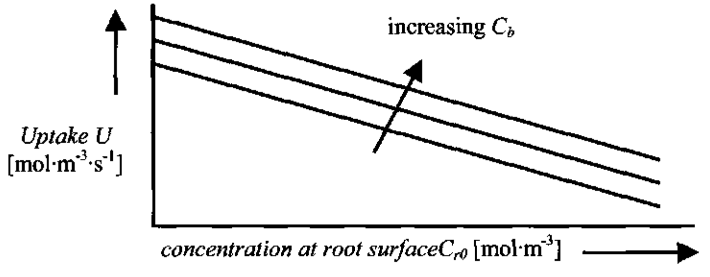

Figure 8 - Increase of C_b will create a set of parallel straight lines, each with their own intercept.

Furthermore, several authors (Barber, 1962; Passioura, 1963; Wild *et al.* 1979) stated, that for some ions nutrient uptake can be related to the concentration at the root surface by a Michaelis-Menten type of expression:

$$U = \frac{(C_{r0} - C_{r0,\min}) \cdot U_{\max}}{k_m + (C_{r0} - C_{r0,\min})}$$; Michaelis-Menten equation, can be rewritten as: **(18a)**

$$(U - U_{\max}) \cdot (C_{r0} - [C_{r0,\min} - k_m]) = -k_m \cdot U_{\max}$$, and is of the form: **(18b)**

$$(y - y_0) \cdot (x - x_0) = -1/2 \cdot a^2$$ **(18c)**

Equation 18c, as a conic section, is an orthogonal hyperbole in the x_0,y_0-plane. The minus sign in de right-hand term of equation 18c indicates that the two function branches are in the second and fourth quadrant of the x_0,y_0-plane. (x_0,y_0) is the point of intersection of the asymptotes of the orthogonal hyperbole and a the shortest distance from (x_0,y_0) to each function branch (Figure 9).

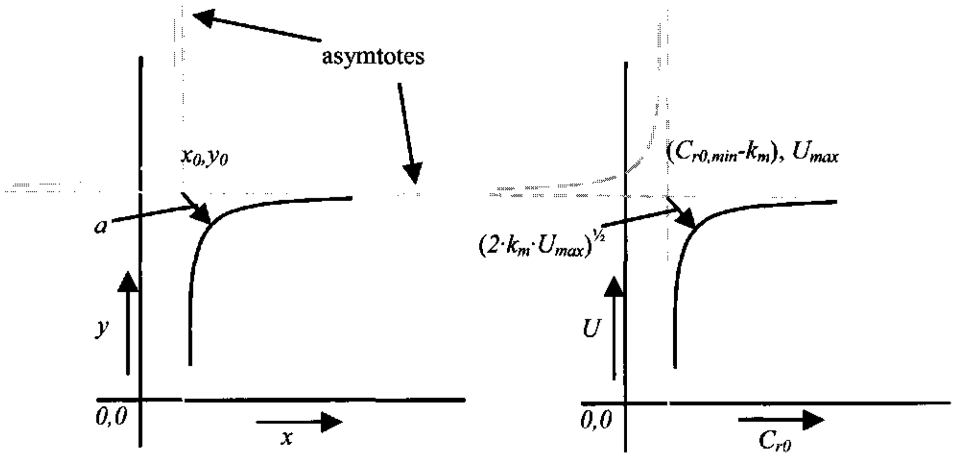

Figure 9 – Representations of equation 18. In real water- and nutrient supply systems only values in the first quadrant of the *x,y* -plane ($C_{r0} \geq C_{r0,min}-k_m$) and ($0 \leq U \leq U_{max}$) have a physiological meaning.

The physiological meaning of the asymptotes of the function in equation 18b is:

$U = U_{\max}$ and $C_{r0} = C_{r0,\min} - k_m$

Figure 10 shows a representation of equation 18, the nutrient uptake U as a function of concentration C_{ro} at the root surface. It shows how much the uptake is impaired with respect to the uninhibited U_{max}, where U_{max} corresponds to the needs of unrestricted crop growth (here, unrestricted means unrestricted availability of nutrients). Moreover, Figure 10 shows that the uptake is almost independent of root concentration in a large range of C_{ro}. Only at low values of C_{ro}, in the neighbourhood of $C_{r0,min}$, a concentration change will influence the uptake.
The status of the plant (health, phase) will determine the position of the curves I or II (potential growth rate). The photosynthesis (micro-climate, global radiation, CO_2 uptake) will determine the actual demand. The value of C_{r0} and the effectiveness of the ion transfer processes in the root membrane determine the actual uptake.

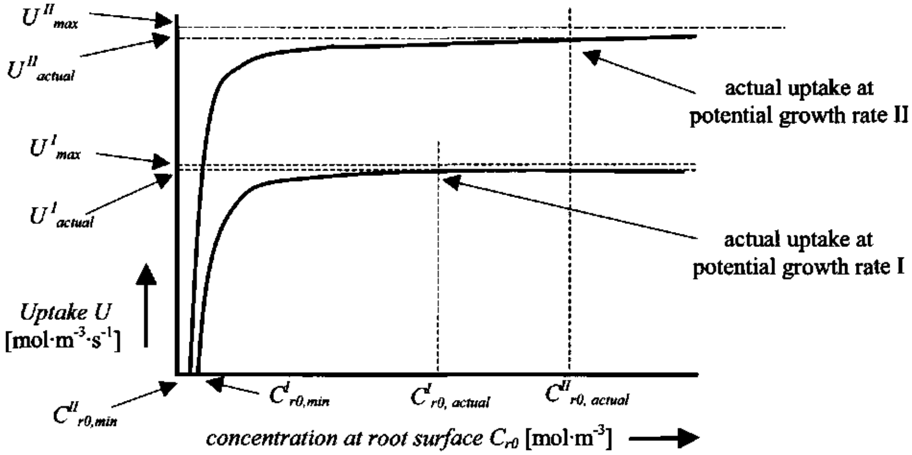

Figure 10 - Uptake U as function of ion concentration at the root surface C_{r0} according to equation 18, at two different Michaelis-Menten curves belonging to plant potential growth rate I and II.

When the uptake of equation 17 is set equal to the kinetic expression of equation 18 (Figure 11), an indication of the demand for a C_{ro} value will result. The intersection point of the line expressing the availability of nutrients in the substrate at the root surface due to the pair (D_{r0}, W), and the curve expressing the demand range in relation to the plant's status and its growth rate, will mark the actual C_{r0}.
At the intersection point C_b and W determine the available nutrients for uptake. The growth rate of the plant determines the demand for nutrient uptake U.
Nutrient limitation can be enforced by manipulating the value of C_b, but equation 17 shows that the extend depends upon the water uptake.

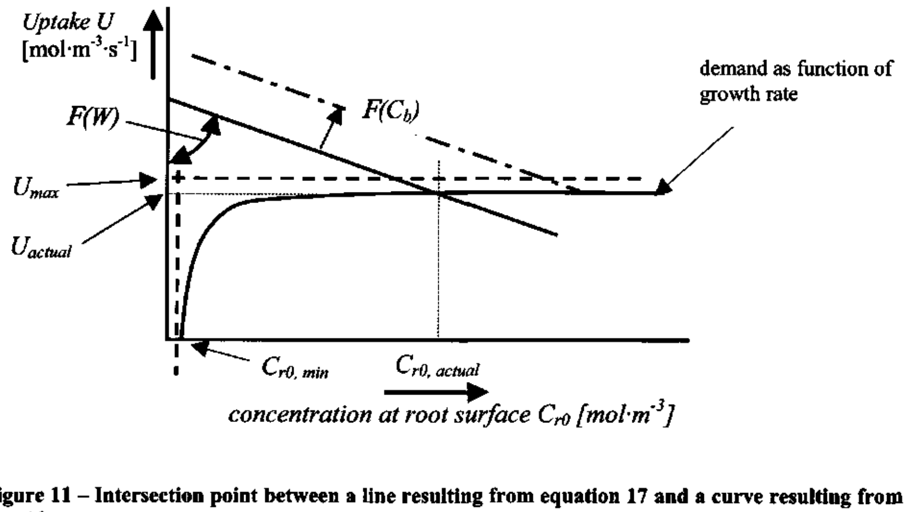

Figure 11 – Intersection point between a line resulting from equation 17 and a curve resulting from equation 18.

Conversely, the graph may help to show which values of C_b do not cause nutrient inhibition. Furthermore, Figure 11 shows that the plant can take up nutrients at a rate of U_{actual} with C_{r0} at $C_{ro,actual}$ at its potential growth rate (determined by plant status, actual photosynthesis, actual temperature and actual transpiration).
As is apparent from the intersections of the C_b set of lines with curve II in Figure 12, C_b can only be used to influence uptake, if C_{r0} is in the neighbourhood of $C_{r0,min}$. If the intersection point is in the C_{ro}>>$C_{ro,min}$ region, Figure 12 curve I shows that variation of C_{ro} does not cause a change of uptake U.

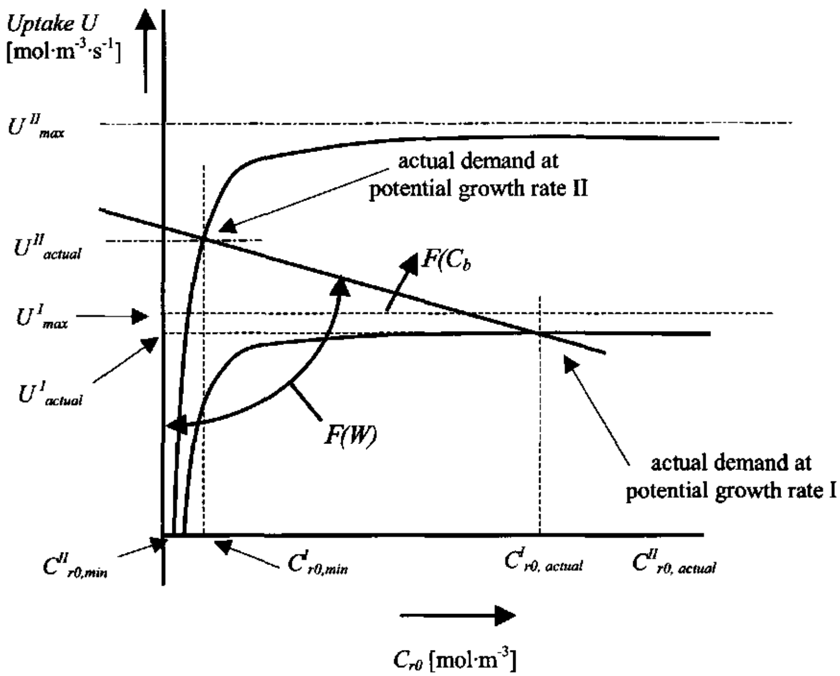

Figure 12 - Combining Figures 7 till 10 shows that C_b can only be used to influence uptake if C_{r0} is in the neighbourhood of $C_{r0,min}$, as is apparent from the intersections of the C_b set of lines with curve I and II.

The significance of equation 17 is that it can be used to estimate whether a particular bulk concentration will lead to concentrations at the root surface at which uptake might be impaired. Working out equation 17 for C_{ro} leads to:

$$C_{r0} = \frac{\frac{D_{r0} \cdot f}{r_0} \cdot C_b - U}{\frac{D_{r0} \cdot f}{r_0} - W} \qquad \textbf{(19)}$$

Define an influx concentration $C_x = U \cdot W^{-1}$. Then U can be eliminated: $U = C_x \cdot W$, leading to:

$$C_{r0} = \frac{\frac{D_{r0} \cdot f}{r_0} \cdot C_b - W \cdot C_x}{\frac{D_{r0} \cdot f}{r_0} - W} \quad \text{and} \quad C_x = C_{r0} + \frac{D_{r0}}{r_0} \cdot \frac{f}{W} \cdot (C_b - C_{r0}) \tag{20}$$

The (virtual) influx concentration C_x is determined by the demands of the plant. Suppose we could make $C_b = C_x$. Then the concentration at the root surface C_{ro} will become equal to C_b and there is no concentration gradient towards the root. Diffusion will not play a part.
Note, however, that there is no freedom in choosing C_x: the plant determines the "no-diffusion value"! It is not clear (yet) whether this will always be a value at which no nutrient limitation occurs. For instance, in situations with a high evaporation, C_x may become low enough to bring the uptake U in limiting ranges.

Combining macroscopic and microscopic steady state conditions
Assume a true steady state, containing the steady state version of equation 19:

$$C_{r0,ss} = \frac{\left[\frac{D_{r0} \cdot f}{r_0}\right]_{ss} \cdot C_{b,ss} - U_{ss}}{\left[\frac{D_{r0} \cdot f}{r_0}\right]_{ss} - W_{ss}},$$

and from equation 10: $F_{in,ss} \cdot (C_{dr,ss} - C_{in,ss}) = V \cdot S_r \cdot (W_{sup,ss} \cdot C_{dr,ss} - U^*_{sup,ss})$ the steady state mass balance:

$$F_{in,ss} \cdot (C_{dr,ss} - C_{in,ss}) = V \cdot S_r \cdot (W_{ss} \cdot C_{dr,ss} - U^*_{ss})$$

If $U^* = U$ (i.e. no hold-up variations in the boundary layer), then this leads to:

$$C_{r_0,ss} = \frac{-F_{in,ss} \cdot (C_{in,ss} - C_{dr,ss}) + V \cdot S_r \cdot \left[W_{ss} \cdot C_{dr,ss} - \left(\frac{D_{r0} \cdot f}{r_0}\right)_{ss} \cdot C_{b,ss}\right]}{V \cdot S_r \cdot \left[W_{ss} - \left(\frac{D_{r0} \cdot f}{r_0}\right)_{ss}\right]} \tag{21}$$

Further simplification needs another assumption: $C_{dr,ss} \approx C_{b,ss}$. Then this results in:

$$C_{r_0,ss} = \frac{-F_{in,ss} \cdot (C_{in,ss} - C_{dr,ss}) + V \cdot S_r \cdot C_{dr,ss} \cdot \left[W_{ss} - \left(\frac{D_{r0} \cdot f}{r_0}\right)_{ss}\right]}{V \cdot S_r \cdot \left[W_{ss} - \left(\frac{D_{r0} \cdot f}{r_0}\right)_{ss}\right]} \tag{22}$$

The interpretation of the above is: if the controller tries to realise an incoming concentration equal to the drain concentration $C_{in,ss} = C_{dr,ss}$, then under the assumption $C_{dr,ss} \approx C_{b,ss}$, the steady state root concentration $C_{ro,ss}$ will be equal to the drain concentration $C_{dr,ss}$, and no diffusion limitation can occur. Under this assumption, also equation 22 holds. It shows that the plant will determine the level of fulfilment. And as said before, this need not always be an optimal non-limiting case, since the latter depends upon the ratio of nutrient uptake and evaporation.

Remark: The settings of this controller must be derived from the dynamics of the transfer between $C_{in,ss}$ and $C_{dr,ss}$. This can be done either experimentally or by model simulations under additional assumptions, which need to be verified by experiments.

3. Conclusions

If the nutrient uptake U goes up, the mass flow needs to remain according to the plant's need, even if the bulk concentration C_b is kept the same. In that case, the concentration at the root will go down. Thus, a higher uptake will be supported by a higher diffusive flux through the boundary layer. Since uptake is not dependent on C_{ro} (Figure 12), it will continue at the same level of fulfilling the plant's needs until C_{ro} reaches C_{limit}. Uptake limitation will only occur when C_{ro} drops below this critical concentration. Macroscopically, the following might happen: a higher diffusive flux will lead to a drop in bulk concentration when the incoming concentration C_{in} remains the same. This, in turn, will reduce the mass flow, leading to the necessity of even larger diffusive flux, and an excessively increasing drop in root surface concentration. The conclusion is that the system is becoming unstable, and nutrient uptake limitations will inevitably occur. The same conclusion can be derived from the overall mass balance of the system as a whole.

From a control point of view, this situation can be detected by observing the drain concentration, and be remedied by increasing the incoming concentration. Therefore, the natural question arises whether the drain concentration should be regulated to a constant value, by manipulating the incoming concentration, similar to how the water supply controller aims at keeping the drain solute flow constant.
Suppose U increases, and increasing C_{in} such, that the drain concentration (and bulk concentration) was kept constant, counteracted this. Although this will lead to a new steady state, this steady state will have to be with a higher diffusive flux, which still is possible only when the root surface concentration is lower. And, consequently, a limitation might occur. Equation 16 may be used to obtain a crude check about this situation (setting $C_b = C_{dr}$).

A strategy that will avoid this, ensures that the diffusive flux towards the roots is zero, so that the nutrients are carried to the plant by the mass flow. This can be achieved microscopically if $C_{ro} = C_b = C_x$, provided that $C_{ro} > C_{limit}$, and macroscopically, if $C_{in} = C_{dr} = C_x$. There are two situations:

- suppose information is available about W - for instance from evaporation measurements - and about U, for instance by a growth model. Then, C_x can be computed, and C_{in} could be set accordingly.
- the other approach would be to increase C_{in} proportional to the difference between C_{in} and C_{dr}, until $C_{dr} = C_{in}$. Although these control strategies have the desired overall static behaviour, it should be noted that their dynamic properties still need to be evaluated.

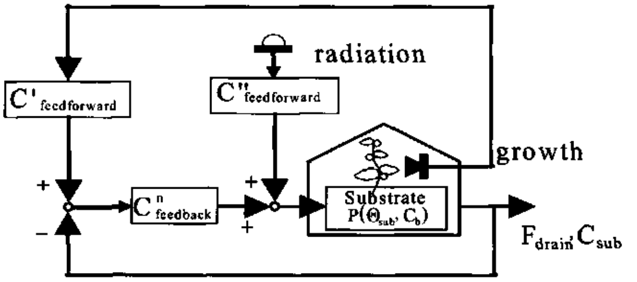

Figure 13 - Feed forward and feedback actions.

In particular, it can be expected that the first approach may lead to the necessity of frequent C_{in} adjustments, in view of the large fluctuations of the water uptake over a day. Perhaps this can be remedied by averaging the flow fluctuations over a day. The second control approach has a positive feedback, which may lead to instability. An upper limit to C_{in} may perhaps be employed to avoid this. In both cases, the short-term dynamic effects, plus the gradients in the substrate slab, may still cause temporary limiting conditions for uptake. This can only be investigated by using more sophisticated models of the behaviour of water and nutrients in the substrate. Feed forward action for water supply should be derived from transpiration (radiation) and for nutrient application from growth rate (Figure 13).

CHAPTER 3

SENSORS IN HORTICULTURE

§3.1 SENSORS AND MEASUREMENT

§3.2 CHEMFETS TO MONITOR ION CONCENTRATION

§3.1 Sensors and measurement

Based on:
Sensors and measurement. In: *Acta Hort. 421*. Th.H. Gieling and K. Schurer, 1995a.
Sensors and measurement. In: J.C. Bakker, G.P.A. Bot, H. Challa, N.J. van de Braak (Eds.) *Greenhouse Climate Control, an integrated approach*. Wageningen Pers, 279p. Th.H. Gieling and K. Schurer, 1995b.

1. Introduction

Present developments in horticulture are towards the use of automated systems for both control and management of crop growth. These can range from classical temperature control systems to expert systems for strategic planning based on growth models and economic outlooks. These systems require as input a continuous flow of quantitative data. Most of these data result from measurements of physical, chemical or physiological phenomena in and around the greenhouse. The continuous measurement of an increasing number of quantities requires the use of sensors with an electrical output, connected to an automatic data acquisition system. Existing sensors have to be modified and new sensors have to be developed to suit these new requirements. Improved methods of measurement and newly emerging semiconductor technologies result in better and/or cheaper sensors. Moreover, these methods and technologies provide opportunities to adapt sensors to the specific requirements of horticulture. Opportunities are found in improvements in classical measurement methods with extra features and options like digital output, smaller dimensions, lower cost and higher reliability, as well as in the development of hitherto not existing sensors.

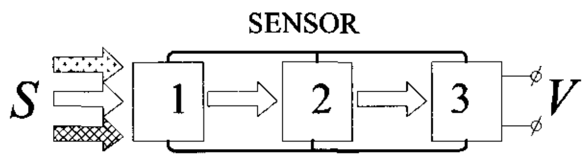

Figure 1 - *S* = signal, *V* = output signal, 1 = selector, 2 = transducer, 3 = detector

The word '*sensor*' has been created in American English to describe the device that performs a 'sense' action. A sensor incorporates three different functions: to select the information sought from an abundance of information offered, to transduce the information into a measurable form and to detect the signal (Figure 1). As an example consider an infrared radiation sensor, where a filter acts as the *selector* (1) and only admits the infrared part of the whole radiation spectrum to increase the temperature of a blackened *transducer* (2). The temperature rise is then converted into an electrical signal by a thermopile *detector* (3).

1.1 Sensor calibration

The relationship between V and S often cannot be described by simple laws of physics. Consequently, an empirical relationship is determined: the function $V = f(S)$ is found from a calibration action. The result of calibration can change over time. To ensure a lasting reliability of

measured values, a scheme of calibrations has to be established, with due regard to the severe conditions imposed on equipment by the greenhouse climate.
In horticulture, sensors are used to measure quantities in fields like local meteorology, indoor greenhouse climate, water and nutrient supply and feedback from greenhouse appliances (ventilators, valves, screens etc.).The position of the sensor is of importance, especially when measuring climate conditions. Horizontal and vertical gradients are intrinsic to all climate variables, both inside and outside a greenhouse. The greenhouse climate is characterised by moderate temperatures, a high to very high humidity, an intense solar radiation and little air movement. The last three circumstances make the measurement of air temperature and air humidity a not straight forward.

1.2 The 'meteo-station'

In The Netherlands, on top of most greenhouses one finds an outdoor measuring set-up. These are equipped with meteorological instruments like air temperature and air humidity sensors in a measuring box. The box should provide adequate shielding from solar radiation and rain (Visscher and Schurer, 1995). A standard so-called "meteo-station" also contains a radiation sensor, a precipitation sensor and sensors for wind direction and wind speed. In some cases, a sensor is installed for measuring the outdoor CO_2 level as well.
The meteo-station itself ranges from a yoke-like support on top of the ridge of the greenhouse roof, to a sophisticated weather station on a tower. Care has to be taken that the sensors are easily accessible for preventive maintenance (cleaning of sensors and refilling the water reservoir). To get good results from measuring outdoor climate variables, it is important to position the meteo-sensors correctly. The most important points of interaction between indoor and outdoor climate are the ventilators in the greenhouse roof. Consequently, it is of considerable importance that the measurements are made at a level about at the height of the greenhouse roof, rather than trying to keep international standard heights for meteorological measurements (WMO, 1971).
Disturbing influences have to be taken care of in positioning the sensors: the boiler chimney, a tree or a nearby building can cause problems such as local increase in temperature and CO_2, or the overshadowing of the radiation sensor. Care should be taken that the sensors are at a fair distance from the ventilators to avoid artefacts introduced by measuring greenhouse exhaust air.

2. Overview on sensors in horticulture

2.1 Climate related sensors

Air temperature
Sensors for temperatures are often of the resistor type. In horticultural practice platinum sensors according to DIN-IEC 751 and standard ceramic NTC sensors (thermistors) are used. In research mainly Pt100, Pt500, Pt1000 are used. To minimise the heat conductance from the temperature sensor to the wall of the measuring box, the casing of the temperature sensor should preferably be of thin-walled and elongated glass or ceramic tubing. The heat conductivity of these materials is fairly low compared to the metal casing of some heavy-duty industrial sensors. With air temperature measurements the uncertainty of the sensors should not exceed +/-0,3 °C. For platinum resistors the optimum choice is a tolerance one third of that of DIN-IEC 751 class B. To prevent the cable resistance from playing a role in the reliability of

the resistance measurement, it is good practice to use a four-wire connection between the resistance sensors and the measuring electronics (Figure 2). One pair of wires is used to conduct the measuring current from a current source to the resistance sensor. The other pair of wires is used to connect the measured voltage across the resistance sensor to a differential instrumentation amplifier with high input impedance. The value of the measuring current is derived from the voltage across a reference resistor in series with the temperature sensor.

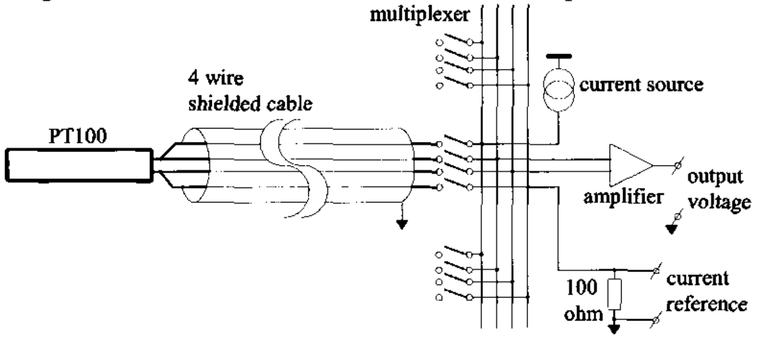

Figure 2 - Four wire connections to resistance sensors for temperature.

The value selected for the measuring current is about 1 mA for Pt100 and Pt500, to keep the influence on accuracy of self-heating of the sensor within the uncertainty limits. A current of 0,2 mA should not be exceeded for the high resistance NTC sensors. Often the current is just switched on for a few milliseconds during the actual measurement. This permits a higher value of the measuring current and hence a more reliable signal at the same level of self-heating. Yearly maintenance should include a check on the calibration at two temperatures, e.g. at 0 °C and at ambient.
Thermocouples are only used in research, especially when temperature has to be measured in places with little heat-capacitance or if a temperature difference should be measured. Examples are: a set of thermocouples to measure the difference between air temperature and leave temperature of a plant, or temperature difference between inside and outside air across the glass pane.

Humidity
The greenhouse climate is characterised by moderate temperatures, a high to very high humidity, an intense solar radiation and little air movement. The last three factors make the measurement of humidity complex. Usually sensors for air temperature and humidity are mounted in a ventilated box (Gieling and Schurer, 1995). Two types of humidity sensors are in common use in Dutch greenhouses. Most widespread is the dry- and wet-bulb instrument or psychro-meter. It has the advantage of sturdiness and reliability. These have long outweighed the amount of labour involved in keeping it going: regularly refilling the water reservoir and replacing the wick. The second type is the thin-film capacitive sensor (Visscher and Schurer, 1985).
The greenhouse climate presents severe conditions for 'electronic' humidity sensors. In fact, of all the situations occurring during growing and storage, only the outdoor climate is still worse. In particular the transition from condensing conditions during the night, with free water on the sensor, to a much lower humidity after sunrise often results in erroneous readings. It is only recently that a choice of sensors able to cope with these conditions has come onto the market. This class of sensors is based on the measurement of the change in capacitance (dielectric constant) of a thin polymer film upon a change in humidity.

CO_2 concentration

Instruments for the continuous monitoring of CO_2 concentration are relatively expensive. It is therefore customary to use a multiplexed sampling system and one analyser. A steady flow of air is maintained in all sampling lines, so that a fresh sample is available the moment a line is connected to the analyser. Sampling lines can best be made from good quality gas-tight tubing, like nylon or high-density polyethylene. The diameter has to be chosen such, that no undue pressure-drop over the length of tubing is required. Attention should be given to possible errors due to pressure differences between the sample in the analyser and the greenhouse atmosphere. Though the result of the determinations is usually presented as a pressure independent volume fraction (expressed as parts per million, ppm), the actual measurement performed is a concentration measurement (in mol/m^3 or sometimes kg/m^3).

Generally, an infrared analyser is used (Long, 1986). Alternatives, such as a conducto-metric or a photo-acoustic measurement have hardly found practical application in Dutch horticulture. Photo-acoustic instruments are in fact very recent; an adaptation for horticultural application has only just become available.

Wind speed and wind direction

Outdoor wind speed is measured with a cup anemometer. Various detectors are used in cup anemometers, such as a tacho generator or a switch giving an on-off signal for every revolution (Hanan, 1984). The on-off signal comes from a mechanically or magnetically operated switch or an interrupted light-beam. Nowadays, an interrupted light-beam type is generally used. Many anemometers show non-linearity errors at low wind velocities and a threshold value due to friction at near zero wind velocity.

The calibration of a cup anemometer should be checked yearly. Special attention should be paid to changes in starting speed, stopping speed and linearity. Wind direction is measured with a wind-vane. The angle is determined from the measurement of the value of a variable resistance or from the read-out of a rotating coded disk (Met.Office, 1969). An interesting

$C = |D - DF_{N-1}|$
    IF ($C < 180$) THEN
        IF ($D \geq DF_{N-1}$) THEN $C = -C$ ENDIF
    ELSE
        $C = 360 - C$
        IF ($D < DF_{N-1}$) THEN $C = -C$ ENDIF
    ENDIF
    IF ($FC \neq 0$) THEN
        $DF_N = D + C \cdot (FC - 1)/FC$
        IF ($DF_N \geq 360$) THEN $DF_N = DF_N - 360$ ENDIF
        IF ($DF_N < 0$) THEN $DF_N = DF_N + 360$ ENDIF
    ENDIF
    $DF_{N-1} = D$

C = change, D = unfiltered wind direction, DF = filtered wind direction, FC = filter constant ($FC \leq 1$), N = this cycle, N - 1 = last cycle.

Frame 1 - Smoothing algorithm for wind direction.

problem occurs when wind direction has to be filtered by a computer algorithm for smoothing a rapidly changing signal. When a signal is changing around the North, e.g. between 350 degrees and 10 degrees (-10 degrees and +10 degrees around North), a normal smoothing algorithm would give the incorrect result: $(350 + 10) / 2 = 180$ degrees, so it would indicate South.

An example of a smoothing algorithm that always will yield the correct wind direction is given in Frame 1.

Rain detector
Most rain detectors consist of two comb-shaped, interlaced, gold- plated tracks on a printed circuit board. Each track acts as an electrode. The printed circuit board is exposed to rain. Rain drops will bridge the gap between the two electrodes, thus generating a yes/no signal for (Met.Office, 1969). A small electrical heating element is mounted below the printed circuit board to accelerate the evaporation of the rain drops. The electrodes should be cleaned now and then, to remove the salt crystals left behind after the water has evaporated.
A quantitative measurement is performed with a tipping-bucket instrument. A small bucket or spoon collects the rain water. Each time a fixed level is reached, the weight of the bucket/spoon exceeds a spring force and empties automatically. The tipping-over of the bucket increments a counting device. At low precipitation levels interpolation is possible by weighing the bucket.

2.2 Radiation

The balance between solar radiation received and heat (energy) lost to the environment is one of the factors that determine greenhouse air temperature. The photosynthetic active radiation (PAR) determines the potential production of the crop.
Sometimes radiation measurements are made inside the greenhouse. However, it is common practice to mount radiation sensors on top of the greenhouse, because shading by constructional parts at various times of the day is a serious problem in relation to monitoring of radiation inside the greenhouse.
Transmission-losses caused by the greenhouse cover are commonly determined under an evenly covered, overcast sky. The transmission is derived from measurements with an outside sensor in open field and a second instrument held at various places inside the greenhouse.
Electromagnetic radiation of optical wavelengths provides the driving force for the processes in the greenhouse. Four different quantities are measured more or less regularly:
- Total global short wave radiation (300 to 2500 nm) [$W{\cdot}m^{-2}$],
- Photo-synthetically Active Radiation (PAR, 400 to 700 nm) [$\mu mol.m^{-2}.s^{-1}$],
- Net radiation (300 to 25 000 nm) [$W{\cdot}m^{-2}$],
- Light intensity (380 to 760 nm) [lx].

Total global short wave radiation
The radiation received from the sun at the surface of the earth has wavelengths between 300 and 2500 nm. Its energy is usually measured in a horizontal plane. Midday values on a clear day in summer are about 1000 $W{\cdot}m^{-2}$ at low latitudes and about 800 $W{\cdot}m^{-2}$ at moderate latitudes (CIE, 1989). The common instrument for measuring this quantity has a broadband thermal receiver. A glass dome that restricts the sensitivity approximately to the wavelength-band mentioned earlier covers it. The instrument is known as a pyrano-meter or a solarimeter. The instrument measures the total short wave energy-flux and its angular response follows a cosine curve. Most Dutch growers use a pyrano-meter made by Kipp & Zonen, Delft (Hanan, 1984). The total uncertainty of the short wave irradiation measurement comprises calibration errors, non-linearity, errors in angular response and positioning errors. The uncertainty can be kept well within +/-5%, if the outer dome is cleaned monthly and the instrument is re-calibrated every two years.

Some manufacturers offer silicon-cells with a response flattened from 450 to 1050 nm as 'solid-state' pyrano-meters. These sensors must be equipped with a diffuser to ensure a good angular response. Because of the limitation in spectral response, the instruments measure between 70 and 90 % of the total short-wave radiation, depending on cloudiness and solar height. Linearity, signal-level and price of a silicon pyrano-meter are comparable to those of a thermal instrument. The significantly increased uncertainty associated with the silicon pyrano-meter makes it an inferior substitute for the thermal instrument.
Sometimes it is useful to have a separate measurement of the diffuse sky radiation only. This can be achieved by a pyrano-meter with a shadow ring in an equatorial mount. The elevation of the ring should be adjusted every three to five days (Robinson, 1966; Met. Office, 1969). Tables are available to account for the interception of part of the diffuse radiation by the shadow ring (manufacturers of thermal pyrano-meters include Kipp, Eppley and Schenk).

Photosynthetically Active Radiation (PAR)
Green plants can utilise radiation of between 400 and 700 nm for photosynthesis. Since the process is driven by the absorption of photons rather than energy, the action spectrum of a crop reflects the photon flux between 400 and 700 nm (Figure 3). The corresponding SI-unit is mol[phot].$m^{-2}.s^{-1}$. PAR sensors consist of a silicon photocell with a diffuser and an optical filter (Biggs, 1986). They have a good linearity and stability. A re-calibration every two years suffices. Because of the limited spectrum involved in PAR, it is not possible to give a single conversion factor from total short wave radiation to PAR. The instrument to be used should be tailored to the problem at hand: PAR as input in a plant growth model and total short wave for temperature control and water supply (manufacturers of PAR-instruments include Licor, Skye and Kipp).

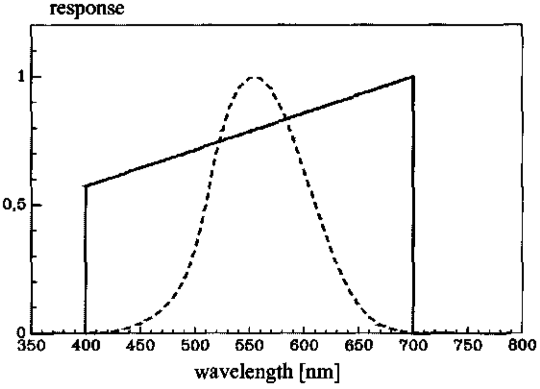

Figure 3 - Relative response: ——— PAR, - - - - - human eye

Net radiation
Net radiation gives the balance of the downward and upward fluxes of short wave and long wave radiation. Since the crop will not only exchange radiation energy with the sky, but with al construction parts of the greenhouse and the installations in it, it should be measured inside the greenhouse. The instrument comprises two thermal radiation receivers, mounted back to back. The receivers have been prepared in the factory so that they have an equal sensitivity to both short wave and long wave radiation. Both receivers are covered with a thin polyethylene cap that can be lightly inflated to preserve their shape. The measurement of net radiation is less straightforward than that of a short wave flux, but the result is two extra terms of the energy balance: the reflected short wave flux and the net long wave flux. At present the net ra-

diometer is still a research instrument, rather than one for every day use. The net radiometer needs a yearly re-calibration (manufacturers include Middleton, Schenk and Swissteco).

Light intensity

The sensitivity of the human eye covers a range very similar to that of photosynthesis. Yet the shape of the sensitivity-curve is rather dissimilar. The eye has a low response in the blue and the red portions of the spectrum and shows a steep maximum in the green. From a maximum at 555 nm, sensitivity drops to virtually zero at 380 nm and 760 nm (Figure 3). The range between these wavelengths is often referred to as the visible. Radiation weighed with the sensitivity curve of the eye is called 'light'. The SI-unit for light flux is the lumen (lm), for flux received per area (illuminance) the lux (lx).

Modern lux meters comprise a silicon photocell with a diffuser and optical filters. Twice a year a re-calibration is needed. The widespread availability of lux meters has led to their use in horticultural lighting. It is common practice to state the level of additional (artificial) lighting in a greenhouse in lx, rather than in $\mu mol_{(phot)}.m^{-2}.s^{-1}$.

To be an efficient source of light, modern lamps have been developed with a high output in the most sensitive part of the human visibility spectrum, rather than of PAR. Consequently, the photosynthetic effect of radiation from high-pressure sodium lamps in comparison to daylight is grossly overestimated. Sensor manufacturers include EG&G, Licor, Minolta, PRC Krochman and UDT.

2.3 Water and nutrients

Chemo-sensors provide an electrical signal in relation to the concentration of particles in fluids or gases. These particles can be atoms, molecules or ions (Hauptmann, 1990). If biological substances like enzymes, bacteria or whole cells are part of a chemo-sensor, the word biosensor is used. In horticulture, chemo-sensors are mainly used in the root environment. In hydroponics EC and pH sensors are common practice. ISE (Ion Selective Electrode) and Isfet sensors are slowly gaining interest (Hashimoto *et al.*, 1989; Bailey *et al.*, 1988; Gieling *et al.*, 1988).

Electrical conductivity and pH

In horticulture EC (Electrical Conductivity) and pH sensors are the simplest form of chemosensors.

EC is measured using three ring-shaped electrodes, mounted inside the water transport pipe at equal distances. The two end-electrodes are connected to each other and to ground. The temperature of the fluid is measured and is used to modify the value of the AC voltage applied between the central electrode and the ground electrodes as a means of temperature compensation. A normal value for this AC voltage is approximately 1 V. The frequency may range from 400 Hz to 50 kHz. An AC voltage is used to avoid polarisation. The EC is measured as the current between the central electrode and the two end-electrodes. The current ranges from 0,1 mA to 10 mA. The currents in the upstream and downstream parts of the sensor are summed at the central electrode. Thus, parasitic effects like the one caused by the speed of the supply water are eliminated. Grounding both end-electrodes allows the sequential or parallel use of more EC electrodes in one water supply system. In horticultural practice two distinct EC electrodes are used in parallel, thus enabling a check on the functioning of both EC sensors against each other. EC normally ranges from 2 to 10 [$dS \cdot m^{-1}$].

The pH sensor is the most well-known potentiometric electrode. Here the potential across a glass membrane is an indication of the activities of H_3O^+ on both sides of the glass membrane.

In horticulture, pH is measured with standard pH combination sensors. The sensors are filled with a gel, which means that replenishing is not needed anymore. Slow deterioration of the sensor is avoided in this way. The lifetime expectancy of the pH sensors normally used in horticulture is about one year. Again, two sensors are used, so that one sensor checks the other. As an additional check, the values obtained with the EC and pH sensors are compared with the results of a bi-weekly lab analysis.

Chemo sensors

The chemo-sensors referred to in this paragraph are potentiometric sensors, based on the measurement of a potential difference across a membrane. Commercially available ISE sensors are mostly combined electrodes, where one electrode is mounted together with the membrane in an easy to handle sensor body. A second electrode is placed inside the ISE sensor body, which is filled with an electrolyte. A well-defined potential difference exists between the electrode and the electrolyte material.

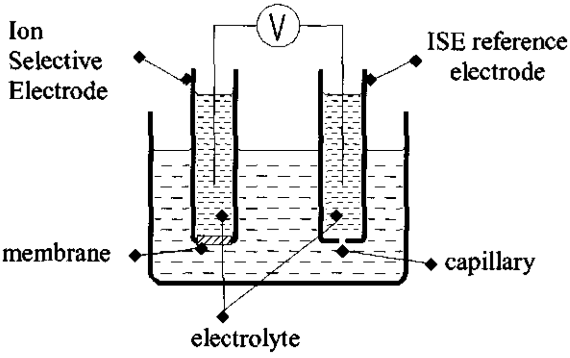

Figure 4 - Basic principles of an Ion Selective Electrode

An ISE is always used with a reference electrode. Usual reference electrodes are the SCE (Saturated Calomel Electrode) and the Ag/AgCl electrode. The membrane-electrode potential is then measured against the reference potential (Figure 4) (Albery *et al.*, 1986). The membrane used in an ISE determines the quality of the sensor. Some popular types are: solid membranes (silverhalogenide, fluoride, silicate), liquid organic electrolyte membranes, solvent polymeric membranes. The membrane separates the sample solution from the inner filling solution of the sensor (Figure 4). The function of the membrane in an ISE sensor is to contain ligands that can selectively catch ions from a fluid or gas and use their charge to develop an electric potential E, as in equation 1 (Nicholsky equation), across the membrane (Morf *et al.*, 1973, Chang, 1990).

$$E_i = E_{0,i} + \frac{R \cdot T}{z_i \cdot F} \cdot \ln(a_i + \sum_{j \neq i} K_{i,j}^{Pot} \cdot a_j^{z_i/z_j})$$

$$E_{0,i} = -\frac{R \cdot T}{z_i \cdot F} \cdot \ln(a_i + \sum_{j \neq i} K_{i,j}^{Pot} \cdot a_j^{z_i/z_j})_{reference\ fluid} \qquad \textbf{(1)}$$

Here, E_i is electrical potential [V], $E_{0,i}$ is a reference potential dependent on the activities in the reference fluid, i is the ion to be determined and j are interfering ions, z is the charge of

the ion, $K_{i,j}^{pot}$ is the selectivity coefficient characteristic of a given membrane and is dependent on the activities a_i,a_j [mol·m^{-3}] of both the i and j ions. R is the gas constant [J·mol^{-1}·K^{-1}], T is temperature [K] and F is the Faraday constant [C·mol^{-1}]. $R \cdot T \cdot F^{-1}$ is often referred to as the Nernst coefficient. ISE sensors are available for most macro-nutrients, like K^+, Ca^{2+}, NO_3^-, SO_4^{2-}, NH_4^+ and ions interfering with growth, such as Na^+ and Cl^-.
Since the logarithm of activity is measured, a measuring uncertainty of 1 mV implies an uncertainty in the ion activity of 8% in the case of a Ca^{2+} ISE sensor ($z_i = 2$), (Heinen, 1991). The output impedance of the sensor is very high, which means that special precautions have to be taken with respect to connecting cables, signal grounding and input impedance of the subsequent amplification electronics.

Ion Sensitive Field Effect Transistors
Isfet sensors have first been developed at Twente University in The Netherlands (Bergveld, 1970). These integrated silicon chip based sensors produce an output signal as a function of the activity a [mol·m^{-3}] of hydrogen ions. When covered with a suitable membrane they are able to distinguish different ions from each other and are preferably called Chemfets. Now, their output signal mainly reflects the activity of one specific ion.
The Organic Chemistry Research Department of Twente University developed a special type of membrane that shows a good performance in lifetime experiments (3 to 6 months *in situ*). These polysiloxane membranes contain different side groups to tune their intrinsic properties to obtain sensors of high durability (Chapter 3.2). The ion selectivity has been tuned by incorporation of various novel ion receptor molecules, yielding sensors with high selectivity for sodium, potassium, calcium, nitrate and dihydrogen phosphate.
Integrating Chemfets for different ions and their amplification and data-handling electronics on the same sensor body, offers opportunities to built smart-sensors. The Chemfet sensor does not use polluting reagents and it does not need excessive maintenance.
Because of their role in the research projects accompanying this thesis, they are described more in detail in Chapter 3.2.

2.4 Soil or substrate moisture

Greenhouse economy and protection of the environment both require the close monitoring of soil moisture. We shall use the word soil moisture in the more general sense of substrate moisture, since the same reasoning refers to any kind of substrate. The present practice of providing a slight overdose of nutrient solution and letting the excess run off into the surface water implies both a waste of valuable material and a threat to the environment. In the closed-loop systems now evolving, the main objective of a moisture monitoring system is to guarantee an optimum water supply to the rooting area.
The driving force for water uptake by roots is the difference in waterpotential (Schurer, 1986) between the substrate and the root-tissue. For any well-defined substrate there is a unique relationship between waterpotential and water content. Measurement of either of these is sufficient for greenhouse control. Current methods of measurement comprise deriving water content from EC of the bulk nutrient solution and of the substrate, from the dielectric properties of the substrate in the time domain (TDR) or in the frequency domain, and from the attenuation and scattering of a beam of thermal neutrons. Waterpotential can be determined from dielectric measurements and from measurements with a hydraulic tensiometer.
Modern growing methods like NFT and aeroponics have no substrate in which measurements can be made. In these methods watering is controlled by the detection of excess water at the end of a drain. An EC sensor is suitable for this purpose.

Time Domain Reflectance
Dielectric methods to determine water content from the dielectric constant of the substrate are rapidly gaining ground. In a calibration procedure the relationship between dielectric constant and water content for each specific soil type has to be established. In time domain reflectometry (TDR), a short electrical pulse is sent into a pair of electrodes and the time dependent reflected signal is analysed to give the water content of the medium between the electrodes (Werkhoven, 1992).

Dielectric measurement
In an alternative approach the real and imaginary part of the complex impedance between two electrode needles is measured at one, carefully chosen (high) frequency (Hilhorst *et al.*, 1992). This method can give both water content and EC. It is easier automated and miniaturised than TDR. A miniature version of the sensor can be incorporated into a well-defined substrate, of which the relation between water content and water potential is known. When this system is brought into a soil or substrate, equilibrium will develop, in which the waterpotential in both media will be the same. Thus, a measurement of the water content of the known medium allows a statement about the waterpotential of the soil. Special designs of the two electrodes offer an opportunity to built sensors with one electrode.

Hydraulic tensiometer
A porous cup filled with distilled water can be used for high (near-zero) waterpotentials. When the cup is brought in contact with the soil an equilibrium will develop in which the tension inside the cup equals the suction of the soil or the substrate (Slavik, 1974). The tension inside the cup is measured with a pressure transducer. The method works for suction pressures down to -80 kPa. At lower pressures, there is a risk of air entering the cup. Errors will arise when contact between cup and soil is lost. Hydraulic tensiometers are available commercially.

2.5 Shielding sensor electronics against RFI and LEMP interference

Interference
Present-day measurement and control involve the application of electronic circuits. These circuits generally are sensitive to RFI (Radio Frequency Interference) and LEMP (Lightning Electro Magnetic Pulse). They can be designed either with discrete electronic components or with microchips. The trade-off for microchip technology is between low cost and good reproducibility versus increased electrical vulnerability (Clark & Povey, 1985). Historical data on damage to crop and livestock from the files of a major Dutch insurance company show that considerable damage to production in agriculture is caused by failures in control equipment (Gieling & Van Meurs, 1984). Furthermore, it was shown that lightning and lightning-induction is the main cause of damage to computer equipment (87%) in agriculture and horticulture. Of course, trivial causes like a loose sensor wire can be equally detrimental.
At a first glance the problem only seemed significant when livestock were involved. Careful analysis indicated that a correlation exists between the response time of the agricultural production system to react on equipment failure and the extent of damage to any type of product. Damage increases considerably where there is a shorter response time.
The introduction of new and fast responding cultivation techniques in horticulture decreases the overall response time of a crop to failures in equipment (Table 1). Examples of these easy to disturb cultivation techniques are: hydroponics (e.g. nutrient film technique, growing on rockwool, aeroponics) or critical climatic circumstances caused, for example, by measures for

energy saving or cultivation in closed systems. Extreme summer or winter outdoors-climatic conditions also present an increased risk.

Table 1 - Estimation of worst-case response time for agri-processes to loose 10%, 50% or 100% of their product as a result of equipment failure

Product loss [%]	Pigs for breeding [min]	Pigs for meat production [min]	Tomato grown in soil [min]	Poultry [min]	Tomato Grown soilless [min]
-10	60	30	40	10	2
-50	120	60	120	20	4
-100	480	120	360	40	8

RFI and LEMP shielding

Since it is the main cause for failure, most preventive measures taken against electro-magnetic interference are concerned with lightning and lightning-induction. Already for years and years, sensitive analogue and digital equipment have been applied to control critical processes in the petrochemical industry. Here good results have been achieved with respect to preventive measures against LEMP and RFI (Högberg *et al.*, 1985), measures that could be successfully applied to agriculture as well (Hasse and Wiesinger, 1985).

Preventive measures include:

- filters on incoming cables, to short-circuit all transient voltages to a central ground electrode (e.g. mains power, telephone, terminals to other buildings),
- an efficient potential equalisation. All electrically conducting metallic parts should be connected to each other and to the central ground electrode (e.g. all piping and appliances of heating installations). So-called 'clean' grounding electrodes must also be connected to the central ground,
- cables to sensors and actuators should have double shielding. The inner shield is only connected to the mass terminal of the computer electronics as a shield against RFI noise. The outer shield is connected to ground on both ends of the cable to function as a shield against lightning-induction,
- the greenhouse construction can act as a so-called 'Faraday cage' and offers some extra shielding against RFI and LEMP noise. For this purpose all construction parts (columns, gutters, glazing bars) should have a galvanic interconnection and be connected to the central ground.

3. Some reflections on sensors in horticulture

The grower is an innovating entrepreneur, passionately driven by his professional skill. This becomes manifest in the quality of the product and the quality of the production process. It is the origin of a natural urge to work with high-tech equipment in a high-tech production facility. The greenhouse, the control systems, the harvesting equipment and the computer supported management system, they should all meet his expectations.

It is because of this urge that horticulture is such an appreciative application area for automation by controlled systems, sensors and modern information and communication technology.

Model-based control, that applies a 'speaking plant' approach, will need even more information directly online from the process - like greenhouse atmosphere, crop and rizosphere - and the direct environment of the greenhouse, like the outside climate, radiation levels and soil conditions.

In the foreseeable future, decision support systems - as management tools - lean on these models. They will be directly coupled by dedicated intranet to databases that are distributed over geographically dispersed locations and which will make use of the sensors mentioned in this section. Most of these sensors involved are a spin-off from meteorology, the process industry or developments for automotive applications.
However, the sensor described in the following section is an example of a development that evolved just the other way around. Modern greenhouse industry, and its water and nutrient supply systems, was the clear mainspring and guideline of the research and development, that ultimately will lead to durable Chemfet analyser systems.

§3.2 Monitoring ion concentration

Based on:
Application of Isfets in closed loop systems for greenhouses. In: *Adv. Space Res.* 18, no. 4/5, p. 135-138. Th.H. Gieling, H.H. van den Vlekkert, 1996.
Chemically modified field effect transistors to monitor ion concentration in nutrient solution. In: *Proceedings of the 3rd International Symposium on sensors in horticulture*, Tiberias, Israel. Th.H. Gieling, J.F.J. Engbersen, J.J.W. Westra, 1998.

1. Introduction

This paragraph describes a measurement system that is based on ion sensitive field effect transistors (Van den Vlekkert and de Rooij, 1988; Engbersen *et al.*, 1995; Gieling and Van den Vlekkert, 1996; Gieling *et al.*, 1998a; Engbersen *et al.*, 1997; Van den Vlekkert, 1992; Van den Vlekkert *et al.*, 1992). The measurement system was built in the course of the research for this thesis. It was intended to serve as a measuring device for the feedback of signals to control the concentration of specific ions in the solution of a greenhouse water and nutrient supply system.

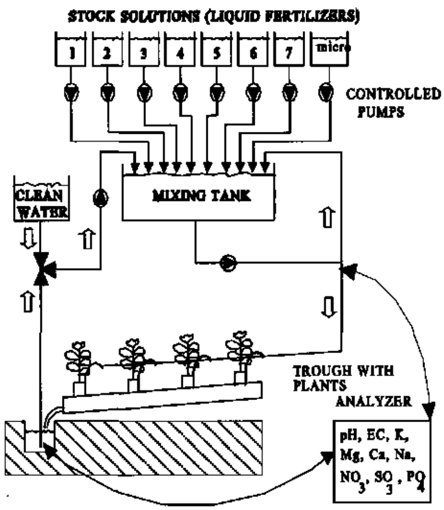

Figure 1 - Closed loop growing system with ion concentration control.

Applying closed growing systems needs precise knowledge of the composition of the recirculating nutrient solution. In this chapter basic principles of a measuring system are elucidated, which can monitor continuously the concentration of nutrients in water. The sensor system measures on-line and real-time at intervals of approximately 20 seconds.
The sensors in the system are based on the chemically modified field effect transistor (Chemfet). They are intended to be used as a set of eight sensors in a flow-through cell.
Due to considerable variation in nutrient and/or water uptake by the plants (Gieling *et al.*, 1989) - and in contrast with current methods of discontinuous sampling followed by analysis

in the laboratory - it is preferable to measure continuously on-line the composition of the drainage water.
Figure 1 shows a mixing tank layout of a nutrient diluter in a closed-loop growing system with monitoring and control for water and nutrient supply. Albury *et al.* (1986) and Heinen, (1991) report on the application of commercial ISE electrodes for monitoring purposes in relation to research in greenhouses.
Although novel miniaturised sensors for the (on-line) detection of low concentrations of ions in aqueous solution can find useful application in many areas (e.g. monitoring of potable water quality, localisation of environmental pollution and biomedical analysis), it is hard to find continuously operating measurement systems that comply with the demands of horticulture. Only very recently, a/o as a result of the contributions made by the research at the IMAG-DLO institute, such miniaturised sensor/data-acquisition/fluidics combinations in one analyser system of sufficient stability have been fully developed.
Consequently, hitherto analysis is carried out with conventional techniques like chromatography, atomic absorption or emission spectrometry and various wet analytical techniques.
Innovative technology in semiconductor materials, micro-engineering and molecular nano-engineering show great promise for the cheap fabrication of large series of micro-sensors by IC technology (Engbersen and Reinhoudt, 1994). Nowadays, solid state pH-sensors based on Isfets are commercially available and it is expected that these will soon be followed by the full range of commercially available Chemfets, capable to measure the activity of other ionic species in greenhouse nutrient solutions (Engbersen *et al.*, 1997).

2. Chemfets for monitoring ion activity

The membrane potential
The electric potential that is measured with ion selective sensors is formed across a membrane that is dependent on the ions in the sample solution. Engbersen *et al.* (1995) report extensively on the functioning of ISE and Chemfet microsensors in the notes of their lecture on chemical micro-sensors. They report on two groups of ion selective membranes:

- solid state membranes, made of insoluble salts,
- liquid-type membranes that are divided into three sub-groups: liquid membranes, polymer supported membranes and all polymer membranes.

They stress that - although all kind of combinations of membrane types and transducer types are possible - liquid-type membranes are commonly used in ISE or Chemfet sensors.
The liquid-type membrane itself is generally not selective towards a specific ion but serves as the solvent for the ionic sites and ionic receptors which are capable of a selective complexation of specific ions. These electro-active components determine the selectivity and sensitivity of the membrane (Figure 2).

Polysiloxanes are all-polymer liquid-type hydrofobic membranes that are used on the Chemfets in this research. Their easily modifiable monomers allow for a covalent attachment of the electro-active ionic sites and ionic receptors to the membrane matrix, which prevents leaching out of the membrane (section 3.3). The active lifetime of the membrane is to a large extend dependent on this process of leaching out and was one of the main issues, together with sensitivity and selectivity, in all former developments in relation to ion selective sensor membranes.
The membrane contains ion receptors, which selectively bind one specific type of ions from the sample solution, thus increasing the charge of the membrane capacitance with the charge

of that specific type of ion. This results in an increase of the membrane potential E_{mem} [mV] (Figure 2).

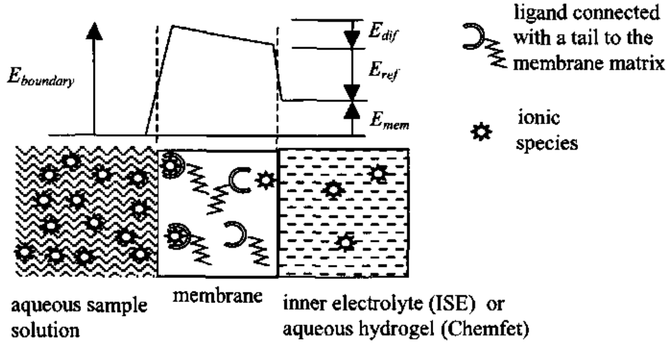

Figure 2 – Ion sensitive membrane separating the sample solution from a reference solution. The reference solution in contact with the membrane of an ISE electrode is the inner electrolyte of the electrode. The reference solution of a Chemfet is a polyHEMA hydrogel, containing an ion- and pH-buffer solution.

As is shown in Figure 2 the membrane electrical potential E_{mem} [mV] consists of the sample-membrane electrical boundary potential $E_{boundary}$ [mV], the electrical membrane reference-boundary potential E_{ref} [mV] and a possible electrical diffusion potential E_{diff} [mV] across the membrane (Engbersen *et al.*, 1995).

The membrane potential is given by:

$$E_{mem} = E_{boundary} + E_{diff} + E_{ref} \tag{1}$$

Since E_{ref} and E_{diff} usually are independent of the activity of the ionic species in the sample solution, the rate of change (as function of the activity of a specific ionic specie in the sample) of the membrane potential is directly related to the rate of change of the sample-membrane boundary potential.

The Chemfet as an electronic device

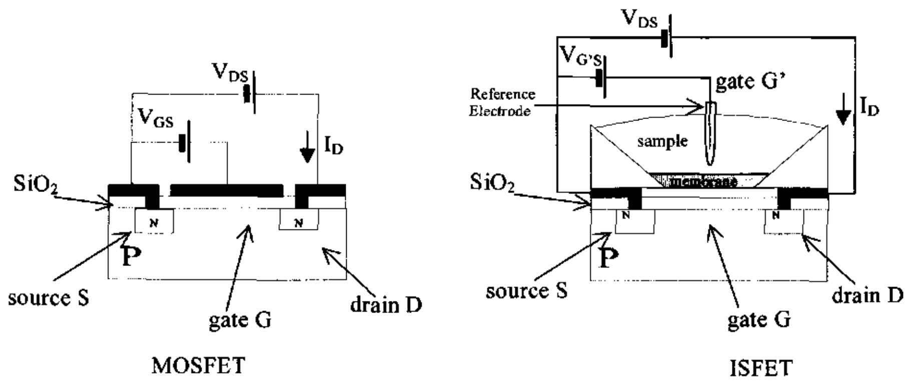

Figure 3: Schematic presentation of a Mosfet and an Isfet

A Chemfet is an Isfet with a chemically modyfied surface and as such a member of the family of MOSfets. A reference electrode replaces the gate electrode of the mosfet. The reference electrode is immersed in the solution to be measured, which is in contact with an ion selective membrane material layer deposited on top of the gate insulator (Figure 3and 4).

The drain current I_D [mA] in a Mosfet is described by equation 2.

$$I_D = \frac{C_{ox}\mu W}{L}\left\{\left(V_{GS} - V_T\right) - \tfrac{1}{2}V_{DS}\right\}\cdot V_{DS} \qquad \textbf{(2)}$$

Here, C_{ox} is the gate insulator capacitance [pF], μ is the electron mobility [J·mol^{-1}] in the channel and $W{\cdot}L^{-1}$ is the width to length ratio of the channel [1]. V_{GS} is the gate-source potential [V], V_{DS} is the drain-source electric potential [V], V_T is the threshold electric potential [V].

When V_{GS} exceeds V_T, the minority-charge carriers in the substrate of a FET transistor start to form a conducting channel between drain and source. The conductance between source and drain is a function of the electrical field perpendicular to the gate oxide surface (Figure 3 and 4).
In contact with an aqueous solution, the state of ionisation of the surface SiOH groups of a SiO_2 gate oxide determines the surface potential and therefore the source-drain current I_D in the transistor. A change in pH of the solution will produce a change in the Nernst surface potential. The theoretical Nernst value is 59 [mV·pH^{-1}], which is influenced by the surface properties of the gate material of the Isfet. Typical responses thus obtained are 37- 40 [mV·pH^{-1}] in case of SiO_2 or 50-55 [mV·pH^{-1}] in case of Al_2O_3 (used in the sensor devices here).

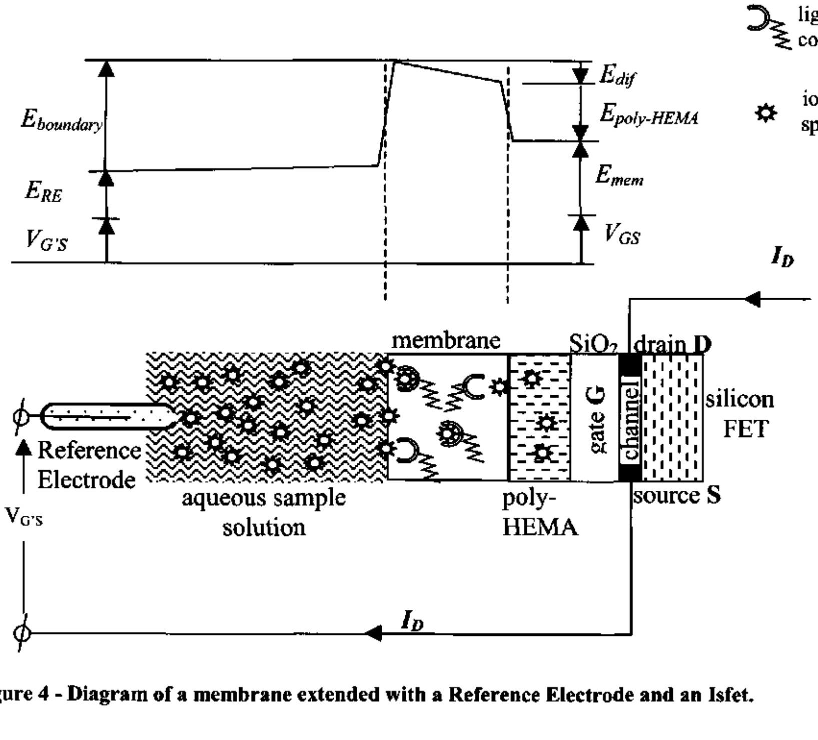

Figure 4 - Diagram of a membrane extended with a Reference Electrode and an Isfet.

The diagram of Figure 2 may be extended with the electronic circuitry of a FET (Figure 4). $V_{G'S}$ is the electrical potential from G' to S [V], or between Reference Electrode and the source connection on the FET transistor (Figure 4). The drain current is modulated by the conductance change of the FET channel due to changes in the gate voltage V_{GS}. If the connection terminals of $V_{G'S}$ are short-circuited, then the ion specific change in V_{GS} is due to changes in E_{mem}, which is caused by an increase in electric charge by the capture or release of specific ions by the ligands. The Reference Electrode causes a parasitic potential E_{RE} in the loop. The E_{RE} potential is subject to temperature and to poisoning by ions from the sample solution.
If - by a short-circuit between the connection terminals - $V_{G'S}$ becomes 0, then:

$$V_{G'S} = V_{GS} - E_{mem} + E_{boundary} + E_{diff} + E_{pol\,HEMA} + E_{RE} \tag{3}$$

Then again, I_D can be described as in equation 2.

The voltage change in $V_{G'S}$ can be measured by the change in channel conductance of the transistor. In practice, the drain current is kept constant by the feedback action of an operational amplifier in a simple but smart circuit (Figure 5).

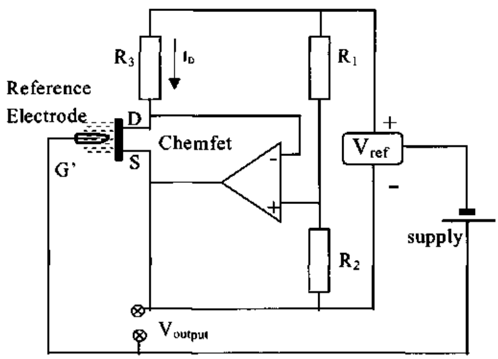

Figure 5 - The Chemfet amplifier circuit

The circuit of Figure 5 transforms the changing channel resistance of the Isfet into an electrical potential signal source V_{output} with a low output impedance.
The reference electrode in Figure 5 acts as the gate electrode G' for the Chemfet. A feedback action of the operational amplifier adjusts the voltage across drain D and source S of the Chemfet (V_{DS}), which keeps the current I_D at a constant value. Both parameters values - I_D and V_{DS} - affect the electronic functioning of the Chemfet. The I_D parameter influences the transconductance g_m (electrical sensitivity) and the V_{DS} parameter influences the drain conductance g_D (output resistance).
Since the voltages at both input terminals of the operational amplifier are the same (due to feedback), the voltage across R_3 equals $V_{R3} = V_{ref} \cdot R_1 \cdot (R_1 + R_2)^{-1}$. This is a constant value since V_{ref}, R_1 and R_2 are constant.
As a result, a constant current ($I_D = V_{R3} \cdot R_3^{-1}$) is superimposed on the Chemfet. The output impedance of the circuit is very low, since it is the same as the internal output impedance of the operational amplifier. Now the output signal reflects accurately the membrane to reference electrode voltage E_{mem} of equation 3, which is a function of the ion activity of the ionic solution.

Since the output impedance of the circuit is very low, the output signal may be loaded with follow-up circuitry for data-acquisition.
A backside-contacted chip is used as the basic pH sensitive Isfet chip (Figure 6). Here, the contacts are at the backside of the chip and are plated through to connect to the drain and source semiconductor islands. Because the ionic solution is on the front side of the chip, it cannot get in touch with the connection pods if these are at the backside and no electrical insulation precautions have to be taken. Backside contacted chips have the disadvantage of a more complicated etching process during production, at the price of higher production cost per chip. Their advantage over more conventional chips is that before encapsulation of a conventional chip, very thin wires have to be bonded to the contact pods on the front side. Since these contacts are at the front side, they have to be covered with epoxy to insulate these wires from the sample solution. Therefore, the connection will be more expensive and the choice of the membrane material will be less flexible, since both epoxy and membrane material have to be compatible.

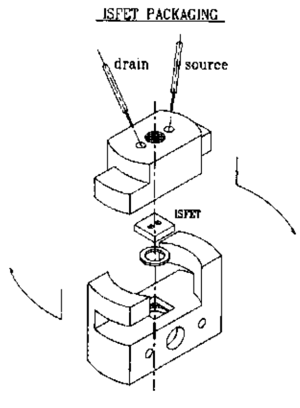

Figure 6 - Encapsulation of a backside-contact chip

The sensor encapsulation of Figure 6 was a special design for the purpose of application in horticulture. However, during the utilisation of the sensors in a lifetime test, it showed that the encapsulation itself was the cause of quite a lot of the problems.
These problems encountered are concerned with leakage of fluid, damage of the chip or its membrane during assembly and bad contact of the spring-loaded contact pins to the backside contacts of the chip.
For these reasons a new design was made, where the backside contacted Chemfet chips are separately packaged in a teflon encapsulation (Figure 7, right). A perspex flow-through cell was designed, in which a combination of Chemfet sensors can be mounted (Figure 7, left).

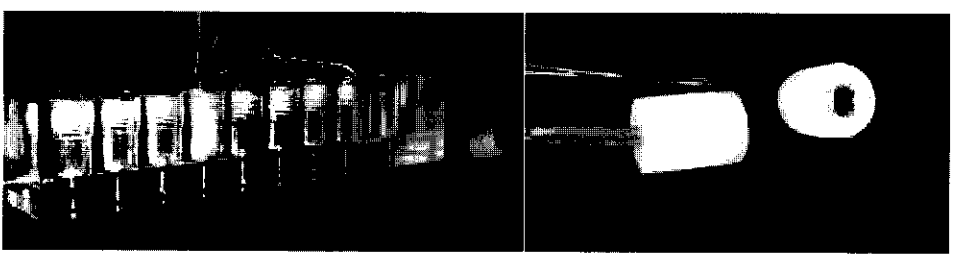

Figure 7 - A flow through cell with holes (left) for individually packaged Chemfet sensors (right)

3. Chemical modification of Isfet transistors

Basically, the Chemfet is a special modification of an Isfet. The latter shows sensitivity for the activity of hydrogen ions in solution, whilst the former is sensitive to other ionic species in solution (Reinhoudt, 1995). The Isfet's measurement principle is - like for the ion selective electrode and glass electrode - based on potentiometric determination of ion activities in aqueous solutions. This detection technique is particularly useful when a large dynamic range of ion activities has to be measured. Chemfets have some important advantages compared to ion selective electrodes, like fast response time, low noise level, small size and opportunities for mass production.

Detection of other ionic species than protons requires the introduction of ion receptors that can selectively recognise these species. The intrinsic pH sensitivity, caused by reaction of hydroxyl groups at the gate oxide surface, has to be suppressed.

Covering of the gate oxide of an Isfet with a plasticised PVC membrane, that contains the potassium-selective natural ionophore valinomycin, already gives a good potassium response upon variation of the potassium concentration. However, this construction has the severe drawback, that the physical adhesion of the membrane to the surface of the semiconductor is not stable. Furthermore, the plasticiser and ionophore leach slowly from the membrane upon prolonged contact of the sensor with the aqueous solution. Moreover, such a sensor suffers from interfering pH-sensitivity (and carbon dioxide sensitivity) due to the uncontrolled ionisation of the surface hydroxyl groups of the gate oxide.

The latter problem has been overcome by placing a buffered hydrogel between gate oxide and sensing membrane (Sudhölter *et al.*, 1990). A layer of polyhydroxyethylmethacrylate (poly-HEMA) is covalently attached to the gate oxide surface by photopolymerising the monomer on the gate electrode, which is pre-treated with methacryloylpropyltrimethoxysilane. The methacrylated siloxane groups on the surface ensure the covalent binding of the hydrogel.

In the next step of sensor preparation, the poly-HEMA layer is covered with a sensing membrane. For a limited life time plasticised PVC membranes can give quite satisfactory results with ionophores as sensing membranes: no CO_2 and pH interference and a low noise signal. A durable sensor, however, requires the chemical attachment of the sensing membrane to the semiconductor and a membrane material that does not need a plasticiser.

In order to prevent leaching out, the electro-active components in the sensing membrane - receptor molecules and ionic sites - have to be covalently bound to the membrane matrix or must be of high lipophilicity.

Requirements that are needed to produce a sensing membrane suitable for these purposes are:

- The sensing membrane must be an elastomer (glass transition temperature below zero).
- The membrane must be moderately hydrophobic, i.e. it must possess a low partition of ions from the aqueous phase but must have sufficient conductivity in order to obtain fast response times. For the permselectivity of the analyte ions, ionic sites of opposite charge must be present in the membrane or allowed to be added. The presence of charged species in the membrane also lowers the electrical resistance of the membrane.

In order to make sensor fabrication compatible with IC-technology, linkage of all components in the membrane matrix and attachment of the membranes to the gate surface must occur by photo-polymerisation.

A reproducible synthesis for well-structured siloxane terpolymers was developed by a group of researchers at Twente University (Engbersen *et al.*, 1997). It is based on anionic co-polymerisation of cyclotrisiloxanes (Figure 8). The covalent attachment of the membrane to the transducing part of the sensor is enabled by the photo-polymerisation of the methacrylate groups.

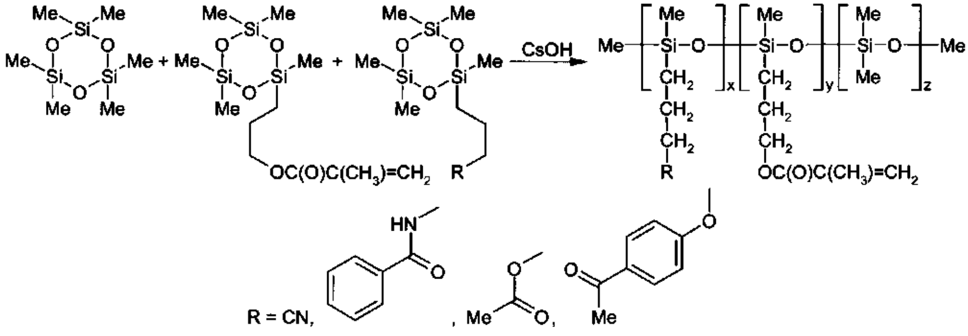

Figure 8 - Anionic co-polymerisation of different cyclotrisiloxanes.

The cross-linking of the methacrylate groups also enhances the mechanical strength of the membrane. The new polymers offer opportunities to tune the polarity and the character of the membrane by changing the amount and type of polar substituents. These changes can have a profound effect on the partition of various ions between sample and membrane phase, resulting in changes in the selectivity of the sensor.

Receptors applied in sensor membranes should posses high selectivity, especially over interfering ions that will possibly also be present in high concentrations in the sample. Furthermore, the receptor molecule must be lipophilic in order to make it soluble in the membrane matrix and to prevent fast leaching to the contacting aqueous solution.

Calix[4]arene (Figure 9-1) is a versatile lipophilic three-dimensional building block that can be functionalised with various ligating substituents for selective ion binding and can be provided with a functional group that enables covalent anchoring to the membrane matrix.

The selectivity of the receptor can be influenced by the type and number of substituents and the conformation of the calix[4]arene. For example, functionalisation of the calix[4]arene at the lower rim with amide moieties (Figure 9-2) results in the right positioning of the coordinating carbonyl and phenol oxygens atoms for complexation of Na^+ with selectivity over other alkali cations. The selectivity of Na^+ over K^+ can even be improved by the use of two diametrically positioned amide ligands instead of four, in combination with two ester ligands (Figure 9-3).

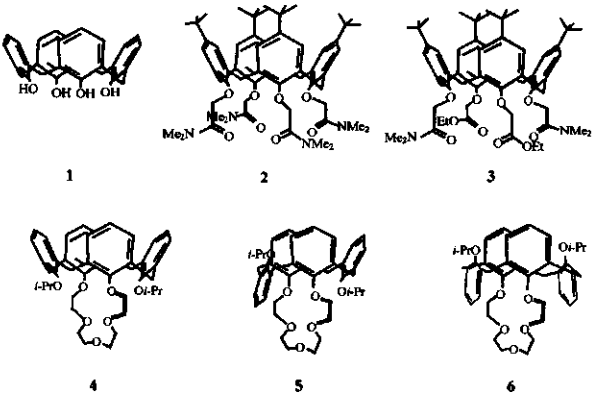

Figure 8 - Calix[4]arene and its functionalisations

A crown ether moiety can easily be combined with the calix[4]arene building block. The pre-organisation of the binding cavity of the crown ether by the calix[4]arene skeleton enhances the binding selectivity and the molecule becomes more lipophilic.
The Twente University research group developed a number of calix[4]arene crown ether ionophores. For K^+ selective sensors, ionophores with five oxygen atoms in the crown ether bridge were developed. These receptors clearly show the influence of the conformation of the calix[4]arene on the selectivity.
They found the construct of Figure 9-4 to be of the lowest selectivity of K^+ over Na^+ ($\log^{pot}_{K,Na} = -2.5$) and the construct of Figure 9-5 of much better selectivity ($\log^{pot}_{K,Na} = -3.9$).
The highest K^+ selectivity ($\log^{pot}_{K,Na} = -4.2$) was obtained by the construct of Figure 9-6.
At Twente University, the durability of the Na^+ selective sensors have been tested by the exposure of these sensors to a continuously refreshed stream of tap water (25 mL·min^{-1}). Here, the Chemfets were conditioned in a 0.1 M NaCl solution for one night before measuring their characteristics (i.e. selectivity and sensitivity). The polysiloxane based Chemfets retained their Na^+ selectivity in the presence of different alkali and alkaline earth metal ions for a period of more than 40 weeks (Reinhoudt, 1995). Despite of the decrease in Na^+/K^+ selectivity from -2.6 to -1.4 after 40 weeks, the Chemfets still have (near) Nernstian responses. Even after 40 weeks of continuous exposure to streaming tap water, they found that the Chemfets were still very selective ($\log K_{Na,j}$ = -3·0 and -2.9) for Na^+ in the presence of Mg^{2+} and Ca^{2+} ions, respectively. They obtained similar results with nitrate-selective Chemfets, incorporating a polysiloxane membrane containing covalently bound quaternary ammonium groups and with potassium-selective Chemfets incorporating covalently bound crown ether analogues.

4. The analyser equipment

The hardware
The Chemfets discussed in this chapter are intended to be used on-line in a controlled supply system for water and nutrients in a greenhouse. For this purpose a suitable device was developed that fulfils all expectations and demands that are of concern to this application environment.

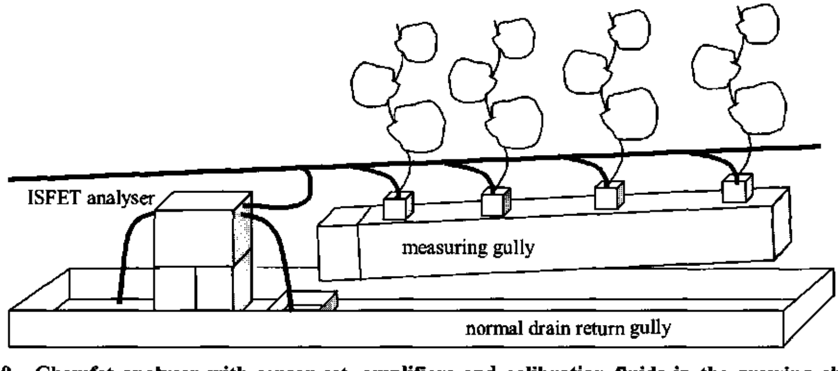

Figure 10 - Chemfet analyser with sensor set, amplifiers and calibration fluids in the growing channel, closely positioned next to the drain exit of the measuring gully

The analyser device incorporates the sensors, the sampling fluidics (valves and pump), the calibration fluids, the data acquisition and data mining software and communication software and hardware.

The delay time between the moment of taking a sample of the fluid to analyse and the moment of measuring the sample in the Chemfet analyser should be minimised. Consequently, the distance between the analyser and the point where the sample is taken (e.g. a small measuring gully in the greenhouse as depicted in Figure 10) has to be as short as possible. The more so, since the amount of drain available from the measuring gully per supply cycle is too small to successfully fill up a sample hose of enough length to bring it to an analyser when it is placed in a corridor outside the greenhouse compartment.
A solution is found in placing the Chemfet analyser next to the measuring gully in the greenhouse (Figure 10 and 12). However, inside an equipment box situated in a greenhouse, temperature may fluctuate 50 °C and humidity may rise to 95% RH. Moreover, only limited space is available in between the plant rows. This calls for a compact, watertight and airtight housing of the analyser equipment and an adequate compensation for influence of ambient temperature and radiation variations.
To minimise temperature fluctuations of the sensors, the calibration fluid containers are positioned in the drain water gully, which forces an equal temperature of drain water and calibration fluids (Figure 11).

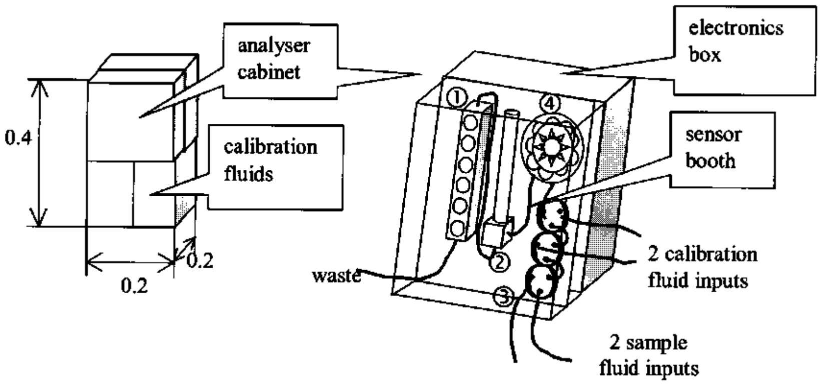

Figure 11 – Analyser cabinet with sensor booth, electronics box and two calibration fluid tanks. The analyser consists of: (1) sensor encapsulation, (2) reference sensor, (3) three selection valves, (4) hose pump. The analyser connects either to one of the two samples or one of the two calibration fluids by the valves.

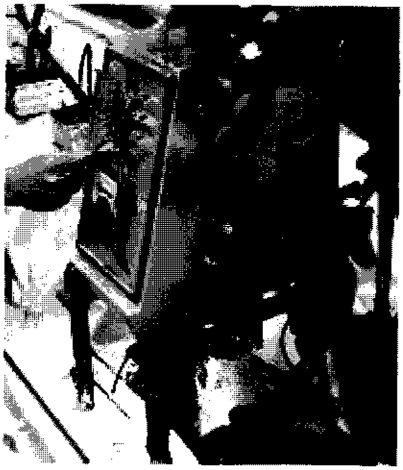

Figure 12 - Chemfet analyser hardware in use in a greenhouse

Data Acquisition

Only small amounts of fluid samples are needed because of the small size of Chemfet sensors, which is an advantage of the applied technology, because it saves on the amount of calibration fluid needed. The intended greenhouse instrumentation measures two sample solutions from the irrigation system (e.g. supply solution and return solution). Two calibration fluids (Cal 1 and Cal2) per ion, of which the concentrations are exactly known, are measured every two to six hours (Figure 13).

Extrapolation outside of the calibration range should be avoided by choosing the activity of the calibration fluids above and below the expected measurement's activities. A small temperature sensor, in thermal contact with the fluidics channel, measures the sample's temperature. These calibration signals are used to convert mV readings in concentration values and to compensate the effects of temperature drift and ageing drift.

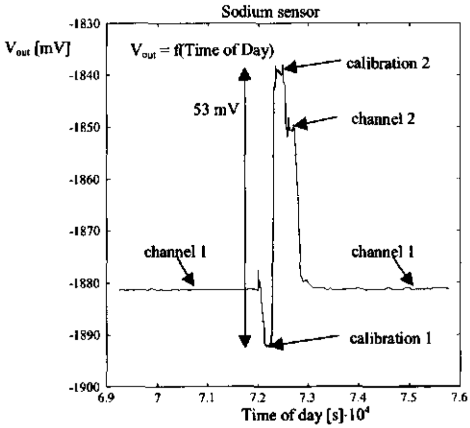

Figure 13 - Output signal of electronic circuit (Figure 5) of a sodium sensor as function of time, with values of two sample fluids (channel 1 and channel 2) and for two calibration fluids (cal 1 and cal2).

In general, the output signal (Figure 13) of the electronic circuit (Figure 5) is of the form:

$$V_{GS} = V_{GS}(pI, T, t)$$

A version of the above relation, linearised around a working point (e.g. pI^I, t_0, T_0, is given in equation 4

$$V_{GS} = V^{I}_{GS} + \left(\frac{\partial V_{GS}}{\partial pI}\right)_{T_0, t_0} (pI - pI^{I}) + \left(\frac{\partial V_{GS}}{\partial T}\right)_{pI^{I}, t_0} (T - T_0) + . \\ . + \left(\frac{\partial V_{GS}}{\partial t}\right)_{pI^{I}, T_0} \cdot (t - t_0) + \left(\frac{\partial^2 V_{GS}}{\partial pI\ \partial T}\right)_{t_0} \cdot (pI - pI^{I}) \cdot (T - T_0) \qquad \textbf{(4)}$$

In equations 4, 5 and 6 the following variables and parameters are used:

pI [1]: logarithm of the ion activity a_I [$10^{-pI} \cdot 10^3$ mol·m^{-3}] in the sample to measure,
V_{GS} [mV]: gate-source output signal of the Chemfet,
t_0 [yy:dd:hh:mm:ss]: start of the sensor's lifetime,

t [yy:dd:hh:mm:ss]: current time, $(t - t_0)$ [s]: the age of the sensor,
T_0 [°K]: temperature at initial calibration at t_0,
T [°K]: actual temperature of the fluid passing through the sensor, averaged over i.e. 20 readings taken in one minute,
pI^1, pI^2 [1]: logarithm of the ion activities a_I of a specific ion I in the calibration fluids Cal1 and Cal2, determined at temperature $T_{ambient}$ in a lab before application in the analyser (e.g. pK, pCa, pNO_3),
T^1, T^2 [°C]: temperatures of the sensor during calibration in Cal1 and Cal2 fluids, averaged over i.e. 12 readings taken in one minute,
V_{GS}^1, V_{GS}^2 [mV]: output signals of the Chemfet during calibration in Cal1 and Cal2 fluids, averaged over i.e. 12 readings taken in one minute,
$S_{T_0} = \left(\frac{\partial V_{GS}}{\partial pI}\right)_{T_0, t_0}$ [mV·pI^{-1}]: initial sensitivity (at time t_0 and temperature T_0),
$TD = \left(\frac{\partial V_{GS}}{\partial T}\right)_{pI^1, t_0}$ [mV·°C^{-1}]: initial temperature drift, in Cal1 fluid at time t_0,
$AD = \left(\frac{\partial V_{GS}}{\partial t}\right)_{pI^1, T_0}$ [mV·s^{-1}]: initial ageing drift, in Cal1 fluid at time t_0,
$STC = \left(\frac{\partial^2 V_{GS}}{\partial pI\ \partial T}\right)_{t_0}$ [mV·pI^{-1}·°C^{-1}]: initial temperature dependency of S_{T0}, at time t_0.

The initial time dependent drift of S_{T0}: $\left(\frac{\partial^2 V_{GS}}{\partial pI\ \partial t}\right)_{T_0}$ and the initial ageing of the temperature dependency $\left(\frac{\partial^2 V_g^s}{\partial T\ \partial t}\right)_{pI}$ are discarded. If the coefficients TD, AD, S_{T0}, STC are known and do not change from the first moment of activation at time t_0, then the resulting measured ion activity pI of a sample is as in equation 5.

$$pI = pI^1 + \frac{(V_{GS} - V_{GS}^1)}{S_{T0} + STC \cdot (T - T_0)} - TD \cdot \frac{(T - T_0)}{S_{T0} + STC \cdot (T - T_0)} - AD \cdot \frac{(t - t_0)}{S_{T0} + STC \cdot (T - T_0)} \tag{5}$$

Although the initial values of the coefficients TD, AD, S_{T0}, STC of the Chemfet sensor are determined in the lab, their value will not remain constant during their use in a lifetime of approximately 6 months. The value of the parameters in the Isfet transistor, as well as in the membrane on top of it, will change due to temperature influence and ageing. Moreover, there will be changes in the membrane parameters due to prolonged exposure of the membrane to variations in pI, pH, EC.

In Table 2, the calibration procedures Cal1 and Cal2 were automatically activated every 2 hours, with pI^1 and pI^2 respectively as ion activity. The temperature-drift parameter TD and sensitivity parameter S_{T0} have been established. The ageing parameter AD is found to be equal to zero, since the time difference between start and end of the sequence is too short to show for a measurable ageing effect.

Table 2 - Calibration values V_{GS}^{1} and V_{GS}^{2} taken on 10 April 2000 in a test on a Na sensor.

Calibration time [hh:mm:ss]	pI^1 [1]	pI^2 [1]	V_{GS}^1 [mV]	V_{GS}^2 [mV]	T [°C]	TD [mV·°C]	S_{T0} [mV·pI^{-1}]
0:08:00	-3	-2	-1910.9	-1860.8	20.51	0.634	50.1
2:08:00	-3	-2	-1910.9	-1861.0	20.18	0.653	49.9
4:08:00	-3	-2	-1910.0	-1859.1	20.52	0.666	50.9
6:08:00	-3	-2	-1907.0	-1856.2	22.10	0.666	50.9
8:08:00	-3	-2	-1905.5	-1854.1	22.96	0.661	51.4
10:08:00	-3	-2	-1902.4	-1849.6	27.46	0.680	52.8
12:08:00	-3	-2	-1901.8	-1847.3	33.43	0.666	54.5
14:08:00	-3	-2	-1902.3	-1847.8	34.51	0.634	54.4
16:08:00	-3	-2	-1903.1	-1849.0	33.82	0.612	54.1
18:08:00	-3	-2	-1906.9	-1853.9	29.81	0.591	53.0
20:08:00	-3	-2	-1910.4	-1859.2	25.10	0.597	51.2
22:08:00	-3	-2	-1912.7	-1862.7	21.30	0.614	50.0

Figure 14 illustrates the relationship between temperature and the *pNa* and *pK* measurement signals. It also shows the high and low calibration points (Cal1 and Cal2). The Cal1 and Cal2 peaks are of the same shape as in Figure 13. Table 2 shows the exact set of calibration data for the Na^+-sensor.

Both the sample fluid signals as well as the calibration 1 and 2 signals clearly show temperature dependencies. Although not so apparent from Figure 14, the signal is also dependent on variations in the other parameters of the sensor.

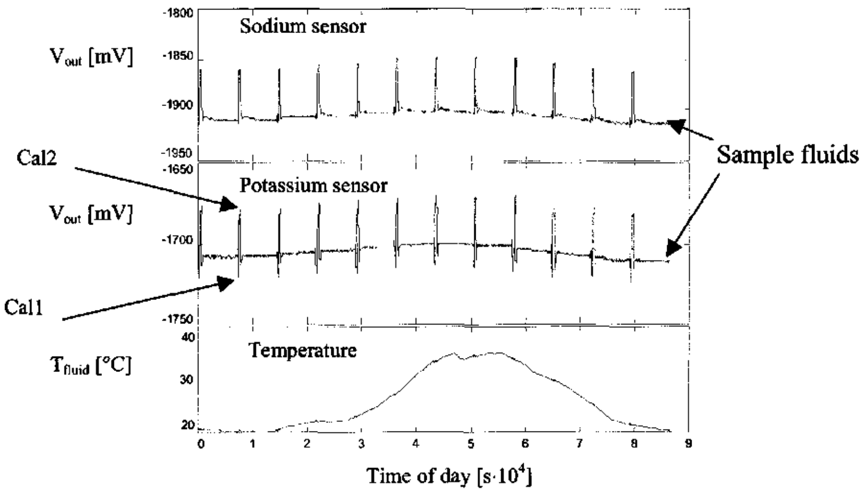

Figure 14 - Output signal [mV] of Na^+ and K^+ sensor (two upper graphs) and temperature [°C] of fluid (lower graph) as function of time of day [s]. A calibration procedure is performed every 2 hours.

In view of the dependencies mentioned, the value of the S_{T0} parameter can be adjusted continuously during subsequent calibration procedures.

In order to adjust for short-term variations due to electronic noise and digitalisation noise, the two values V_{GS}^1 and V_{GS}^2 are measured i.e. 12 measurements in one minute of which the mean value is determined. This mean value is stored in memory, together with the known pI^1 and

pI^2 values determined at the laboratory. This stored information is used in a two-point algorithmic calibration calculation (equation 6).

$$S_{T_0} = \frac{\overline{V}^2_{GS} - \overline{V}^1_{GS}}{pI^2 - pI^1} \tag{6}$$

The pI^1 and pI^2 values are determined at a lab at a standard temperature of i.e. 25°C, whilst the Cal1 and Cal2 fluids are applied to the analyser at temperature *T*. The S_{T0} parameter is corrected for it by means of the parameter *STC* (see equation 5). Now, at each calibration instance, the new value for S_{To} [mV·pI^1] is calculated online (Van den Vlekkert and De Rooij, 1988). Then, application of equation 5 will automatically adapt the *pI* calculated result of the measured sample for variations in S_{T0}.

The algorithm of equation 5 shows dependencies on the *AD* and *TD* parameters. Equation 5 only correctly calibrates for effects of lifetime drift and temperature drift of the Chemfet sensor if the *AD* and *TD* parameter values are established and adjusted online during the data acquisition process. The frequency of repeating the adjustments is dependent on the expected rate of change over time of these parameters.

The temperature process shows a diurnal pattern (Figure 13) in the same order of magnitude as the greenhouse air temperature, whilst the ageing process is expected to show variations over weeks (Figure 15).

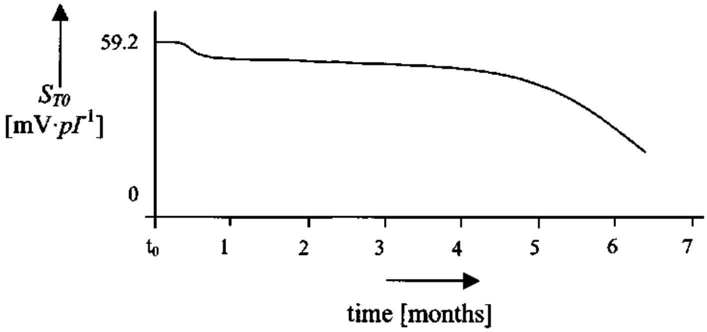

Figure 15 – Relation between sensor response (Nernstian behaviour) and lifetime (Engbersen *et al.*, 1995). The *AD* parameter is related to this ageing effect.

Calibration will take place three or four times each day. Only at each new calibration procedure new information for this purpose becomes available. Therefore, the most reasonable and feasible instance of adjustment, which fulfils both mentioned time horizons for variations due to temperature and ageing, is during each calibration procedure.

The disentanglement of parameters acting on the output signal at the same time

The output signal of a Chemfet is not only a function of S_{To}, temperature (*TD*) and lifetime (*AD*), but also of the activity of all the different ions present in the sample.

As is indicated by the Nicholsky-Eisenman relation (equation 1, Chapter 3, §2.3), interfering ions exert their specific influence on the output signal in relation to the non-zero cross-sensitivity of the membrane for the interfering ions. To overcome these cross-sensitivities, one way would be to build better sensors with higher selectivity. Another option is found in the application of multi-component/multi-variate calibration models.

Engbersen *et al.* (1995) describe a number of methods from chemometrics, where mathematical calibration models use simultaneously measured signals from non-ideal sensors to calculate the result. These multi-component/multi-variate calibration models can be subdivided in two classes: linear and non-linear calibration models.
As non-linear model, a neural network and fuzzy logic solution are suggested.
As linear models, the authors present singular value decomposition or multiple regression after principal components analysis. These methods need mathematical libraries with routines from linear algebra (matrix algebra).
Neither of the above-mentioned methods has been used in the analyser under development in this research project. Mainly, because an in-depth disentanglement of the cross sensitivities could not be subject of research in this study. Only a few series of prototype Chemfet sensors of only one type were available at the same time (either sodium or nitrate) during the research for this thesis. Only after the project stopped a set of potassium and sodium sensors were available. So, at the time there was not an urging reason to incorporate sophisticated methods to disentangle a multitude of dependent measurement signals.
Nevertheless, from experience with earlier versions of the Chemfet sensor it was clear, that both the *TD* and *AD* parameter values change over time. Moreover, at the same instance they act together on the output signals $V_{GS}, V_{GS}^1, V_{GS}^2$ of the analyser. Their mutual entanglement (dependent measurement) is comparable to the cross sensitivity of the sensors for different ions.
In close contact with the company that commissioned this PhD-research project, it was decided to use a less sophisticated solution, because it should fit into a small embedded computer system with simple fixed point rather than floating point calculus. The consequences of it are that routines allowing for matrix inversion are not available.
For this purpose an on-line routine has been incorporated in the analyser system that will invoke adjustment of the *TD* and *AD* parameters each time the calibration routines for Cal1 and Cal2 are activated, according to a procedure described below.
In this procedure, the last 25 calibration measurements V_{GS}^1, V_{GS}^2 of pI^1 and pI^2 are kept as a timeseries in a FIFO buffer (Figure 16).

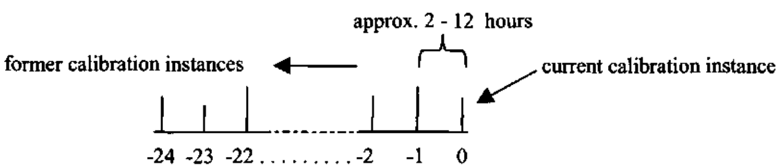

Figure 16 – Calibration instances prior to the current calibration. The time gap between calibration instances is a parameter chosen at the start of data-acquisition and may range from 2 to 12 hours.

At the end of each calibration procedure, the last measured calibration signal values are stored in the row 0. The former calibration measured values shift one row upward. The oldest values, in row -24, move out. The iterated regression procedure mentioned uses all 25 stored calibration values in the buffer to determine the errors due to ageing (*AD*) and due to temperature (*TD*) respectively and disengages the entanglement of both the *AD* and *TD* parameters.

In the procedure an iterative method from non-linear algebra has been used, which solves the pair of equations $x = F(x, y); y = G(x, y)$, by an iterative method using

$x_n = F(x_{n-1}, y_{n-1}); y_n = G(x_{n-1}, y_{n-1})$

If $x = AD$ and $y = TD$, then: $AD_n = F(AD_{n-1}, TD_{n-1}); TD_n = G(AD_{n-1}, TD_{n-1})$.
The F and G functions find AD_n and TD_n by prediction from a linear regression on the last 24 final AD and TD values during the past 24 calibration instances and AD_{n-1} and TD_{n-1}.
If both AD_n and TD_n sequences converge, the routine stops. If both AD_n and TD_n sequences do not converge, the procedure stops after a fixed number of iteration loops and takes the (AD_n, TD_n) values of the former calibration instance as valid values.
It is an advantage that the procedure always has a defined stop condition, i.e. no hold-up of the processor due to endless loops. It will never show singular values due to division by zero, since only multiplication, addition, subtraction and comparison are used. Consequently, there is only need for a processor with simple calculus and fixed point arithmetic.
In the routine mentioned, a set of sub-routines in the C programming language is used. These sub-routines, developed according to the functional design of an offline conversion program by Bentvelsen *et al.* (1997), have been enhanced for online usage. First, the procedure was tested in Matlab®, then it was generalised in an algorithm in the C^{++} programming language and incorporated in the firmware of the analyser.

5. Testing drift compensation on artificial and real world data

Artificial values may be used to replace V_{GS}^1 and V_{GS}^2 readings for the calibration signals in a real measured data set for the purpose of testing the functioning of the drift compensation routine. These artificial values consist of their theoretical values, each increased with a user-defined component of ageing drift and temperature drift. To check on the stability of the procedure a noise component may be superimposed on it and the number of data points used may be altered. When the iterative drift compensation model is applied on these artificial data, the calculated ageing and drift components that result from it may be compared with their artificial user-defined values.
Adding noise or changing the number of data points used in the calculation determines the sensitivity of the iterative model for these parameters. The squared error of the linear regression, remaining after the last iteration, is a quality indicator on the reliability of the approximation. As noise increases, more data points have to be available for the calculation and more iteration loops are needed. In the ideal case, no noise and independent measurements, only 2 iteration loops with 2 data points are needed (solve two equations with two unknown variables) and the squared error of regression is 1. When noise with a value of $1 mV_{top\text{-}top}$ is added, it needs 5 iteration loops and 10 data points to reach a squared error of 0.9.
Table 2 shows a measured data set of calibration data (the same data as in Figure 14) for the Na-sensor, where each set of values is taken at a two hours difference during one day. It is clear that the ageing effect during this short period is not very significant. However, diurnal temperature variations in this greenhouse are considerable (14°C).
A Matlab® routine to test the procedure shows results as in Figure 17. Here the Cal 1 and Cal 2 fluids have a value determined in the laboratory of $pI^1 = -2$ and $pI^2 = -3$. The routine determines the drift values for this data set as: $AD = -0{,}038$ [$mV \cdot h^{-1}$] and $TD = 0{,}325$ [$mV \cdot °C$]. The Matlab® routine uses these parameters to correct the measured pI value of the samples taken each 2 minutes from the greenhouse.
No laboratory determined data of the concentration from the greenhouse sample solution was available to check for correctness of the applied routine. Because of it, improvement of the

quality of the overall data-acquisition and calibration process - due to the method described above - can not be proven on real-world measured sample data.
However, there is an option of back-substitution, that gives an alternative method to show improvements due to *AD* and *TD* correction, as is depicted in Figure 17. The Matlab® routine has an option to calculate the *pI* values of Cal1 and Cal2 by back-substitution.
By substituting the uncorrected values of the *AD* and *TD* parameters in the calibration model, the *pI* value of the Cal1 or Cal2 fluid can be calculated back. In the ideal case, this would give a straight line at -2 and -3, being the laboratory determined calibration values of Cal1 and Cal2 respectively. Remaining errors in the calibration model will become manifest as deviations (Figure 17, left set of lines, first two lines) from the expected straight line.
Back-substitution of the corrected values of *AD* and *TD* show an improvement in the order of a factor 4 reduction on the squared error on the *pI* values (Figure 17, right set of lines, first two lines) in comparison with the results of the uncorrected case (Figure 16, left set of lines, first two lines). It increases the signal to noise (S/N) ratio by $20 \cdot {}^{10}\mathrm{Log}\, 4 = 12\,[\mathrm{dB}]$.
Noise is produced by the sensor itself, by the reference sensor, by the analog to digital conversion (quantisation noise) and by electro-magnetic induction into the measuring circuitry.
In a measuring experiment in the greenhouse, noise signals were established of 0.5-2.5 $\mathrm{mV}_{top\text{-}top}$ on a V_{GS} signal of 1800 mV. However, this signal of 1800 mV only contains ion activity information in the order of: $pI \cdot S_{T_0} \cong 3 \cdot 55 = 165\,[\mathrm{mV}]$. Here, the signal to noise ratio is in the order of $20 \cdot {}^{10}\mathrm{Log}(\frac{165}{2.5}) = 36.4\,[\mathrm{dB}]$. Therefore, improvement of 12 [dB] on the S/N ratio by the simple iterative method is considerable.

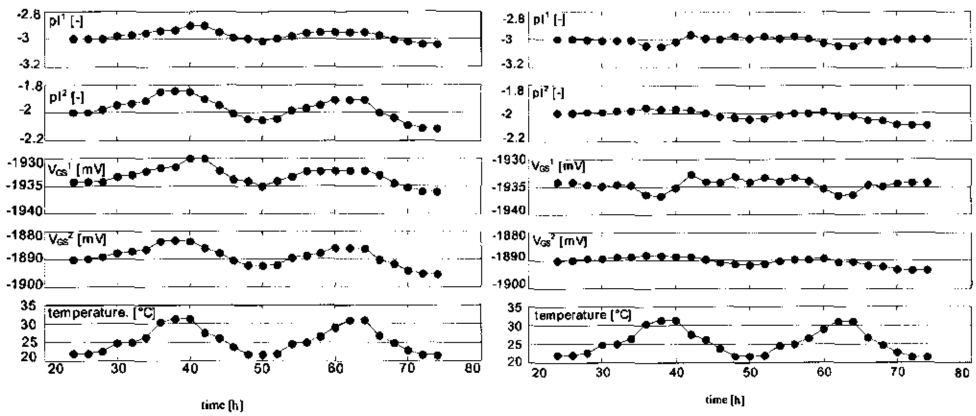

Figure 17 – The graphs at the left and right show calibration data of Table 2. The left-side shows the uncorrected data set, the right-side shows the corrected data set.

From the data in Table 2, a sequence of S_{T0} values can be determined. This calculated sequence of S_{T0} values (dots in Figure 18) reveals correlation with the fluid temperature. A linear regression of these data on fluid temperature results in the solid line in Figure 18.

The slope of the line is 0.3 [$\mathrm{mV \cdot pI^{-1} \cdot {}^{\circ}C^{-1}}$] and represents the $S_{TC} = \left(\frac{\partial^2 V_{GS}}{\partial pI\, \partial T}\right)_t$ parameter.

If the dots in Figure 18 are interconnected in sequence with the timestamp of the measurements, the connecting line (Figure 18, broken line) reveals a backlash between the warming up and cooling down trajectories.

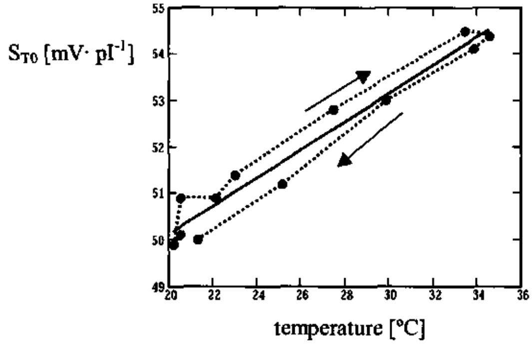

Figure 18 - S_{T0} [mV·pI^{-1}] as function of fluid temperature [°C] (dots). The solid line is the linear regression of all measured values (dots) on fluid temperature. The dotted line connects successive data points in sequence with the timestamp of the measurements.

6. Discussion and conclusions

The Chemfet can be successfully applied in horticulture, when the advantages of this class of sensors are exploited to its full extend. To be of use in applications in everyday horticultural practice, the lifetime expectancy of a sensor should not be shorter than 6 months, preferably even not shorter than 9 months.

Application of electronic signal-conditioning circuitry ensures that the sensors have a low output impedance. Consequently, the signal is less susceptible to electrical noise and may be loaded by the electronic circuitry for data acquisition. To keep the tubes for sample transport short, the analyser with the sensors should be applied on a short distance from the sampling point, preferably in the greenhouse next to the measuring gully by the design described. However, as is shown in this chapter, the S_{T0} parameter value is dependent on fluid temperature. Greenhouse air temperature may vary between 10 and 35 [°C] and supply water temperature may show the same variation. Radiation levels will vary between 0 and 600 [W·m^2], which means that equipment in the greenhouse will show a strong warming up effect due to radiant energy. Therefore, it is advisable to apply an automatic readjustment of the parameters S_{T0}, as realised in the developed algorithm.

Although the latest series of Chemfet sensors have never been working long enough to do a reliable lifetime test, knowledge from literature about the sensitivity in relation to lifetime - as depicted in Figure 15 - indicates the need for a reliable ageing correction that is activated automatically every calibration procedure.

Ageing drift *AD* [mV·h^{-1}] does have a different timing than temperature drift. As temperature changes take place in a diurnal pattern, changes due to ageing will stretch out over months. Nevertheless, determining it at the same time as temperature drift simplifies the procedure.

The simple iterative drift compensation model described above, is suitable for the purpose it is used for: determine the *AD* and *TD* parameters. However, it is sensitive to noise. As Figure 17 shows, there is room for improvement, because back-substitution still does not produce a straight line at the *pI* value of Cal1 and Cal2.

Compensation of cross sensitivity could not be studied, because only one type of sensor was available at a time. Since the membranes of almost all sensors available show cross sensitivity for almost all ions, multi-component/multi-variate calibration models are needed to improve

the fidelity of the output signal of the sensor. The simple iterative routine, which has been used for drift compensation, will not be sufficient.
During the research project the functioning of the equipment was often hampered by an ill functioning of the reference sensor. The bigger part of the problems during the last - more or less successful - measurements were caused by it. At the start of the project, a glass type of reference sensor was used that we managed to break several times. This ISE-type of reference sensor introduces again the clumsy, hard to handle properties that one tried to get rid of by the development of the Chemfet sensors. Later, it was replaced with a plastic tube with a gel-filling that was more easy to handle. Because of the slow release of gel through the contacting capillary into the sample, this sensor was often poisoned by ions and algae penetrating from the sample into the gel-filling. A lot of effort has been put into new types of semiconductor reference sensors, the so-called REFET sensors, which originate from the same type of technology as the Chemfet sensor. If the application of Chemfet sensors in horticulture should become a success, the search for these REFET sensors or other type of novel reference instrumentation or reference methods should better be successful.
As Chemfets will become available for more ions, on-line *in situ* monitoring in supply water and drainage water of a greenhouse will come within reach of quantities like: pH, potassium, calcium, nitrate, sodium (and possibly phosphate). It will be an important step towards advanced ion specific nutrient control in closed recirculation systems.

CHAPTER 4

SIMULATION AND CONTROL

§4.1 GREENHOUSE WATER SUPPLY CONTROL

§4.2 ROBUST CONTROLLER DESIGN

§4.3 INJECTION OF FERTILISER STOCK FLUIDS

§4.1 Greenhouse water supply control

Based on:
A greenhouse water supply controller: a design based on system identification of closed growing systems. In: *Computers and Electronics in Agriculture, Vol 26 (2000)*, p. 361-374, Elsevier. Th.H. Gieling, G. van Straten and H.J.J. Janssen, M. Suurmond, 2000.
Feedback control of water supply in an NFT growing system. In: *Proceedings 3[d] workshop on "Sensors in Horticulture"*, Tiberias. Th.H.Gieling, H.J.J. Jansen, H. de Vree and P. Loef, 1998.
Control of water supply in closed growing systems in a greenhouse. In: *Proceedings of the IFAC/CGIR/ASAE Workshop, Athens*. p. 167-170. Th.H. Gieling, G. van Straten, H.J.J. Janssen and A. Berge, 1998.

1. Introduction

Environmental protection laws enforce greenhouse growers to reduce pollution. To comply to these laws, growers need to grow plants in closed growing systems. In closed growing systems channels capture the drain water. The water is disinfected, enriched with nutrients and used again. Optionally, a growing medium (e.g. sand bed, perlite, rockwool, glasswool, gravel etc.) is used to support the plants in the channel and lead the water and nutrients to the roots. In a Nutrient Film Technique (NFT) system the plants are bare rooted. The type of closed growing system - and the growing medium in it - influence to a great extend the dynamic properties of the supply process.
In a NFT growing system the root mat will gradually fill the growing channel in the course of the growing season and alter the delay time and dead time of the overall system. In growing systems with rockwool substrate as growing medium, the substrate and the roots in it behave as a porous medium through which the nutrient solution is transported. Moreover, due to the ageing of the growing medium, the physical characteristics of the material will change during the growing season. Most commercially available supply systems are tuned conservatively to possess some intrinsic robustness against these time dependent perturbations, (Chapter 2).
Chotai *et al.* (1991) suggest a concept based on modern control theory. In a top-end supplied NFT system they propose a 'Proportional Integral Plus' controller to suppress these kind of system perturbations. However, in their approach, they did not consider trickle irrigation nor growing systems with rockwool as growing medium.
The basic idea of the central concept developed in this thesis is a Tichelmann layout of the water supply system (Chapter 2. Section 1.) and a control approach that keeps the drain flow and drain concentration at a fixed level (Chapter 2. Section 2.).
This paragraph deals with the design of stable controllers for water and nutrient supply in the before mentioned approach. The sections first describe experiments to identify the dynamic behaviour of the growing system in relation to water supply. In order to be able to design stable controllers for water and nutrient supply, an identification of the dynamic properties of the different growing systems is preformed. The measurement data are used to build dynamic I/O models needed in controller design. Finally, the actual design and implementation of the water supply system is presented, followed by design considerations for a nutrient system.

2. Materials used in the experiments

A 300m^2 greenhouse is equipped with water and nutrient supply. A standard commercial fertiliser dispenser system (PRIVA Universeel Substraat Computer®) is applied (Figure 1).

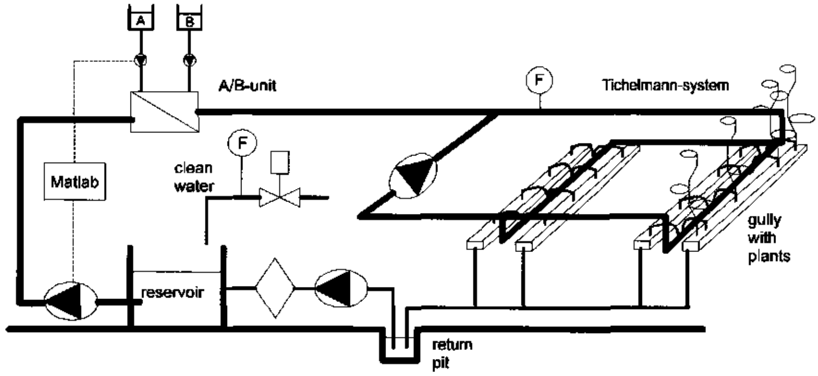

Figure 1 - Layout of a closed growing system with reservoirs, pumps and A-B nutrient supply system. Channels capture the drain water of the plants. The supply pipes are interconnected at the end, to enable the supply water to circulate over the supply system through an extra circulation pump ("Tichelmann" layout). A Matlab® program controls the supply of nutrient solution.

It dilutes A- and B liquefied nutrients (100-fold concentrated) based on EC and pH measurements. In order to minimise dead time in the supply tubes, a so-called Tichelmann layout of the water supply pipes has been applied (Chapter 2.1). In comparison with a standard layout, a Tichelmann layout enables a continuous circulation of supply water over the supply system through an extra circulation pump, invoking a faster transport of nutrients from inlet to nozzle that is mainly determined by the circulation pump.

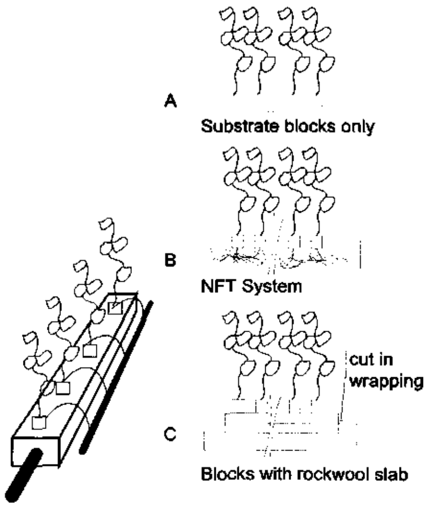

Figure 2 - Different types of growing channels:
a - cubes of rockwool in NFT,
b - rockwool cubes with artificial 'roots' in NFT,
c - rockwool slabs wrapped in plastic foil, with an opening cut in the down stream foil edge. The opening acts as drain.

Identification procedures are carried out on the water supply and nutrient supply systems with a short measuring channel in a fully equipped greenhouse. Drain flow is measured with a tip-

ping bucket sensor at the drainage output of the measuring channel. Three different types of artificial substrates were used to mimic the normal growing medium (Figure 2).
The identification procedure of the growing systems and their growing media is carried out without plants. In case of a NFT growing system, for one part of the experiment the measuring channel contains just seedling blocks. To mimic the root mat in a second part of the NFT experiment, the seedling blocks were extended with bundled pieces of rope, 0.5m in length and 5mm in diameter
In case of a 'substrate' growing system, the channel was filled with rockwool slabs wrapped in a plastic foil (Figure 2), with rockwool seedling blocks on top of the slab.

Details of the feed pump operation
The control system activates a pump during a fixed on-time. The off-time between the previous and the next on-time is modulated according to the output of the feedback controller, within the limits of a minimum (2 min.) and a maximum (14 min.). A full cycle is called a supply cycle. In the concept of constant drain return, the amount of unused water (drain flow) is kept at a constant value by means of a feedback controller. The controller uses the difference between measured drain flow and a set value to adapt the water supply. Thus, water uptake by the plants is - intrinsically - compensated for (Figure 3). The water supplied to the whole greenhouse is related to the ratio between the total amount of plants in the greenhouse and the plants in the short measuring channel.

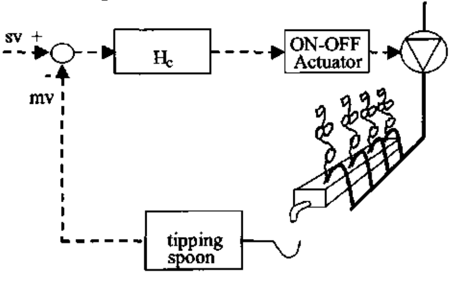

Figure 3 - Growing channel with water supply by means of a pump, which is activated by a controller with a fixed-pulse-width ON-time and a modulated OFF-time. Drain flow is measured with a tipping spoon sensor.

The tipping-bucket instrument is a cheap and simple alternative to measure flow in the severe circumstances found in a greenhouse. When the spoon or bucket is full, it will tip over and cause a pulse on the output of the instrument. However, the instrument shows problems with linearity. When the spoon is in the down position, water will leave the reservoir without touching the spoon. Hence it will not be counted. This effect increases when the water flow from the reservoir is large. A calibration procedure handles this problem by counting the time the spoon is in the down position and interpolates this time period in a table.

3. Identification of the dynamic behaviour of a water supply system

Dynamic model representation of the growing system
System identification is performed in open loop with a 'limited band universal noise' input signal that has been applied to the supply pump. The output response and the noise excitation that caused it, were analysed with the System Identification Toolbox of Matlab® to fit a set of models on the data.

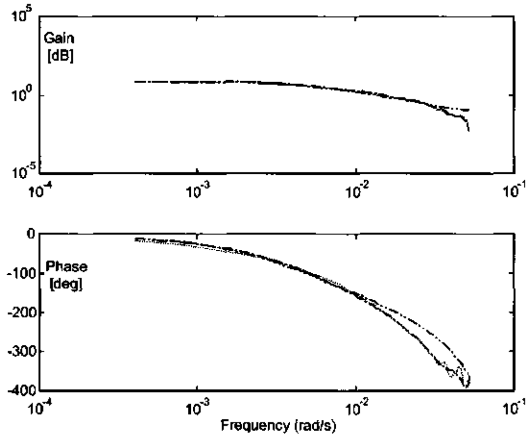

Figure 4 - Bode plot derived from response on noise excitation in a growing system with rockwool cubes on a root mat. - - - - - - = Spectral model, · — · — · — = ARX591 model, ·· — ·· — ·· — ·· N4S2 model.

Both ARX as well as State Space models were tested using the Matlab® toolbox. Figure 4 shows Bode plots for a fifth order ARX model, with nine input delays and no time delay (ARX591), and a two states and four order State Space model (N4S2).
As can been seen in Figure 4, the gain as function of frequency of both the ARX and the N4S2 model nicely fit to the experimental Bode diagrams derived from a spectral analysis of the data. The phase response of the N4S2 model shows some divergence, which can be explained from the fact that dead time is not accounted for in a state space model representation.

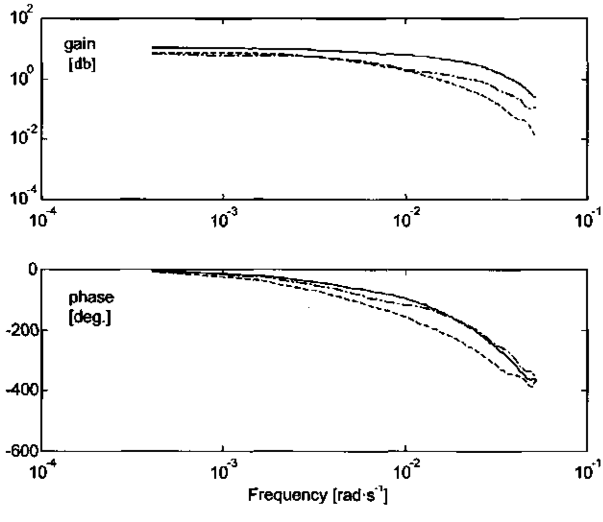

Figure 5 - ARX441 model of the three growing systems depicted in Figure 3. rockwool cubes (——),cubes on root mat (- - - -) and rockwool slab (– · – · –).

Figure 5 shows the Bode plots of an ARX441 model of the three different types of growing systems. The difference in corner frequencies shows that plain rockwool cubes (Figure 2a) clearly react the fastest to excitation and the rockwool cubes on an artificial root mat (Figure 2b) the slowest.

The system identification experiment shows that rockwool cubes on a root mat are the slowest. On a first glance, this result does not seem to be very obvious. It is not easily explained from the physical properties of the systems.
The rockwool slabs (Figure 2c) are of the same material and are larger in volume than just the cubes. So, one would expect that water will take a longer time to flow through the slabs.

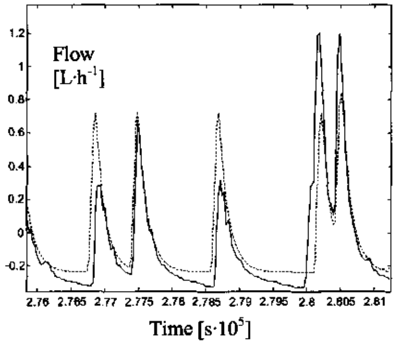

Figure 6 - The validation part of measured data (———) compared to simulation data (– · – · –). The mean value of the data is zero.

The models have been constructed with two third of the data set and were validated with the remaining part of the data. Figure 6 shows a part of the measured and simulated data in the validation stage for model ARX441 for the substrate seedling blocks without roots. It can be concluded that the model gives a fair representation of the dynamics of the supply system during each water supply cycle.

Continuous simulation

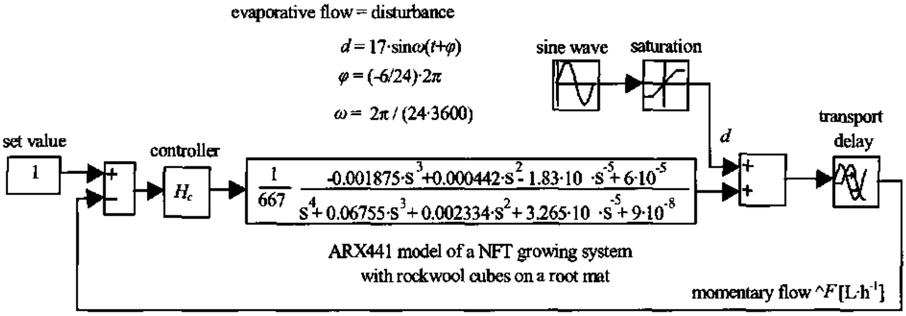

Figure 7 - Block diagram (in Simulink®) of a continuous time simulation of an ARX 441 model.

The results of the system identification can be expressed in terms of the process transfer function H_p:

$$H_p = \frac{1}{667} \cdot \frac{-.001875 \cdot s^3 + .000441 \cdot s^2 - 1.834 \cdot 10^{-5} \cdot s + 6 \cdot 10^{-5}}{s^4 + 0.06755 \cdot s^3 + .002334 \cdot s^2 + 3.265 \cdot 10^{-5} \cdot s + 9 \cdot 10^{-8}} \qquad (1)$$

Equation 1 shows the transfer function of the ARX441 model of a growing system with cubes on an artificial root mat. Similar functions are obtained for the other systems.

The transfer function representation is applied in a simulation of a feedback control system in continuous time for supply of water and nutrients to the plants as depicted in the Simulink® diagram in Figure 7. The disturbance (d) on the controlled system by the plants is introduced as a simulation of the water uptake. Water uptake is a function of global radiation, which is simulated by the positive half of a sine function, with a period time of 24 [h], shifted in such a way that the peak value is at 12:00 [h] (Equation 2). A transport delay of 75 [s] was introduced according to real measured values.

$$d = \hat{d} \cdot \max(0, \sin(\omega \cdot t + \varphi)) \quad [t \text{ in } s], \tag{2}$$

$$\omega = \frac{2 \cdot \pi}{24 \cdot 3600} \quad [\text{rad} \cdot \text{s}^{-1}], \quad \varphi = -\frac{6}{24} \cdot 2\pi = -\frac{\pi}{2} \quad [\text{rad}]$$

A simple PI algorithm was used, that allows playing around with controller tuning in order to get some feeling for the system. Results of the simulation procedure and the response of the system on a variation of the water uptake are shown in Figure 8. The set value for the drain flow is 0.4 [$L \cdot h^{-1}$]. In addition, Figure 8 shows that the response is within acceptable limits. Problems arise at the sharp breakaway points of the radiation curve. In the approach with continuous time simulation blocks, all discrete timing aspects are disregarded (i.e. the pulse-pause time of the controlled pump as well as the discrete time characteristics of the tipping spoon flow sensor).

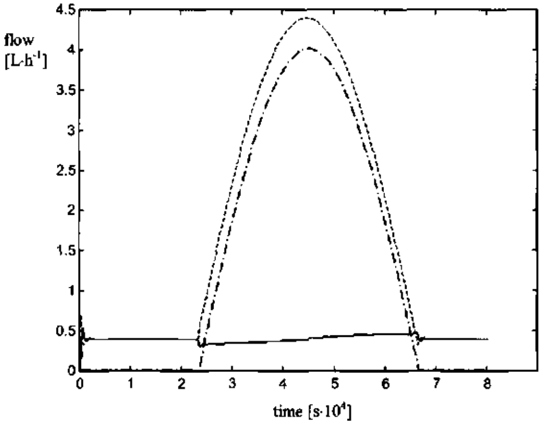

Figure 8 - Drain flow (——), water supply (– · – · –) and global radiation (- - - -) as function of time of day. Global radiation is here interpreted as potential evaporative water uptake ($L \cdot h^{-1}$).

Simulation with discrete elements

A detailed design of the real system should include an accurate discrete time representation in Simulink® of the fixed-pulse-width/modulated-pause-time (Figure 11-lower) actuator and the tipping spoon flow sensor. Figure 9 shows the design of a discrete approach, with specifically designed discrete subsystems for the controller, the total controller delay, the actuator and the sensor. The actuator subsystem converts a flow set value on its input into modulation of OFF-time with a constant ON-time pulse width. It also presents a value for the total controller cycle time $T_s = t_{on} + t_{off}$.

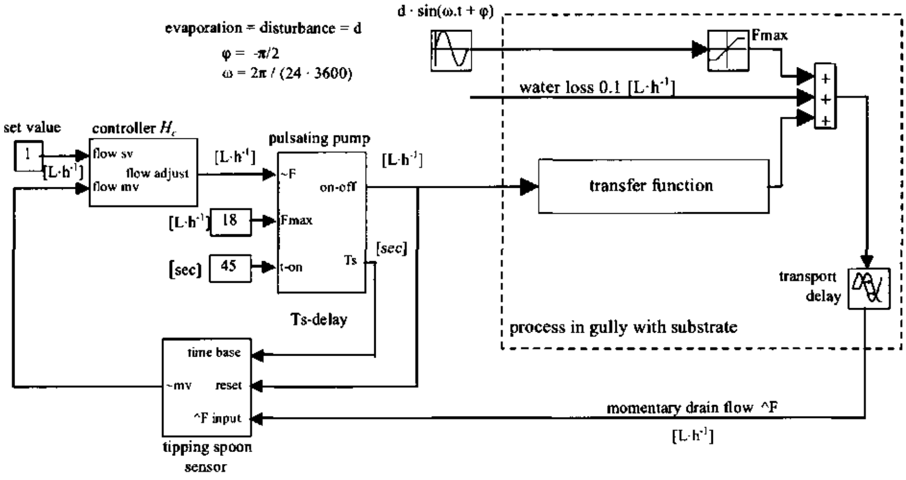

Figure 9 - Diagram (in Simulink®) of the controlled loop used for the discrete time simulation.

The momentary drain flow ^{F} is averaged over the total cycle time T_s, by the subsystem block of the tipping spoon sensor. This is achieved by integrating the momentary flow ^{F} at the end of the T_s cycle and divide it by the value of T_s. Now, $F_{average} = Ts^{-1} \cdot Sum(^F)$. As a consequence, the design of Figure 9 controls the value of an average over a T_s cycle of the momentary flow ^{F}. In this way, the average drain flow during each cycle of the active control time is kept constant.

In Figures 10, 12 and 13 details of the Simulink® blocks 'pulsating pump', 'Ts delay' and 'tipping spoon sensor' are elucidated.

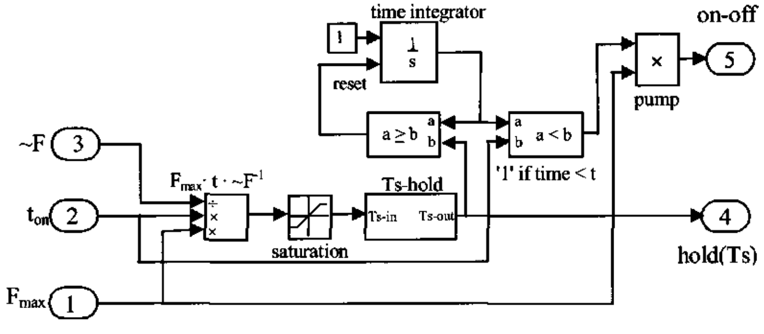

Figure 10 - Simulink® model of a pulsating pump. Inputs: 1) pump capacity F_{max} at continuous operation [$m^3 \cdot h^{-1}$], 2) puls duration t_{on} [s], 3) ~F (flow averaged over cycle time) [$m^3 \cdot h^{-1}$]. Outputs: 4) pulsating flow [$m^3 \cdot h^{-1}$], 5) supply time Ts [s] (available on this terminal during whole supply cycle).

In Figure 10 a Simulink® representation of a pulsating pump is shown. The time Ts is calculated from the capacity of the pump F_{max}, the on-time of the pump t_{on} and the pump flow, averaged over the whole supply cycle. The value Ts is kept during the whole water supply cycle at output 5 by means of a hold function as is depicted in Figure 13. As long as the time integrator value is smaller than t_{on}, the pump supplies water. As soon as t_{on} time is up, supply is stopped until the new cycle starts.

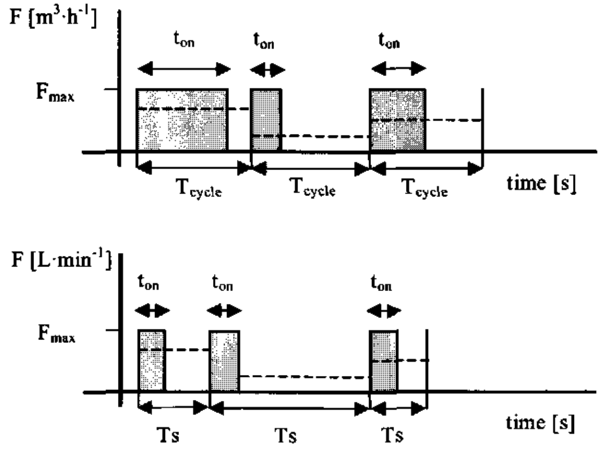

Figure 11 - The average flow during one cycle (- - - -) due to a pulse operated pump. In the upper diagram the cycle time (T_{cycle}) is fixed and the ON-time is modulated, in the lower diagram the ON-time is fixed and the repetition or cycle time is modulated ($Ts = t_{on} + t_{off}$).

In Figure 11 the averaged flow is shown when a fixed ON-time is chosen and when a fixed cycle time is chosen. A fixed ON-time is a disadvantage for practical application. With a fixed on time it is hard to combine the water supply of a number of valve operated sections in a greenhouse together on one nutrient dispenser. In this situation, an orderly ON and OFF switching sequence of section valves may not be possible anymore.

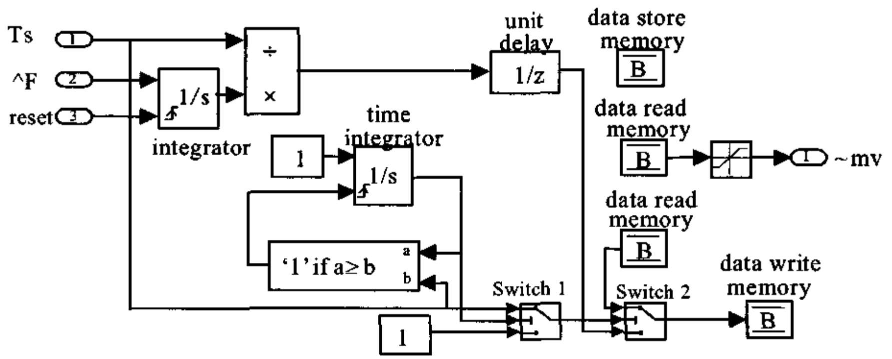

Figure 12 - Simulink® representation of the tipping spoon sensor. Inputs: 1) Ts input, *Ts* [s] value should be present during the whole supply cycle, 2) momentary flow *^F* [L·h^{-1}], 3) reset signal for the integrator. Output: *~mv* is the measured value of the of the drain flow [L·h^{-1}], averaged over one supply cycle.

The Simulink® block of Figure 12 simulates the tipping spoon sensor. It has as input signal the momentary measured value of the flow at the end of the measuring gully. The time integrator resets at the *Ts* value.
At the output of the tipping spoon simulator, the averaged drain flow over the past cycle is presented. The *Ts* value is needed to calculate the average value of the drain flow and to de-

termine when the water supply period finishes. For this purpose, the *Ts* time value has to be available over the whole cycle time.
For the controller H_c a simple PID algorithm was used. The tuning of the controller was manually set by playing around with the parameters until a response with a reasonable overshoot was realised.

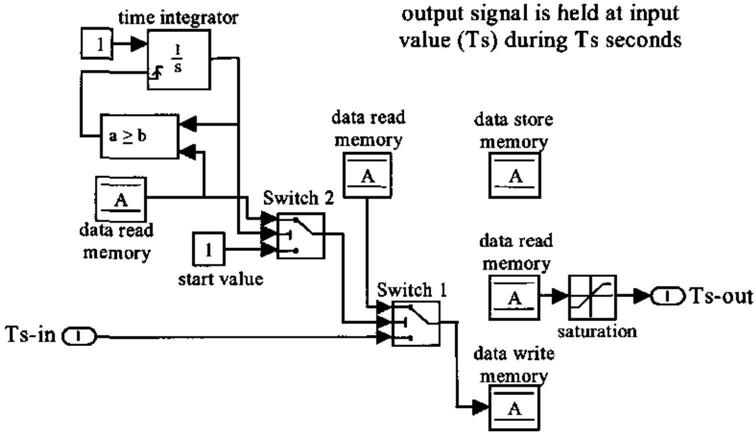

Figure 13 - The Ts hold block keeps the calculated *Ts* value during te whole watersupply cycle of duration *Ts* by means of memory function block A. The time integrator functions as time counter.

The basic PID was enhanced with a first order filter to yield a proper controller.

$$H_c = K_c \cdot \frac{\tau_I \tau_D s^2 + \tau_I s + 1}{\tau_I \tau_D s^2 + \tau_I \cdot s}$$

This resulted in: $K_c = 17$, $\tau_I = 900$, $\tau_D = 2$.

$$H_c = 17 \cdot \frac{1800 \cdot s^2 + 900 \cdot s + 1}{1800 \cdot s^2 + 900 \cdot s}$$

In the Figures 14, 17 and 18 the simulation results are shown of different system types (continuous or discrete components) or different kind of feed forward (dynamic or passive).

Figure 14 shows the results of a simulation run of the system with discrete elements as described before. Comparison with Figure 8 indicates that inclusion of the discrete elements of the real system results in a deterioration of the controller performance at sunrise and sunset. The cycle averaged drain flow is not constant but runs away above and below its constant set value. The controller is not able to timely compensate for this sudden change.

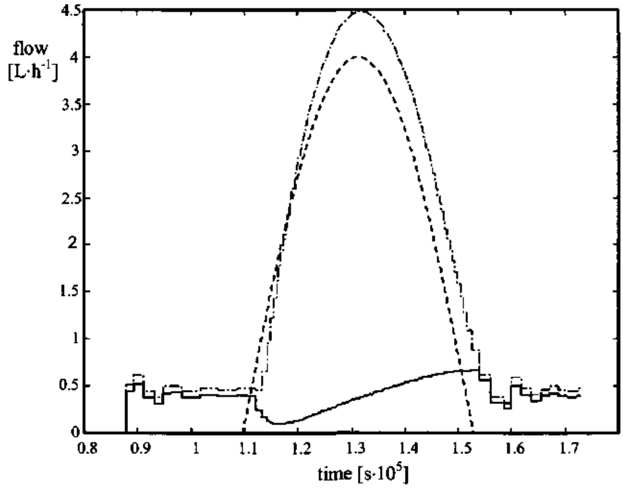

Figure 14 - Drain flow (——), water supply (– · – · –) and global radiation (– – –) as function of time of day. Global radiation is interpreted as potential evaporative water uptake (L·h^{-1}).

Feed forward compensation of the disturbance

A closer look at the results of the simulation in Figure 14 gave rise to the idea that a feed forward action of the disturbance on the ON-time of the pump control action might solve the problem.

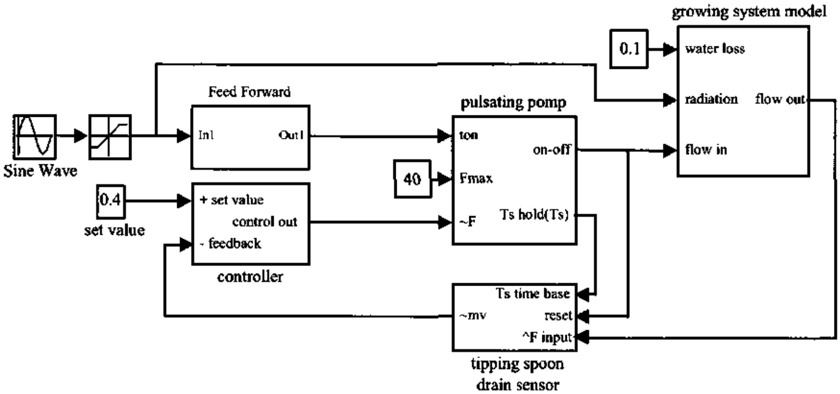

Figure 15 - Diagram (in Simulink®) of the controlled loop used for the discrete time simulation, with extra feed forward compensation of the disturbance.

The Simulink® diagram of Figure 15 depicts a representation of this approach. Here a function of the global radiation (Φ_g), as the cause of water uptake, is fed into the ON-time input (t_{on}) of the controlled pump actuator. An algorithm that anticipates on the rate of change of the global radiation improves the performance of the controller. Figure 16 shows two types of feed forward elements that have been tested in simulation runs.

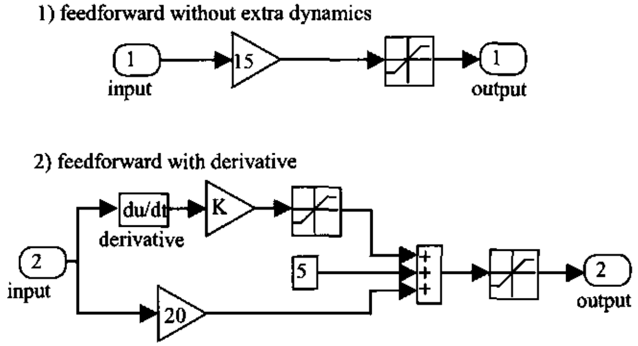

Figure 16 – Feed forward elements in Simulink®. Element 1) is time independent. Element 2) contains a derivative component.

The algorithm taken for the derivative feed forward function of Figure 16 is as in equation 3:

$$t_{on} = k_1 \frac{d\Phi_g}{dt} + k_2 \cdot \Phi_g + k_3 \qquad (3)$$

In this algorithm parameters k_2 and k_3 are chosen as 20 [$s\cdot m^2\cdot W^{-1}$] and 5 [s] respectively, to bring the system in its steady state position. The parameter k_1 [$s^2\cdot m^2\cdot W^{-1}$] is used to tune the influence of the change of global radiation on the system performance.

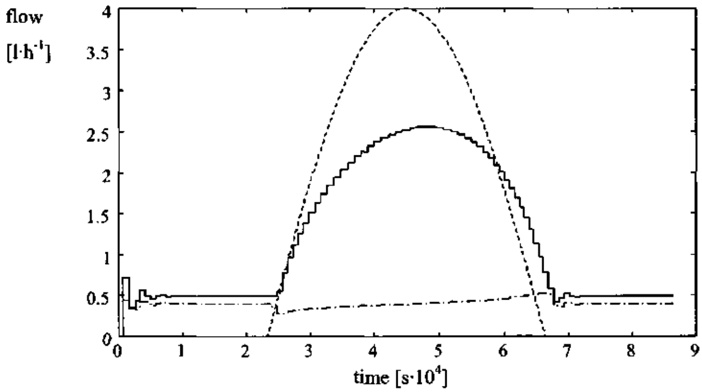

Figure 17 - Feed forward performed by the time independent element (component 1, Figure 16). The set value for drain flow $F_{dr,sv}$ = 0.4 [$L\cdot h^{-1}$]. Disturbance: (- - - -); Water supply: (——); Drain flow: (– · – · –). Global radiation is interpreted as potential evaporative water uptake ($L\cdot h^{-1}$).

Figure 17 shows the improvement in performance as a result of the combination of a feedback and a feed forward component. In Figure 8, 14, 17 and 18 the global radiation represents the potential water uptake. The feed forward component adjusts the range of the global radiation signal to the range of the Simulink® signals used blocks and adapts it to the desired nature of the feed forward action (dynamic or passive).

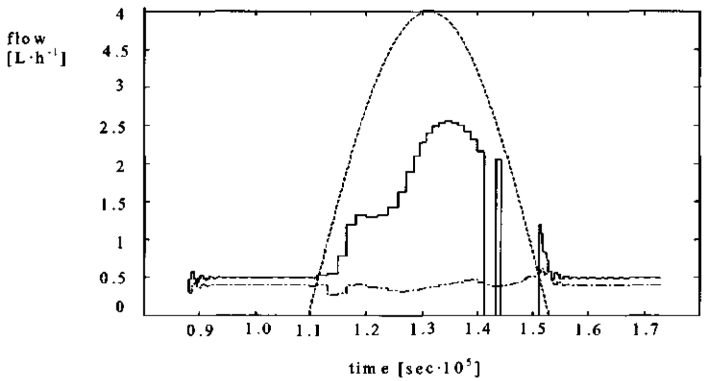

Figure 18 – Feed forward performed by the component (component 2, Figure 16), the element with a derivative action. The set value for drain flow is 0.4 [L·h^{-1}]. Disturbance: (- - - -); Water supply: (——); Drain flow (· — · — ·). Global radiation is interpreted as potential evaporative water uptake (L·h^{-1}).

Figure 18 shows the simulation results of a controlled system with feedback and a feed forward component with a derivative nature. The desired set value of 0.4 [L·h^{-1}] of the drain flow is achieved with fewer problems than the system without feed forward (Figure 14), but it does not show improvements in comparison with the system with passive feed forward.

Figure 19 shows results from a simulation run with the system from Figure 15. However, when real measured data of global radiation were used (the radiation data set of Figure 20-1, between approximately 06:00-20:00 h), where - as before - the radiation data values are interpreted as a flow (potential evaporative water uptake [L·h^{-1}]).
Comparison of Figures 17 and 14 for smooth radiation input already showed that - in general - addition of a feed forward component improves the system performance.
With real measured radiation data, the three diagrams in Figure 19 confirm that feed forward action improves the performance of control (compare drain flow in Figure 19, diagram a and both b and c).
Here, the difference between passive and derivative nature of the feed forward component also shows that passive feed forward is sufficient (compare drain flow in Figure 19, diagram b and c), and has preference over a feed forward with derivative nature, as was already the case with the stylised radiation in Figures 17 and 18.

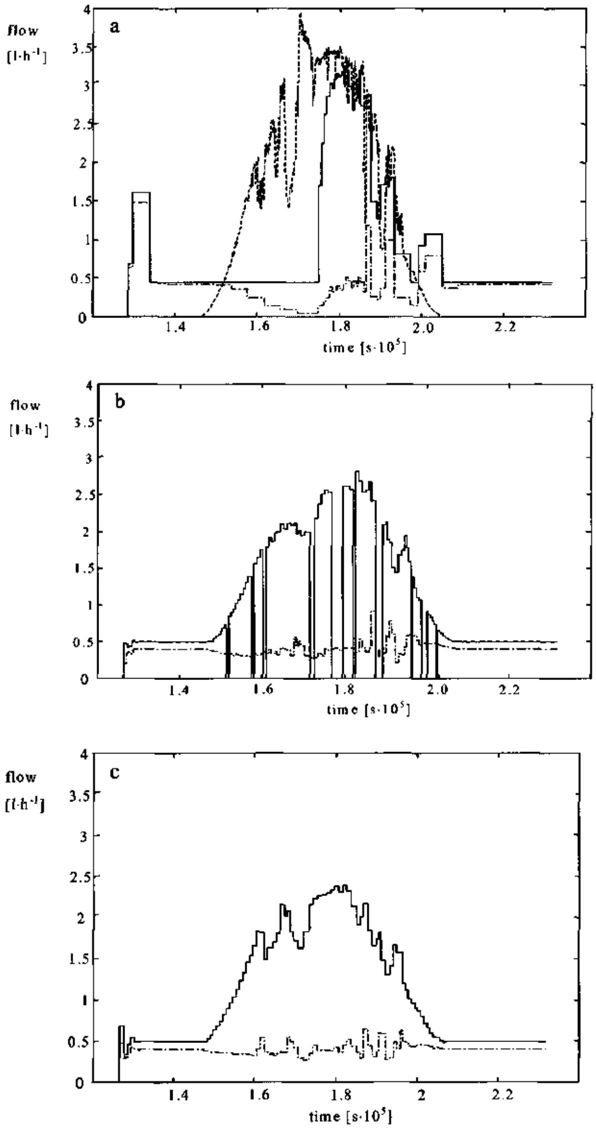

Figure 19 - Disturbance (- - - -), water supply (——) and drain flow (· — · — ·). Global radiation is interpreted as potential evaporative water uptake (L·h^{-1}). *In diagrams a, b, c the same global radiation pattern* is applied in the simulation run. a: just feedback control; b: feedback and derivative feed forward component; c: feedback and passive feed forward component.

4. Experimental verification

Figure 20 shows results from experiments using the feed forward/feedback controller in a greenhouse with a real crop. Figure 20-2b shows a diagram with constant drain flow curves. The water supplied to the system (Figure 20-2a), as a result of the controller action in order to keep the drain flow constant turns out to be a direct function of the global radiation (Figure

20-1). The small time delay between the radiation diagram and the diagram for water uptake by the plants (approximately 5-10 min.) cannot be explained by the delayed reaction of the plants to the change in radiation.

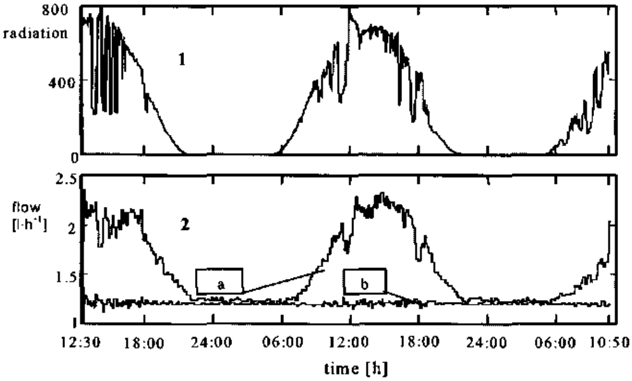

Figure 20 - Two consecutive days with radiation and flow data 4-5 June 1997:
1. radiation as function of time of day,
2. water supplied to the plants (a) and the resulting constant level of the drain flow (b).

Research by Bruggink *et al.* (1988) and Van Ieperen (1996) asserts that the time delays between radiation and water uptake are negligible on the time scale at hand. The time delays are better explained by the lingering time of the water in channel, root mats and return pit.

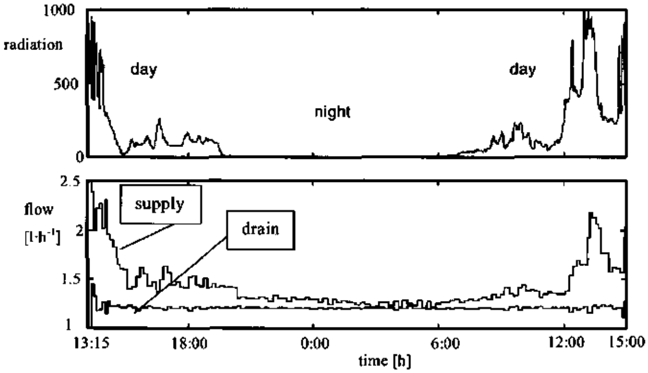

Figure 21 - Radiation and flow data recorded on 20-21 May 1997.

Figure 21 shows an additional data set of an extra day of measurements in the greenhouse. During the period shown, the global radiation is much lower than in Figure 20. Both for high radiation and low radiation, the controller can cope with the changes in the water uptake.

5. Conclusions

The above presented simulation experiments and the real time application in a controlled supply system show that different types of models (i.e. ARX, State Space), constructed from noise response data of a real system in a greenhouse, have a good resemblance with the actual response of the system and predicted time responses from validation data. The concept of feedback control aiming at keeping the drain flow constant, in conjunction with feed forward compensation on global radiation, is functioning well for a wide range of uptakes acting as disturbances upon the process.

§4.2 Robust controller design for nutrient supply

Based on:
Modelling and simulation for control of nutrient application in closed growing systems. In: *Netherlands Journal of Agricultural Science.* 45, p. 127-142. Th.H. Gieling, J. Bontsema, E.A. van Os, T.W.B.M. Bouwmans and R.H. Steeghs, 1997b.
Monitoring and control of water and nutrient supply in closed growing systems. In: E. Goto *et al.* (Eds). *Plant Production in Closed Ecosystems.* P. 103-121, Kluwer Acad. Publishers. Th.H.Gieling, J.Bontsema and E.A. van Os, 1997a.

1. Introduction

Nowadays, commercially available equipment for water and nutrient supply uses classic analogue or digital P, PI and PID controllers. In so called A/B type of systems, A or B type of stock solute mixtures - 100 times higher in concentration then the concentrations in a fertiliser solution - are subsequently added into a mixing tank. These diluters add the solute in relation to the EC value measured in the supplied nutrient solution. The pH value of nutrient supply is kept within the range of approximately 5.5-6.5. These systems have problems in compensating relatively fast changes of the nutrient uptake or - in case of closed growing systems - the drain water returning from the plants (Chapter 1).
Some publications on new strategies for system identification and new algorithms for control of water and nutrient application consider feedback of ion selective measurements in relation to the control of the supply of individual fertilisers. Hashimoto *et al.* (1989) used ion selective sensors to study and elucidate the dynamic characteristics of nutrient uptake. They propose the application of fuzzy logic and a neural network to control water and nutrient supply and the pH level of a 'deep flow' hydroponic growing system. Young *et al.* (1991), Chotai and Young (1991) and Chotai *et al.* (1991) describe what they call true digital control of a nutrient film technique (NFT) system with top-end water supply. They suggest a self-adaptive and self-tuning control method for systems whose dynamic characteristics change over time. Their papers report on the development of an adaptive control approach with a Proportional Integral Plus controller.
Honjo and Takakura (1991) suggest the use of a simple neural net structure for the identification of water and nutrient supply to a hydroponic tomato plant growing system. By using 8 hours of input data from 5 environmental factors and a neural net with one hidden layer (4 nodes), the amount of water and nutrient supply is calculated from the time series of these 5 environmental factors.

2. Robust nutrient controller design methodology

The design method described in this chapter is taken from robust control theory and results in a controller with robust performance and stability properties. In relation to nutrient supply this means in general, that the controlled process remains stable and within chosen allowable margins, in spite of uncertainties in the process models (i.e. seasonal changes in the root mat or models which do not describe the real process precisely in all details). The controller compensates disturbances caused by the nutrient uptake of the plants. In this section the use of the technique of loopshaping is described, where Bode plots enable well-defined choices to determine the properties of the controller.

General layout of the supply system

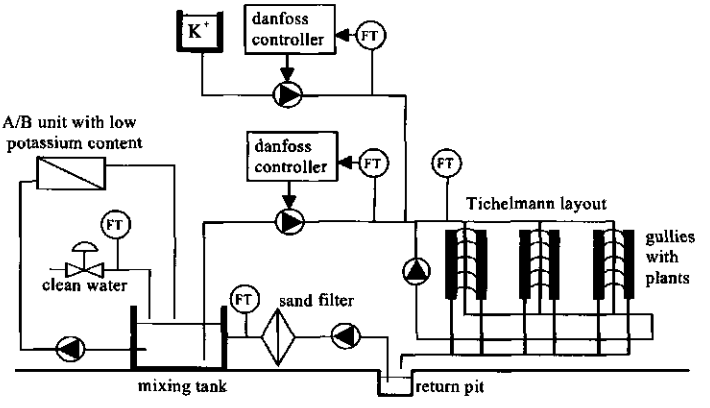

Figure 1 - Layout of a solute supply system

A nutrient supply system, situated in a $150m^2$ greenhouse with a NFT closed growing system and eight rows of tomato plants in gullies, is used for testing the system. Each gully is covered with a lid. Seedlings stay in 10x10x10 cm rockwool seedling blocks. Water is supplied by means of a trickle irrigation system (Steeghs and Bouwman, (1996).

The layout of the water supply system follows the Tichelmann design (Figure 1). In a Tichelmann system an extra pump circulates the nutrient solution through the supply pipes in order to reduce the dead time of nutrient supply (Chapter 2, Section 1). The drain water from the gullies is collected in a small return pit below the surface of the greenhouse floor and pumped into a mixing tank.

The nutrient solution in the mixing tank is kept at the standard nutrient concentration by means of an A/B diluter system. In the A/B solutes the K^+ is kept at a low value (Figure 1), in order to allow for a separately controlled injection of K^+. The potassium concentration is measured in the return pit, using an analyser with Chemfet sensors (Chapter 3, Section 2). A flow-controlled pump injects potassium - e.g. as KNO_3 - in the main stream of the nutrient solution (Figure 1).

All these parts are connected to form a closed growing system. Dead times as found in the real system were used in simulations performed on the system. Dead times of appendages and pipes add together as one overall dead time. Simplifications have been made to understand better the type and shape of the overall transfer functions of some of the sub-processes.

A model of the controlled process.

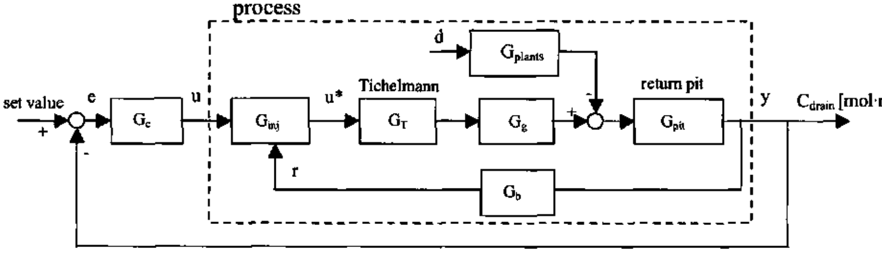

Figure 2 - Diagram of the nutrient supply process with controller.

In terms of transfer functions, the layout is shown in Figure 2. In the SISO case, which is considered here, a transfer function is defined as the quotient of the Laplace transform of the output response and its related input excitation, both as functions of time.
In this figure, G_g, G_b, G_{inj}, G_{pit}, G_T and G_{plants} represent the transfer functions of the gully, the mixing tank, the injector, the return pit, the Tichelmann supply lines and the influence of the plants respectively. G_g, G_b and G_{pit} are assumed to behave as first order systems. G_c is the transfer function of the controller, which is subject of research and is described in this section.
As was confirmed by simulations with a more complex model in which also non-linearity's were accounted for, the Tichelmann process can be approximated well by a first order system, as is shown in Figure 3.

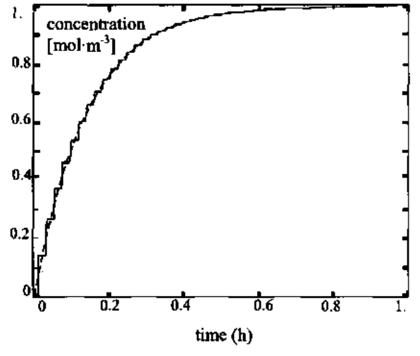

Figure 3 - Step response of potassium (solid) and first order approximation (dashed) of the Tichelmann system.

The solid line is the output of a simulation of a detailed transport model of the system. The staircase shape is due to the water pumped around in the supply pipes. During the first circulation cycle the water reaches the injection point with a constant concentration and it remains constant during the time it takes for the injected ions to reach the output. Each next cycle the concentration is increased at the injection point.
The dashed line is the step response of the first order approximation model. As can been seen the approximation is quite good.

In the injector, fluids u and r (Figure 2) are added each with their respective concentration. The derivation of the transfer function of the injector needs some extra considerations. Equation 1 describes the actual mixing process in the injector. F_{ion} is the ion flow [$m^3 \cdot s^{-1}$], C_{ion} is the concentration of the injected ion flow [$mol \cdot m^{-3}$] and F_r, C_r are respectively the flowrate [$m^3 \cdot s^{-1}$] and concentration [$mol \cdot m^{-3}$] of the return stream. C_T is the concentration of the fluid at the Tichelmann inlet.

$$\frac{F_{ion}(t)\cdot C_{ion}+F_r(t)\cdot C_r(t)}{F_{ion}(t)+F_r(t)}=C_T(t)\Leftrightarrow \quad \textbf{(1a)}$$

$$u^*(s)=\frac{C_{ion}}{F_{ion}+F_r}u(s)+\frac{F_r}{F_{ion}+F_r}r(s)=\alpha\cdot u(s)+\beta\cdot r(s) \quad \textbf{(1b)}$$

Here, *u(s)*, *r(s)* and *u*(s)* are the Laplace transform of $F_{ion}(t)$, $C_r(t)$ and $C_T(t)$respectively.
Since F_{ion} shows up in both numerators and denominators of equation 1a, this part of the process is non-linear. By stating that the potassium flow is always very small compared to the main solution flow - or $F_{ion} << F_r$ - equation 1 may be linearised by using F_{ion} as variable *u(s)* in the numerator and as a small constant increment of value F_{ion} on the value of F_r in the denominator. This leads to the transfer function approximation of the injector shown in equation 1b.

If all transfer functions are considered, the overall transfer from *u(s)* and *d(s)* to *y(s)* has the form:

$$y(s) = \frac{\alpha \cdot G_T(s) \cdot G_g(s) \cdot G_{pit}(s) \cdot u(s) - G_{plants}(s) \cdot G_{pit}(s) \cdot d(s)}{1 - \beta \cdot G_T(s) \cdot G_g(s) \cdot G_b(s) \cdot G_{pit}(s)} \tag{2}$$

The minus sign in the numerator arises because a positive disturbance (nutrient uptake) results in a negative response. All transfer functions used in equation 2 are shown in Figure 2. The model in equation 2 is the basis of the design of the controller.

The controller should work at various flow rates. Since the transfer functions depend upon the flow rates, the dynamics of the system is uncertain and the actual system is perturbed with respect to the system at nominal flow rate. In order to cope with this kind of perturbation, the controller has been designed by using the 'robust design' method (Doyle *et al.*, 1992). The uncertainty is modelled by taking a range of fixed flow rates around the nominal value.
By using the robust design method, a whole class of system models can be controlled based on a controller that has been designed for the nominal model. Robustness in control distinguishes between robust stability and robust performance. In this particular case, the robust design method deals with uncertainties in the model description of the real process, i.e. variability of the mainstream flow and seasonal changes of the models. Loopshaping is used as a design tool for the controller. This way of designing the controller takes into account the uncertainties mentioned above and a desired performance.

Performance and Stability

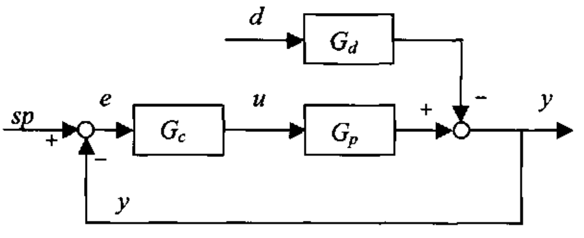

Figure 4 – Generalised transfer diagram.

Performance is expressed in terms of the maximum allowable difference between set value *sp* and *y* as output value. From the generalised transfer diagram in Figure 4, the sensitivity function *S* is defined as the transfer from set value *sp* to deviation *e*. Additionally a complementary sensitivity function *T* is defined as the transfer from set value *sp* to output *y*:

$$S=\frac{1}{1+G_c\cdot G_p};\quad T=\frac{G_c\cdot G_p}{1+G_c\cdot G_p} \qquad \textbf{(3a,b)}$$

Nominal performance is stated in terms of a weighting function W_1. If the performance is defined as the maximum allowable deviation between set value and output, this performance can be reformulated as a weighting of the sensitivity function S by W_1 as in equation 4a and 4b.

In a SISO system the maximum allowable deviation can be formulated mathematically by the infinite norm of the magnitude of the transfer function, i.e.:

$$\|H\|_\infty=\sup_\omega |H(j\omega)|$$

So:

$$\frac{e}{sp}<\varepsilon \Leftrightarrow \|S\|_\infty<\varepsilon \Leftrightarrow \left\|\frac{1}{\varepsilon}S\right\|_\infty<1 \qquad (4a)$$

$$\|W_1\cdot S\|_\infty<1\Rightarrow W_1=\frac{1}{\varepsilon} \qquad (4b)$$

Here, instead of a performance directly related to *sp,* a performance is considered which is related to the disturbance as a result of variations in nutrient uptake by the plants. Again this performance is - indirectly - expressed as a maximum deviation related to a set value *sp* that is kept constant. In other words, how good will the controlled process track a (constant) *sp* when it suffers from a varying disturbance.
The frequency spectrum of nutrient uptake by the plants (the disturbance *d* in Figure 4) is only of interest to a maximum frequency of about $7.2\cdot10^{-5}$ rad·s^{-1}, namely one cycle of a negative cosine during a period of one day, as an approximation of the smoothed diurnal curve of solar radiation.
From Figure 4 the transfer *V* from disturbance *d* to deviation *e* with constant *sp* can be derived as:

$$V=\frac{G_d}{1+G_c\cdot G_p}=G_d\cdot S \qquad \textbf{(5)}$$

The performance requirement, chosen as a goal for design, states that the maximally allowable deviation from the set value should be smaller than ε, while disturbances are acting on the process. Considering disturbance rejection thus introduces a new weighting function $\widetilde{W}_1$, in a similar fashion as equation 4a and 4b, as follows:

$$\left\|\frac{1}{\varepsilon}V\right\|_\infty<1\Rightarrow\left\|\frac{G_d}{\varepsilon}S\right\|_\infty<1\Rightarrow\|\widetilde{W}_1\cdot S\|_\infty<1\Rightarrow\widetilde{W}_1=\frac{G_d}{\varepsilon}=W_1\cdot G_d \qquad \textbf{(6)}$$

Since only disturbances are considered with a frequency spectrum till ω_{max} = $7.2\cdot10^{-5}$ rad·s^{-1}, $\widetilde{W}_1(\omega)=0$ for $\omega>\omega_{max}$. For ε the value of 0.1 was chosen. This means that maximal deviations of + or - 10% around the set value are accepted. A second weighting function W_2 is introduced to allow for the design of a controller C. It not only achieves internal stability for the nominal process, but also stabilises an entire class of models with allowable multiplicative perturbation. This class $\tilde{G}_p$ is given by:

$$\left\{\tilde{G}_p(s) | \tilde{G}_p(s) = (1 + \Delta(s) \cdot W_2) \cdot G_p(s), \|\Delta\|_\infty < 1\right\} \tag{7}$$

This class consists of all transfer functions $\tilde{G}_p$, such that the relative error between a perturbed model $\tilde{G}_p$ and the nominal model G_p is bounded by the weighting function W_2, as expressed by equation 8. A set of $\tilde{G}_p(j\omega)$ enables determination of $W_2(j\omega)$ in equation 8.

$$\left|\frac{\tilde{G}_p(j\omega)}{G_p(j\omega)} - 1\right| \leq |W_2(j\omega)|, \forall\, \omega \tag{8}$$

Then, the robust stability condition with respect to these perturbations is determined by:

$$\|W_2 \cdot T\|_\infty < 1 \tag{9}$$

Robust Performance

Doyle *et al.* (1992) explain the general notion of robust performance as: internal stability and performance of a specified type, which hold for all process models in $\{\tilde{G}_p\}$. The robust controller for nutrient supply is designed with an internally stable nominal feedback system, that satisfies the conditions in equation 10.

The first condition ensures the robust stability and the second condition guarantees that the closed loop system has the required performance for all perturbed process models.

$$\|W_2 \cdot T\|_\infty < 1 \text{ and } \left\|\frac{\tilde{W}_1 \cdot S}{1 + \Delta \cdot W_2 \cdot T}\right\|_\infty < 1, \forall \Delta \tag{10}$$

Equation 11 is a necessary and sufficient condition for the robust performance.

$$\left\| |\tilde{W}_1 \cdot S| + |W_2 \cdot T| \right\|_\infty < 1 \tag{11}$$

Once both weighting functions are known, loopshaping is used as a tool to design the controller C. For this purpose the robust performance inequality in equation 11 is rewritten as:

$$\Gamma(j\omega) = \left|\frac{\tilde{W}_1(j\omega)}{1 + L(j\omega)}\right| + \left|\frac{W_2(j\omega) \cdot L(j\omega)}{1 + L(j\omega)}\right| < 1, \forall\, \omega \tag{12}$$

In equation 12, ω is the frequency ($rad \cdot s^{-1}$) and L is the open loop transfer function. A Bode plot is made of both weighting functions. For all ω along the horizontal axis they should satisfy equation 13:

$$\min\left\{\left|\tilde{W}_1\right|, \left|W_2\right|\right\} < 1, \ \forall \omega \tag{13}$$

If equations 12 and 13 are satisfied, it can easily be seen that both the nominal performance (equation 6) and robust stability (equation 9) are ensured. Equation 12 implies, that at a certain frequency an improved nominal performance ($\tilde{W}_1$ is large) entails a decreased robustness (W_2 is large) and vice versa, because both $\tilde{W}_1$ and W_2 can not be large at the same frequency. The loopshaping process now consists of finding a transfer function L in the Bode diagram that fulfils the inequalities in equation 12. In order to ease this process, it should be noted that these constraints mean that in general equations 14 and 15 should hold in the high and in the low frequency range respectively.

$$|L| < \frac{1 - |\tilde{W}_1|}{|W_2|} \tag{14}$$

$$|L| > \frac{|\tilde{W}_1|}{1 - |W_2|} \tag{15}$$

Now an L, which satisfies the inequalities in equations 14 and 15, is chosen in such a way that the inequality in equation 12 holds. Since (Figure 4) $L = G_c \cdot G_p$ and G_p are known, G_c can be calculated. However, in the specific approach described here, G_c rather than L is calculated directly in order to have some influence on the complexity of the controller.

3. Results and discussion

The Weighting function $\tilde{W}_1$

Weighting function $\tilde{W}_1$ can be determined only if the transfer function from disturbance d to y is known (equation 6). A simulation with the Simulink® model of the nutrient injection process produces the transfer function G_d. By analysing the Simulink® model and after some minor simplifications it could be shown that the transfer function from d to y was of the form as in equation 16. Since the form of the transfer function was known it was sufficient to fit the parameters in equation 16 on the basis of step responses of the disturbance d in the Simulink® model, with constant input u. Five simulations were carried out for the following set of pairs of disturbance d and drain flow r: {($7.5 \cdot 10^{-5}$ $m^3 \cdot s^{-1}$, nominal), ($1.5 \cdot 10^{-4}$ $m^3 \cdot s^{-1}$, nominal + 10%), ($1.5 \cdot 10^{-4}$ $m^3 \cdot s^{-1}$, nominal - 10%), (0, nominal + 10%), (0, nominal - 10%)}.

$$G_d(s) = \frac{A \cdot s^2 + B \cdot s + C}{D \cdot s^4 + E \cdot s^3 + F \cdot s^2 + s} \tag{16}$$

It resulted in a series of five values for A through F as in Table 1. Equation 16 and the five simulation runs produced five different $\tilde{W}_1$ functions. In order to choose the best function for $\tilde{W}_1$, $|\tilde{W}_1(j\omega)|$ was calculated for all five simulations and depicted in a Bode plot (Figure 5a). The upper line (simulation run 2) exceeds the other four lines, thus satisfying best the conditions of equation 13.

Table 1 - Parameter values of $G_d(s)$ as in equation 16 for five simulation runs.

run	parameter	A	B	C	D	E	F
1		$4.83 \cdot 10^{2}$	$5.49 \cdot 10^{-1}$	$1.16 \cdot 10^{-4}$	$6.32 \cdot 10^{9}$	$1.03 \cdot 10^{7}$	$5.55 \cdot 10^{3}$
2		$5.61 \cdot 10^{2}$	$8.22 \cdot 10^{-1}$	$2.49 \cdot 10^{-4}$	$3.32 \cdot 10^{9}$	$6.67 \cdot 10^{6}$	$4.47 \cdot 10^{3}$
3		$7.55 \cdot 10^{2}$	$9.46 \cdot 10^{-1}$	$2.54 \cdot 10^{-4}$	$5.44 \cdot 10^{9}$	$9.28 \cdot 10^{6}$	$5.28 \cdot 10^{3}$
4		$1.37 \cdot 10^{-2}$	$2.43 \cdot 10^{-6}$	$1.08 \cdot 10^{-10}$	$1.21 \cdot 10^{11}$	$9.02 \cdot 10^{7}$	$1.94 \cdot 10^{4}$
5		$9.25 \cdot 10^{-3}$	$1.99 \cdot 10^{-6}$	$1.08 \cdot 10^{-10}$	$1.00 \cdot 10^{11}$	$6.81 \cdot 10^{7}$	$1.46 \cdot 10^{4}$

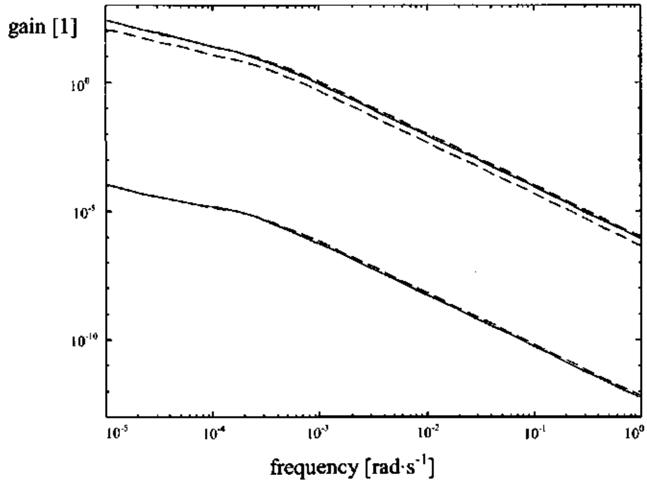

Figure 5a - Weighting function $\widetilde{W}_1$ run 2, 3, 1, 4 and 5 counting from above respectively.

Inspection of the diagram of simulation run 2 of the Bode plots in Figure 5b revealed, that the transfer function of $\widetilde{W}_1$ could be reduced to the much more simpler form:

$$\widetilde{W}_1 = \frac{2.7 \cdot 10^{-3}}{1.3 \cdot 10^{-3} \cdot s^2 + s} \tag{17}$$

Since the reduced form still encloses the Bode plots of the other five functions (Figure 5b), it was used to continue the loopshaping process.

The second weighting function W_2 takes into account the perturbations of the nominal model. The nominal model will be perturbed as a result of dynamics in the flows. All flows were related to the three most important flows, i.e. the potassium injection flow, the nutrient solution flow due to plant uptake and the drain flow. These three flows had $2^3 = 8$ combinations of upper and lower boundaries, which had to be taken into account in the same type of simulation-fit procedure as described before for the $\widetilde{W}_1$ weighting function, however, now with a step function on u and a constant value for d.

The W_2 weighting function was determined by equation 8. The set of transfer functions $\widetilde{G}_p$ were found to be of the type as in equation 18:

$$\widetilde{G}_p = \frac{A \cdot s + B}{C \cdot s^4 + D \cdot s^3 + E \cdot s^2 + s} \tag{18}$$

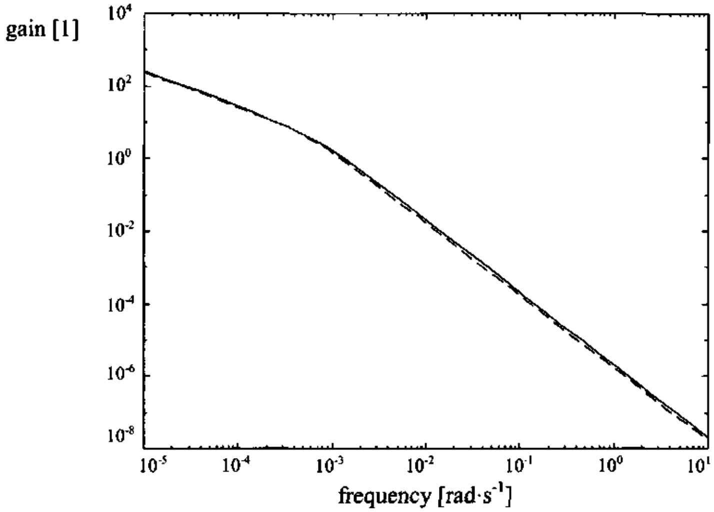

Figure 5b - Reduced form (solid) and $\widetilde{W}_1$ for run 2 (dashed).

The simulation procedure together with Equations 8 and 18 produced eight series of parameters A through E. The resultant Bode plots for $|(\widetilde{G}_p \cdot G_p^{-1}) - 1|$ are depicted in Figure 6a.

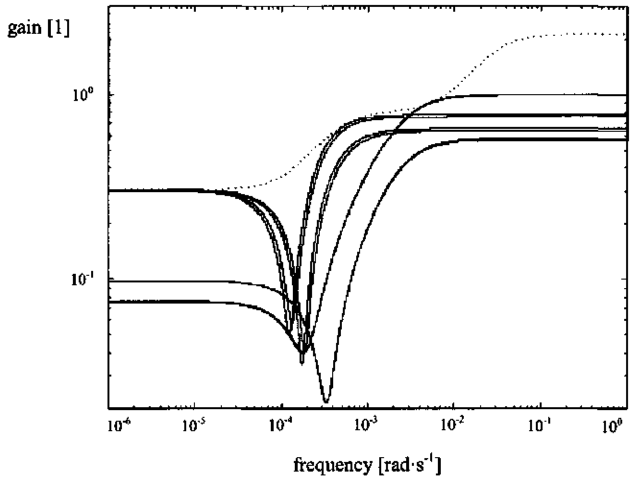

Figure 6a - Results of the eight simulation runs (solid) and of $\widetilde{W}_2$ function (dots).

The function values (for all ω) represented by the dashed line in Figure 6a exceed the values of all simulation outputs and thus - according to the constraint in equation 8 - is a sufficient representation of the weighting function W_2 in equation 19:

$$W_2 = \frac{2.29 \cdot 10^5 \cdot s^2 + 2.21 \cdot 10^3 \cdot s + 3.03 \cdot 10^{-1}}{1.08 \cdot 10^5 \cdot s^2 + 2.74 \cdot 10^3 \cdot s + 1} \qquad (19)$$

Since step functions were used for the excitation of the system the high frequency end of the W_2 function (dashed line in Figure 6a) was kept at a relatively large distance from the uppermost of the eight graphs.

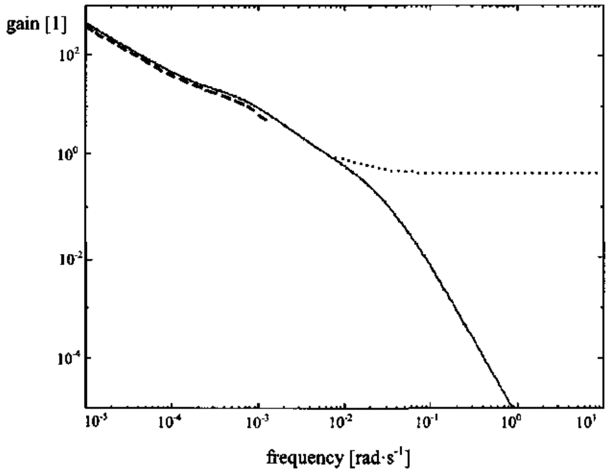

Figure 6b - Diagram shows /L/ (solid) and its limits in the upper (dots) and lower (dashed) frequency area.

Now $\widetilde{W}_1$ and W_2 were known and the controller could be determined by means of "loopshaping". For this purpose $L=G_p \cdot G_c$ was used.

As a result, G_p is known and G_c is chosen to determine L in such a way, that inequalities in equation 14 and 15 were satisfied for the high and low frequency range respectively.
Halfway through the frequency range the shape of L could be chosen freely, as long as equation 12 was satisfied.
Finally, it produced the controller transfer function, that satisfied all constraints as depicted in equation 20 with an $|L|$ as in Figure 6b (solid).

$$G_c(s) = \frac{5.92 \cdot 10^2 \cdot s^3 + 5.15 \cdot s^2 + 1.18 \cdot 10^{-2} \cdot s + 2.9 \cdot 10^{-6}}{2.62 \cdot 10^5 \cdot s^3 + 1.23 \cdot 10^4 \cdot s^2 + 1.92 \cdot 10^2 \cdot s + 1} \qquad \textbf{(20)}$$

4. Test of the control algorithm

A simulation test of the control algorithm was performed with a simulation set-up as is shown in Figure 7. The results are presented in Figure 8. A unit step was applied to simulate *sp*.

From the tenth hour onwards a negative cosine was applied, as a disturbance acting on the process, with a mean value of 5.7 [mol·s^{-1}], mimicking the nutrient uptake by the plants.

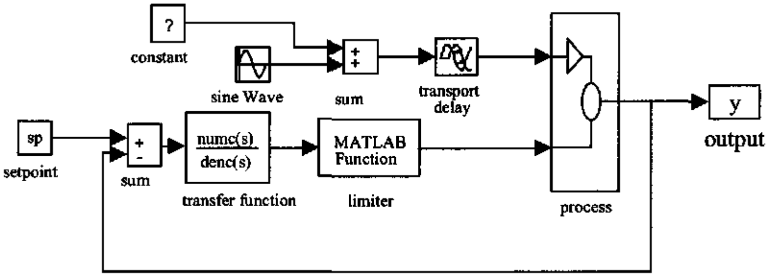

Figure 7 - The controlled system in Matlab Simulink®.

The process in Figure 7 is a Matlab-Simulink® model of the controlled system. Three different flow rates (minimum, nominal and maximum) were simulated for the potassium pump, the plant uptake and the gully. The extreme values of the flow rates induce the maximum expected perturbation of the model. In Figure 8, curve (a) is the response with nominal flow rates, curve (b) is the response with high flow rates and curve (c) is the response with low flow rates. Curve (d) shows the simulated flow through the potassium injection pump and shows the compensation for the unit step in the first hours and for the negative cosine of plant uptake from the tenth hour onwards. All three simulation results a) through c) show almost no residue of the disturbance in the output signal, hence the controller is able to keep the maximum deviation well within the indicated allowable margin of 10%.

The simulation data shows that the dynamics in the nutrient supply process are more complicated than expected at a first glance. More standard design procedures (PI, PID etc.) can lead to a stable controlled process, but might be less robust than the controller presented.

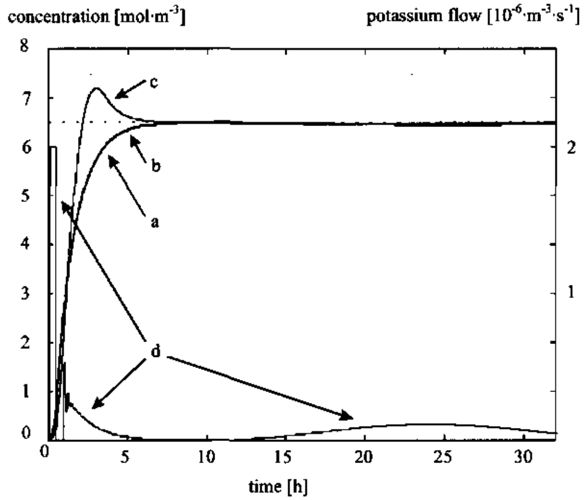

Figure 8 - Simulation responses at nominal (a), at high (b) and at low flowrates (c) (left axe) with a set value of 6.5 [mol·m^{-3}]. Example of nutrient injection exitation at nominal flowrate (d) (right axe).

Preparing the controller for implementation

The system under test was implemented as a Direct Digital Controller, using a SCADA measurement and control system. The smallest time period between samples of measured data was 6.4 seconds. The same time was needed for the control actions to be effective at the valves and pumps. To implement the control algorithm in a Direct Digital Controller, the continuous time transfer function G_c of equation 20 was transformed into a discrete time transfer function. First, the continuous time transfer function was transformed into a state space system (equation 21).

In equation 21 variables $x(t)$, $y(t)$ and $u(t)$ are the state variable, the output and the input of the controller respectively. $\boldsymbol{A}$, $\boldsymbol{B}$, $\boldsymbol{C}$ and $\boldsymbol{D}$ are system matrices, the values of which are given in equation 22.

$$\begin{aligned} \dot{x}(t) &= \boldsymbol{A}\cdot x(t)+\boldsymbol{B}\cdot u(t) \\ y(t) &= \boldsymbol{C}\cdot x(t)+\boldsymbol{D}\cdot u(t) \end{aligned} \tag{21}$$

$$\boldsymbol{A}=\begin{bmatrix} -4.7\cdot10^{-2} & -7.3\cdot10^{-4} & -3.8\cdot10^{-6} \\ 1 & 0 & 0 \\ 0 & 1 & 0 \end{bmatrix};\boldsymbol{B}=\begin{bmatrix}1\\0\\0\end{bmatrix};\boldsymbol{C}^T=\begin{bmatrix}-8.6\cdot10^{-5}\\-1.6\cdot10^{-6}\\-8.6\cdot10^{-9}\end{bmatrix};\ \boldsymbol{D}=2.3\cdot10^{-3} \tag{22}$$

The discrete time version of the controller transfer, with $\Delta t = 6.4$ [s], is depicted in equation 23. $\boldsymbol{A}_d$, $\boldsymbol{B}_d$, $\boldsymbol{C}_d$ and $\boldsymbol{D}_d$ in equation 23 are the discrete time system matrices. A Matlab® procedure is used to transform the continuous time system matrices (equation 22) into discrete system matrices (equation 24). The Matlab® Control Toolbox, which is connected to the SCADA system, directly accepts the matrices of equation 24 to control the real process.

$$\begin{aligned} x((n+1)\cdot T) &= \boldsymbol{A}_d\cdot x(n\cdot T)+\boldsymbol{B}_d\cdot u(n\cdot T) \\ y(n\cdot T) &= \boldsymbol{C}_d\cdot x(n\cdot T)+\boldsymbol{D}_d\cdot u(n\cdot T) \end{aligned} \tag{23}$$

$$\boldsymbol{A}_d=\begin{bmatrix} 6.0\cdot10^{-1} & -5.9\cdot10^{-3} & -3.0\cdot10^{-5} \\ 7.9 & 9.7\cdot10^{-1} & -1.6\cdot10^{-4} \\ 42\cdot8 & 9.9 & 1 \end{bmatrix};\ \boldsymbol{B}_d=\begin{bmatrix}7.9\\42.8\\148\end{bmatrix};\ \boldsymbol{C}_d^{\,T}=\begin{bmatrix}-8.6\cdot10^{-5}\\-1.6\cdot10^{-6}\\-8.6\cdot10^{-9}\end{bmatrix};\ \boldsymbol{D}_d=2.3\cdot10^{-3} \tag{24}$$

5. Conclusions

As is shown, robust control solves problems if a model of the process contains uncertainties. It keeps the performance of a controlled process within pre-set limits. Robust performance and robust stability - as qualities of the controlled process - are shown to be feasible for the control of nutrient application in closed growing systems. Loopshaping as a design tool gives a lot of insight into the process and its control. It helps the engineer to find his way around design pitfalls. Especially in this application, robust design and the loopshaping method results in a controller, which meets the desired performance, despite the uncertainties in the process. It shows to be a straightforward design procedure, useful to non-specialists with the aid of some mathematical toolboxes.

A simulation test (Figure 8) shows very good results in terms of disturbance suppression of the controlled process: the response on an excitation with a negative cosine disturbance stays well within the pre-set 10% limits.

A response to a change in set value is dictated by the intrinsic dynamics of the substrate (residence time) as the initial dynamics of the response on the switch-on bump shows (either a response as result of over critical damping or sub-critical damping). Nevertheless, the responses of Figure 8 show that the controller tracks the set value for the full range of the flow.
From the peak in disturbance in the second halve of the curve (after the initial condition has vanished) the disturbance is suppressed very well. The response to disturbance is well within the limits of 10%.
If the controller is implemented, however, there are some considerations that may hamper direct application in practice. The flow actuator is designed as a continuous dosage system. The amplitude of the dosage flow is continuously modulated in time in accordance with the controller output. It implies that the dosage equipment should be connected to this one greenhouse continuously and can not be multplexed over subsequent nutrient solution supply loops in the greenhouse.
In practice, the supply systems are pulse operated, where the time duration or the repetition frequency is modulated (Chapter 1 and Paragraph 4.1). The design of controllers that are able to cope with the peculiarities of pulsed flow injection of nutrients in a substrate needs more knowledge of the physics of substrate behaviour problems related to pulse modulated control. This work for further research in new projects.

§4.3 INJECTION OF FERTILISER STOCK FLUIDS

Based on:
Supply of nutrient ions by injection of multiple chemical fertilisers. Internal report IMAG. Th.H.Gieling, J.J.W Westra, 2000.

1. Introduction

The procedure to design a liquid fertiliser controller that produces a nutrient solution for plants in closed growing systems has been evaluated in Gieling *et al.* (1998c) and has been discussed in Chapter 4.2. This design was based on the generalised single-input single-output (SISO) diagram of Figure 1.

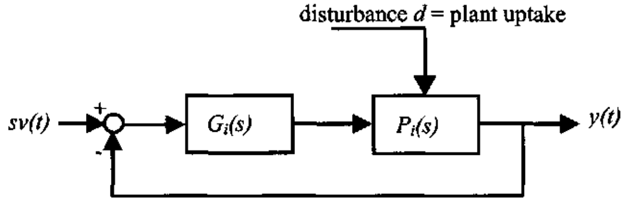

Figure 1 - Diagram of a controlled system, with the uptake of the plant as disturbance on the controlled process.

The output of the controlled nutrient application system is $y_i(t) = {}^{\langle i \rangle}C_{dr}(t)$, with ${}^{\langle i \rangle}C_{dr}$ as the drain concentration of ion *i*. The transfer function of the controlled process is $P_i(s)$ and that of the controller $G_i(s)$. The controller could very well be of the kind as described in Chapter 4.2. The goal of the controller action is to keep the concentration of the solute, which drains from the root zone (growing medium + roots), at a value equal to $sv_i(t)$. The absolute value of $sv_i(t)$ is probably constant or it is changing as a function of i.e. growth rate, with a time base that stretches out over days. The latter is very slow, compared to the dynamics of the drain process in the root zone (time base of hours during a day).

Table 1 - Examples of multiple and single nutrient ions in liquid fertiliser stock solutions.

Fertiliser name	Nutrient ion	Multiple nutrient-ion fertiliser fluid	Single nutrient-ion fertiliser fluid
potassium nitrate	Ca^{++}, NO_3^-	$Ca\text{-}(NO_3)_2$	
magnesium nitrate	Mg^{++}, NO_3^-	$Mg\text{-}(NO_3)_2$	
caustic potash	K^+		K-OH
bitter salt	Mg^{++}, SO_4^-	$Mg\text{-}SO_4$	
sulphuric acid	SO_4^-		$H_2\text{-}SO_4$
phosphoric acid	PO_4^-		$H\text{-}H_2PO_4$
nitric acid	NO_3^-		$H\text{-}NO_3$
ammonium nitrate	$NH_4\text{-}NO_3^-$	$NH_4\text{-}NO_3$	

In a real-world system, the nutrient ions needed for crop growth are commercially available in a set of highly concentrated stock fertiliser liquids. In these liquids some nutrient ions are present in more than one fertiliser stock fluid and some chemical stock fluids contain more than one nutrient ion (Table 1).
A diagram of a typical nutrient supply system is depicted in Figure 2, where a nutrient injection unit dilutes and distributes concentrated liquid stock chemicals. In Figure 2 a generalised block diagram is given of the nutrient application control.

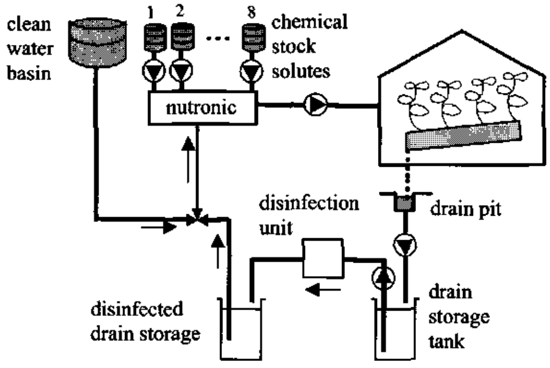

Figure 2 - Nutrient injection (NUTRONIC®, Priva Hortimation), with storage tanks and disinfecting unit

It is of importance for controller design to know, whether the nutrient supply system should be controlled by a MIMO controller, with *N* (possibly interrelated) inputs and *N-K* (possibly interrelated) outputs, or whether it should merely been seen as a vector of *N* independent SISO controllers. *N* is the number of nutrient ions as in column 2 of Table 1, and *N-K* is the number of available stock solutions as in column 3 and 4 of Table 1 (*K* may be positive or negative). So, instead of Figure 1, a realistic controller structure looks more like Figure 3.

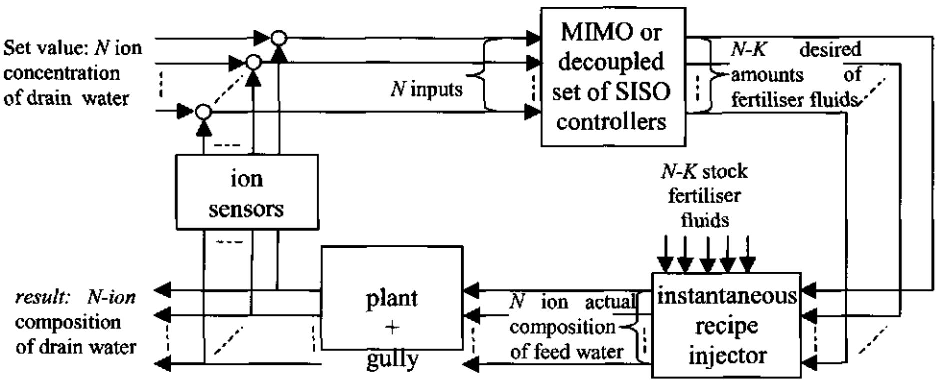

Figure 3 – Control diagram of *N* setvalues for drain concentration, which result in *N-K* desired amounts of fertiliser fluids (*K* may be positive or negative).

The purpose of this paragraph is to examine whether it is possible to consider the nutrient control system as a set of decoupled SISO systems, rather than one complex MIMO controlled system (section 2). Furthermore, it should be determined how to apply the nutrients while taking into account the various stock solutions (section 3).

2. MIMO and SISO controllers

The diagram of a SISO controlled process in Figure 1 will do for each ion of a single element fertiliser fluid (Table 1), if - and only if - it is present in one stock-tank. The process control diagram is bound to be more complicated when the ion is from a multiple ion fertiliser, or when there are more stock tanks containing that ion (multiple sources) (Figure 4). These last two options exist in all direct injection or mixing tank systems that utilise liquid fertiliser chemicals in stock tanks. An optimisation routine in the controller should determine how the recipe of chemical fluid volumes, needed to fulfil the crop's demand, is divided over the available source tanks.

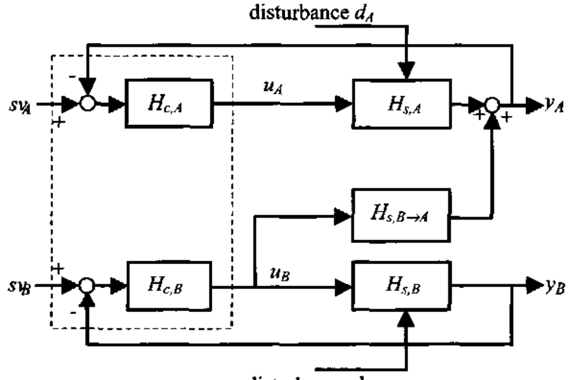

Figure 4 - A two-input, two-output controlled process with one relation between the two. Each section consists of a feedback-controlled process as in Figure 2. The controllers have resp. a transfer of $H_{c,A}$ and $H_{c,B}$, the supply process $H_{s,A}$ and $H_{s,B}$, the transfer from u_B to y_A: $H_{s,\,B\to A}$

In order to determine whether a MIMO or an independent set of SISO controllers is needed, a situation is considered of two ions A and B. Ion A is present as a single ion fertiliser, controlled by output u_A. Ion B together with ion A is part of a multiple ion fertiliser, controlled by output u_B. Figure 4 shows two processes each with its own controller, where the controller output of controller B (u_B) also excites the output of process A (y_A).

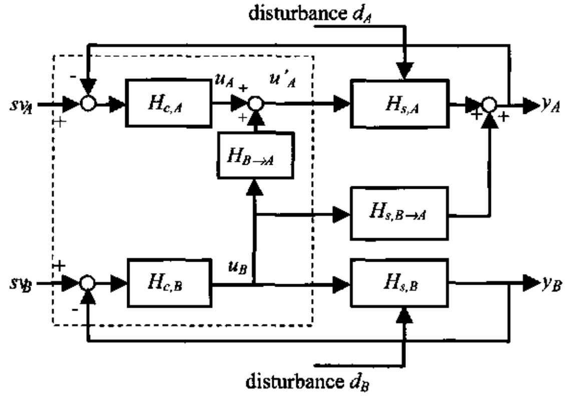

Figure 5 - A two-input, two-output MIMO controlled process with one relation between the two. Dashed line: the actual controllers. The controllers have respectively a transfer of $H_{c,A}$ and $H_{c,B}$, the supply process $H_{s,A}$ and $H_{s,B}$, the transfer from u_B to y_A: $H_{s,\,B\to A}$ and the transfer of the decoupler $H_{B\to A}$.

Figure 5 depicts a MIMO controller with two inputs and two outputs. One section controls the application of a fertiliser with only the A-ion and the other section controls the application of a fertiliser with ions A+B.

Due to the fact that ion A as well as ion B is supplied, when the set value of ion B is changed, manipulating the control u_B acts as a disturbance upon y_A, which is shown in Figure 4 by the transfer function $H_{s,B\rightarrow A}$. To counteract this, a decoupler element $H_{B\rightarrow A}$ should compensate for the changed y_A by providing an adjustment to the input u_A. The total amount of A-ion supplied will remain the same by reducing the flow of fertiliser liquid A in order to compensate for the amount of ion A-ion provided by liquid B.

According to Stephanopoulos (1984) the relations governing the decoupling are:

$$H_{B\rightarrow A} = -\frac{H_{s,B\rightarrow A}}{H_{s,A}} \quad \textbf{(1)}$$

$$y_A = (u_A + u_B \cdot H_{B\rightarrow A}) \cdot H_{s,A} + u_B \cdot H_{s,B\rightarrow A} = (u_A - u_B \cdot \frac{H_{s,B\rightarrow A}}{H_{s,A}}) \cdot H_{s,A} + u_B \cdot H_{s,B\rightarrow A} = u_A \cdot H_{s,A} \quad \textbf{(2)}$$

$$y_B = u_B \cdot H_{s,B} \quad \textbf{(3)}$$

Both fertiliser addition actions (A and A+B) are applied on the same supply process, i.e. the same type of pumps, valves, flowmeters, nozzles and the same substrate. As a result, $H_{s,A}$ and $H_{s,B}$ are equal, i.e. H_s:

$$y_A = u_A \cdot H_s \text{ and } y_B = u_B \cdot H_s \quad \textbf{(4)}$$

The above equations show that the process of supplying fertilisers that are coupled by one ion, can be de-coupled by a de-coupling controller as in Figure 4 provided that the process involved in both the A and the B fertiliser fluid application channels are the same.

Of course, this will only hold for the relation $sv_A \rightarrow y_A$ and $sv_B \rightarrow y_B$, because the process here only involves the gully+substrate, which will be the same for the A fertiliser fluid as well as the B fertiliser fluid.

The relation between disturbances and outputs, like $d_A \rightarrow y_A$ and $d_B \rightarrow y_B$, which depict the plant's uptake of the A and B ions, is not affected by the de-coupler.

The result of the above findings is, that controllers for the application of nutrients are a set of SISO controllers, rather than one complex MIMO controller.

Furthermore, this implicates that with proper design of the decouplers the controllers can be developed as a set of SISO controllers, thus avoiding the need for complex MIMO design.

3. Routines from Linear Algebra to optimise fertiliser application

Some stock fertiliser fluids contain the same ions, however, each in different combinations. Nevertheless, the calculations to determine a vector of fertiliser additions in order to realise a certain desired nutrient composition, can be made independent of each other by means of a set of linear transformations. A method from Linear Algebra is described that performs these transformations and calculates the amount of millilitres of fertiliser fluids that have to be taken from each liquid fertiliser stock tank to produce a fertiliser solute according to a given recipe. A simplex algorithm is applied as a mathematical optimisation technique to find the optimal solution within a set of given constraints that concern the individual ions. A recipe asked for by a controller does not necessary lead to a feasible solution of the matrix calculations, i.e. the desired solute to dispense can not always be produced. Then the procedure finds a solution close to the desired recipe.

Computer programs that calculate nutrient recipes use the so-called 'Sonneveld' algorithms (Sonneveld & Spaans, 1989). These programs are available from the fertiliser producers or from the suppliers of controller equipment. For a standard nutrient solution these algorithms need the following inputs:

- $\sigma_{out,mv}$ = EC = Electrical Conductivity [$dS \cdot m^{-1}$] measured in the mainstream nutrient solution
- $\sigma_{out,sv}$ = EC = set value for the EC of the mainstream nutrient solution
- pH_{mv} and pH_{sv} are measured and set values of the mainstream nutrient solution
- σ_i = EC of the clean water (measured value or operator provided value)
- the new recipe of macro nutrients that the mainstream nutrient solution should have [$mmol \cdot l^{-1}$]
- the new recipe of micro nutrients for the mainstream nutrient solution [$\mu mol \cdot l^{-1}$]

It is nowadays practice to send samples of mainstream solution and root zone solution to a lab and receive back an advice on the composition of a new recipe, which is then inserted by the operator. Only EC and pH are measured automatically (Chapter 1). However, an online-monitored nutrient supply system automatically measures the ion concentration values in mainstream and drain and the controller provides set values for the new recipe of ion concentrations. In both situations, before each new water supply cycle, the program then calculates:

1. the vector of chemical fluid volumes to inject (or mix) in the mainstream solution, to compensate the difference with he desired recipe,
2. the calculated overall EC of the mainstream nutrient solution, as a result of the contribution of each of the amounts of chemical fluids applied in item 1,
3. an extra amount of a specific acidic or basic nutrient to correct pH.

A method to calculate volumes of liquid fertiliser stock solutes

In his thesis, Heinen (1997) gives a clear and thorough description of the computation of the EC of a solution. Starting with the theory of ionic mobility and conductance in electrolyte solutions, he states that EC of a solution should rather be given as a function of ion activity than of ion concentration. The activity coefficient of ion i is $f_{a,i}$ and depends on the total ionic strength σ_s of the solution. Heinen uses the extended Debye-Hückel theory (Chang, 1990) to give precise relations between $f_{a,i}$ and σ_s. He also provides an approximate formula, equation 5, that is accurate enough for practical application. In here, m is the number of distinct ions in solution and ${}^{<i>}C$ is concentration of ion i [$mmol \cdot l^{-1}$].

$$\sigma = \frac{\sum_{i=1}^{m} {}^{<i>}C\,[mmol \cdot l^{-1}] \cdot valency_i\,[-]}{10}\ [dS \cdot m^{-1}] \qquad \textbf{(5)}$$

During the tests in the research project supporting this thesis, a nutrient injector was used (Priva Hortimation Nutronic® Injector) with an onboard nutrient calculation program (Priva Hortimation Nutricalc®). In this program the expression in equation 5 is used to calculate the resulting EC (Figure 6).

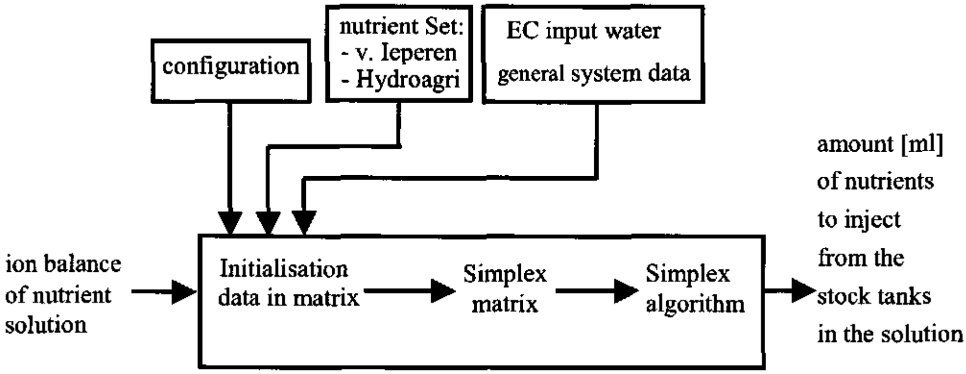

Figure 6. Data structure to calculate the new nutrient recipe.

Most nutrient calculation programs apply the simplex algorithm from Linear Algebra as a mathematical optimisation technique to find the optimal solution within a set of given constraints that concern the individual ions in a mixture of ions These constraints are concerned with avoidance of precipitation and desired EC and pH levels. In order to control nutrient supply, the sum of ions changes in relation to the set value. This is done by linearly balancing the macro-nutrients, except H_2PO_4 and NH_4.

The Naaldwijk Horticultural Station (PBG) prescribes a standard nutrient recipe vector for a number of commercial crops (the so-called 'schema' or blueprint). The nutrient calculation program calculates all additional changes (e.g. set value changes by the grower and additional recalculations due to H_2PO_4 and NH_4 influence) as relative changes to the standard nutrient vector. The output is the so-called "Sonneveld vector" and is put in the correct format into the Simplex Matrix template.

Micro-nutrients are added as a ready-made mixture via a separate injection channel. Micro-nutrient mixtures are commercially available for each type of crop, with recipes according to an advice by the Naaldwijk Horticultural Station (PBG).

In practice, in systems based on EC and pH control only, the grower keeps the input water of the diluter at a constant EC value during a considerable time, by means of a EC pre-control on the mixing of drain water with clean-water (well water, rain water, tap water). Moreover, the set value for this pre-controlled EC is manipulated by the grower to optimise the consumption rate of the drain water during recirculation. The grower plays around with the EC of the input water to keep the amount of drain water in stock constant.

However, if the concentration of individual ions is not measured, which is still the case in present-day commercial available systems, EC is considered to be a quality factor of the input water that should not change too much on a short time base, because it is taken into account by the nutrient calculation program to correct the supplied amount of all nutrients by a factor: the actual EC of the input water divided by the EC of standard input water.

4. Discussion

Although fertiliser chemical solutes contain multiple nutrient ions, and some ions are available from multiple stock tanks, yet the controlled process may be organised in such a way that a set of decoupled SISO controllers is used instead of a full-blown MIMO structured controller. As was shown in the previous section, it can be argued that the transfer between output of

the controllers - in the form of nutrient supply rates - and input of the diluter/injector - in the form of a recipe - is a pure algebraic relation without dynamics. The outputs of the SISO controllers are thus combined in order to determine how to apply the nutrients while taking into account the various stock solutions.
A calculation procedure as described above, is perfectly able to fulfil the task of optimising the fluid flows from different stock tanks. However, it should be noted that it is often impossible to find a final solution of a recipe vector of fertiliser fluid volumes that perfectly fits the output commanded by the nutrient controller. Not every desired vector of set values for the concentrations (input of the calculation program) will lead to a set of fertiliser fluids to inject/mix in the mainstream solution (output of the calculation program) in order to bring this solution to the desired ion concentrations $^{<i>}C$. This is due to the constraints that are valid for chemical mixtures: $^{<i>}C_{min} \leq {}^{<i>}C \leq {}^{<i>}C_{max}$. Where, $^{<i>}C_{max}$ is the maximum allowable concentration in the mixture to avoid precipitation. This value depends upon the other ions via the solubility productofthe various precipitates. $^{<i>}C_{min}$ is the concentration available in the mixture of drain water and "clean" water (in the present situation it is impossible to take out ions). Routines are available (i.e. using a simplex optimisation algorithm) that determine the optimal vector of fluid additions that comes closest to the wanted recipe.
It should be noted that any forward compensation of nutrient uptake, calculated on the basis of sensor-based (i.e ISE or Isfet) ion balances, under the assumption that all components will only appear in dissolved ionic form, may fail due to the formation of precipitates (as a function of pH, temperature and total ionic strength).
A feedback control of a single ion that tries to keep the concentration in the drain at a pre-set value - as developed in this thesis - will not suffer from this limitation, provided that conditions are avoided at which clogging of the supply tubes may occur.

CHAPTER 5

PHOTOGRAPHIC PRESENTATION OF EQUIPMENT AND INSTRUMENTS

Photo 1 - Tray with Isfet chips and small sealing rings. The picture shows the chips from their frontside and their backside. Occasionally, the selective membrane is visible on the frontside (e.g. third row from the left, second row from below). The backside shows the two plated through connection holes.

Photo 2 - First encapsulation design for the Chemfet chips, with connection wires and small plug. The housing is of a flow-through design, where the measurant fluid enters one side and leaves the other side. Sensor housings can be stacked to form a set of e.g. eight sensors for eight different types of sensors (e.g. pH, pK, pCa, pMg, pNa, pNO3, EC and temperature).

Photo 3 - Upper and lower parts of this first type of encapsulation are detachable. A spring forces the connection pins to click into the plated-through backside contact holes in the sensor chip. The chip is locked between two small rings, which seal-off the backside of the chip from the flow-through compartment that contains fluid. A big problem in this design is the bad sealing between electric contacts and the fluid compartment.

Photo 4 - A set of stacked sensor encapsulations and a reference electrode. The measurant is entering and leaving through tubes with 3 mm cross section, connected in-line with the flow-through path of the sensor set.

Photo 5 - A second design of a sensor set. Here, six backside-contacted chips are glued in one strip. The flow-through channels are milled into the supporting construct, thus separating electrical contact area from the flow-through compartments. The same spring loaded contact pins are used to click into the chip contact holes.

Photo 6 - The set is completed with a temperature sensor and a reference sensor. A disadvantage of this design is the complexity of the set. Because of the many parts it is difficult, time consuming and expensive to assemble all parts into a complete set.

Photo 7 - A third prototype of the flow-through cell has been designed, where - again loose - sensor bodies are put in-line with the fluid flow.

Photo 8 - The latest version of the SENTRON Chemfet sensors used in the equipment of PRIVA Hortimation. In the background the red coloured Chemfet, in the foreground a miniature version of an EC sensor.

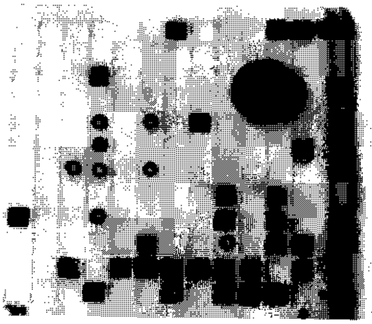
1

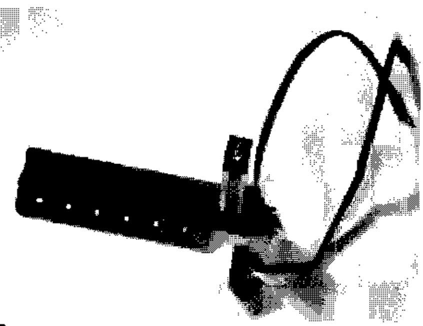
5


2


6

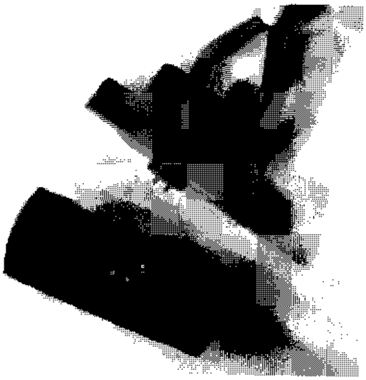
3


7

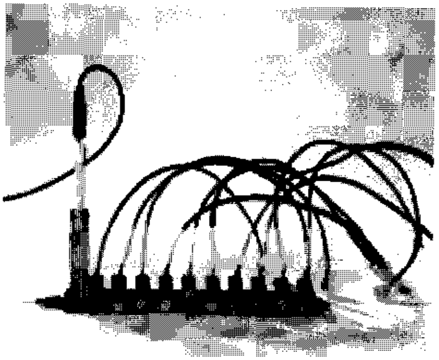
4

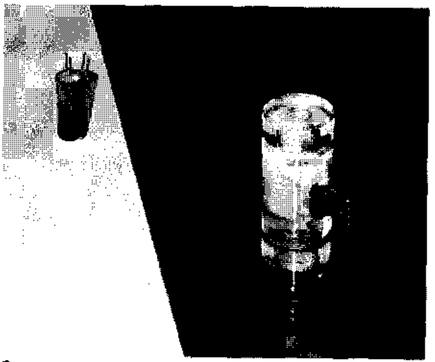
8

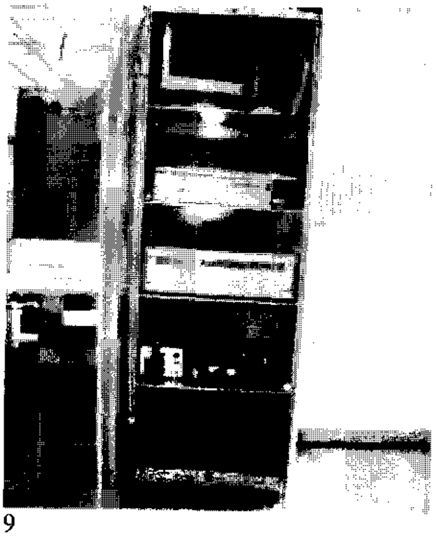

9

12

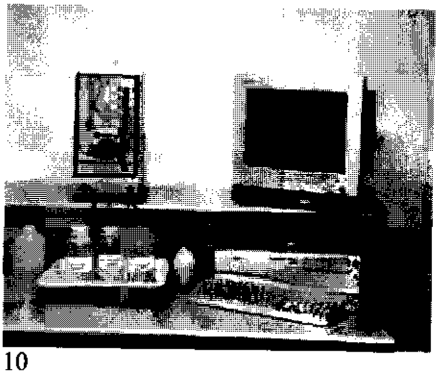

10

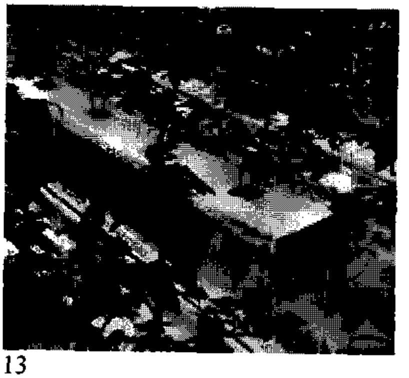

13

11

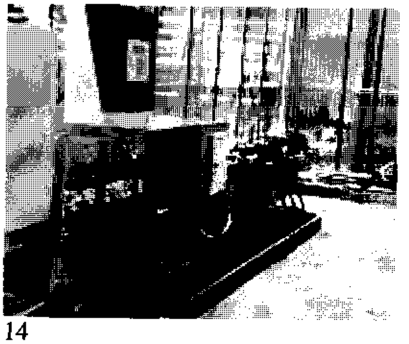

14

Photo 9 - The first IMAG analyser prototype with all the original hardware and software.

Photo 10 - The stand-alone analyser shown here in a laboratory set-up with calibration fluids. The analyser is connected to a computer for parameter input, report generation, acquisition of data and data representation in graphs.

Photo 11 - The IMAG analyser prototype in its 'natural' environment, next to the model gully in the greenhouse. The measurant inlet tubes collect fluid from the model gully. The analyser drains its used fluids in the same channel that captures the drain water of the plants. An RS232 line connects the analyser with a computer system for data acquisition.

Photo 12 - The first prototype of a PRIVA Hortimation analyser. All Chemfet sensors, the reference sensor, the 6 calibration fluids, the fluidic multiplexer, the pump and the analog and digital electronics are integrated in a 1.3m x 0.3m x 0.3m box.

Photo 13 - The model gully as it is situated in the greenhouse, amidst the plants in the canopy.

Photo 14 - Front view of the nutronic injector/dilutor.

CHAPTER 6

DISCUSSION AND CONCLUSIONS

§6.1 DISCUSSION AND CONCLUSIONS

§6.1 Discussion and conclusions

As has been stated before in this thesis: the grower is an innovating entrepreneur, passionately driven by his professional skill. This becomes manifest in his striving for high product quality. It is the origin of a natural urge to work with high-tech equipment in a high-tech production facility. The greenhouse, the control systems, the harvesting equipment and the computer supported management system, they should all meet his expectations.

It is because of this urge that horticulture is such an appreciative application area for automation by controlled systems, sensors and modern information and communication technology.

Substrates

Since the main process of interest for control takes place in the substrate, attention should be paid to the question: is the substrate able to deliver, in time, the water and nutrients to the root system according to the plant's needs and the grower's intention.

If the nutrient uptake U goes up, the mass flow needs to remain according to the plant's need, even if the bulk concentration C_b is kept the same. Thus, a higher uptake will be supported by a higher diffusive flux through the boundary layer. Since uptake is not dependent on C_{ro} (Figure 12, Chapter 2.2), it will continue at the same level of fulfilling the plant's needs until C_{ro} reaches C_{limit}. Uptake limitation will only occur when C_{ro} drops below the critical concentration. Macroscopically, the following might happen: a higher diffusive flux will lead to a drop in bulk concentration when the incoming concentration C_{in} remains the same. This, in turn, will reduce the mass flow, leading to the necessity of even larger diffusive flux, and an excessively increasing drop in root surface concentration. The conclusion is that the system is becoming unstable, and nutrient uptake limitations will inevitably occur. The same conclusion can be derived from the overall mass balance of the system as a whole.

From a control point of view, this situation can be detected by observing the drain concentration, and be remedied by increasing the incoming concentration. Therefore, the natural question arises whether the drain concentration should be regulated to a constant value, by manipulating the incoming concentration, similar to how the water supply controller aims at keeping the drain solute flow constant.

Suppose U increases, and increasing C_{in} such, that the drain concentration (and bulk concentration) was kept constant, counteracted this. Although this will lead to a new steady state, this steady state will have to be with a higher diffusive flux, which still is possible only when the root surface concentration is lower. And, consequently, a limitation might occur.

A strategy that will avoid this, ensures that the diffusive flux towards the roots is zero, so that the nutrients are carried to the plant by the mass flow. This can be achieved microscopically if $C_{ro} = C_b = C_x$, provided that $C_{ro}>C_{limit}$, and macroscopically, if $C_{in} = C_{dr} = C_x$.

There are two situations:

- suppose information is available about W - for instance from evaporation measurements - and about U, for instance by a growth model. Then, C_x can be computed, and C_{in} could be set accordingly.
- the other approach would be to increase C_{in} proportional to the difference between C_{in} and C_{dr}, until $C_{dr} = C_{in}$. Although these control strategies have the desired overall static behaviour, it should be noted that their dynamic properties still need to be evaluated.

In particular, it can be expected that the first approach may lead to the necessity of frequent C_{in} adjustments, in view of the large fluctuations of the water uptake over a day. Perhaps this can be remedied by averaging the flow fluctuations over a day. The second control approach has a positive feedback, which may lead to instability. An upper limit to C_{in} may perhaps be employed to avoid this. In both cases, the short term dynamic effects, plus the gradients in the substrate slab, may still cause temporary limiting conditions for uptake. This can only be investigated by using more sophisticated models of the behaviour of water and nutrients in the substrate. Feed forward action for water supply should be derived from transpiration (radiation) and for nutrient application from growth rate.

Sensors

Very recently, phyto-monitoring is finding an increasingly large number of supporters amongst growers. It may be considered as a first real proof of appreciation of the 'speaking plant' approach, were sensor-supported models are used in control. It is a justifiable expectation that the next generation of control systems of processes in greenhouses (e.g climate control, water- and nutrient application control) will apply model-based control.

Model-based control systems and decision support systems lean on models, which need direct online information from the process and its environment. These models will be directly coupled by dedicated intra-net to databases that are distributed over geographically dispersed locations and make use of sensors as are mentioned in this thesis.

Most of the sensors in horticulture are a spin-off from meteorology, the process industry or developments for automotive applications. However, the Chemfet sensor, as described in this thesis is an example of a development that evolved just the other way around. Modern greenhouse industry, in its search for better control of water and nutrient supply, was the clear mainspring and guideline of the research and development that - ultimately - will lead to durable analyser systems to measure ion concentrations.

The Chemfet can be successfully applied in horticulture, when the advantages of this class of sensors are exploited to its full extend. To be of use in applications in everyday horticultural practice, the lifetime expectancy of it should not be shorter than 6 months, preferably even not shorter than 9 months.

From a point of view of control, delay-times and dead-times in the measuring loop should be avoided. Hence, the tubes to transport the sample from the growing system to the analyser should be kept short. Therefore, it is advisable to mount the analyser on a short distance from the sampling point, preferably inside the greenhouse, next to the measuring gully.

Greenhouses are a harsh environment for the application of vulnerable equipment. Greenhouse air temperature may vary between 10 and 35 °C and supply water temperature may show the same variation. Radiation levels will vary between 0 and 600 W·m^2, which means that equipment in the greenhouse will show a strong warming up effect due to radiant energy. Inside metal equipment boxes temperature may rise to 70 °C.

Ageing drift does have a different timing than temperature drift. As temperature changes take place in a diurnal pattern, effects of ageing will stretch out over weeks or even months. Nevertheless, determining it at the same time as temperature drift simplifies the procedure.
Since the membranes of almost all available sensors show cross sensitivity for almost all ions, multi-component/multi-variate calibration models are needed to improve the fidelity of the output signal of the sensor. Compensation of cross sensitivity was not studied. The simple iterative routine, which has been used for drift compensation, is only a first step.
For all the reasons mentioned above, reliable equipment for measuring ion concentration in a greenhouse for the purpose of automatic control of water and nutrients should contain:
1. electronic signal-conditioning and surge voltage protection circuitry,
2. automatic on-line readjustment of the analyser's parameters,
3. compensation for the sensor's temperature drift,
4. compensation for the sensor's ageing drift
5. compensation for the sensor's cross sensitivity for other ions.

During the research project the functioning of the equipment was often hampered by an ill functioning of the reference sensor. The bigger part of the problems during the last - more or less successful - measurements were caused by it. At the start of the project, a glass type of reference sensor was used that we managed to break several times. This ISE-type of reference sensor introduces again the clumsy, hard to handle properties that one tried to get rid of by the development of the Chemfet sensor. During the course of the project, it was replaced by a plastic tube with a gel-filling that was more easy to handle. However, the slow release of gel through the contacting capillary into the sample, caused this sensor often to be poisoned by ions and algae, which penetrate from the sample into the gel-filling.
A real quest is going on in the search for a new type of semiconductor reference sensor, the so-called REFET sensor, which originates from the same type of technology as the Chemfet sensor. If the application of Chemfet sensors in horticulture should become a success, the search for a REFET sensor or other type of novel reference instrumentation or reference method should better be successful.

Growers are not very meticulous about sensor maintenance, as the lack of maintenance of the wet-bulb air humidity sensor showed in the past. Therefore, refilling calibration fluids might become a problem. In instruments developed and used during the project, each ion needs two calibration fluids, one above and one below the expected concentration. For some ions the fluids may be combined. The first production series of the prototype instrument provides 6 different fluids. A proper preparation and calibration of the sensors in a laboratory, before they are shipped to the customers, and some changes to the calibration procedure might make it possible to use one instead of two calibration fluids per ion.
As Chemfets will become available for more ions, on-line *in situ* monitoring in supply water and drainage water of a greenhouse will come within reach of quantities like: pH, potassium, calcium, nitrate, sodium (and possibly phosphate). It will be an important step towards advanced ion specific control of nutrient application in closed recirculation systems.

Controllers
As is shown in this thesis, robust control solves problems if a model of the process contains uncertainties. It keeps the performance of a controlled process within pre-set limits. Robust performance and robust stability - as qualities of the controlled process - are shown to be feasible for the control of continuous, uninterrupted application of nutrients.
Loopshaping as a design tool gives a lot of insight into the process and its control. It helps the engineer to find his way around design pitfalls. Especially in this application, robust design

and the loopshaping method results in a controller, which meets the desired performance, despite the uncertainties in the process. It shows to be a straightforward design procedure, useful to non-specialists with the aid of some mathematical toolboxes.
A simulation test shows very good results in terms of disturbance suppression of the controlled process: the response on an excitation with a disturbance as may be expected in practice stays well within the pre-set 10% limits.
However, there are some considerations that may hamper direct application in practice. The flow actuator is designed as a continuous dosage system. The amplitude of the dosage flow is continuously modulated in time in accordance with the controller output. It implies that the dosage equipment should be connected to this one greenhouse continuously and can not be multiplexed over subsequent nutrient solution supply loops in the greenhouse.
In practice the supply systems for nutrient solution are pulse operated, where the time duration or the repetition frequency is modulated, which enables multiplexing.
Both the simulation experiments and the real time application in a controlled water supply system presented in this thesis, show that different types of models (i.e. ARX, State Space), constructed from noise response data of a real system in a greenhouse, have a good resemblance with the actual response of the system and predicted time responses from validation data. The concept of feedback control aiming at keeping the drain flow constant, in conjunction with feed forward compensation on global radiation, is functioning well for a wide range of water uptake acting as disturbances upon the process.

Solutes

Although fertiliser chemical solutes contain multiple nutrient ions, and some ions are available from more than one stock tank, the controlled process may be organised in such a way that a set of decoupled SISO controllers is used instead of a full-blown MIMO structured controller. It is shown that the transfer between output of the controllers -in the form of nutrient supply rates- and input of the diluter/injector -in the form of a recipe- is a pure algebraic relation without dynamics.
It should be noted that it is often impossible to find a final solution of a recipe vector of liquid fertiliser fluid volumes that perfectly fits the output, as commanded by the nutrient controller, in respect to ion concentrations, EC and pH. Not every desired vector of set values for the concentrations will lead to a set of fertiliser fluids to inject/mix in the mainstream solution. Routines are available (i.e. using a simplex optimisation algorithm) that determine the optimal vector of fluid additions that comes closest to the wanted recipe.
Ion balances, calculated on the basis of potentiometric sensor measurements (i.e. ISE or Isfet) may fail due to the formation of precipitates (as a function of pH, temperature and total ionic strength). These precipitates might leave the system through the drain or be stored as crystals in the substrate and not be accounted for because they are not 'visible' to potentiometric sensors.
Forward compensation of nutrient uptake based on these models, under the assumption that all components only appear in dissolved ionic form, may lead to wrong decisions. Feedback control of a single ion that tries to keep the concentration in the drain at a pre-set value - as developed in this thesis - will not suffer from this limitation, provided that conditions are avoided at which clogging of the supply tubes may occur.

Thesis

It is the challenge of the technological research at the basis of this thesis, to lay down the prerequisites for a system with the mentioned properties and negotiate different paths to success. In the due course of the research it became evident that the set values for EC, pH and the concentration of each single ion in the nutrient recipe are related to plant behaviour and the

plant's status and should come from outside this so much technologically oriented research and thesis. They should be determined in relation to the water status of the plant and the need for nutrients as building blocks in the photosynthetic process, e.g. related to photosynthesis, growth rate, water uptake, turgor, evapo-transpiration, radiation, temperature and CO_2.
Consequently, these items are not part of this thesis, but of subsequent follow-up projects (Van Kooten, 2000). Yet, the realisation of the technological basis for appropriate control systems, as pursued in this thesis, are of paramount importance. It is a step towards a fully integrated system that allows for the control of nutrient uptake in relation to demand of the plant. This, in turn, will contribute to a better quality of the product as well as the horticultural production process.
In an applied research project as described in this thesis, in the back of our mind the question should always be: which additional tomato of higher quality is present on the tomato plant, or which cost are going to be saved extra, or which rules in environmental legislation are going to be met, as result of our research effort?
This PhD project produced the onset for the development of an instrument that will be useful in more specific research on the real problems related to water and nutrient uptake by plants. Control engineering studies, applying plant models for controller design and for model based control, can use the presented results and equipment design very fruitfully. The determination of relations between greenhouse climate and root environment, the influence of greenhouse parameters on the state variables, the use of water and nutrient control based on plant models, these are all a challenge that can be answered by the use of this design as a research instrument.

SAMENVATTING

De tegenstelling tussen het high-tech karakter van de klimaatregelaar en de relatief low-tech aanpak rondom het doseren van water en nutriënten, zoals dat tot nu toe nog steeds in de glastuinbouw gangbaar is, was mede de uitdaging voor het ondernemen van een project gericht op het besturen van de processen in het wortelmilieu. Tevens is er in de teelttechniek een groeiend besef dat er voordelen zijn te behalen uit een koppeling tussen de besturing van het bovengrondse klimaat en de besturing van de omstandigheden in het wortelmilieu.

Gedurende de looptijd heeft de promotiestudie, waarvan het resultaat hier voorligt, zich ontwikkeld tot een project gericht op integratie van verschillende technologieën. Technologieën die al voorhanden zijn of in nog ontwikkeling zijn, maar waarvan in ieder geval mag worden verwacht dat de resultaten binnen afzienbare tijd ter beschikking staan van de glastuinbouwpraktijk. Echter, er was een doorbraak op het gebied van de sensortechniek nodig om de ontwikkelingen daadwerkelijk mogelijk te maken.

Indien een nieuwe manier van besturen iets meer moet betekenen dan hetgeen nu wordt bereikt met regelen op basis van EC en pH van het gietwater, dan komt bij specialisten op dit gebied onmiddellijk de wens naar voren om te sturen op basis van de concentratie van ieder afzonderlijk meststof-ion. Daarnaast de vraag, om via de regeling de opname van water en individuele meststoffen door de plant te compenseren. Om dit te bereiken zijn twee dingen nodig: 1) het kunnen meten van de concentraties van individuele ionen in water; 2) een recept samenstellen van individuele ion concentraties als output van een regelaar dat door een installatie van vloeibare meststoffen kan worden gedoseerd.

Indien even wordt uitgegaan van de beschikbaarheid van de bovengenoemde apparaten en installaties, is het nodig een filosofie te ontwikkelen rondom het regeldoel. De vraag moet daarmee worden beantwoord, welke grootheden uiteindelijk onderwerp van een besturingsysteem moeten zijn.

Die filosofie kan eenvoudigweg bestaan uit het regelen van het water- en nutriënten transport naar het substraat toe en het verpompen, schoonmaken en hergebruiken van drain water. Het uitgangspunt kan echter ook zijn het volledig compenseren van de behoefte van de plant aan water en nutriënten. Ook kan met opzet worden gekozen voor het maar gedeeltelijk voldoen aan de plantbehoefte aan nutriënten. Dit kan dan worden gebruikt om groeiprocessen van de plant te beïnvloeden.

In de onderhavige studie is de compensatie van de opname van de plant als uitgangspunt gekozen. Om dit uitgangspunt goed te kunnen nastreven, is het nodig te weten hoe het opnameproces op het scheidingsvlak van wortel en substraat in zijn werk gaat en of het substraat in staat is, op het moment dat de plant er om vraagt, de gevraagde hoeveelheden water en nutriënten aan te leveren. In de thesis is daarom veel aandacht besteed aan deze overwegingen en zijn algoritmen uitgewerkt die ingaan op deze filosofie rondom het regeldoel. De vraag hierbij is tot in welk detail en met welke nauwkeurigheid deze processen bekend moeten zijn

voor regeltechnische doeleinden, zeker ook gezien de diversiteit in beschrijving van de werking van de opnameprocessen die er in de literatuur voorkomen.
Om aan bovengenoemde vragen te voldoen is het nodig een criterium te ontwikkelen, waarmee de opgenomen hoeveelheden kunnen worden afgewogen t.o.v. een gewenste situatie. Gedurende het verloop van het onderzoek is er voor gekozen hiervoor setpoints voor de drainflow en de drainconcentratie als uitgangspunt te nemen, waarbij deze setpoints over grote delen van de dag constant worden gehouden. De compensatie van veranderingen in de drainflow en in de drainconcentratie ten gevolge van plantopname, is uiteindelijk het balanceerpunt waarop de doseerinstallatie voor toediening van water en meststoffen wordt aangestuurd.

Al in 1985 is de ontwikkeling van een nieuw type sensor in gang gezet, door een pH Isfet (Ion Selective Field Effect Transistor) te voorzien van een actief membraan, dat daarmee in staat is de concentratie van één type ion te meten. De ontwikkeling van de membranen op deze Isfet sensoren is door onderzoek tot stand gekomen in het Laboratorium voor Organische Chemie van de Universiteit Twente in een groot aantal PhD studies voorafgaand aan en ook nog tijdens deze hier voorliggende studie.
De resultaten zijn zo nieuw dat - ofschoon de ontwikkeling van de sensoren als zodanig niet tot deze studie behoort - ook in deze thesis de typische eigenschappen van de Isfet en de essentiële eindresultaten van het Twentse onderzoek worden toegelicht en weergegeven.
Een set van Isfet sensoren, waarbij elke sensor gevoelig is voor een ander type ion, is in staat per ion de concentratie van de belangrijkste meststofionen in samples uit het gietwater van de kas te meten. De hier voorliggende studie gaat dieper in op de ontwikkeling van een on-line analyser en het gebruik van Isfet sensoren in de analyser.
Voor deze analyser is een voorhanden idee verder uitgewerkt en is een eerste vorm van hardware en software ontwikkeld tot een werkend prototype. De hard- en software van de analyser is zodanig ingericht, dat een aantal ionen *in situ* in de kas gemeten kunnen worden. Op basis van het onderzoek aan dit prototype is een commerciële lijn van analysers in productie genomen door een toeleverend bedrijf aan de glastuinbouw.
De kas is een omgeving die een sterk storende invloed heeft op signalen van sensoren, o.a. door temperatuurvariaties, hoge luchtvochtigheid, hoge stralingsniveaus, verouderingseffecten en meetruis t.g.v. electro-magnetische invloeden. In een analyser, die on-line in de kas wordt geplaatst, hebben deze verstoringen een grote invloed op de nauwkeurigheid en de betrouwbaarheid van de signalen. De thesis omschrijft hoe de sensoren m.b.v. calibratievloeistoffen, die op gezette tijden door de sensorset worden geleid, worden gecorrigeerd voor de verstoringen. Extra routines worden beschreven, die in de software van de analyser zijn aangebracht, en in staat zijn het meetsignaal te ontdoen van de verstoringen via calibratieprocedures, signaalbehandeling en data-mining.

Het is nu al gangbare praktijk om vloeibare meststoffen van hoge kwaliteit toe te passen, die zijn ontdaan van ballaststoffen en waarvan de samenstelling nauwkeurig bekend is. Ook nu al kunnen in de praktijk van de hedendaagse glastuinbouw vloeibare meststoffen nauwkeurig worden toegediend, via menging in een tank of injectie in de hoofdleiding. In de opstelling voor het onderzoek werd deze bestaande commerciële apparatuur toegepast.
Echter, menging van hooggeconcentreerde elektrolyten kan aanleiding zijn voor problemen met het uitkristalliseren en tot situaties leiden met ontploffingsgevaar door overdruk t.g.v. vrijkomend CO_2 gas. Door gebruik van speciaal ontwikkelde algoritmen kunnen recepten aan de doseerunit worden opgegeven, die worden doorgerekend op deze mogelijke problemen.
Deze algoritmen, in de vorm van software routines, dragen zorg voor het voldoen aan de beperkingen (constraints) die gepaard gaan met het mengen van de hooggeconcentreerde elektrolyten. In die gevallen, waarin wegens de beperkingen niet precies het gewenste recept

kan worden aangemaakt, wordt via een optimalisatie routine het gewenste recept zo dicht mogelijk benaderd, waarbij rekening wordt gehouden met alle constraints.

In eerste instantie is een regelaar ontwikkeld, die uitgaat van een permanente vloeistofstroom richting planten, waarvan de hoeveelheid [$m^3 \cdot s^{-1}$] continue kan worden geregeld. Gezien het feit dat de parameters van een eenmalig bepaald dynamisch model van het teeltsysteem gedurende het teeltseizoen een langzaam veranderingsproces ondergaan, o.a. door aanpassingen van het wortelpakket door de plant, is hiervoor een ontwerptechniek toegepast die een robuuste regelaar oplevert.
Dit uitgangspunt, een contimue vloeistofstroom richting plant, blijkt ver van de werkelijke toepassingen in de praktijk te liggen. Het is namelijk gebruikelijk de kassen op te delen in z.g. kraanvakken, waarbij delen van de kas - elk apart - worden voorzien van water door een electro-magnetisch bediende kraan (ventiel). De dure doseerinstallatie wordt zo gebruikt voor ieder kraanvak. De doseereenheid wordt als het ware ge'multiplex't over de verschillende kraanvakken.
Dit heeft tot gevolg dat het water in de vorm van een puls wordt afgeleverd, waarbij de tijdsduur en de pompcapaciteit bepalend zijn voor de afgeleverde hoeveelheid. Eenmaal per cyclus van de multiplexer wordt zo elk kraanvak bediend om weer opnieuw te beginnen met een puls in de volgende cyclus. Bijvoorbeeld elk half uur 3 minuten water geven per kraanvak. Elk kraanvak krijgt zo een gemiddelde hoeveelheid water en nutriënten per cyclus, waarbij de hoeveelheid kan worden bestuurd door de tijdsduur van de puls.
In vergelijking met een permanent bewaterd systeem is dit een keuzebeperking. Deze beperking maakt het noodzakelijk de gekozen regelmethode aan te passen. De graden van vrijheid beperken zich tot correctie door één schakelactie op een kraanvakventiel per cyclustijd, hetgeen betekent dat de regelmethode zich moet richten op het compenseren van de gemiddelde opname over een cyclus. Informatie over het gedrag van het bestuurde proces tijdens de watergeefpuls is wel van belang voor de modelvorming, echter de informatie wordt daarna niet meer voor de besturing gebruikt.
De thesis gaat in op de manier waarop de regelaar ontwikkeld kan worden, ook in situaties met een praktijkkas, waarbij de omstandigheden en parameters afwijken van een gekozen standaardsituatie. Aan deze omstandigheid kan worden tegemoet gekomen door in het uiteindelijke ontwerp per kraanvak een z.g. 'model-meetgoot' (+/- 2.5m lang) op te nemen in de gewashaag, waarop +/- 10 planten zijn opgesteld. De regelaars worden zodanig ontworpen dat in feite het proces op die model-meetgoot wordt geregeld. Omdat de rest van het kraanvak hetzelfde water ontvangt als deze model-meetgoot, staat de meetgoot dus echt model voor de besturing van het kraanvak. Direct naast de uitgang van de modelmeetgoot wordt de analyser opgesteld, die van de drain de flow en de concentratie per ion bepaald. Het drainwater van zo'n meetgoot is onmiddellijk beschikbaar en hoeft niet een retourgoot van enkele honderden meters te doorlopen, voordat het in een drain bassin is aangekomen om te worden gesampeld door de analyser. Het procesmodel dat moet worden bepaald om de regelaar te ontwerpen, is dus in feite het model van het proces dat zich op deze meetgoot afspeelt. Het kan dus éénmalig worden ontworpen voor een bepaald type substraat en een bepaalde soort plant. Het geldt dan - behoudens enkele parameters zoals pompcapaciteit, setpoint voor drain flow en drain concentratie - voor iedere situatie bij die plant en dat substraat in elke willekeurige kas.
Indien er meer dan één kraanvak per kas is die allen hetzelfde zijn uitgevoerd, kan er ook nog voor worden gekozen dezelfde hoeveelheid water van dezelfde samenstelling door de andere kraanvakken naar de planten te sturen. De meetgoot staat dan niet alleen model voor het eigen kraanvak, maar voor een hele kas. Dit laatste is alleen mogelijk als de procesomstandigheden van de verschillende kraanvakken voldoende aan elkaar gelijk zijn.

Het project is niet af. Er is in feite een basale regelaar ontwikkeld voor watergeven op basis van drainflow. Een regelaar voor drainconcentratie kon uiteindelijk niet worden gerealiseerd, omdat de benodigde Isfet sensoren steeds weer nieuwe problemen vertoonden. Problemen van een zodanig ernstige aard, dat meten t.b.v. regelen er steeds weer niet inzat. Waarmee weer eens is bewezen dat het uitvoeren van onderzoek, met behulp van resultaten van gelijktijdig plaatsvindend ander onderzoek, uiteindelijke frustrerend kan gaan werken op het totale resultaat. Kort na beëindiging van dit promotie onderzoek zijn de ionsensoren uiteindelijk toch nog gereed gekomen.

SUMMARY

The contrast between the high-tech character of the climate control system in a greenhouse and the relatively low-tech approach in relation to supply of water and nutrients, as is still common practice in greenhouse industry, was an additional challenge to undertake a project aimed at the control of the processes in the root environment of the plant. In addition to this, there is an ever-increasing understanding amongst horticulturists that advantages might be taken of a connection between the control of variables in the plant's atmosphere and the plant's rizosphere.
During the research for this thesis, the project developed into the direction of integrating different technologies that are already available or still under development, but are expected to be available for horticulture industry within short. However, it needed a breakthrough in the area of sensor technology to really make it happen.

When a new method of control of the application of fertilisers should be meaning more than what has been achieved in the field of EC and pH control of the supply water, then in the mind of specialists in this area the desire arises to control on the basis of concentration of each individual ion. Next to it, the question arises to compensate the plant's uptake of water and nutrients by means of a control system.
To achieve this, two things are needed: 1) to be able to measure the concentrations of individual ions; 2) to be able to establish as the output of a controller a recipe of individual ion concentrations, adequate for a dispenser of simple liquid fertilisers.

Given the availability of the above mentioned equipment and installations, it is a prerequisite that a control philosophy is developed that answers the question which quantities ultimately are subject of the control action. This can simply be the efficient transport of water and nutrients towards the substrate and the recirculation, cleaning and reuse of the drain water. But the main issue can also be the full - or deliberately partial - compensation of the plant's demand. Partial compensation of the plant's demand for nutrients can be used to influence the growth process. In the present study compensation of the plant's demand is chosen as the basic principle.
To fulfil the basic principle, compensation of the plant's demand, a clear understanding is needed on the processes of plant uptake that are active on the interface between root and substrate. In addition, the question arises whether the substrate is able to deliver the required amounts and to deliver them in time.
Therefore, attention is paid to these considerations. Algorithms have been specified, which elaborate on a philosophy in relation to the subject of control. It is of interest to know to which detail and accuracy these processes should be negotiated, in order to meet the needs of the control engineer. The more so, since literature shows much diversity in the description of the functioning of the uptake process of the root.

Since the questions: 1) is the substrate limiting, and 2) can these effects be compensated by adequate control measures, can (or should) be answered by 'yes', the thesis issues the need for the development of a criterion that can be used to balance uptake against a set value.
During the course of the research project the choice has been made to take as a base the set values for drain flow and for concentration of individual ions in the drain. These set values are kept constant during large parts of the day. Compensation of the change in flow and concentration of the drain due to plant uptake, by means of feedback, is the ultimate balancing point on which the supply of water and fertilisers is controlled.
Already in 1985 a development was started with a new type of measuring device. A pH sensitive Isfet sensor was covered with an active membrane, enabling it to measure the concentration of one specific type of ion. The development of the membranes was performed by the Organic Chemistry Department of the Twente University, during a number of PhD studies, preceding and during the here presented study.
The results are so new that - although the development of these sensors as such are not part of this study - this thesis elucidates and presents the typical properties of the Isfet sensors and the essential end results of the research at the Twente University.
A set of Isfet sensors, of which each sensor is able to measure one individual ion, is able to measure the most important fertiliser ions in a small (5mL) sample taken from the supply- and drain water of a greenhouse. The sampling rate can be as high as one sample reading per 20 seconds.
This thesis emphasises the need for an on-line analyser *in situ* in the greenhouse. An available idea has been evaluated and was worked out from a first specification of hardware and software into a functional prototype. Hardware and software are established in such a way that samples can be measured in the greenhouse. On the basis of the experience gained during the research that produced this prototype, a commercial line of analysers has been taken into production by the main supplier company of control equipment to greenhouse industry.

The interference on sensor signals from electrical noise and environmental influences in a greenhouse are manifold: temperature variations, high humidity of the air, high radiation levels, ageing due to high UV radiation, electromagnetic noise from on/off switching of high-power relay contacts. In a greenhouse, these disturbances exert a big influence on the accuracy and reliability of the signals of the *in situ* and on-line analyser.
The thesis describes calibration procedures that are used for signal correction. Intermittently, calibration fluids are passed through a set of sensors. Calibration software routines are elucidated, which have been incorporated in the analyser and are able to free the signals from these disturbances by statistics on the measured samples values from the greenhouse and on the calibration signal values stored in memory.
Nowadays, it is common practice in horticulture to use simple liquid fertilisers of high quality, of which the composition is accurately known and have been freed from ballast materials. In present day horticultural practice, commercial available equipment administers simple liquid fertilisers by mixing exact dosages in a tank or by injecting them directly in the main water supply line. In the research set-up for this thesis, directly injecting commercial equipment was used.
However, mixing highly concentrated electrolytes from an independently established recipe of simple fertiliser elements, may lead to problems with crystallisation and with detonation of high pressure CO2 gasses. Taking into account the restricting constraints in specially designed algorithms, recipes may be supplied to the fertiliser diluter/mixer that are optimised to avoid those problems. If the exact recipe can not be produced, it will administer an amount as close to the optimum as possible.

As a start a controller has been designed that operates on a permanent solute flow to the plants, of which the amount [$m^3 \cdot s^{-1}$] can be controlled continuously by means of the rotation speed of a pump. Since the parameters of the model of a growing system change gradually during the season, including changes of the root mat, the robust controller design method has been applied. This design has been elucidated and leads to a controller that keeps the maximum deviation well within an allowable margin of 10%.
However, manipulating the rotational speed of a pump is not realistic in practical circumstances. It is good practice in greenhouse engineering to split up a greenhouse water supply system into several valve controlled sections. Parts of the greenhouse get their own electromagnetically operated valve to control water supply to that section. In this way the expensive water- and nutrients dispenser is multiplexed over the different valve controlled sections. As a result, the water is supplied in subsequent cycles as a repetition of pulses, of which time duration and pump discharge determine the delivered amount. Once per cycle of the multiplexer each valve-operated section is served, to start again with a pulse in the next cycle, e.g. each half hour 3 minutes of water supply per section. On average, each section gets an equal amount of water and nutrients, of which the amount can be controlled by the time duration of the pulse. However, in comparison with a permanently watered system this is a limitation in choice, since it restricts the degrees of freedom. This limitation to one controlled variable, the pulse duration for water supply, forces to adjust the method of control. Now the controller action should be aimed at the compensation of the uptake, averaged over the time duration of one cycle. Information of the dynamic behaviour of the controlled process during the supply pulse in its cycle is of interest for establishing the model, but from then on it is not used for control.
The method and the procedures to design a controller are presented for situations of a greenhouse in practice, of which the circumstances and parameters will differ from a standard situation. These demands are met by the introduction of a so-called "model gully" (+/- 2.5m long) in a valve operated section. The model gully contains approximately 10 plants and is integrated in the crops canopy. Since the rest of the valve section receives the same amount of water and nutrients as the model gully, the gully is really a model for the rest of the valve section. The controller is developed to control the process on the model gully. The analyser is situated next to the model gully, which enables a short response time of the measured drain flow and drain concentration. To design a controller, only the process model of the measuring gully needs to be determined. It allows a once-only design that is applicable for all greenhouse types, apart from some parameters like pump capacity, setpoint for drain flow and drain concentration.
If there are more valve-sections that are equipped the same, there is an option to supply the same amount of water with the same nutrients to the plants in the other valve-sections. Then, the model gully is not only a model for its own valve section, but for the whole greenhouse. This last option is only valid, if the different valve sections are sufficiently equal to each other.

The project is not finished yet: in fact a basic controller has been designed for the control of water supply only. In the end, a controller for nutrient concentration could not be realised, because the required Chemfet sensor was never available long enough to allow for a decent controller design. This again proves that research, carried out with results of simultanous research, finally may frustrate the overall goal. Shortly after the end of the research efforts for this thesis the Isfet sensors were finally ready.

REFERENCES

Agricultural Structure Memorandum, 1989. Ministry of Agriculture, Nature Management and Fisheries, The Hague, 174 pp.

Albery, W.J., C.C.Haggett, L.R. Svanberg, M.D.Neville, 1986. The development of electrochemical sensors. In: W.G. Gensler (Ed.), *Proceedings of the NATO Advanced Study Institute on 'Advanced Agricultural Instrumentation'*, Il Ciocco, 1984. Martinus Nijhoff, Rotterdam. p. 429-456.

Bailey, B.J., B.G.D. Haggett, A. Hunter, W.J. Albery and L.R. Svanberg, 1988. Monitoring nutrient film solutions using ion selective electrodes. In: *Journal of Agricultural Engineering Research*, 40(1988)2, p. 129-142.

Baille, A., 1993. Specific objectives and constraints in irrigation management of greenhouse crops under Mediterranean conditions. In: *Proceedings Workshop on environmentally sound water management of protected agriculture under Mediterranean and arid climates*, CIHEAM IAM-B.

Balendonck, J., M.C. Kuyper, M.A. Hilhorst, 1998. A water management method for non-closed crop production. In: *Proceedings of the AgEng 98 Conference*, Oslo Norway.

Barber, S. A., 1962. A diffusion and mass-flow concept of soil nutrient availability. In: *Soil Sci.*: 93(1962) p. 39-49.

Bentvelsen, B., R. de Wit, F. van den Holst, 1997. Functioneel ontwerp MSGRAPH. PRIVA Agro Research & Development. Intern Rapport.

Bergveld, P., 1970. Development of an ion sensitive solid state device for neurophysical measurements. In: *IEEE Trans.Biomed.Eng.* BME-17:70

Biggs, W., 1986. Radiation measurement. In: W.G. Gensler (Ed.), *Proceedings of the NATO Advanced Study Institute on 'Advanced Agricultural Instrumentation'*, Il Ciocco, 1984. Martinus Nijhoff, Rotterdam, p. 3-20.

Bowling, D.J.F., 1976. Uptake of ions by plant roots. Chapman and Hall London.

Bruggink, G.T., H.E. Schouwink and Th.H. Gieling, 1988. Modelling of water potential and water uptake rate of tomato plants in the greenhouse. In: *Acta Hort. 229*, p. 77-85.

Buitelaar, Th., H de Kroon and L. de Jong, 1975. Verwarmingstechniek in de tuinbouw. Centrale school voor de tuinbouwtechniek, Ede. 152 pp.

Chalabi, Z. S. and Bailey, B. J., 1989. Simulation of the energy balance in a greenhouse. In: *Divisional Note DN.1516*, AFRC Institute of Engineering Research, Silsoe, UK.

Chang, R., 1990. Physical chemistry with applications to biological systems. In: *Maxwell Macmillan International Editions.* Second edition. Macmillan, New York.

Chotai, A. and P.C.Young, 1991. Self-adaptive and self-tuning control of a Nutrient Film (NFT) System. In: Y.Hashimoto and W.Day (Editors). In: *Mathematical and Control applications in agriculture and horticulture*, Elsevier, Kidlington-Oxford, p. 33-40.

Chotai, A., P.C. Young, P. Davis & Z.S. Chalabi, 1991. True digital control of glasshouse systems. In: Hashimoto Y. & W. Day (Eds.), *Mathematical and Control Applications in Agriculture and Horticulture*. Pergamon Press, p. 41-46.

CIE, 1989. Solar Spectral irradiance. In: *Technical report, publ.no CIE-85*, Vienna Austria

Claassen, N and S.A. Barber, 1986. A method for characterising the relation between nutrient concentration and flux into roots of intact plants. In: *Plant Physiol.* (1974) 54, p. 564-568.

Clark, O.M. and M.A. Povey, 1985. Integrated protection for computer systems. In: *Conference proceedings of the 18th conference on lightning protection (ICLP-85)*; VDE-Verlag GmbH Berlin Offenbach. p. 325-331.

Cornell, J. A., 1990. Experiments with mixtures. Designs, models, and the analysis of mixture data. John Wiley & Sons, New York, 632 pp.

De Veld, P., 1997. Teeltvoordeel uit tensiometers. In: *Groenten & Fruit/Glasgroenten, wk 27*, p. 14-15.

De Willigen, P. and M. van Noordwijk, 1987. Roots, plant production and nutrient use efficiency. PhD Thesis Wageningen Agricultural University, 279 pp.

Deane-Drummond, C.E., 1982. Mechanisms for nitrate uptake into Barley (Hordeum Vulgare L. cv. Fergus) seedlings grown at controlled nitrate concentrations in the nutrient medium. In: *Plant Science Letters*, 24 (1982), p. 79-89.

Doyle, J.C., B.A. Francis & A.R. Tannenbaum, 1992. Feedback control theory. Maxwell Macmillan International Editions, New York, 227 pp.

Engbersen, J.F.J. and D.N. Reinhoudt, 1994. Chemically modified field-effect transistors for measurement of ion activities in aqueous solution. In: *Analusis Magazine*, 1994, V22, no 9, p. M16-M18.

Engbersen, J.F.J., W. Olthuis, M. Bos, 1995. Chemical Microsensors. In: *Comett-FSRM Training Course in UETP-MEMS*. Swiss foundation for research in microtechnology. Neuchâtel Swiss Confederation.

Engbersen, J.F.J., M.M.G. Antonisse, R.J.W. Lugtenberg and D.N. Reinhoudt, 1997. Chemically modified field-effect transistors for measurement of ion activities in aqueous solution. In: *J.Electrochem.Soc.*, Paris 1997.

Epstein, E. and C.E. Hagen, 1952. A kinetic study of the absorption of alkali cations by barley roots. In: *Plant Physiology*, 27, p. 457-474.

Fick, A. 1855. The process of translational diffusion. In: *Ann. Physik*, 94, 59.

Gieling, Th.H. and W.Th.M. van Meurs. 1984. Damage to climate control equipment and crop caused by lightning. In: *Acta Hort.* 148. p. 297-303.

Gieling, Th.H., E.A. van Os, A. de Jager. 1988. The application of chemo- and bio-sensors for soilless cultures. In: *Acta Hort. 230*, p. 357-362.

Gieling, Th.H., J. Bontsema and L.J.S. Lukasse. 1994a. The dynamic behaviour of salinity changes in a closed NFT growing system. In: *Acta Hort. 361*, p. 218-225.

Gieling, Th.H., J. Bontsema, A.W.J. van Antwerpen & L.J.S. Lukasse. 1994b. Monitoring and control of water and fertilizer distribution in greenhouses. In: *Acta Hort. 401*: p. 365-372.

Gieling, Th.H. and K. Schurer, 1995a. Sensors and measurement. In: *Acta Hort. 421*.

Gieling, Th.H. and K. Schurer, 1995b. Sensors and measurement. In: *J.C. Bakker, G.P.A. Bot, H. Challa, N.J. van de Braak (Eds.) Greenhouse Climate Control, an integrated approach.* Wageningen Pers, 279p.

Gieling, Th.H., E.A. van Os, P. Hamer, 1996. Greenhouse water supply, application of nutrients and their environment. In: *Macqu Final Report EU AIR3-CT93-1603*. Chapter 2.

Gieling, Th.H. and H.H. van den Vlekkert, 1996. Application of ISFET's in closed loop systems for greenhouses. In: *Adv. Space Res.* Vol.18, no 4/5, p. 135-138, Pergamon.

Gieling, Th.H., J.Bontsema and E.A. van Os, 1997a. Monitoring and control of water and nutrient supply in closed growing systems. In: E. Goto *et al.* (Eds). *Plant Production in Closed Ecosystems*. P. 103-121, Kluwer Acad. Publishers.

Gieling, Th.H., J. Bontsema, E.A. van Os, T.W.B.M. Bouwmans and R.H. Steeghs. 1997b. Modelling and simulation for control of nutrient application in closed growing systems. In: *Neth. Journal of Agricultural Science.* 45(1997), p. 127-142.

Gieling, Th.H., J.F.J. Engbersen, J.J.W. Westra, 1998a. Chemically modified field effect transistors to monitor ion concentration in nutrient solution. In: *Proceedings of the 3^{d} International Symposium on sensors in horticulture*, Tiberias, Israel.

Gieling, Th.H., H.J.J. Jansen, H. de Vree and P. Loef, 1998b. Feedback control of water supply in an NFT growing system. In: *Proceedings 3^{d} workshop on "Sensors in Horticulture"*, Tiberias Israel.

Gieling, Th.H., G.van Straten, H.J.J. Janssen and A. Berge, 1998c. Control of water supply in closed growing systems in a greenhouse. In: *Proceedings of the IFAC/CGIR/ASAE Workshop on Control and Ergonomics in Agriculture*. pre-prints: p. 167-170.

Gieling Th.H. J.W. Westra, 2000. Supply of nutrient ions by injection of multiple chemical fertilisers. Internal report IMAG.

Gieling, Th.H., G van Straten and B.W. Veen, 2000. Analysis of solute movement in inert substrates. In: *Proceedings of IFAC Conference on modelling and control in agriculture, horticulture and post-harvest processing*, pre-prints: p. 357-363.

Gieling, Th.H., G. van Straten and H.J.J. Janssen, M. Suurmond, 2000. A greenhouse water supply controller: a design based on system identification of closed growing systems. In: *Computers and Electronics in Agriculture Vol 26 (2000)*, p. 361-374, Elsevier.

Hamer, P. J. C., 1997. Simulating the irrigation requirements of a greenhouse crop. Proceedings of the International Conference and British-Israeli Workshop on Greenhouse Technologies, Tel-Aviv and Bet Dagan, Israel. In: *Acta Hort.* 443 p. 147-154.

Hamer, P. J. C., 1998. Validation of a model used for irrigation control of a greenhouse crop. Proceedings of the International Symposium on Water Quality and Quantity in Greenhouse Horticulture, Tenerife. In: *Acta Hort.* 458 p.75-81.

Hanan, J.J., 1984. Plant environmental measurement. Bookmakers Guild Inc. 1430 Florida Avenue Longmont Colorado 80501.

Hashimoto, Y., T. Morimoto, T. Fukuyama, H. Watake, S. Yamaguchi and H. Kikuchi, 1989. Identification and control of hydroponic system using ion sensors. In: *Acta Hort.* 245. p. 490-497.

Hasse, P. and J. Wiesinger, 1985. Schutz von Rechenanlagen und -Geräten gegen Blitzstörungen. In: *Conference Proceedings of the 18th conference on lightning protection (ICLP-85)*; VDE-Verlag GmbH Berlin Offenbach. p. 299-304.

Hauptmann, P., 1990. Sensoren, Prinzipien und Anwendung. Carl Hanser Verlag München Wien.

Heinen, M., 1991. Control of composition of nutrient solution in NFT systems, Experiment and Simulation. In: *Acta Hort. 304*, p. 281-289.

Heinen, M. and K. Harmanny, 1992. Evaluation of the performance of ion selective electrodes in an automated NFT system. In: *Acta Hort*. 304. p. 273-280.

Heinen, M., 1997. Dynamics of water and nutrients in closed, recirculating cropping systems in glasshouse horticulture. PhD Thesis Wageningen Agricultural University.

Heuvelink, E. and J. Miguel Costa, 2000. Greenhouse horticulture in Almería (Spain): report on a study tour.

Hietbrink, O., H.B. van der Veen, J.K. Nienhuis, M.N.A. Ruijs, 1999. Bedrijfs- en milieueffecten AmvB Glastuinbouw 2000-2010. In: *LEI, Den Haag, report 1.99.08*, 59 pp.

Hilhorst, M.A., J. Groenwold and J.F. de Groot, 1992. Water content measurements in soil and rockwool substrates: Dielectric sensors for automatic in situ measurements. In: *Acta Hort.* 304. p. 209-218.

Högberg, R, E. Lötberg and V. Scuka, 1985. Lightning protection of electronic installations - design considerations. In: *Conference proceedings of the 18th conference on lightning protection (ICLP-85)*; VDE-Verlag GmbH Berlin Offenbach. p. 291-298.

Honjo, T. & T. Takakura, 1991. Identification of water and nutrient supply to hydroponic tomato plants by using neural nets. In: Hashimoto Y. & W. Day, *Mathematical and Control Applications in Agriculture and Horticulture*. Pergamon Press, Oxford, p. 285-288.

Jacobs, J.M., 1995. The history of greenhouse cultivation. In: J.C. Bakker, G.P.A. Bot, H. Challa and N. J. van de Braak (Eds.), *Greenhouse climate control, an integrated approach*. Wageningen Pers, Wageningen, p. 3-7.

Jacobson, K., E.D.Sheets and R.Simson, 1995. Revisiting the fluid mosaic model of membranes. In: *Science*, Vol. 268: p. 1441-1442.

Jolliet, O. and B.J. Bailey, 1992. The effect of climate on tomato transpiration in greenhouses: measurements and models comparison. In: *Agricultural and Forest Meteorology*, 58, p. 43-62.

Jolliet, O., 1994. HORTITRANS, a model for predicting and optimizing humidity and transpiration in greenhouses. In: *Journal of Agricultural Engineering Research*, 57: p. 23-37.

Jongebreur, A.A., Th.H. Gieling and J.J.W. Westra, 1999. Closed growing systems for supply of water and nutrients. In: *Proceedings of BRAIN International Symposium 2000*. IAM-BRAIN, Japan, November 1999, p. 44-51.

Jungk,, A., C.J. Asher, D.G. Edwards and D. Meyer, 1990. Influence of phosphate status on phosphate uptake kinetics of maize and soybean. In: *Plant Nutrition-physiology and applications*, p. 135-142. Kluwer Academic Publishers.

Knoll, W.H. and E.J. Wagenaar, 1994. Handboek installatietechniek, uitgave 1994. TVVL Amersfoort, ISSO Rotterdam and NOVEM Sittard. 1201pp, p760-762.

Kupers, G., J. van Gaalen, Th.H. Gieling and E.A. van Os, 1992. Diurnal changes in the ion concentration of the supply and return water of a tomato crop grown on rockwool. In: *Acta Hort. 304*.

KWIN, Quantitative information for greenhouse horticulture 1999 - 2000 (Kwantitatieve Informatie voor de glastuinbouw), 1999. PBG, Research Station for greenhouse vegetables and floriculture, Naaldwijk/Aalsmeer, 166 pp (in Dutch). p. 291-300.

Long, S.P., 1986. Instrumentation for the measurement of CO_2 assimilation by crop leaves. In: W. Gensler (ed.), *Proceedings of the NATO Advanced Study Institute on 'Advanced Agricultural Instrumentation'*. Martinus Nijhoff, Rotterdam. p. 39-91.

Lukasse, L.J.S., 1994. MSc Thesis Agric. Universtity Wageningen .

Meteorological Office, 1969. Handbook of meteorological instruments, I, Instruments for surface observations. H.M. Stationary Office, London.

Monteith, J. L. and M. Unsworth, 1990. Principles of environmental physics. Edward Arnold, London, 291 pp.

Morf, W.E., D. Ammann, E. Pretsch and W. Simon, 1973. Carrier antibiotics and model compounds as components of selective ion sensitive electrodes. In: *Plenery lectures at the International Symposium on Selective Ion sensitive Electrodes*. Cardiff, Uk, 1973. p.421-439.

Mulder, M., 1991. Basic principles of membrane technology. Kluwer Academic Publishers, Dordrecht, The Netherlands, 363 pp.

Multi-Year Crop Protection Plan, 1991. Ministry of Agriculture, Nature Management and Fisheries. The Hague, 298 pp.

National Environmental Policy Plan, 1989. Ministry of Housing, Planning and the Environment. The Hague, 258 pp.

Passioura, J. B., 1963. A mathematical model for the uptake of ions from the soil solution. In: *Plant and Soil* XVIII, no 2.

Reinhoudt, D.N., 1995. Durable chemical sensors based on field-effect transistors, *Sensors and Actuators B* 1995, *24*, 197-200.

Robinson, N., 1966. Solar Radiation. Elsevier Publishing Company, Amsterdam

Ruijs, M.N.A. and E.A. van Os, 1991. Economic evaluation of business systems with a lower degree of environmental pollution. In: *Acta Hort. 295*, p. 79-84.

Ruijs, M.N.A., 1994. Economic evaluation of closed production systems in glasshouse horticulture. In: *Acta Hort. 340*, p. 87-94.

Schrevens, E. and J.A. Cornell, 1990. Design and analysis of mixture systems: Applications in hydroponic plant nutritional research. In: *Plant and Soil* 154: p. 45-52.

Schurer, K. 1986. Water and plants. In: W.G. Gensler (Ed.), *Proceedings of the NATO Advanced Study Institute on 'Advanced Agricultural Instrumentation'*, Il Ciocco, 1984. Martinus Nijhoff, Rotterdam. p. 429-456.

Singer, S.J. and G.L.Nicholson, *1972*. The fluid mosaic model of the structure of cell membranes. In: *Science*, Vol.175: p. 720-731.

Slavik, B., 1974. Methods of studying plant water relations. Springer Verlag Berlin, Heidelberg, New York.

Sonneveld, C., 1988. Rockwool as a substrate in protected cultivation. In: *Horticulture in high technology era*, Tokyo, Japan, p.173.

Sonneveld, C. and L. Spaan, 1989. A universal model for calculations on nutrient solutions. Horticultural Station Naaldwijk, The Netherlands.

Sonneveld, C., 1996. Watergift kan terug, zonder negatieve gevolgen voor gewas. Vakblad voor de Bloemisterij no. 46, p.72-73.

Stanghellini, C., 1987. Transpiration of greenhouse crops, an aid to climate management. Ph.D. Dissertation, Agricultural University, Wageningen, 150 pp.

Steeghs, R.H. and T.W.A.M. Bouwman, 1996. Het ontwerp van een robuuste regeling voor de dosering van meerdere voedingsionen in een N.F.T.-teeltsysteem. MSc thesis Wageningen Agricultural University.

Steiner, A.A., 1996. Foreword. In: Proceedings of the 9^{th} international congress on soilless culture. p. 13.

Stephanopoulos, G., 1984. Chemical process control. Prentice-Hall Inc, Englewoods Cliffs, NY, USA

Sudhölter, E.J.R., P.D. van der Wal, M. Skowronska-Ptasinska, A. Van den Berg, P. Bergveld, D.N. Reinhoudt, 1990. Modification of ISFETs by covalent anchoring of poly (hydroxyethyl methacrylate) hydrogel. Introduction of a thermodynamically defined semi-conductor sensing membrane interface, In: *Anal. Chim. Acta, 230*, p. 59.

Van Antwerpen, A.W.J., 1995. Ontwerp van een watergeefsysteem aangelegd volgens de Tichelmann methode. MSc thesis Wageningen Agricultural University, 68 pp.

Van den Muijzenberg, E.W.B., 1980. A history of greenhouses. IMAG-DLO, Wageningen.

Van den Vlekkert, H.H., N.F. de Rooij, 1988. Design, fabrication and characterization of pH sensitive ISFETs, In: *Analusis*, Vol.16 nr.2, p. 110.

Van den Vlekkert, H.H., 1992. Ion Sensitive Field Effect Transistors. In: *Acta Hort. 304*, p. 113-126.

Van den Vlekkert, H.H., J.P.M. Kouwenhoven and A.A.M. van Wingerden, 1992. Application of ISFETs in closed loop systems for horticulture. In: *Acta Hort. 304*. p. 309-320.

Van Ieperen W., 1996. Consequences of diurnal variation in salinity on water relations and yield of tomato. Ph.D. Thesis Wageningen Agricultural University.

Van Kooten, O., 2000. Hydrion-line II: online monitoring- en besturingssysteem voor proceswater in gesloten teeltsystemen in de glastuinbouw. Project put into effect under the authority of the Dutch Ministry of Economic Affairs.

Van Meurs, W.Th.M. and C. Stanghellini, 1991. Use of an off-the shelf electronic balance for monitoring crop transpiration in greenhouses. In: *Acta Hort. 304.* pp 219.

Van Os, E.A., M.N.A. Ruijs and P.A. van Weel, 1991. Closed business systems for less pollution from greenhouses. In: *Acta Hort. 294.* p. 49-57.

Van Os, E.A., 1994. Closed growing systems for more efficient and environmental friendly production. In: *Acta Hort.* 396: p. 25-32.

Van Os, E.A., 1998. Closed soilless growing systems in the Netherlands: the finishing touch. *Acta Hort.* 458, p. 279-291.

Van Os, E.A., 1999. Closed soilless growing systems: a sustainable solution for Dutch greenhouse horticulture. Water Science & Technology, Vol. 39, No 5, p. 105-112.

Van Os, E.A. and F. Benoit, 1999. State of the art of Dutch and Belgian greenhouse horticulture and hydroponics. *Acta Hort.* 481, p. 765-767.

Van Os, E.A., 2000. New developments in recirculation systems and disinfection methods for greenhouse crops. Proceedings 15th Workshop on Agricultural Structures and ACESYS IV Conference, p. 81-91.

Vernooy, C.J.M., 1992. Op weg naar een schonere glastuinbouw (1): Het verbruik van water en meststoffen op praktijkbedrijven. *LEI-DLO publication 4-131*, The Hague, 64 pp.

Verwer, F.L., 1976. Growing horticultural crops in rockwool and NFT. In: *IMAG publication no. RR76-6.*

Visscher, G.J.W. and K. Schurer, 1985. Some research on the stability of several capacitive thin film (polymer) humidity sensors in practice. In: *Moisture and humidity 1985, Measurement and control in science and industry.* Instrument Society of America. Research Triangle Park, North Carolina USA. p. 515-323.

Von Zabeltitz, Chr., 1978. Gewächshäuser: Plannung und Bau. In: *Handbuch der Erwerbsgärtner*, 267p, Ulmer, Stuttgart.

Werkhoven, C., 1992. Sensors for irrigation scheduling of cultures in the field. In: *Acta Hort. 304.* p. 259-264.

Wild, A., P.J. Woodhouse, and M.J. Hopper, 1979. A comparison between the uptake of potassium by plants from solutions of constant potassium concentration and during depletion. In: *J.Exp.Bot.*Vol. 30, no.117, p. 697-704.

World Meteorological Organisation, 1971. Guide to meteorological instrument and observing practices. In: *WMO no 8*, TP3-4th ed., Geneva.

Young, P.C., W. Tych and A. Chotai, 1991. Identification, estimation and control of glasshouse systems. In: Hashimoto Y. & W. Day (Eds.), *Mathematical and Control Applications in Agriculture and Horticulture.* Pergamon Press, Oxford, p. 307-317.

Zimmerman, A.L., 1997. Cell membranes and transport. In: *Syllabus Fall 1997.* Brown University, Providence, Rhode Island 02912 USA.

CURRICULUM VITAE

Theodorus Hendrikus Gieling, was born on 14-3-1947 in Zevenaar, The Netherlands. After his study at a college for electronic engineering, he earned a BSc in Electronic Engineering and in addition he successfully finished a BSc in Control Engineering.
In 1970, he started working for the Dutch Ministry of Agriculture and Fisheries, as a staff member of the Institute of Horticulture Engineering, that later was merged to form the Institute of Environmental and Agricultural Engineering (IMAG-DLO), where he has been appointed as head of the cluster "Mechatronics and Process Control" at the IMAG institute.
From the start of his job in horticulture, he has been working on climate control in greenhouses. Especially work related to the introduction of analogue climate controllers for greenhouses (1974) and related to climate control by means of a digital computer (1978) were his first contributions to horticulture science. With a team of researchers, he participated in the development of an innovative computer network system that controls the greenhouses on the IMAG premises.
As an extension to this, he is doing research on a broader scale, i.e. in the application of sensors (1985) and control systems in other horticulture processes. Especially sensors related to "the speaking plant approach", climate control, control of water supply and nutrient concentration. In a co-operative research project of universities and institutes of five European countries - aimed at product quality in relation to climate control and nutrient supply - he has been working on the control of ion specific nutrient supply in relation to nutrient uptake, water uptake and evaporation.
This EU project resulted in two practice oriented national follow-up projects aimed at the introduction of ion specific application of water and nutrients to plants and in the research for the thesis at hand.

He published papers in international horticulture books and journals and presented invited papers at international symposia. He is chairman of the Working Group on Sensors in Horticulture of the International Society of Horticultural Science and convenor of a series of International Workshops on Sensors in Horticulture.

Printed by Ponsen & Looyen, Wageningen

Cover: Thijs Hoesté, Zevenaar